Monash University

School of Earth, Atmosphere and Environment

Doctoral Thesis

The effect of water sensitive urban design and outdoor water-use practices on urban microclimate

Supervisors:

Prof. Nigel Tapper

Prof. Jason Beringer

Author:

Ashley Broadbent

Dr. Andrew Coutts

Dr. Matthias Demuzere

This thesis is presented for a Doctor of Philosophy at Monash University

February 29, 2016

Copyright notice

Abstract

The excess heat that is stored in urban materials and created by human activities implies that people living in cities are particularly vulnerable to heat stress and heat related illness. In Australia, where extreme weather and prolonged drought are common, heat exposure in urban areas can be significantly exacerbated. The combination of increasing urban development, excessive urban heating, and lower water availability, alongside the impacts of future climate change could have damaging implications for the human health and well-being of urban dwellers. Water management in cities plays an important role in determining urban climates, but minimal work has been done that directly acknowledges these interconnected issues. Integrated water management approaches, such as water sensitive urban design (WSUD), provide a means for retaining water in the urban environment through stormwater harvesting and reuse. This study examines the potential for WSUD to provide cooling benefits and reduce human exposure to heat stress and thermal discomfort.

A high resolution observational field campaign, measuring surface level microclimate variables and remotely sensed land surface characteristics, was conducted in a mixed residential suburb containing WSUD in Adelaide, South Australia. At Mawson Lakes microclimate variability was measured, including air temperature and thermal comfort, to investigate the microclimate effects of WSUD features, including man-made lakes, bio-filtration wetlands, and irrigated open space. Additionally, the SURFEX (SURFace EXternalisée in French) model was used to simulate the potential for irrigation to reduce exposure to heat stress and provide more thermally comfortable conditions during heatwaves.

Clear evidence was found that WSUD approaches and irrigation can provide cooler air temperature and more comfortable thermal urban environments. It was found that the microclimate conditions that people experience in Mawson Lakes vary significantly over small spatial scales. The effects of WSUD features were seen to be highly localised, having little effect beyond 50 m from the source. Air temperature variability was influenced by land surface differences, such as proximity to water bodies. Sites that there were influenced by water bodies were up to 1.8 °C cooler during the day. However, human thermal comfort

(HTC) was less influenced by land surface characteristics, and was mostly determined by contrasts in shading and airflow in the environment. The modelling analysis showed that there is high potential for irrigation to cool air temperature during heatwave conditions; with irrigation a 2.8 °C maximum reduction in daily average temperature was predicted.

From this research some specific recommendations for the implementation of WSUD have been developed. These include consideration of the local wind regime when implementing WSUD; the use of smaller distributed features throughout the urban landscape at targeted locations; the use of irrigation during heatwaves to provide cooling; and the retention of trees in urban areas to provide shade, and augment the thermal comfort benefits provided by WSUD features. Overall, this research argues that distributed WSUD features can be used to capture, store, and treat stormwater, simultaneously providing ecological benefits and thermal benefits. Further, harvested stormwater can be re-integrated into the urban environment, thereby helping to maintain vegetation and providing distributed evaporative cooling benefits.

Declaration

This thesis contains no material which has been accepted for the award of any other degree or diploma at any university or equivalent institution and that, to the best of my knowledge and belief, this thesis contains no material previously published or written by another person, except where due reference is made in the text of the thesis.

Ashley M. Broadbent

Acknowledgments

This research would not have happened without the support of a number of people. I would like to extend my sincerest thanks and appreciation to the following:

- A special thanks to all my supervisors: Nigel Tapper, Andrew Coutts, Jason Beringer, and Matthias Demuzere. You all contributed to this project in different but invaluable ways. Many thanks to you all for the support, guidance, and humour throughout! I look forward to the prospect of working with you all in the near future.

- To all those legends who assisted during the Mawson Lakes field campaign: Andrew Coutts, Darren Hocking, Emma White, Naim Daliri-Milani, Stephen Livesley, Margaret Loughnan, Nigel Tapper, and Jason Beringer. In particular, I am highly indebted to Andrew Coutts for all his work in planning and organizing this campaign.

- Many thanks to Tony Wong and the CRC for Water Sensitive Cities for financial support and providing me with many other unique opportunities throughout my candidature.

- I'd like to thank Valéry Masson and others at Meteo-France who assisted greatly with the SURFEX modelling component.

- I'm grateful to Peter Isaac for assistance with footprint modelling.

- Also, a huge thank you to Jas Thom for helping with SOLWEIG in the middle of her busy honours year!

- Huade Guan at Flinders University provided assistance with sky view factor calculations.

- To my fellow office buddies — Caitlin, Fimi, Lam, and Tess. Thank you for putting up with me and sweary rants, and for helping with those endless pesky problems and coding issues. It's been a pleasure sharing an office with you all. See you around!

- Thanks to the Gracie Street crew for all your PhD distractions and general loveliness.

- And of course, to my loving Fam, thank you to each and everyone of you for supporting me through 9+ years of study. You guys are amazing and I love you ALL dearly! I'll get a job eventually, I promise :) x.

Contents

7　High resolution modelling of air temperature and HTC in Mawson Lakes:
the effect of irrigation on urban microclimate during extreme heat　167

8　Research outcomes, implications, and conclusions.　204

List of Figures

xxi

List of Tables

List of acronyms and nomenclature

- β = Bowen ratio

- **AWS** = automatic weather station

- **CFD** = computational fluid dynamics

- **EHE** = extreme heat event

- **ET** = evapotranspiration

- **HTC** = human thermal comfort

- **ISBA** = Interaction Soil-Biosphere-Atmosphere

- $K\downarrow$ = incoming shortwave radiation

- $K\uparrow$ = outgoing shortwave radiation

- $L\downarrow$ = incoming longwave radiation

- $L\uparrow$ = outgoing longwave radiation

- **LAI** = leaf area index

- **LCZ** = local climate zone

- **LSM** = land surface model

- **LST** = land surface temperature

- **LUMPS** = Local-scale Urban Meteorological Parameterization Scheme

- **MRT** = mean radiation temperature

- **NDVI** = normalised difference vegetation index

- **PCI** = park cool island

- **PET** = physiological equivalent temperature

- Q^* = net radiation

- Q_E = latent heat flux

- Q_F = anthropogenic heat flux

- Q_H = sensible heat flux

- Q_M = metabolic heat flux

- **RH** = relative humidity

- **RSL** = roughness sub-layer

- **SBL** = stable boundary layer

- **SDML** = Sir Douglas Mawson Lake

- **SOLWEIG** = Solar and Long Wave Environmental Irradiance Geometry model

- **SUEWS** = Surface Urban Energy and Water Balance Scheme

- **SURFEX** = SURFace EXternalisée (French)

- **SVF** = sky view factor

- **TEB** = Town Energy Balance model

- **UBL** = urban boundary layer

- **UCL** = urban canopy layer

- **UCM** = urban canopy model

- **UHI** = urban heat island

- **UTCI** = universal thermal climate index

- **WRF** = Weather and Research Forecasting model

- **WSUD** = water sensitive urban design

1   Introduction

1.1   Problem statement

Due to climate change and a global trend towards urbanisation, the cities of the 21st century are facing an increasing number of sustainability problems. It is well known that Earth's climate system is going through a period of warming due to increased anthropogenic greenhouse gas emissions. This unprecedented warming of global climate has accelerated further in last three decades with each 10 year period being successively warmer than any preceding decade since 1850 (see Figure 1.1). This warming includes an increase in the frequency and intensity of extreme heat events (EHE), which is considered a major threat to the health and well-being of human populations (Costello et al., 2009). Extreme events, also known as heatwaves, are expected to occur more frequently and become more severe over most land areas during the 21st century (IPCC, 2014). An unprecedented event in Western Europe in 2003 caused 50,000 to 70,000 excess deaths over a three month period (Brücker, 2005; Robine et al., 2008), and at least 15,000 of those deaths occurred in France in a three week period (Fouillet et al., 2006). Given the global trend towards an increase in heatwaves, heat exposure stands to cause additional heat-related illness, and without mitigation the potential health burden from heat exposure could become a significant public health problem.

In Australia similar climate change trends have been observed. The average temperatures have been increasing with a mean rise in surface air temperature of 0.9 °C since 1910. The last two years: 2013 and 2014 were the 1st and 3rd hottest years on record in Australia (BOM, 2014). The extremes are changing in Australia too; heatwave frequency and intensity are also increasing across many parts of Australia, particularly in the south-east (BOM, 2014). A number of recent heatwaves in Australia have exemplified this trend, including a severe heatwave in 2009
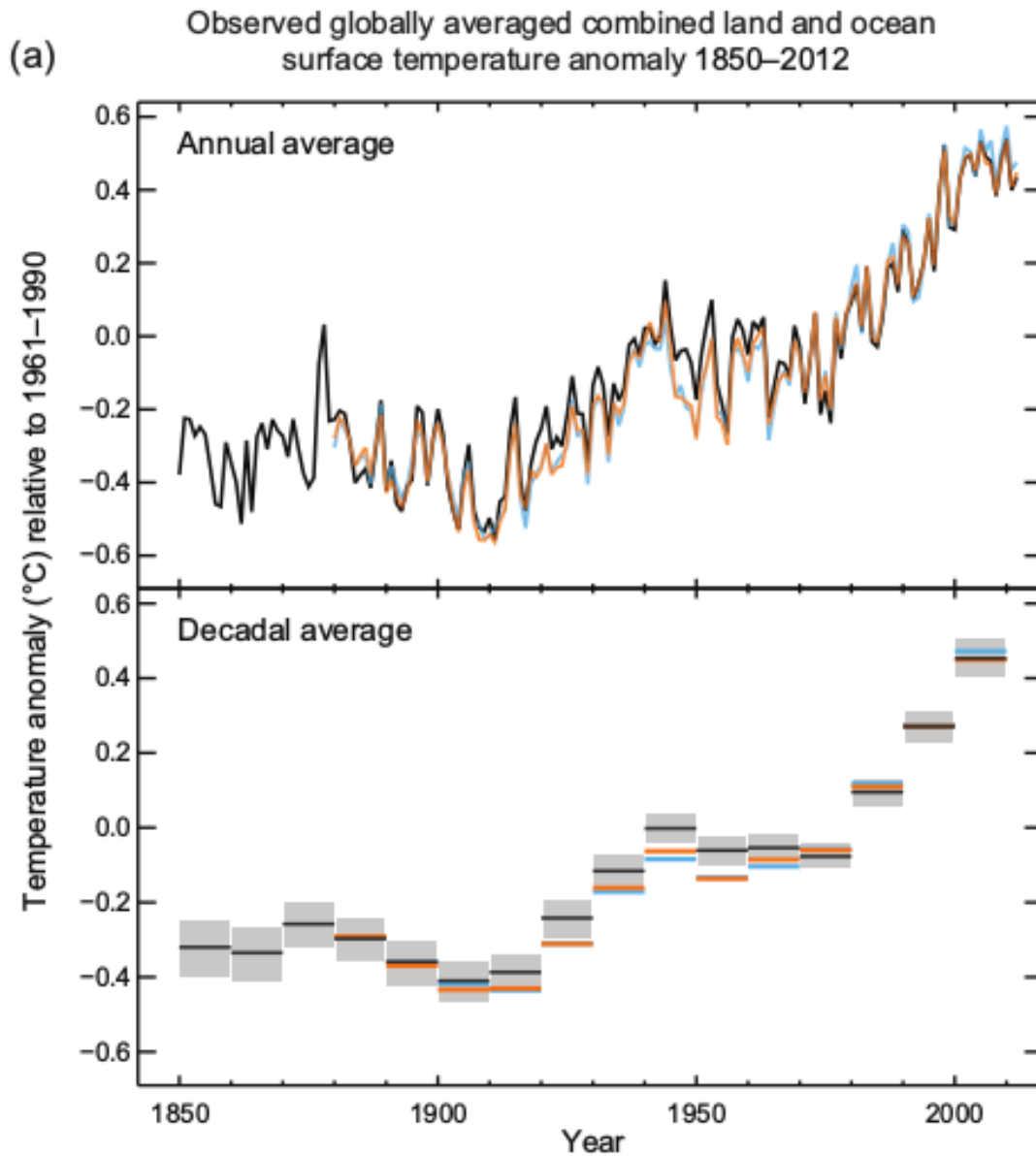
Figure 1.1: The observed global mean combined land and ocean surface temperature anomalies, from 1850 to 2012 from three data sets. Top panel: annual mean values, bottom panel: decadal mean values including the estimate of uncertainty for one dataset (black). Anomalies are relative to the mean of 1961–1990. The increasing average global temperatures also include a trend towards more extreme events. These events stand to increase the health burden associated with human exposure to heat. Source: IPCC (2014).

that affected Australia's south-east over a period of 16 days. At its peak the heatwave caused

temperatures of over 45 °C, which resulted in 374 excess deaths from heat stress in Victoria

(VicGov, 2009). There is no evidence that the warming trend in Australia will halt any time in

the near future. Global climate modelling suggests that the future climate in Australia will be characterised by an increase in warm nights, longer dry spells (Alexander & Arblaster, 2009), and more frequent occurrence of EHE with increased intensity, duration, and extent (CSIRO, 2007). Without some form of mitigation the adverse effects of extreme heat on human health will increase in Australia during the 21st century as climate change progresses and warming continues.

From an epidemiological perspective, the need for mitigation is well recognised. It is well established that in the mid-latitudes, human mortality and morbidity rates increase during EHE (Auliciems & Skinner, 1989; Nicholls et al., 2008; Loughnan et al., 2010a,b). Heatwaves are known to cause a marked short-term increase in mortality and/or morbidity of exposed populations. Analyses of public health records have shown that heat related deaths typically occur quickly, on the same day or within one to four days of exposure (Hajat et al., 2002; Michelozzi et al., 2005), and occur most frequently among the elderly (DIppoliti et al., 2008; Johnson et al., 2005; Pirard et al., 2005). In Australia, researchers have be able to show that there are statistically significant air temperature thresholds at which regional or municipal mortality and/or morbidity rates will increase (heat health thresholds) (Loughnan et al., 2013). Heatwaves are a significant environmental hazard, and have caused more deaths in Australia in the last 200 years than any other natural hazard except disease (Coates, 1996). It can be said that a clear association between extreme environmental heat and mortality has been established through analysis of available public health data (Loughnan et al., 2013).

In addition to the increased intensity and frequency of damaging EHE, the distribution and rate of rainfall is changing in Australia. Broadly, the south of Australia has been experiencing a significant decline in Southern wet season (April – November) winter rainfall (BOM, 2014). This decline is a major problem as traditional water supplies have been stretched, and soil water content in urban areas has dropped. This drop in urban water availability can potentially lead

to further exacerbation of extreme heat in urban areas. A recent prolonged drought (1997–2009) caused major water shortages in Australia's southern cities such as Melbourne, Adelaide, and Perth. The drought saw storage levels in many reservoirs drop to very low levels, and placed pressure on city water resources, leading to water restrictions and irrigation bans. Residents have become diligent at conserving water in response to water restrictions, but existing urban vegetation struggled with reduced water availability during the drought (Coutts et al., 2012). Many residents have adapted gardening approaches to cope with less potable water supplies by planting drought-tolerant species, and new developments are more commonly designed with xeric style landscaping and rock gardens (Coutts et al., 2012). These compounding consequences of drought such as water restrictions, xeric gardening practices, and reduced health of urban vegetation, have the potential to directly contribute to additional warming in urban areas. The additional warming occurs because urban areas have their own distinct climates, which even outside of times of drought, are typically warmer than rural areas. The responses to drought, such as water restrictions, may exacerbate this urban warming process, and in the context of climate change this additional urban warming effect is of particular concern.

Extreme temperatures have been shown to be particularly damaging to the elderly (DIppoliti et al., 2008; Johnson et al., 2005; Pirard et al., 2005). The vulnerability of elderly people is particularly concerning in countries like Australia that have a growing ageing population. The Australian Government's 2015 Intergenerational report claims that the proportion of Australians aged 85 and over will grow from $< 1\%$ of the population in 1974-75, to 4.9% of the total population by 2054-55. It is projected that there will be 40,000 people aged over 100 in Australia by 2054-55. The growing ageing population in Australia, alongside climate change and more EHE, will mean that a greater proportion of vulnerable people are susceptible to bad heat health outcomes. This could represent a significant health cost for society as a whole. The need to mitigate heat and protect vulnerable people, such as the elderly, is essential for maintaining good public health and

well-being in Australia.

The climate of any environment is directly related to the characteristics of the land surface. Broadly speaking, in urban areas the land surface tends to be drier, retains more heat, and becomes warmer than rural areas (Figure 1.2). This means that human exposure to heat in cities is impacted by both climate related factors (e.g. increase EHE) and urban factors (e.g. urban design) (Figure 1.3). The concurrent influences of climate change and increased urban warmth means that urban dwellers are potentially further exposed to heat stress and heat related mortality and morbidity. The tendency for urban areas to become warmer than their surrounding rural environments is a well established phenomenon (Arnfield, 1990). The process of urbanisation modifies the natural energy and water balances that occur at the earth-atmosphere interface causing an increase in urban temperature (Figure 1.2). A range of characteristics in urban areas cause this warming, including the high thermal admittance of urban materials, three-dimensional (3D) geometry of urban surfaces, anthropogenic heat, and widespread impervious surfaces (Oke, 1982). Impervious surfaces are designed to facilitate rapid removal of rainwater away from urban areas, and this removal of water exacerbates the heating and drying of urban climate. The warmth created by urban environments can exacerbate EHE, and heat related morbidity and mortality have been shown to be higher in urban environments during heatwaves (Henschel et al., 1969; Buechley et al., 1972; Jones et al., 1982; Conti et al., 2005; Tan et al., 2010). This means that the combined effects of urban warming driven by urban development, low water availability, and future climate change (including more EHE), could create particularly unfavourable conditions for maintaining good human health and well-being in cities (Figure 1.3).

The human health vulnerability of city dwellers is even more relevant in the 21st century, as Earth's growing population has become increasingly urbanised. Global urban population has increased from 220 million to 2.8 billion people during the 20th century. By 2008 more than half the global population (3.3 billion people) were living in urban areas (UNFPA, 2007). The
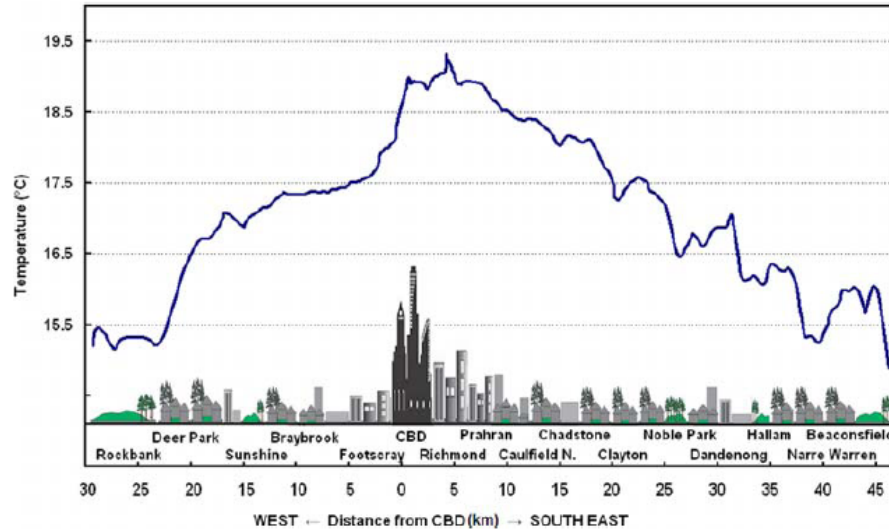
Figure 1.2: Spatial variability of the Melbourne urban heat island at 1 am, 23 March 2006. The characteristics of urban areas cause air temperature to be warmer in cities. This urban warming effect means that urban dwellers are particular vulnerable to being exposed to extreme temperatures during a heatwave. Source: Coutts et al. (2010).
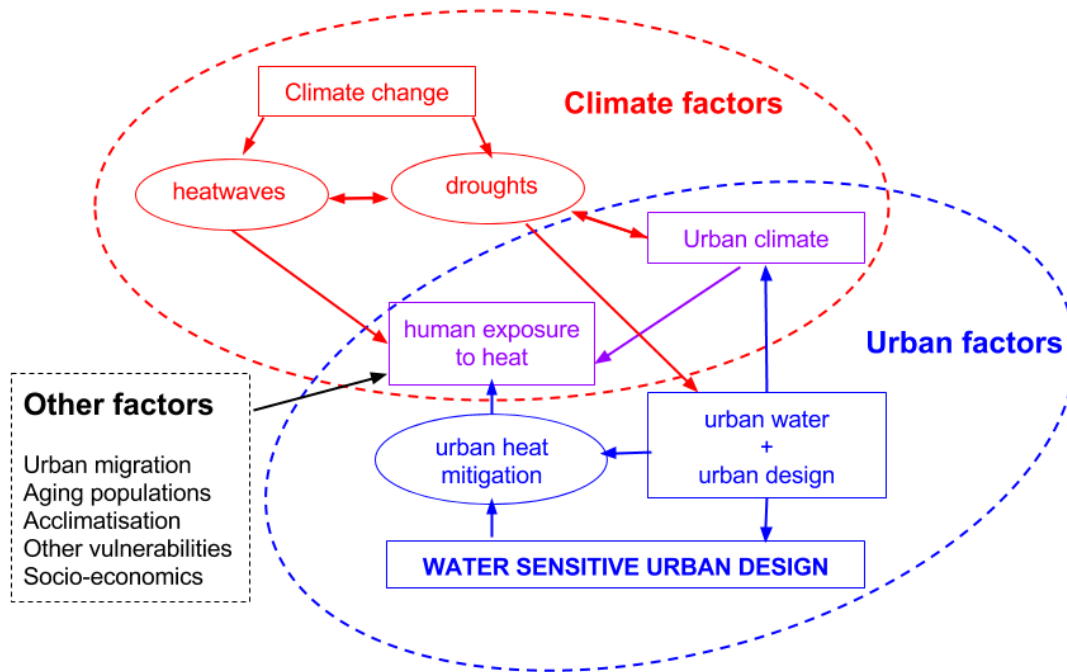
Figure 1.3: An overview of the problem statement of this research. Human exposure to heat is affected by climate and urban factors — these factors interact and may culminate in the 21st century to leave urban dwellers highly exposed to damaging urban climates.

urban population is expected to increase further during the 21st century, and will reach 6.4 billion people (69% of the global population) (UNFPA, 2007) by 2050 (PRB, 2011). Australia's

populace is already consolidated in urban areas with 87% of the population classified as urban (TWB, 2011). Urban migration will drive ongoing and unprecedented city development and densification during the 21st century. These future cities need to be designed in such a way that mitigates urban warmth. Without mitigation, the growth of cities in Australia will likely exacerbate urban warmth and leave an increasingly large number of humans exposed to adverse and uncomfortable climates.

Degraded urban climate and exposure to EHE is an increasingly likely prospect for cities in Australia, many of which are growing rapidly. It is well known that human health and well-being can be negatively affected by exposure to heat. However, as shown in Figure 1.3, the amount of exposure to extreme heat is influenced by a number of interacting processes. These processes may culminate during the 21st century, potentially leaving many urban dwellers regularly exposed to damaging heat stress and thermal discomfort. As such, the need to mitigate urban warmth, provide human thermal comfort (HTC), and minimise exposure to extreme heat, are important tasks for ensuring the good health and well-being of Australia's ever growing urban populace.

1.2 Heat mitigation in cities

The growth of cities and the changing global climate, heighten the risk of exposure to damaging extreme heat. There is a pressing need to mitigate urban warmth and reduce exposure to heat in Australian cities. There are a range of methods that can be used to mitigate urban warmth, including reflective white surfaces (Taha et al., 1999; Kikegawa et al., 2006; Ihara et al., 2008; Zhou & Shepherd, 2010), urban density changes (Gober et al., 2010), ventilation measures (Alcoforado et al., 2009), increased urban vegetation (Bowler et al., 2010), and reduced anthropogenic heat (Kikegawa et al., 2006; Ihara et al., 2008). Increasing vegetation in cities, or so called "urban greening", is probably the mostly commonly cited measure, and vegetation has been shown to be an effective way to reduce urban temperatures (see Bowler et al. (2010) and references

therein). Broadly speaking, vegetation provides cooling by increasing evapotranspiration (ET) and providing more shade in urban areas. From a climate perspective, the magnitude of ET is very important as it affects the partitioning of available energy at the surface, and hence, the amount of atmospheric heating at the surface. There is a relationship between the amount of ET and the strength of urban warming. This linkage between water and air temperature means that water availability directly influences urban temperatures. The focus of most urban greening studies has been the cooling effect of increased vegetation, but few urban warmth mitigation studies have considered in detail the potential for modulating urban warmth through direct modifications of the urban water cycle.

Generally speaking, urban areas are unnaturally dry, as stormwater[1] drainage systems are designed to export rainwater rapidly away from the city. One way to reduce heat in cities, could be to retain more water within the urban environment by reducing this runoff. The removal of rainwater leads to a drying of urban surfaces and soils, which reduces the amount of ET of water to the atmosphere. In Australia the effects of prolonged drought mean that the presence of water in cities is further diminished. Urban ET is generally lower than rural areas, due to the removal of rainwater, but during drought ET rates can drop further still. The linkage between water and climate means that the way water is managed in cities can directly influence urban temperatures. Modifications of the urban water cycle, for example garden irrigation, directly influence urban climate, but have not received a lot of attention in the urban cooling literature. If more water is retained in the urban environment, urban temperatures will potentially be cooler. One approach that could mitigate heat through retention of more water in the urban environment is called Water Sensitive Urban Design (WSUD).

---

[1]In this thesis stormwater is defined as runoff that is generated when precipitation from rain events flows over land or impervious surfaces and does not percolate into the ground.

1.3   Water Sensitive Urban Design

WSUD is an integrated urban water management approach that seeks to reduce urban runoff and retain water in the urban environment (Figure 1.4). WSUD refers to a "holistic" urban water management approach involving a number of technologies for retaining, treating, and reusing stormwater. The three main objectives of WSUD are (CWSC, 2010):

(1) To treat stormwater (through removal of pollutants) to improve the quality of stormwater discharging into streams.

(2) To change the path, and the reduce the rate, at which stormwater travels to streams and aim to restore the pre-urban water cycle.

(3) To capture water in order to reduce demand on potable water supplies imported from outside of the urban area.

The retention, treatment, and diversion of water in the urban environment is done through a host of technologies including: bio-filtration systems, wetlands, rainwater tanks, rain gardens, and stormwater harvesting. These technologies have proven positive benefits for a range of hydrological problems including flood mitigation, water preservation (Burns et al., 2012), and improved downstream ecology (Walsh et al., 2005) (summarised in Figure 1.4). In addition to these hydrological benefits, the retention of water in the urban environment through WSUD can potentially lead to increased urban ET, cooler urban temperatures, and improved HTC in cities (Figure 1.5). The questions surrounding water retention in cities and the interaction with urban climate are particularly important for many cities in Australia where traditionally a large proportion of urban domestic water use (e.g. 25.4% Melbourne) comes from garden irrigation (Roberts, 2005). Potable water is imported into cities, and is used in part, to balance out the water lost as stormwater runoff. This process of importing water is energy intensive

Natural	Urbanised	Harvesting & WSUD

	Natural	Urbanised	Harvesting & WSUD
Stream channel form and biodiversity			
Groundwater recharge	High	Low	Moderate
Evapotranspiration	High	Low	Moderate
Atmospheric heating and heat storage in buildings	Natural	Hotter	Closer to natural
Human thermal comfort	Neutral	Hot	Slightly warm
Surface runoff	Low and infrequent	High and frequent	Infrequent and moderate
Stream hydrology	Natural	'Peaky'	Moderated (both high flows and low flows)
Riparian vegetation	Intact	Degraded	Restored
Channel form	Natural	Severely degraded	Uncertain (may need intervention)

Figure 1.4: A synthesis of urban impacts on the landscape, atmosphere, and hydrology and the benefits of stormwater harvesting and WSUD. Source: Wong et al. (2013).

and wasteful as the stormwater runoff resource is not efficiently utilised. Water scarcity in Australia, is a major factor that has caused some local governments and water authorities to seek alternative urban water management approaches (such as WSUD), which secure a more reliable water supply for growing cities (Mitchell et al., 2008). WSUD technologies could be used to retain and/or re-integrate stormwater in the urban environment, thereby promoting ET, and providing valuable urban cooling (Figure 1.4). WSUD could promote localised cooling at the micro- to local-scales (Figure 1.5), while simultaneously preserving valuable potable water, and providing other sustainability benefits. Therefore, WSUD and stormwater harvesting could be an effective way of cooling the urban environment even during times of drought when traditional

(potable) water supplies are limited.
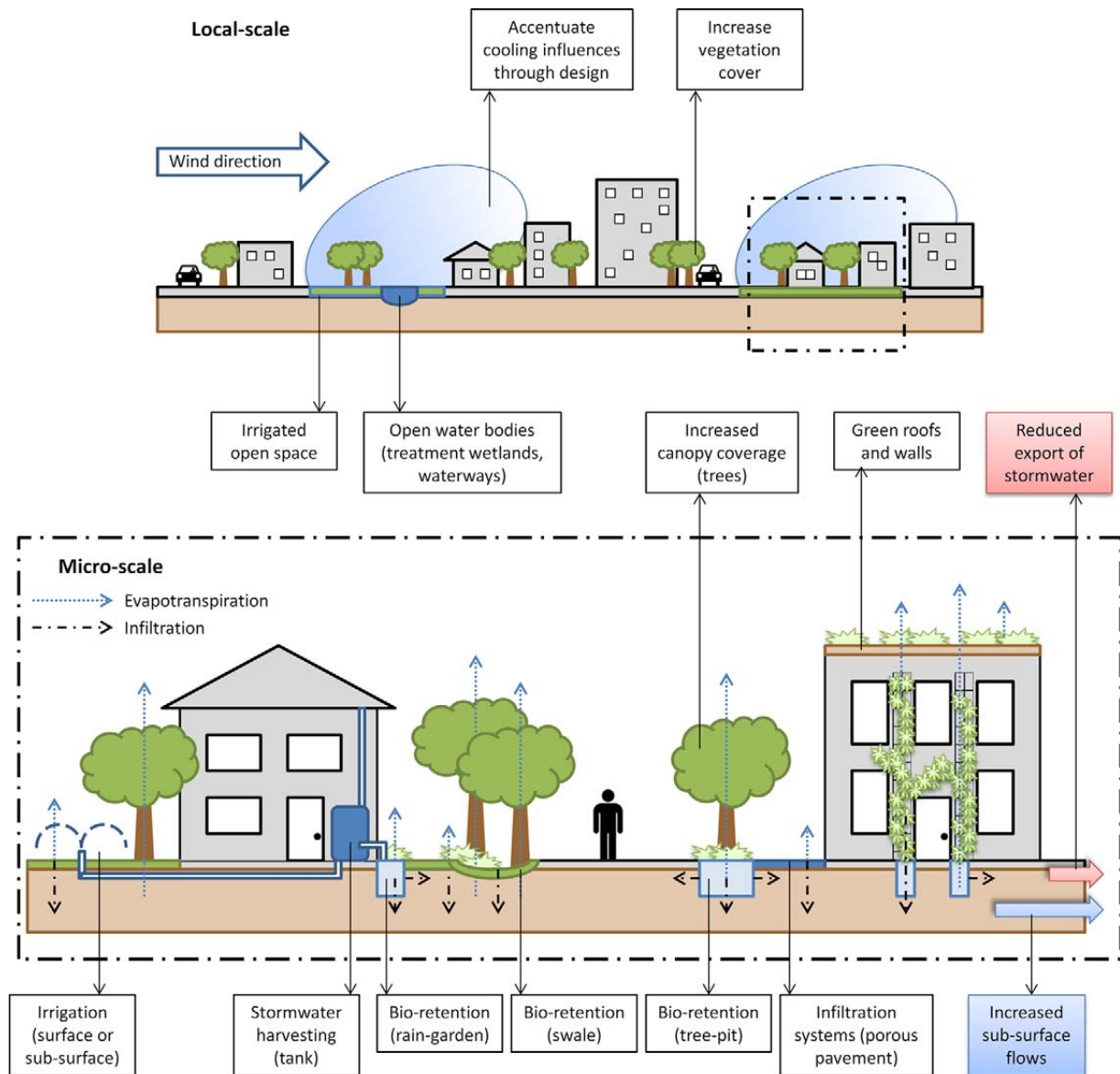
Figure 1.5: A schematic representation of widespread implementation of stormwater harvesting and WSUD, including a more natural water cycle (reduced runoff) and increased vegetation cover. WUSD could enhance urban ET and shading, which should result in local-scale cooling effects that can reduce urban air temperatures and makes cities more thermally comfortable. Source: Coutts et al. (2012).

WSUD and stormwater harvesting leads to the retention of more water in urban soils, provides extra water for outdoor water-use practices, and supports healthy vegetation (Figure 1.4). Due to the non-climatological benefits of WSUD, such as potable water preservation, some water sensitive technologies have begun to be implemented in Australia. However, the potential cooling

effects of WSUD and stormwater reintegration has received very little attention in the urban warmth mitigation literature. The research described in this thesis includes an investigation of one WSUD prototype suburb, in Adelaide South Australia, where water sensitive technologies have already been implemented. Though the WSUD in Mawson Lakes is targeted towards addressing the three main objectives of WSUD (described above), there is also a clear need for heat mitigation in Australian cities. WSUD has begun to gain traction as a sustainable urban water management approach, but very little has been done to investigate its possible cooling benefits (as in Figure 1.5). This research seeks to understand and **quantify the potential for WSUD and stormwater reintegration techniques to mitigate urban warmth and improve HTC, during extreme heat events**. As such, the focus of this research is the cooling potential of WUSD during hot to warm summertime conditions.

1.4 Research objectives

The overarching aim of this research is to understand and quantify the cooling effects of WSUD on urban microclimate. For urban microclimate this research considers both urban air temperature and HTC separately as these are both important metrics for human health and well-being. To achieve the overarching aim of this research four research objectives have been defined. These objectives were identified through a review of the relevant literature (chapter 2). However, for clarity they are outlined below:

Objective 1: Identify the observed microscale air temperature and HTC variability in a WSUD suburb.

This objective will be addressed through an analysis of observational data from a large field campaign conducted in Mawson Lakes, Adelaide. Mawson Lakes is a mixed residential suburb with a number of WSUD features in place (see chapter 3 for a full description of the field campaign). The suburb has been developed with a dual reticulated water supply system, which delivers

potable water and harvested stormwater to homes via separate piping systems. The suburb also contains a range of WSUD features including man-made lakes and bio-filtration wetlands. Mawson Lakes is an example of a WSUD suburb, and provides an excellent case study to investigate the effects of WSUD and stormwater reintegration on air temperature and HTC.

Objective 2: Generate robust estimates for the cooling potential of WSUD features on microscale air temperature.

The data from the Mawson Lakes field campaign are also used to address this objective. This objective is met through a statistical analysis (multiple linear regression) of land surface characteristics and other factors that influence observed microscale air temperature variability.

Objective 3: Calculate the potential for irrigation to reduce exposure to adverse extreme heat conditions (air temperature).

This research focuses particularly on irrigation as a potential cooling measure, because it could provide more flexibility than other heat mitigation measures. Irrigation allows water to be distributed to the locations where cooling is most needed, at the time of greatest need. To examine the cooling potential of irrigation a numerical modelling approach utilising the SURFEX (SURFace EXternalisée in French) model (Masson et al., 2013) will be employed. The SURFEX model is used to calculate the effect of a range of irrigation scenarios on air temperature during an extreme heat event.

Objective 4: Calculate the effect of irrigation on microscale HTC under extreme heat.

To address this goal the SURFEX scheme is used in conjunction with the solar and longwave environmental irradiance geometry model (SOLWEIG) (Lindberg et al., 2008), to calculate any changes in HTC with different irrigation scenarios, during an extreme heat case study.

The overarching aim of this research is to understand and quantify the cooling effects of

WSUD on urban microclimate. An investigation of the cooling effects of WSUD is justified; it has been shown in this introduction chapter there are a range of factors that influence human exposure to extreme heat. The exposure of urban dwellers is influenced by interacting process including: climate change, increased EHE, drought, urbanisation, and the urban warmth (Figure 1.3). The growth of cities and urban populations alongside an increase in the frequency of EHE and drought may leave many urban dwellers regularly exposed to damaging heat stress and thermal discomfort. It's clear that there is a growing need to mitigate urban warmth, provide thermal comfort, and minimise exposure to extreme heat in Australia. The fact that urban design and water management influence urban climate is both a problem and opportunity. The implementation of clever design measures that mitigate warmth in cities can help to reduce exposure to extreme heat. WSUD is a holistic urban water management approach that is already being used in Australia for a range of sustainability benefits. It is thought that WSUD can provide significant cooling benefits for urban micro- and local-scale climates. This research investigates the cooling potential of WSUD, including both HTC and exposure to extreme air temperature. The research approach will utilise both observational and numerical modelling methods to achieve the research objectives.

2 Literature review

2.1 Introduction

The combined effects of an increase in the frequency, duration and severity of EHE, restricted water availability, urbanisation, and urban warmth mean that those living in cities are at a growing risk of exposure to extreme heat and thermal discomfort. Broadly speaking, this potential exposure necessitates heat mitigation in urban environments. WSUD is a mitigation approach that aims to reduce urban runoff and increase urban ET through a range of technologies and stormwater harvesting techniques. The overarching aim of this research is to understand and quantify the cooling effects of WSUD on urban microclimate. Heat mitigation is a very broad concept, and mitigation can be achieved by manipulating the energy balance and water balance in a variety of ways. This chapter provides a detailed review of relevant literature to demonstrate the importance and relevance of the research objectives (outlined in Section 1.4). The literature review will demonstrate that, while WSUD has received minimal attention in the urban climate research space, there is a lot of theoretical potential for WSUD and stormwater harvesting to provide cooling effects. Additionally, the literature review will show that minimal attention has been given to the effect of outdoor water-use practices and irrigation in the urban heat mitigation literature. The research objectives of this thesis will directly address these knowledge gaps.

To help set the context for this research, the literature review provides some important background information, including the definition of HTC and related indices, and a detailed description of the urban energy and water balances. Furthermore, the concept of scale is critical for any discussion of heat mitigation and HTC; in particular, the microscale is important for this research. The literature review provides a clear definition and discusses the significance of microscale climate. Given that this research is interested in the cooling effects of WSUD on

microscale climate, it is necessary to synthesise the relevant literature for this topic. Previous research has been undertaken through both observational and modelling studies, and this literature is discussed in Sections 2.3 and 2.4, respectively. The focus of the literature synthesis is observational and modelling research that has looked at the microscale cooling influence of features that are relevant for WSUD, such as water bodies, vegetation, and irrigation. The research summarised in this chapter will demonstrate the relevance of the research objectives outlined in chapter 1.

2.2 Definitions

2.2.1 Water and energy balance

In any environment the balances of water and energy at the surface are fundamental factors that determine the manifestation of boundary layer meteorology and surface climate characteristics (Oke, 1987). In urban environments, the water and energy balances can become highly modified from their natural states. These modifications are the cause of key environmental problems including urban warmth and excess stormwater runoff. The modification to the water and energy balances directly lead to a general warming and drying of the surface climate in urban areas. The state of the urban water cycle is important because the urban energy balance and the urban water balance are intimately linked. An in depth understanding of the urban water and energy balances is essential for effective urban warmth mitigation, and both balances are formally defined below. The water and energy balance apply to a hypothetical volume which extends from a depth in the substrate below which water and energy exchanges are negligible, to a level roughly equal to roof level (Oke, 1988b) (Figure 2.1). For urban areas the water balance is defined as (mm hr^{-1}) (Grimmond & Oke, 1991):

$$P + I + F = E + r + \Delta S + \Delta A \tag{1}$$
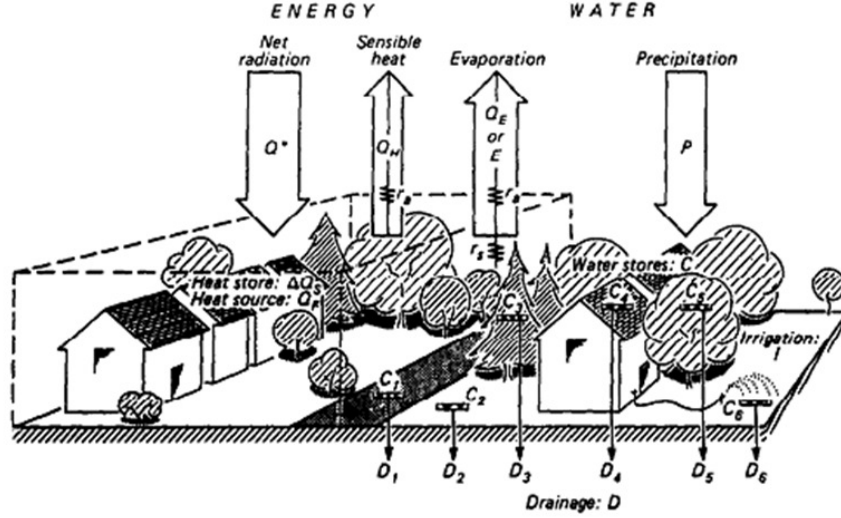
Figure 2.1: A schematic of the conceptual framework of urban energy and water balances. Energy and water fluxes occur within a volume that extends from a depth in the substrate below which water and energy exchanges are negligible to a level roughly equal to roof level. The urban and water energy balance are linked through the evapotranspiration term. This linkage means that modifications to the urban water balances can directly modify the urban energy balance and urban climate. Source: Grimmond & Oke (1991).

the sources of water are precipitation (P), the piped water supply (I), and water released due to anthropogenic activities (F). Sinks of water are evapotranspiration (ET), runoff (r), the change in water storage for the period of interest (ΔS), and net moisture advection (ΔA). In urban environments, runoff is a large sink of water because the drainage infrastructure is generally designed to rapidly export stormwater away from the urban environment (see urban water balance in Figure 2.2). Stormwater drains are designed to drain rain and excess runoff from paved areas, parking lots, footpaths, and roofs. This runoff is diverted into the stormwater network of gutters and underground pipes before being discharged into receiving waterways such rivers, lakes, or the ocean. In urban areas a large volume of potable water is imported, from outside the catchment, directly into the urban water cycle. Some of this imported potable water is added to the urban environment through irrigation processes. Thus, one important characteristic of the urban water cycle is that large volumes of water are imported into the system (Figure 2.3).

17
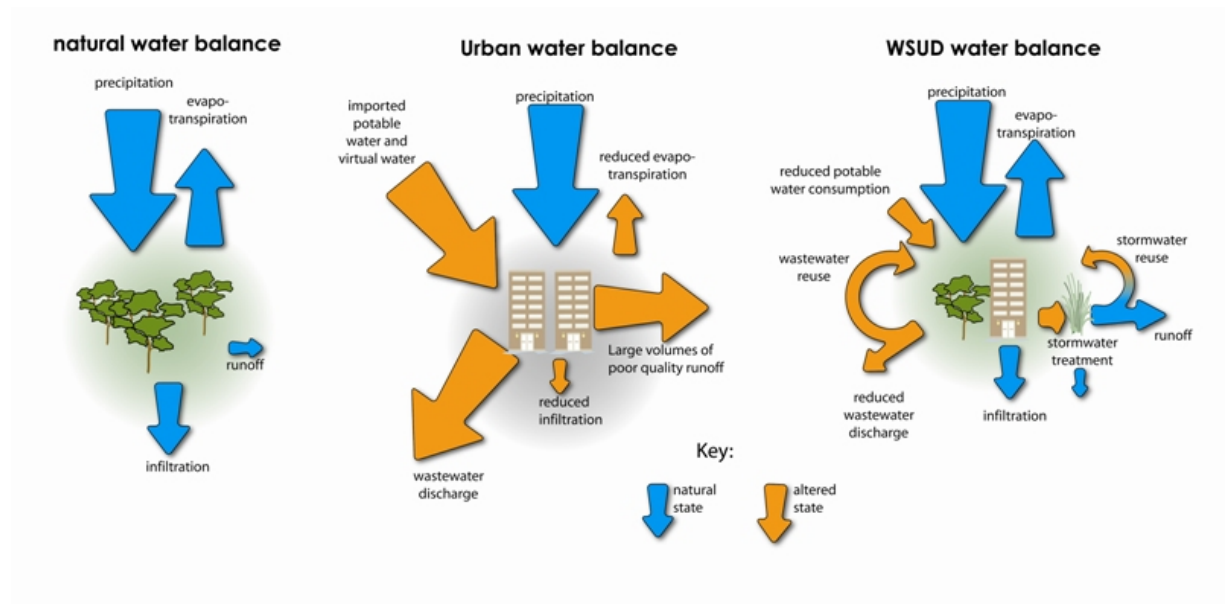
Figure 2.2: A schematic of theoretical natural, urban, and WSUD water balances. The size of the arrow represents the magnitude of the flux. In urban areas the volume of runoff is much larger than in natural areas. This results in a reduced volume of ET from urbanised areas, which influences the urban energy balance through Q_E. WSUD attempts to restore a more natural water balance in urban areas by capturing, re-integrating, and reusing stormwater runoff. This stormwater reuse also reduces the need for imported potable water. Source: Wong & Hoban (2006).

In Australia, this imported potable water (I) generally comes from large inland reservoirs where water is stored. This imported water is a significant addition of water to the water cycle that does not happen in natural areas (Figure 2.2). In some Australian cases, the volume of water imported through the reticulated water supply, is larger than the volume that is lost as runoff (Coombes, 2008) (Figure 2.3). This means that, in conventional urban areas, stormwater runoff is a significant water resource that remains largely unused. In the context of water scarcity in Australia, it is prudent to utilise this valuable water resource. Captured runoff water can be used in many ways in urban areas, such as non-potable domestic uses, including clothes washing, garden irrigation, and toilet flushing. Water scarcity alone justifies alternative water management approaches that minimise runoff and utilise the stormwater resource.

There are also a range of other sustainability benefits that emerge from reducing urban runoff through WUSD. The high volumes of water that are exported via runoff from urban areas have damaging implications for the ecology of receiving waterways and streams (Walsh et al.,
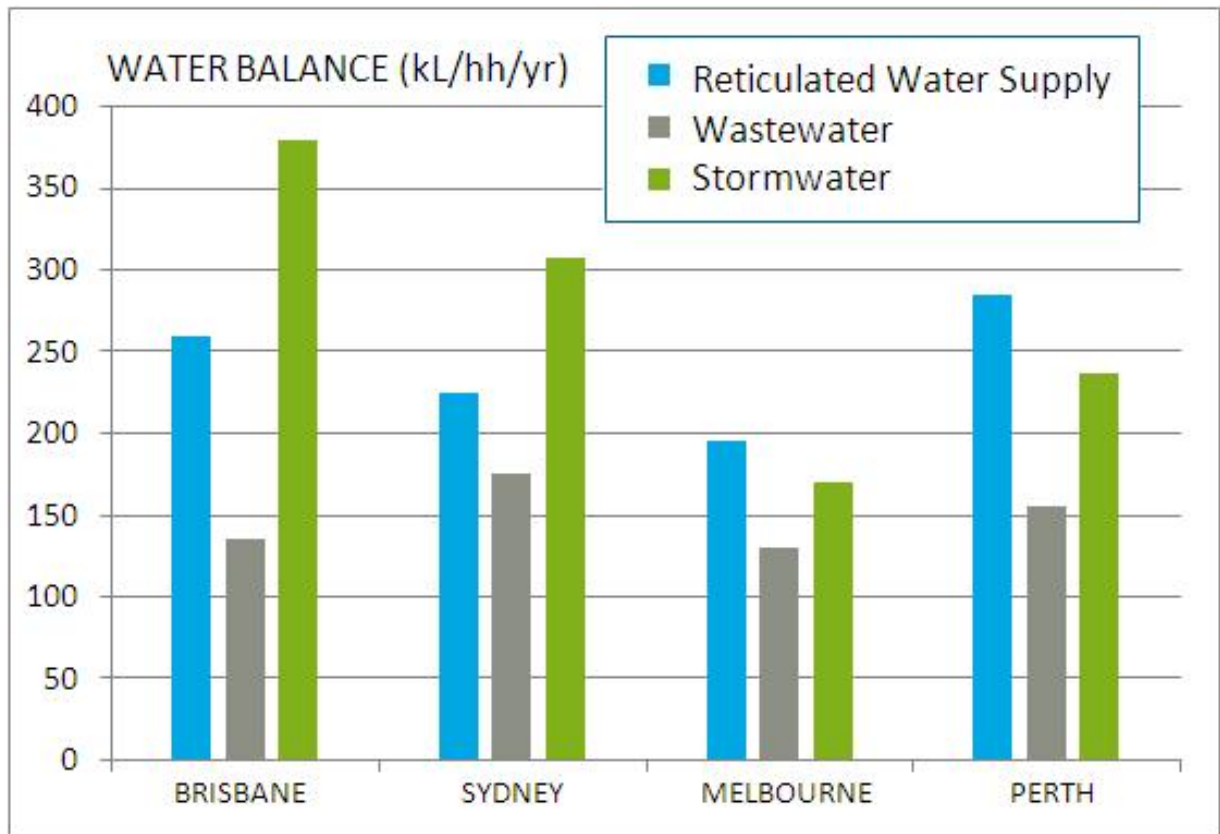
Figure 2.3: The volume of urban water-use and discharge in Australian cities. The volume of water that is lost from the urban water cycle through stormwater runoff is very large in Australian cities. This volume is as large (or larger) than the volume of high quality potable water that is imported through the reticulated water supply. Stormwater runoff should be utilised to reduce demand on imported potable water. Source: Water for Liveability Centre, Monash University — modified after Coombes (2008).

2005). Reducing the volume of water that is discharged into receiving waters is also beneficial for the ecological health of these waterways. The streamflow in urban waterways is typically characterised by very low levels of baseflow, and very high peaks in flow after a rainfall event (Walsh et al., 2005). Heavy rainfall flows rapidly into streams carrying pollutants and sediments from impervious surfaces, increasing the concentrations of pollutants, nutrients and suspended solids (Walsh et al., 2005). This "peaky" flow regime and the pollutant loads that occur in urban streams have been shown to reduce water-quality, algal biomass, and several measures of diatom and macroinvertebrate assemblage composition (Walsh et al., 2005). Furthermore, these peaks in urban flow can increase the susceptibility of the stream to flooding during rainfall events. As such, reducing runoff from WSUD can improve the stream ecology and health of receiving waters and potentially reduces flooding events.

WSUD aims to reduce the runoff (r) term in the urban water budget, by increasing infiltration, ET, and stormwater capture (see WSUD water balance in Figure 2.2). The promotion of ET has positive implications, in this case for urban climate. When urban ET increases this potentially causes a broad cooling of urban climate, because the urban energy balance, which drives urban surface climate, is directly linked to the urban water balance through the ET term. It is this linkage that forms a large part of the basis for the hypothesised cooling potential of WUSD, and this means that an understanding of the energy balance is important for this research. The urban energy balance is defined as (Wm^{-2}) (Grimmond & Oke, 1991):

$$Q^* + Q_F = Q_E + Q_H + \Delta Q_S + \Delta Q_A \tag{2}$$

where values on the left side of Equation (2) are inputs to the system, and positive values on the right are outputs. Q^* is net radiation, Q_F is anthropogenic heat, ΔQ_S is the storage flux, and ΔQ_A is the net advected flux. Q^* is given by:

$$Q^* = (K \downarrow - K \uparrow) + (L \downarrow - L \uparrow) \tag{3}$$

where $K \uparrow$ and $K \downarrow$ are outgoing and incoming shortwave radiation, and $L \downarrow$ and $L \uparrow$ are incoming and outgoing longwave radiation. ΔQ_S is representative of all the energy storage mechanisms within the volume, including all energy that is conducted into the substrate and other surfaces (e.g. buildings) and ΔQ_A is the net advection through the sides of the volume. Urban surfaces modify these fluxes, which causes urban areas to be generally warmer than their rural surroundings. The turbulent fluxes (Q_E and Q_H) determine atmospheric heating; Q_H is the energy used to heat the atmosphere within the volume and Q_E is the energy transferred during a change in state from liquid water to vapour ($Q_E = L_V ET$ where L_V is the latent heat of vaporisation). Broadly, there are four key characteristics of urban environments that can modify the urban energy balance resulting in warmer urban climates (Oke, 1987):

(1) high thermal admittance of urban surfaces can cause increased ΔQ_S during the day, which can cause higher Q_H at night when this stored heat becomes a heat source;

(2) 3D canyon geometry, can increase Q^* , as more $K \downarrow$ is absorbed during the day, and less $L \uparrow$ is lost at night;

(3) Q_F provides additional energy at the surface from sources such as vehicles, buildings and human metabolism, and;

(4) a higher proportion of impervious surfaces (increased drainage) causes more runoff, and in combination with reduced vegetation cover, results in reduced Q_E, and hence increased Q_H.

These characteristics can influence urban climate, but number 4 is of most relevance to this research, as it brings together WSUD and urban climate. In conventional urban areas, (Figure 2.4 - compare urban and natural water balances), the lack of pervious surfaces, and high amounts of
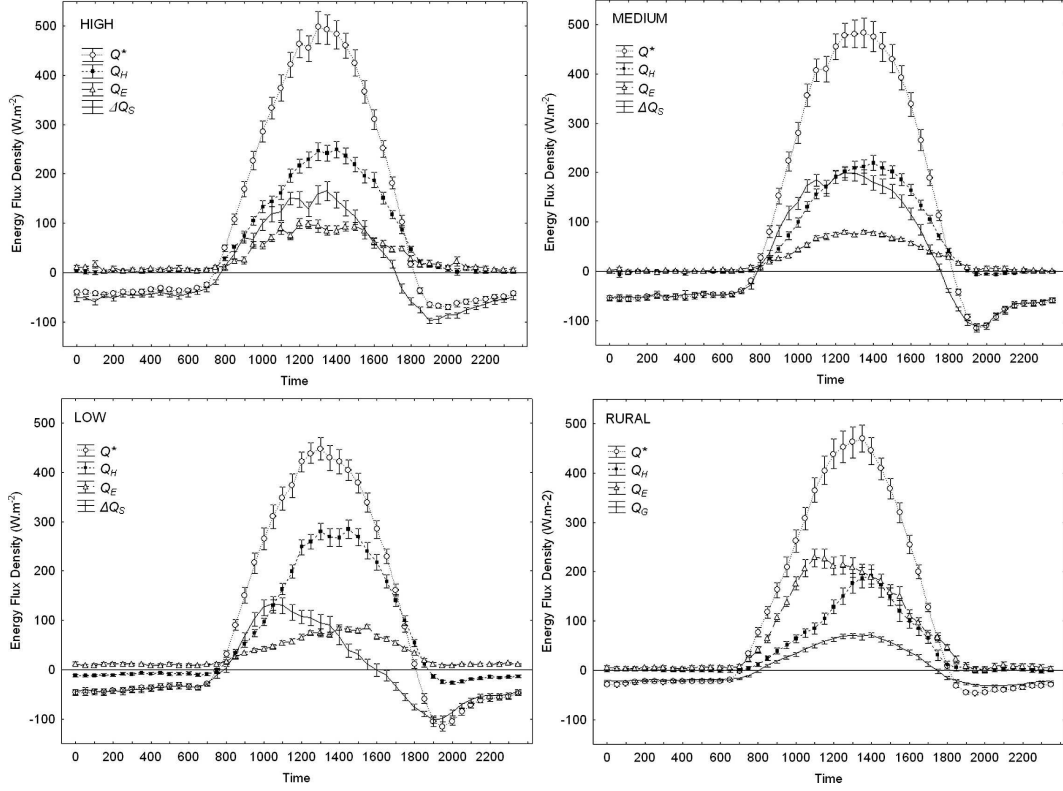
Figure 2.4: The mean (± std error) diurnal surface energy balance for March (austral summer) 2004 at three urban sites and a rural site in (or near) Melbourne, Australia. Note that a much greater proportion of available energy (Q^*) is partitioned into Q_E at the rural site (bottom right). This means that the overall magnitude of the Q_H is smaller. Using WSUD to promote Q_E in urban areas could be an effective way of mitigating extreme heat. Source: Coutts et al. (2007).

runoff, means that during the day, Q_E at urban sites is typically small and Q_H is large (Figure 2.4, see high density sites). WSUD aims to reduce urban runoff and promote more ET, and hence Q_E, thereby reducing the amount of heating of the atmosphere (Q_H) (Figure 2.4, see rural site). These linkages between the urban water and energy balance show the potential to simultaneously and purposefully manage the urban water balance (through WSUD), and cool the urban microclimate (Mitchell et al., 2008).

2.2.2 HTC indices and definition

While managing the amount of ET in the urban environment may be a key method for mitigating urban warmth, when considering HTC, it is important to take into account other factors that

influence the human thermal experience. The fact that thermal comfort is affected by more than just air temperature has lead to the development of a number of HTC indices in order to quantify the human thermal experience. The focus of this research is the potential for WSUD to mitigate urban warmth at the microscale and improve human health and wellbeing. While traditional measures of human health such as morbidity and mortality are important, HTC is a particularly relevant metric that describes the human experience of urban climate at the microscale. HTC seeks to understand the thermal experience of an individual at a given point in space and time. This focus on the individual means that HTC is a microscale metric. HTC indices are key measures of human exposure to heat stress. Broadly, the concept of HTC is defined as the mental state achieved when (1) physiologically: the thermoregulatory mechanisms are minimally activated, and (2) psychologically: the perceiver's satisfied with the thermal comfort (Thompson & Perry, 1997). Further, the ASHRAE Standards 55-1992 define HTC simply as the *"condition of the mind in which satisfaction is expressed as thermal comfort"* (ASHRAE, 1992). The perceived HTC of an individual is generally considered to be influenced by six major variables (Parsons, 2002):

(1) air temperature — the warming of air temperature in cities (urban warmth) is a key measure for human health, but should not be used as a sole measure of HTC (Matzarakis & Endler, 2010).

(2) mean radiant temperature (MRT) — is a measure of the influence of radiant temperature on the human body. Matzarakis et al. (2010)[p.131] state that MRT is defined as *"the uniform temperature of a hypothetical spherical surface surrounding a human (emissivity=1) that would result in the same net radiation energy exchange with the subject as the actual, complex radiative environment"*. MRT is highly influenced by incoming solar radiation ($K \downarrow$), and MRT can be the most important meteorological parameter impacting upon HTC during

the day, particularly during summer and when wind speed is light (Mayer & Matzarakis, 1998).

(3) humidity — the amount of moisture in the atmosphere determines the ability of a person to lose heat by sweating (Q_E), which is a crucial heat loss mechanism for a person under heat stress (Parsons, 2002).

(4) wind speed (air movement) — the speed and direction of wind influences the convective and evaporative losses and therefore influence the heat balance and internal temperature of the human body (Gaitani et al., 2007).

(5) metabolic rate (Q_M) — the internal source of heat generated by human activity (Parsons, 2002).

(6) clothing — the amount of clothing worn also influences HTC. The effect of garment insulation is often described using the clo unit.

HTC indices are focused on the experience of the individual (rather than population averages) and provide a detailed understanding of human behavioural responses to heat. There are a large range of HTC indices that are used throughout the HTC literature. Reviewing them is beyond the scope of this research (see Parsons (2014) or Buzan et al. (2015) for a summary on these indices). This research uses the physiological equivalent temperature (PET) (Mayer & Höppe, 1987). PET is considered as the most comprehensive biometeorological index to assess the outdoor human thermal environment, as it is based on the human energy balance and thermophysiological concepts (Höppe, 1999). PET also has the advantage of a widely known unit (°C), which makes the PET index more comprehensible (Matzarakis et al., 1999). HTC indices such as PET show the specific meteorological and non-meteorological processes that lead to discomfort. With this specific information about HTC our cities can be designed to target

maximum thermal comfort. Thus far in this thesis, the term "microscale" has been used without formally defining what is meant by it. The following section will define and discuss the concept of microscale climate and its relevance in urban climate research.

2.2.3 Scale consideration and relevance in observational urban climate research

Urban climate can be viewed at a range of scales and because of the complex nature of the urban surface, understanding scale in urban climate is important for effective observation and interpretation of urban climate data (Oke, 2009). The microscale is defined as the having spatial dimensions of $10^{-2} - 10^3$ m and temporal dimensions of seconds to hours. Other scales of climate include the local and mesoscales, which are characterised by their own spatial and temporal dimensions (see Table 2.1). Different types of atmospheric phenomena occur at these scales: ranging from mesoscale urban heat plumes to microscale atmospheric phenomena such cross canyon vortices and building wake effects (Figure 2.5). These scales are also associated with a range of physical features in the urban environment, for example the microscale is said to describe the climate of the space between buildings (the urban canopy layer [UCL]) (see microscale box in Figure 2.5), and the local-scale is the average climate associated with a neighbourhood (see local-scale box in Figure 2.5). The UCL is the zone that defines urban microscale climate, and as such the UCL is the focus of this research. The UCL is the zone where urban dwellers live in and experience urban climate. In this research, in order to understand the climate that individuals are exposed to, observations and modelling must be conducted at the microscale.

One key characteristic of microscale climate is that it can be highly variable in both time and space. The climate that urban dwellers are exposed to inside the UCL can vary significantly over short distances (Oke, 2004). This is because the source areas that influence a location in the UCL can be in the order of 10s of meters (Oke, 2004). This small source area means that, the surfaces that define a microclimate can be highly localised in the UCL. Given that urban surfaces are

Table 2.1: A summary of the urban climate scales, associated phenomenon, features, and appropriate observation methods, modified after (Oke, 2006).

Scale	Dimensions	Associated layer(s)	Meteorological phenomena	Physical features	Temperature observations
Micro-scale	$10^{-2} - 10^3$ m	UCL, RSL	Cross canyon vortex, building wake	Building, canyon, tree	Fixed stations, mobile transects
Local-scale	$10^2 - 10^3$ m	Inertial UBL	Urban park breeze	Neighbourhood, park	Tower
Meso-scale	$10^3 - 10^6$ m	Mixed UBL	Urban/city plume, rural/urban breeze	Land-use class, city	Tower, sodar, sonde, remote platforms
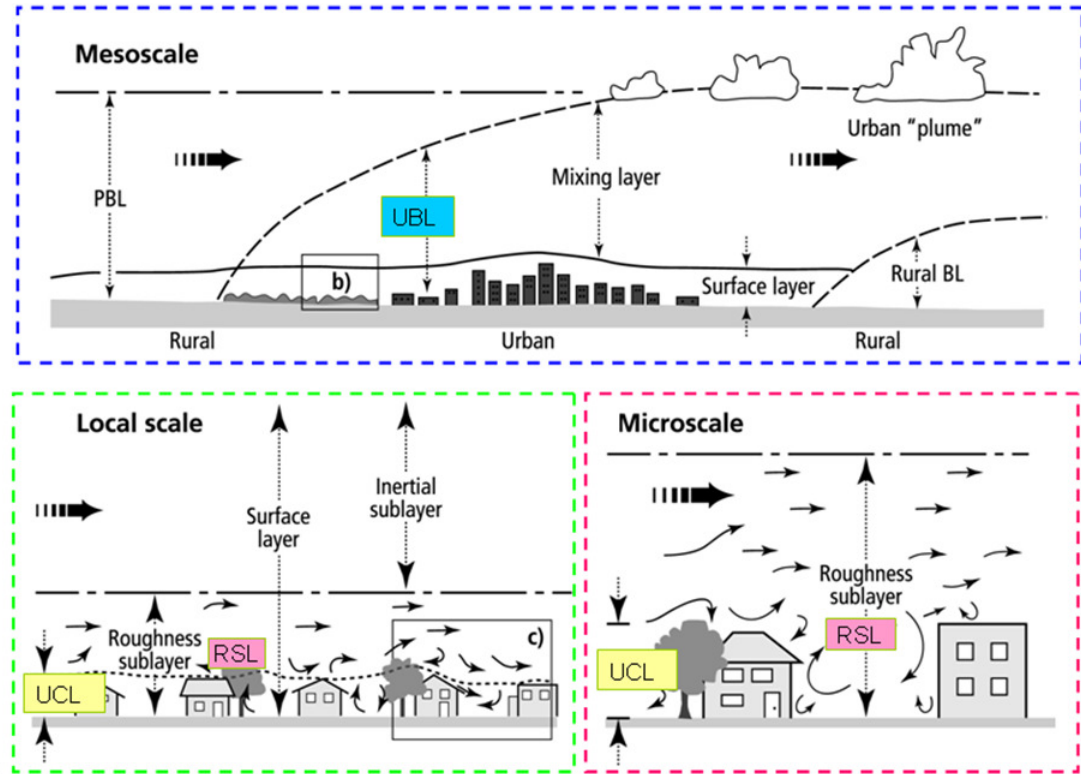
Figure 2.5: A schematic of the different scales of urban climate. UBL = urban boundary layer, UCL = urban canopy layer, and RSL = Roughness sublayer. The top box shows the mesoscale atmospheric phenomena, including the atmospheric heat plume. The bottom boxes show local (left) and microscale (right) representation of the urban boundary layer. The microscale climate is characterised by the turbulent and highly variable conditions within the UCL. Source: Oke (2009).

typically highly heterogeneous, and can be made of patches that have very different thermal and moisture properties, the resulting temperature variability can also be large. The localised source area that is observed in the UCL can create large temperature gradients over short distances. Additionally, the effects of shading and complex turbulence features in the UCL can contribute to this variability. Coutts et al. (2015) note that microscale variability is so significant that the use of a single monitoring station to represent HTC within one urban canyon is not appropriate. This degree of intra-urban microscale variability justifies a high resolution approach, but also represents a significant challenge for those interested in HTC and human exposure to heat. The UCL microclimate is highly variable, and this limits spatial and temporal range of microscale research. The variability of microclimate makes it difficult to observe or model microclimate over a large area/and or time period. This high variability also makes the measurement and interpretation of microscale measurements very challenging.

Observations of microscale climate are difficult to interpret. In particular, it is difficult to attribute microclimate variability to changes in surfaces characteristics, such as increased water availability. One reason for this is that there are a complicated range of variables that influence microclimates including shading effects, turbulence and wind channeling, interactions between canyon air parcels and air parcels aloft, and highly variable energetic contributions from different surface facets in the UCL (Oke, 2004). In order to understand the cooling effects of WSUD, this research must establish a meaningful link between the surface drivers of urban microclimate and observed microclimate variability. However, there is no simple method for estimating the source area of a microscale sensor in the UCL (Oke, 2004). This means that there is no clear way to work out exactly what surfaces an instrument can "see" when it is placed below roof height. Capturing microscale climate variability and understanding the drivers of that variability, in particular the effects of WUSD, are concepts that are fundamental to this research. However, without a meaningful way to connect the land surface characteristics and microscale variability

it is difficult to quantify how much WSUD can influence urban microclimate. This is a question that is addressed through observational analysis in chapter 4 of this research.

A proper understanding of scale is necessary in urban climate research, particularly in observational studies, for the accurate collection and interpretation of data. Observational urban climate research has long been focused around the concept of urban heat island (UHI), which refers to the atmospheric warmth of a city as compared to its surrounding rural areas. UHI studies infer the effect of urbanisation on climate by comparing the air temperature of a rural and urban site. Much emphasis has been placed on observing and documenting UHI magnitudes in cities around the world (Stewart, 2011). However, Oke (2009) emphasised that the notion of "the UHI" is misleading, and he suggests that there are in fact multiple UHI, depending on what part of the urban boundary layer is being observed. A major reason for this characteristic of UHI is related to the issue of scale. Observations of urban climate will differ significantly when observed in the UCL as compared to the inertial sub-layer (Figure 2.5). As shown in Figure 2.5 an observation made in the UCL reflects microscale climate, and an observation made in the inertial sub-layer is representative of local-scale climate. Given the variability at the microscale, the comparison of two sites (one rural and one urban) to describe the magnitude of the UHI, is a very simplistic way to characterise the effects of urbanisation on climate. Furthermore, Stewart & Oke (2012) argue that the simple "urban-rural division" is inadequate because these terms cannot sufficiently describe the complex nature of the urban environment or its local surroundings. The words "urban" and "rural" mean different things in different places, making comparison difficult or irrelevant. In response to this, some researchers have begun to deploy multiple instruments within urban environments, either with static weather stations, and/or mobile weather stations. These intra-urban studies are typically less interested in the UHI, but rather in intra-urban temperature variability. It has been shown that microscale air temperature variability can be as large as the urban-rural contrast (Petralli et al., 2014). This intra-urban

variability reveals the areas within a city that are potentially exposed to negative heat health conditions (Petralli et al., 2012), whereas UHI type studies do not. From the perspective of heat exposure research, the presence or absence of UHI is somewhat irrelevant. Researchers that are motivated by improving heat health outcomes need to consider local-scale variability, while those interested in HTC goals must consider the microscale climate of cities. This research is interested in the cooling potential of WSUD from both a heat health and HTC perspective. For applied heat mitigation studies such as this one, capturing and understanding the microscale and local-scale variability is essential to properly understand the conditions that humans are actually exposed to.

2.3 Microscale climate and land surface — observations

2.3.1 Introduction

Given the importance of microscale intra-urban variability, a critical analysis on the drivers of microscale variability from previous research relevant to WSUD (e.g. trees, parks, water bodies, vegetation, and irrigation), will help to place this research within the existing body of urban climate knowledge. Urban microclimate is important to understand because it represents the conditions urban dwellers are physically exposed to. Significant variations in urban microclimate can be seen over very short distances (Petralli et al., 2014) and this variability is largely driven by the variability in the land surface characteristics and morphology of highly heterogeneous urban landscapes.

Identifying how different urban land surface characteristics contribute to intra-urban climate variability has been a major focus of many international studies (see literature cited below). No observational studies have specifically looked at the effects of WSUD on microclimate, highlighting a critical gap in the literature that needs to be addressed given the mitigating potential of

WSUD and improved urban stormwater management. However, a broad range of research has been conducted looking at urban characteristics, such as trees, parks and green spaces, water bodies, and outdoor water-use. The previous research examined here focuses on the influence of these urban characteristics/features on urban microclimate and the potential implications for WSUD are explored.

2.3.2 Outdoor water-use and irrigation

WSUD seeks to maximize the reintegration of stormwater into the urban environment. A major way to facilitate this reintegration is through irrigation of gardens and public space. In section 2.3.4 the effect of irrigation with respect to urban parks is discussed, this section will discuss general irrigation related research. The effects of irrigation and outdoor water-use on air temperature and HTC has received little attention in observational studies; however a number of observational studies have considered the effects of outdoor water-use practices on the energy balance. Oke & McCaughey (1983) undertook flux measurements of a suburban site and a rural site in Vancouver, Canada, and found that the suburban landscape ($Q_E/Q^* = 0.67$) was evapotranspiring more than the rural landscape ($Q_E/Q^* = 0.59$) during the day. This finding is in stark contrast to many other urban-rural flux comparison studies which show sensible heat as a much more dominant flux in urban areas (Oke et al., 1999, and references therein). Oke & McCaughey (1983) suggest that these high values of suburban Q_E were caused by advectively-assisted ET from irrigated gardens and lawns, especially under high radiation conditions when impervious surfaces were dry and hot. Kalanda et al. (1980) found that abrupt day-to-day changes in energy partitioning between Q_E and Q_H (by considering the Bowen ratio (β) where $\beta = Q_H/Q_E$) were unrelated to precipitation events and suggest it was related to irrigation practices of homeowners. Additionally, Grimmond & Oke (1995) compared summertime suburban energy budgets for four North American cities, and found that at the sites with infrequent rainfall (Tucson,

Los Angeles, and Sacramento) the Bowen ratios were inversely proportional to the amount of irrigated green-space. These early energy balance studies discussed above provide a strong basis for the hypothesis that irrigation can cause a cooling of the daytime urban climate, particularly in suburban areas. Oke (1987) suggested that large scale irrigation can modify the local climate, and especially at arid or semi-arid locations. However, none of these studies attempted to directly quantify the effects of irrigation on local-scale or microscale air temperature, nor HTC. Aside from the research undertaken in urban parks (see section 2.3.4), there has been very few observational studies that have directly related irrigation and outdoor water-use practices to air temperature and HTC variability.

Shashua-Bar et al. (2009, 2011) looked at the water efficiency of a range of common urban cooling approaches, including shade trees, irrigated grass, and shade mesh in two adjacent courtyards in Israel. These studies found that a combination of irrigated grass and shade trees were the most effective in cooling, and that trees alone achieved the highest cooling efficiency per amount of water used. While Diem & Brown (2008) showed that increased ET resulting from extensive irrigation, was contributing to enhanced summer p recipitation totals downwind of Phoenix, Arizona. In another study, Bonan (2000) investigated microclimate variability throughout a residential neighbourhood in Colorado, USA, and found that across the neighbourhood on a hot summer day, air temperatures in areas with irrigated vegetation were several degrees cooler than those with non-vegetated surfaces, and air temperatures observed within areas of native dry grasses were warmer than those in irrigated greenbelts. These studies provide further evidence that irrigation can contribute to cooling in urban areas. However, the effect of irrigation on air temperature at night remains unclear, as does the effect of irrigation on HTC. Given that promoting the reintegration of stormwater is a major goal of WSUD, the thermal effects of irrigation on micro to local-scale air temperature and HTC are important considerations for this research.

2.3.3 Urban trees

Trees are an important part of urban landscapes and increasing tree canopy cover is widely regarded as an effective means for providing daytime cooling benefits, receiving a strong research focus particularly at the microscale. Trees provide daytime cooling via two key mechanisms: (1) decreasing the receipt of solar radiation ($K \downarrow$) at the urban surface (shading), and (2) transpiration (increased Q_E) (Bowler et al., 2010). From the perspective of WSUD, trees are relevant because they require a significant amount of water to provide thriving canopies that actively transpire and block solar radiation. Cities can be stressful environments for trees due to the higher temperature and lower humidity (Peters et al., 2010). Urban tree health in Australia is a particularly important issue because drought, water restrictions, and rapid export of stormwater away from the urban environment has left many urban landscapes water-starved and this can constrain tree transpiration (Coutts et al., 2012). Trees in Australian cities during times of drought have been shown to be adversely affected by low water availability (Coutts et al., 2012; May et al., 2013). A city with WUSD features, utilises an additional water source largely neglected in conventional urban development, and can therefore help to maintain productive tree health in urban areas. Trees that are well supplied with water can provide optimal cooling via transpiration and shading.

During the day, a major benefit of trees is the shade that they provide. Observational studies have shown that the presence or absence of shade can influence air temperature (Tsiros, 2010; Georgi & Dimitriou, 2010), HTC (Picot, 2004; Ali-Toudert & Mayer, 2007; Coutts et al., 2015), and LST (Wong et al., 2003). Tree shade reduces the amount of solar radiation received at the surface, as $K \downarrow$ is absorbed and reflected by the tree canopy, which reduces the Q_H of the UCL, causing lower air temperatures (Figure 2.6). Shading can also reduce the MRT experienced by a person in the UCL, which can greatly improve HTC (Coutts et al., 2015). It is worth

noting that trees are not the only source of shade in urban areas, and the shading effects of buildings have also been shown to be effective at reducing air temperature and MRT during the day (Ali-Toudert et al., 2005; Hwang et al., 2011). However, the focus here is observational studies that have specifically examined the cooling effect of trees on HTC and air temperature. A range of observational studies have observed lower air temperature below urban tree canopies (Souch & Souch, 1993; Lin & Lin, 2010; Coutts et al., 2015). These air temperature reductions, which are usually in the order of 1–2 °C, are smaller than observed reductions in HTC indices beneath trees. A study from Melbourne has shown this effect, where Coutts et al. (2015) found a maximum air temperature cooling of 0.9 °C, while the Universal Thermal Climate Index (UTCI) decreased by up to 6 °C and reduced the level of heat stress. This is because MRT can increase significantly in direct sunlight and become much higher than air temperature (Ali-Toudert et al., 2005) dominating the human energy budget. As HTC is highly influenced by MRT, trees have been shown to be particularly beneficial for cooling that targets HTC. However, other factors that influence HTC have been shown to be affected by tree canopy coverage. Higher humidity has also been observed beneath tree canopies (Souch & Souch, 1993; Zhang et al., 2013) and ventilation (wind speed) may also be reduced below the tree canopy (Park et al., 2012). It's important to recognise that HTC is affected by a range of different factors other than air temperature, such as humidity and wind speed, and given that WSUD seeks to maximise ET in urban areas, it is necessary to be aware of any potential adverse effects on HTC. However, overall, studies that have calculated HTC indices beneath trees have noted improved daytime thermal comfort beneath the tree canopy (Lee et al., 2013; Coutts et al., 2015).

A range of factors influence the daytime cooling benefits of trees, including canopy coverage, tree size, positioning, planting density, and irrigation management (Ali-Toudert & Mayer, 2006b; Shashua-Bar et al., 2010; Pataki et al., 2011; Coutts et al., 2015). The most important characteristic of trees for effective daytime cooling is most likely canopy coverage (Shashua-Bar et al.,
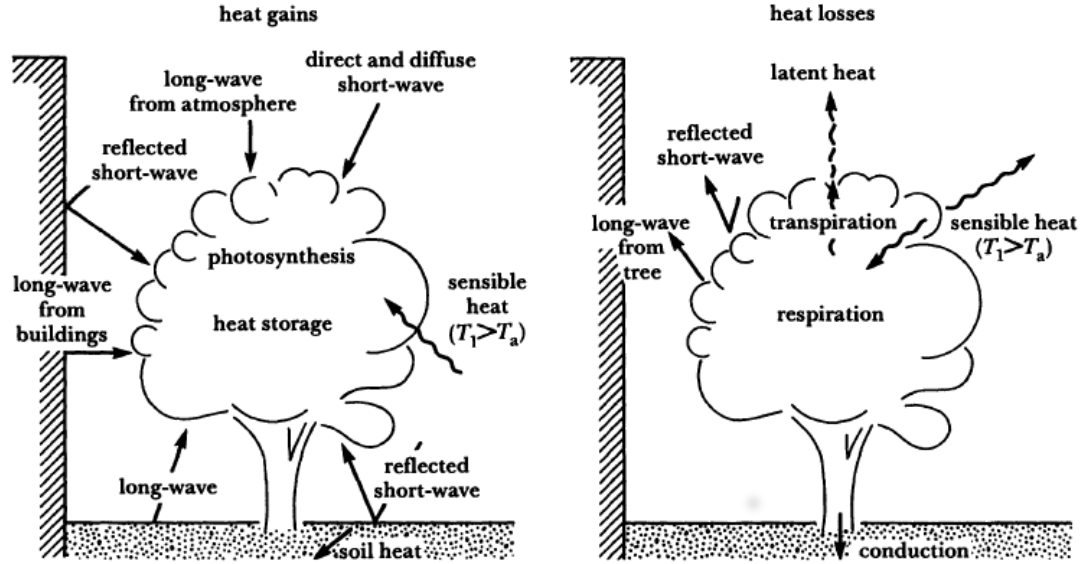
Figure 2.6: A schematic of the daytime energy exchanges between an isolated tree and its street canyon environment. Trees reduce the $K \downarrow$ received at the surface, which can reduce air temperature, LST, and HTC during the day. Source: Oke et al. (1989).

2010). Dense tree canopy coverage can be beneficial for cooling daytime air temperature and improving HTC (Figure 2.7). This research will not be looking at tree canopy coverage. However, this beneficial nature of canopy coverage provides further justification for keeping trees healthy and well-watered via WSUD and harvested stormwater (Figure 2.7). Coutts et al. (2015) suggest that the strategic placement, density of planting, and species selection of street trees should be taken into account to maximize cooling. These findings emphasise one of the complexities associated with trying to quantifying the cooling benefits of any land surface feature; in the UCL a range of variables influence air temperature and HTC variability and it's difficult to disentangle the effect of any given variable.

It is well known that street trees can provide a cooling benefit during the day. However, a few studies observe that nocturnal air temperature below trees can be slightly higher than nearby open sites (Bowler et al., 2010) due to reduced sky view factor (SVF) inhibiting longwave cooling (via $L \uparrow$) at night (Figure 2.6). Souch & Souch (1993) observed air temperature was 0.5 °C warmer under canopies than at an open site due to longwave radiation absorption and re-
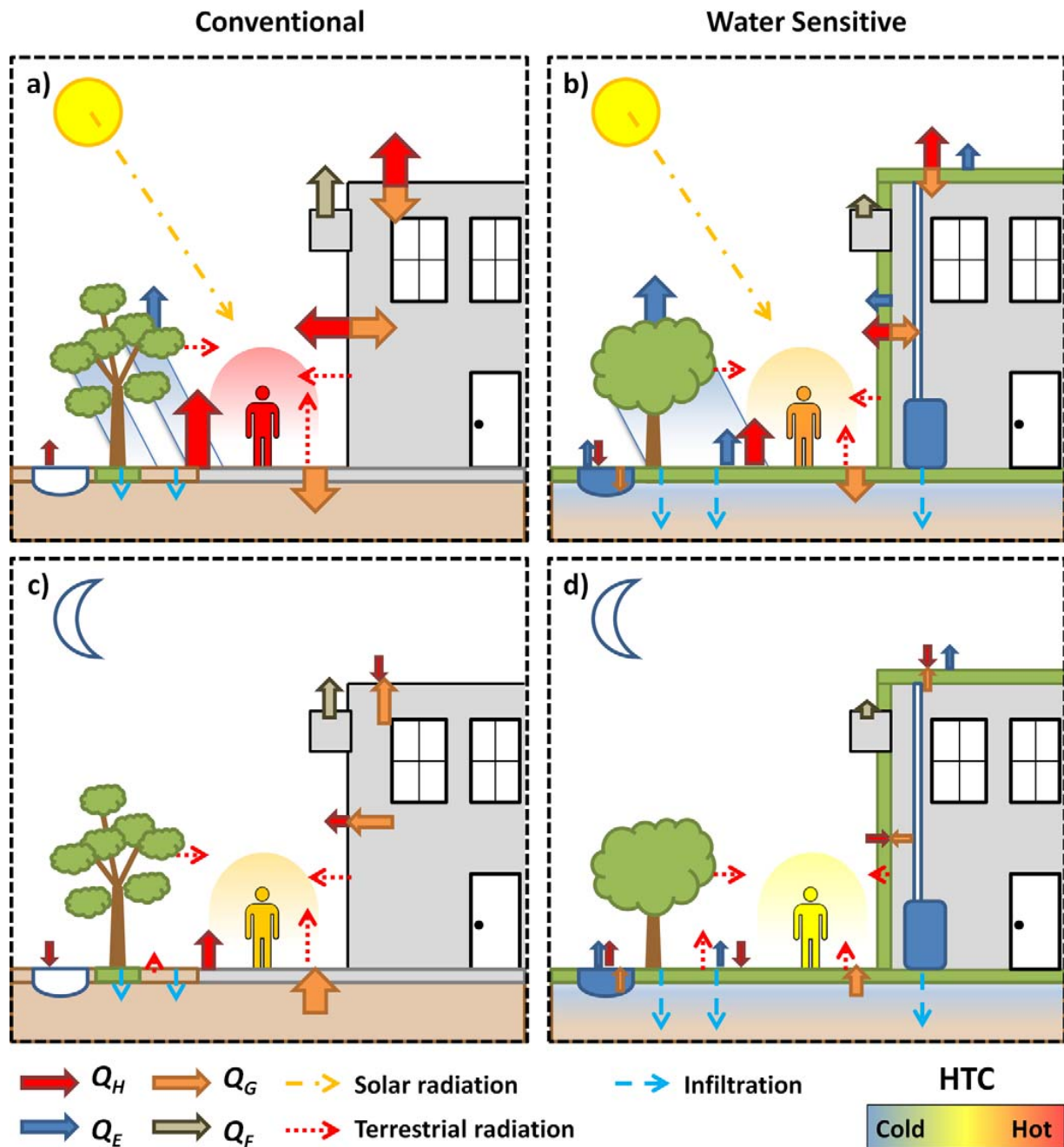
Figure 2.7: Generalisation of key processes in the formation of urban microclimates during summer for conventional (water limited) urban landscapes (a and c) and water sensitive urban landscapes (b and d). Day (a and b) and night (c and d) conditions are presented. Surface radiative and energy balance processes are presented with arrows denoting direction and relative strength of fluxes. The relative level of HTC experienced in each case is presented. In the conventional urban landscape during the day, a combination of high sensible heat fluxes and strong radiative heat loading results in a hotter environment. In contrast, the water sensitive landscape provides higher water availability to soils and waterways, along with healthy, full canopied vegetation, compared to conventional water limited, xeric urban landscape. WSUD increases ET and shading, and reduces surface temperatures, limiting radiative heating, and resulting in improved HTC. Reduced heat storage during the day is beneficial at night, as less energy is available to support ongoing warming. Cooler outdoor environments along with reduced heat transfer into buildings limits the need for indoor air conditioning and associated anthropogenic heating. Other factors may also be influential, such as air pollution effects on radiation and wind flows. Source: Coutts et al. (2012).

36

emission by the tree canopy. This process of longwave radiation absorption also occurs in urban canopies due to decreased SVF from buildings. As such, higher air temperature can occur at night when SVF is decreased and this must be accounted for when considering the microclimate variability in urban areas and the heat mitigation potential of trees.

Overall, trees have been shown to be an important measure for mitigating urban temperatures during the day. Cooling is most pronounced during the day, and the majority of this cooling comes from the shading effect that trees provide. Because the cooling effects of trees are primarily related to shading effects, this means that one may not necessarily expect to see cooling directly adjacent to trees. Furthermore, it can be said that trees tend to have larger effect on HTC than on air temperature as MRT is a key variable that influences HTC. Despite the relatively clear message that trees can reduce daytime air temperature and HTC, there are in reality a range of factors (e.g. airflow and SVF) that must be further considered when quantifying the thermal benefits of trees. These complexities reinforce a wider point about urban microclimate: that it is difficult to quantify the effect of single feature (e.g. a tree) on microscale climate. This is a major challenge of this research, which is interested in quantifying the cooling of WSUD on urban microclimate. Overall, maintaining healthy urban trees can provide valuable daytime cooling benefits, particularly for HTC. However, the reduced water availability in cities threatens the health of urban trees. WSUD can be used to maintain more water in urban areas, which means tree health can be supported even during times of low water availability. Healthy urban trees, supported by WSUD, are likely to have greater canopy coverage and therefore provide more shading (Figure 2.7). Trees are just one important part of WSUD that can increase urban infiltration and ET. There are a range of other thermally beneficial vegetation features in urban areas, which require water to be sustained, including parks and green space.

2.3.4 Parks and greenspace

Urban parks have generally been shown to have cooler air temperature than surrounding built up areas (Barradas, 1991; Oke et al., 1989; Saito et al., 1990; Ahmad, 1992; Lindqvist, 1992; Spronken-Smith, 1994). Broadly speaking, the presence of vegetation, open space, small amounts of impervious surfaces, irrigation (in some parks), and a lack of Q_F in parks leads to a relative cooling effect compared to their surrounding urban areas. Urban parks are coherent with WSUD concepts because widespread pervious surfaces encourage infiltration of water and reduce runoff. Additionally, captured stormwater could be reintegrated into parks, increasing ET and potentially providing a cooling effect. The cooling phenomenon in parks is most common at night (Upmanis et al., 1998) but can occur throughout the day, and is often referred to as the Park Cool Island (PCI) effect. The cooling influence of parks can extend beyond the park and reduce temperature in built-up areas. Spronken-Smith (1994) suggest the air temperature cooling can extend to about one park width, but the influence reduces rapidly with distance away from the park boundary. Parks are generally considered to be cooler than built-up urban areas throughout the diurnal cycle, but the processes associated with PCI vary between the night and daytime.

At night, urban parks are cooler because open areas lose heat quicker than urbanised areas due to greater SVF (greater $L \uparrow$ / less $L \downarrow$) and the lower thermal conductivity of natural surfaces. This means that the air temperature in parks can become lower than urbanised areas during nocturnal hours. However, the effect of water availability at the surface (from irrigation) has been shown to cause slightly higher land surface temperature (LST) in irrigated parks compared to dry parks. Spronken-Smith & Oke (1998) examined PCI effects in a number of parks in North America. They found that irrigation caused higher LST in Vancouver, because moist grass has a higher heat capacity than dry grass, and retains more heat throughout the night. However, Spronken-Smith & Oke (1998) observed that PCI (air temperature) still formed in

irrigated parks, meaning the effects of irrigation did not completely negate PCI, especially in Sacramento, which has a drier and warmer climate than Vancouver. Overall, Spronken-Smith & Oke (1998) concluded that all other factors being equal, air temperature in drier parks (i.e. less irrigated parks), was cooler than irrigated parks throughout the night. Therefore, surface water availability may increase nocturnal LST and air temperature of grassed areas. This irrigation issue is quite relevant with respect to this research, as WSUD seeks to maximise water availability in cities, which could have a mild warming effect at night, although LST of irrigated grass still remains cooler than hard impervious surfaces at night. However, this processes has only received limited attention and it is unknown how air temperature in parks will respond to irrigation during extremely hot and dry nocturnal conditions.

The amount of trees also affects the nighttime characteristics of nocturnal PCI. In Malaysia, it was observed that the air temperature of well-treed parks was only slightly cooler (about 1 °C) than their urban surrounds (Sani, 1990). As discussed above trees reduce $L\uparrow$ heat loss at night, and can have a slight nocturnal relative warming effect. Additionally, nocturnal PCI has also be shown to be affected by wind speed. Spronken-Smith (1994) observed the air temperature of the some parks to be up to 6–8 °C cooler than their suburban environs, and noted that PCI are inversely related to wind speed. Lastly, park size and surrounding urban geometry have also been shown to be important factors that determine the intensity of PCI (Upmanis et al., 1998). The strength of nocturnal PCI typically increases with the horizontal size of the park (Spronken-Smith & Oke, 1998; Upmanis et al., 1998), and there is evidence that more tightly spaced buildings around urban parks can reduce Q_E/Q^* (Pearlmutter et al., 2009). Broadly, it is clear that parks have a nocturnal cooling effect, but this effect is complicated as parks vary significantly in a range of characteristics, such as water availability, exposure to wind, and tree coverage. This means that all these factors must be accounted for when examining the nocturnal microclimate of parks and grassed areas.

During the day, park climates are generally cooler than surrounding urban areas too (Saito et al., 1990). However, Jauregui (1991) found that, at noon, a park in Mexico City was warmer than the surrounding built-up area, because of the lower thermal inertia of park materials relative to the surrounding urban landscape. This means that, sometimes urban parks can heat up quicker than urban areas, particularly when water availability is low. However, lower daytime temperatures in urban parks have also been commonly reported (Saito et al., 1990), but the reason for this cooling remains unclear. Spronken-Smith & Oke (1998) state that the presence or absence of shade, the surface albedo, and water availability in parks have the most control on air temperature during the daytime. They found that parks with greater tree coverage and more irrigated grass had the coolest air temperature in the afternoon. WSUD can facilitate daytime irrigation (reintegration of stormwater) in parks which will provide potential daytime cooling benefits. Irrigation will likely provide cooling benefits for air temperature in urban parks and greenspaces, but it is also likely to increase humidity, which may influence HTC. The effect of irrigation on HTC has rarely been directly considered in urban climate research. Spronken-Smith & Oke (1998) reinforce that fact that although parks can provide cooler air temperature conditions during the day, these cooler conditions emerge due to a range of different factors, such as exposure, tree coverage, and irrigation. It is important to remember that a range of processes influence daytime microclimate in parks.

Park design can vary significantly and a number of factors have been shown to influence the magnitude of relative cooling in parks. These are matters of important consideration for this research. How can the water retention in the urban environment be maximised, while simultaneously optimizing the urban thermal environment? Parks and greenspace are an important part of WSUD considerations, they provide pervious surfaces for infiltration, and they are also an area where captured stormwater can be easily reintegrated. Previous research suggests that reintegration of stormwater is likely to be thermally beneficial during the day, but not necessarily

at night. For WSUD to be effective at achieving urban cooling, these issues require investigation.

2.3.5 River, lakes, and water bodies

Water bodies are a key component of WSUD. Constructed wetlands are a common means for treating stormwater before it reaches local waterways and lakes can be built to store stormwater throughout the urban environment. While these water bodies have functional and amenity value, they are also potential cooling features in the urban landscape. The cooling potential of lakes and wetlands therefore are a key consideration for this research. A few studies have observed the cooling effect of lakes, rivers, and other water bodies, which have shown a general daytime cooling effect (Murakawa et al., 1991; Saaroni & Ziv, 2003; Kim et al., 2007; Chen et al., 2009). Water bodies are well known to provide a downwind cooling benefit, which is sometimes referred to as the lake effect (Saaroni & Ziv, 2003). This cooling occurs because water has a very high heat capacity and tends to remain cooler than urban materials during the day and water provides a source for evaporation. Wind moving across the water body is cooled and transported into nearby urban areas (advection). Saaroni & Ziv (2003) observed the microscale cooling effect, downwind of a small lake in Tel Aviv, Israel, where they observed a maximum cooling effect of 1.6 °C at midday. The highest temperatures were observed upwind of the lake and the lowest were observed immediately downwind of lake. However, Saaroni & Ziv (2003) added that the influence of water on downwind cooling is difficult to quantify because wind also affects turbulence which can increase Q_H and increase the transport of heat away from the surface. In another study, Murakawa et al. (1991) investigated the effects of a river on urban microclimate in Hiroshima, Japan. The results showed that sites near the river were up to 5 °C cooler (between 12 pm and 5 pm) than the surrounding area. However, Murakawa et al. (1991) state that the cooling from the river was more evident in places where the density of buildings were low and the width of streets and rivers were wide. Both Saaroni & Ziv (2003) and Murakawa et al. (1991) noted that

the downwind cooling effects of water bodies are affected by other variables, which are difficult to account for. This reinforces the fact that many factors influence urban microclimate and isolating the influence of a single factor can be difficult.

The effect of water bodies on nocturnal air temperature is less definitive. Water bodies can maintain warmer temperatures at night due to the high heat capacity and thermal inertia of water. The high heat capacity of water means that the cooling potential of water bodies at night is uncertain, and they may have a relative warming effect if the surrounding urban areas cool more rapidly. The effect of water bodies on nighttime climate is an area that requires attention in this research. WSUD encourages the implementation of distributed water bodies throughout the urban environment, and it is important to ascertain what the thermal effects of these water bodies could have.

Saaroni & Ziv (2003) also observed an increase in humidity downwind of the lake, which could potentially have adverse effects for HTC. Studies looking specifically at the effects of water bodies on HTC are limited. Höppe & Seidl (1991) looked at HTC for a coast beach site and an inland location. The authors found that heat stress was less likely at the beach location due to sea breeze effects. Lakes, wetlands, and water bodies provide daytime air temperature cooling benefits. However, HTC will be dependent on other factors that are potentially affected by the presence of the water body, such as humidity and wind speed. Therefore, the effect of water bodies on HTC needs to be considered as part of this research.

Overall, WSUD water bodies are likely to bring daytime downwind cooling benefits for air temperature. However, the thermal effects of artificial water bodies, such as those used in WSUD, have seldom been considered. Furthermore the nighttime effect of water bodies in general has received minimal attention and it is important to consider if any microscale warming occurs due to WSUD water bodies. Finally, the effect of WSUD water bodies on HTC is an important consideration for this research as well. Water bodies are likely to increase microscale humidity

and that could have adverse implications for HTC. Overall, a full appraisal of WSUD water bodies is needed both with respect to night and daytime climate and in the context of air temperature and HTC is needed.

2.3.6 Microscale observational studies summary

- A range of energy balance studies from urban areas in North America suggest that irrigation directly influences the partitioning of the urban energy balance. As such, there is strong evidence to suggest that irrigation can directly influence urban temperatures through evaporative cooling.

- The cooling potential of outdoor water-use or irrigation has received very little attention in observational studies. In particular, the effects of nighttime irrigation remain unclear. While daytime irrigation is expected to provide some cooling, the magnitude of this cooling remains unclear, as are the implications of daytime irrigation for HTC.

- Parks and greenspace are generally considered to provide some urban cooling benefits. However, a range of factors, including water availability, influence the cooling effects of parks and greenspace.

- Trees are an effective way of providing daytime cooling, and are particularly beneficial for improving HTC. However, at night trees may cause some retention of warmth in the urban environment. Stormwater reintegration can be used to maintain healthy urban trees, which is particularly important during times of drought.

- The thermal effects of artificial WSUD water bodies have not been sufficiently researched. Generally speaking, water bodies are known to cause downwind cooling of air temperature, but little is known about their effect at night. Moreover, the effect of water bodies on HTC needs to be assessed further.

- Inferring the effect of single feature type (e.g. tree or water body) is difficult as many factors influence urban microclimate. Comparative observational studies such as most of the studies discussed above often neglect this fact. In order to understand the cooling potential of WUSD, a robust analysis of urban microclimate that considers the many factors influencing urban microclimate is needed.

Urban microclimate is important to understand because it represents the conditions urban dwellers are physically exposed to. Observational studies are a necessary way of understanding what controls microclimate variability. However, a major limitation of microscale observational approaches is that it is difficult to ascertain the influence of a single variable or feature. Numerical modelling allows for controlled sensitivity tests to be conducted, and the influence of a single variable to be estimated. Additionally, numerical models provide high spatial coverage and allow users to forecast climate under hypothetical/future conditions. This means that numerical modeling of urban climate is useful way to study urban climate and understand how different characteristics of the land surface influence climate.

2.4 Urban climate modelling

2.4.1 Introduction

Numerical modelling techniques are a useful tool for urban climate investigations because they provide high spatial coverage and allow different scenarios to be tested. For these reasons, numerical modelling techniques have been used for urban climate related research at range of spatial and temporal scales. Thus far, this literature reviewed has focused around observational research. However, this project also utilises numerical land surface modelling to investigate the effects of irrigation on microclimate (HTC and air temperature) during heatwave conditions. The main reason for this modelling is the opportunity to conduct controlled experiments and test the

44

effects of different irrigation scenarios. This research focuses on the cooling potential of irrigation because it is a potentially effective way to distribute water across the urban landscape, timing and volume can be controlled, and can be applied when most needed (i.e. prior to and during a heatwave). Irrigation scenarios allow us to isolate the effects of irrigation on microclimate, which is not a simple task when working with observational data. There have been many modelling techniques used in previous urban climate research. To provide context and justification for the modelling in this research an overview of modelling techniques, and a synthesis of previous research is provided below.

2.4.2 Modelling techniques

There are a number of different modelling approaches that can be used for urban climate applications including computational fluid dynamics (CFD) approaches, land-surface models (LSM), and radiation models. This research utilizes a LSM as the primary modelling tool. All modelling approaches have limitations, but LSM simulate the urban energy balance and are computationally efficient, which allows users to conduct a large number of simulations in time and space. Furthermore, LSM are very commonly used, and the techniques are widely tested, including in a series of large inter-comparison projects (PILPS-urban) (Grimmond et al., 2010, 2011). A large number of urban LSM have been developed, which simulate urban energy and water balances with varying complexity (for example see Table 1 Grimmond et al. (2011)). Grimmond et al. (2010, 2011) include a thorough summary of different modelling methodologies and representations used, as part of the PILPS-urban project (Figure 2.8). LSM approaches are designed to account for the complex atmospheric processes associated with urban surfaces. These models calculate the fluxes of heat, moisture, and momentum between the surface and the atmosphere for different land surfaces and can be used to provide the lower boundary conditions to atmospheric models (Figure 2.9). Urban LSM use a number of different methods for parameterising

the urban morphology including: slab (bulk), single-layer, and multiple-layer approaches. Slab models represent the urban form as a single flat horizontal surface with bulk radiative, aerodynamic, and thermal characteristics (Grimmond et al., 2010). By contrast, some urban LSM have a more complicated representation of the UCL (single and multi-layer urban morphology in Figure 2.8), with roofs, walls, and a roads represented, which allows for more realistic representations of radiative trapping and turbulent exchange (Masson, 2000; Kusaka & Kimura, 2004; Harman et al., 2004; Lee & Park, 2007). Urban LSM have varying complexity, and when coupled with atmospheric models are often used for mesoscale UHI mitigation research.

Coupled approaches ("online modelling") are commonly used in mesoscale urban climate studies (Rosenzweig et al., 2009; Zhang et al., 2009; Grossman-Clarke et al., 2010; Zhou & Shepherd, 2010). Such mesoscale studies often consider city-scale UHI mitigation measures. Urban heat mitigation research investigates ways to intentionally modify the urban surface energy balance and decrease urban air temperature. The most common approach to UHI mitigation modelling is to use a mesoscale atmospheric model coupled with a LSM to simulate atmospheric conditions over the area of interest (Taha et al., 1999; Civerolo et al., 2000; Kikegawa et al., 2003; Tong et al., 2005; Kikegawa et al., 2006; Velazquez-Lozada et al., 2006; Rosenzweig et al., 2009; Zhang et al., 2009; Grossman-Clarke et al., 2010; Zhou & Shepherd, 2010). Mitigation scenarios can be implemented in models by changing the relevant surface characteristics, such as vegetation cover or albedo, to the desired configuration and the effectiveness of the mitigation scenario is modelled as the change in air temperature from a default (unmodified) modelling run. The cooling effects of different UHI mitigation measures varies from study to study, and is typically calculated to be up to 2 °C.

A major focus of mesoscale urban climate modelling has been the effects of vegetation (including trees) in urban area (Ashie et al., 1999; Civerolo et al., 2000; Tong et al., 2005; Kikegawa et al., 2006; Velazquez-Lozada et al., 2006; Mitchell et al., 2008; Takebayashi & Moriyama, 2009;
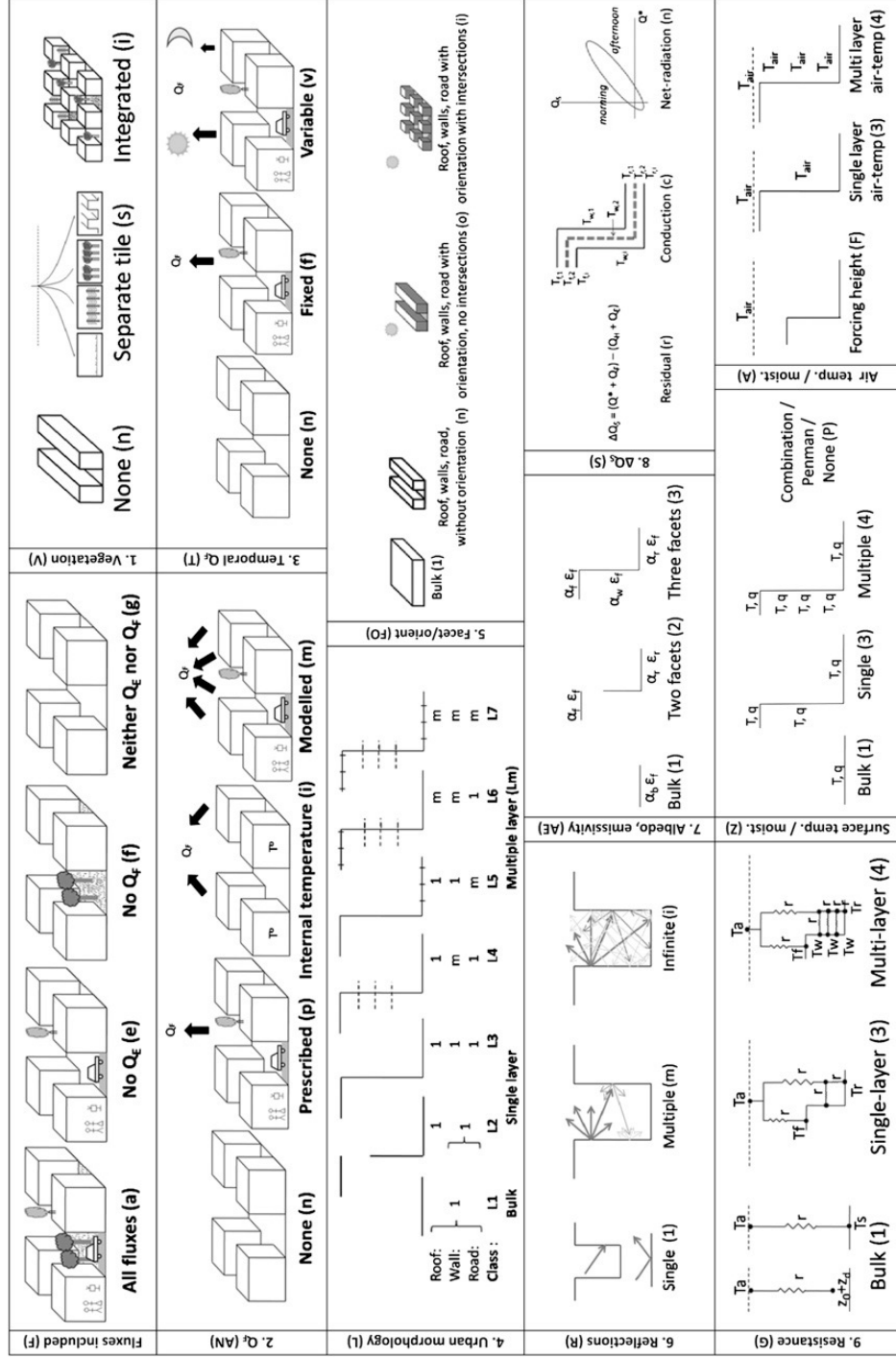
Figure 2.8: An overview of the characteristics of urban LSM. Many different approaches are used by urban LSM. Note that some models do not include vegetation or urban water balance representation. Source: Grimmond et al. (2010).
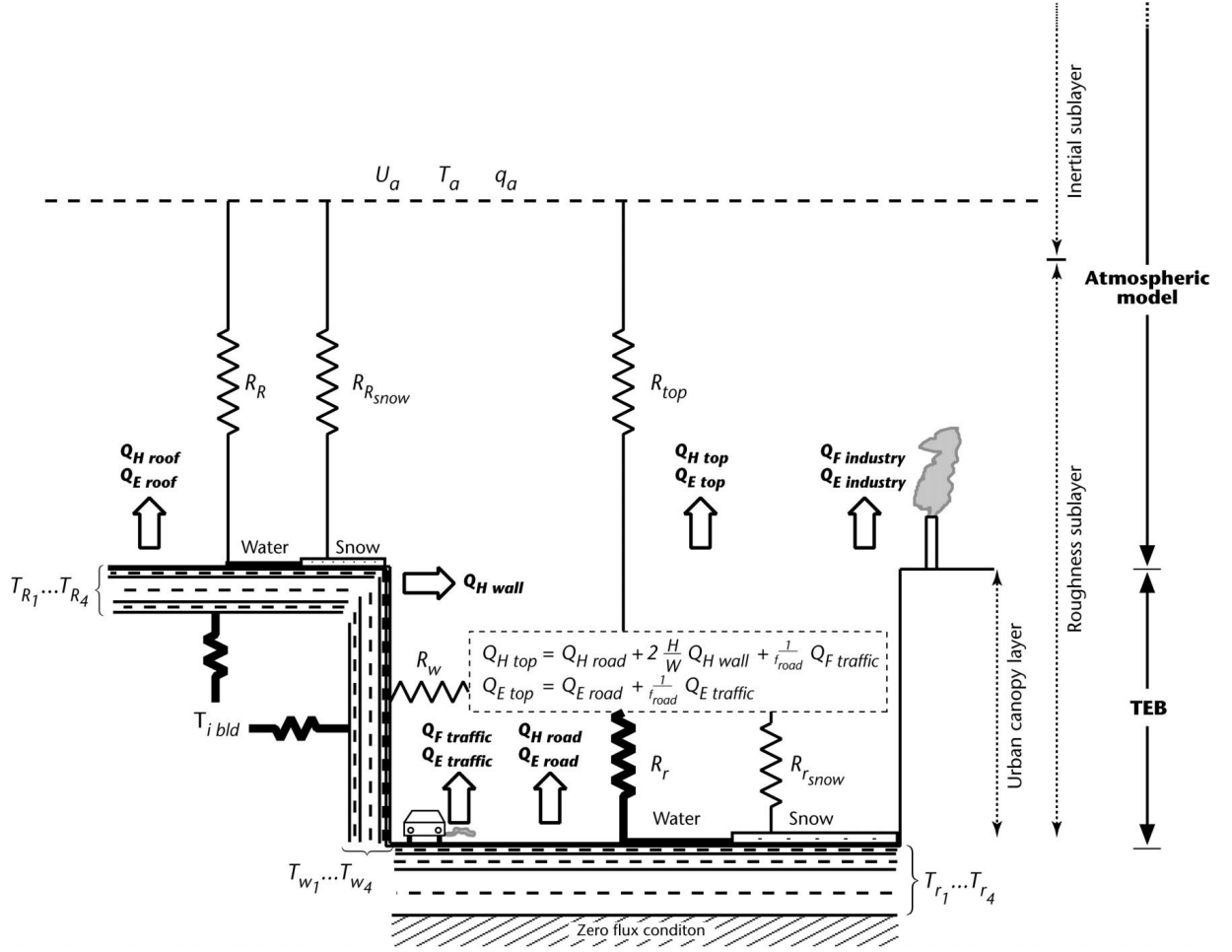
Figure 2.9: A schematic representation of the surfaces (roof, wall, road indicated by subscript R, w, and r, respectively), prognostic temperatures (T), and aerodynamic resistances (R) used in TEB and the output fluxes modelled. Source: Masson et al. (2002).

Zhang et al., 2009; Zhou & Shepherd, 2010; Gober et al., 2010). Inter-comparison of these studies is difficult because different models, cities, regional climates, scenarios, and measures of abatement success were used. However, broadly speaking, these vegetation focused studies are in agreement with the observational research, and show that increased urban vegetation can reduce air temperatures in urban areas. Modelled reductions in maximum air temperature of around 0.5 – 1.5 °C have been observed in New York (Rosenzweig et al., 2009); Hong Kong (Tong et al., 2005); Virginia to Massachusetts (Civerolo et al., 2000); Kobe City Takebayashi & Moriyama (2009); and Tokyo (Ashie et al., 1999; Kikegawa et al., 2006). These studies are encouraging as they suggest that increasing vegetation in cities can significantly decrease urban

air temperature. These coupled LSM-atmospheric model approaches tend to be conducted at a spatial resolution of 1 km or more and do not capture microscale climate. A major limitation of all these vegetation-UHI-mitigation modelling studies is that they do not consider the amount of water that would be needed to maintain increased vegetation, nor the effects of providing this water through stormwater harvesting and WSUD. This means these studies have not fully considered the implications of adding large amounts of vegetation to urban areas. Much like the observational research, there have not been many studies that have directly looked at the role of water in moderating and modulating urban climate.

Despite the potential influence of irrigation shown in observational studies irrigation is largely not included in commonly used urban LSM. A recent study from Monaghan et al. (2014) noted that irrigation is a common activity that should be, but is generally not, represented in urban canopy models. Further, Best & Grimmond (2014) have suggested that irrigation is a critical process that needs to be taken into account by urban surface energy balance models. The authors showed that by adding water to the soil profile in the JULES model, the partitioning of urban Q_E and Q_H was better simulated at sites where urban vegetation fraction was quite high ($> 35\%$) (Figure 2.10). Monaghan et al. (2014) also found that including irrigation in their simulations with the High-Resolution Land Data Assimilation System (HRLDA), improved the accuracy of surface radiative temperature prediction in Houston, TX. These findings support the observational work discussed in section 2.3.2, which showed that urban irrigation can influence urban energy balance, and must be taken into account by modellers and observationalists.

A number of studies exploring the effect of outdoor water-use on urban climate have used the Local-scale Urban Meteorological Parameterization Scheme (LUMPS) (Grimmond & Oke, 2002) or the Surface Urban Energy and Water Balance Scheme (SUEWS) (Grimmond & Oke, 1991; Järvi et al., 2011) to conduct simulations. Gober et al. (2010) used LUMPS to address urban climate and water-use in Phoenix, Arizona. Phoenix has a hot desert climate (BWh
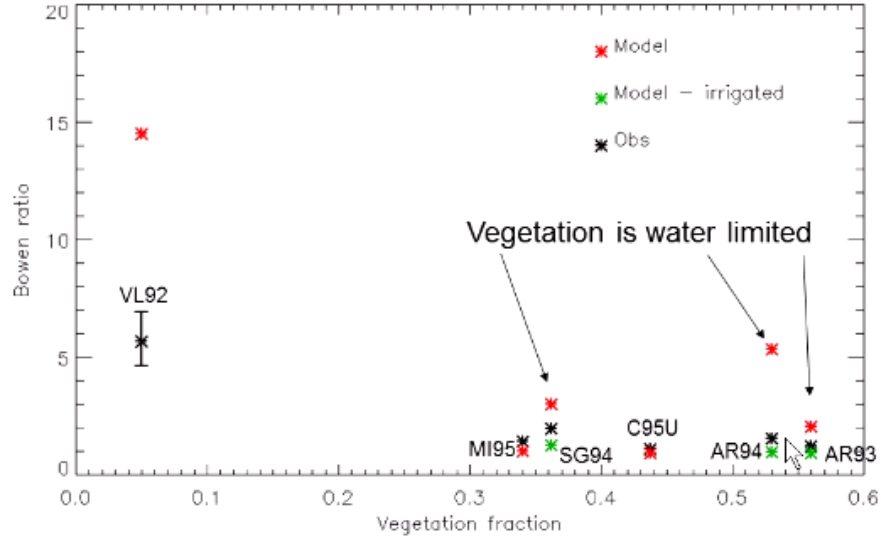
Figure 2.10: The modelled (JULES model) vs. observed Bowen ratios for a range of North American sites. Best & Grimmond (2014) found that simulating irrigation improved model performance at a number of sites where irrigation was commonly observed. Irrigation processes can significantly influence urban water and energy balances and should be taken into account by urban LSM. Source: Best & Grimmond (2014).

under Köppen climate classification), which means conditions are extremely dry and irrigation is essential for maintaining non-native vegetation. LUMPS was used to calculate monthly average ET and nighttime cooling changes over 10 census tracts with different planning and water-use characteristics. They found that increasing irrigated vegetation by 20% led to nighttime cooling but required 32.8% more outdoor water-use. With regards to effectiveness of water-use, a key finding from Gober et al. (2010) was that the relationship between ET and nighttime cooling was nonlinear (Figure 2.11 describes the relationship between ET and cooling rate), indicating that the magnitude of nighttime cooling levels off when ET rates (and irrigation) are high. This relationship means more cooling can be achieved through increased ET in dry areas. This implies that adding water is a thermally inefficient strategy for reducing temperatures in densely vegetated and well watered neighbourhoods. This raises an important question for this research, as the relationship between ET and nighttime cooling is non-linear, methods for optimising cooling via water-use must be considered. WSUD can provide additional water for irrigation,

and applying this additional water in such a way that maximises cooling is preferable.

In another simulation, Gober et al. (2010) explored the urban climate effects in the city during water shortages, by replacing 10% of vegetation with unmanaged soil. The water shortages scenario showed that nighttime cooling rates would decrease by 0.16–0.39 °C hr^{-1} while 12.8% less water was used. Gober et al. (2010) addressed the notion of water availability indirectly, as water-use was calculated as a function of ET, which varied due to the percentage of vegetation cover in their simulations. However, water-use practices can vary significantly within urban areas, especially when there is shortage of supply and water is expensive. Undoubtedly, the percentage of urban vegetation cover will decrease during sustained drought (as the Gober et al. (2010) scenario simulated) but so too will the overall in situ water content of all urban surfaces. Gober et al. (2010) do acknowledge that modelled ET and water-use diverged most significantly in areas that were highly heterogeneous and had low levels of irrigated vegetation. As such, an approach where irrigation is actively simulated within the urban LSM is needed for directly capturing the effects of irrigation on temperature variability, especially at higher spatial and temporal resolutions.

The Gober et al. (2010) study is an important piece of work because, unlike most urban climate modelling studies, it acknowledges the intertwined issues of water-use and urban climate. However, there is another methodological issue that should be mentioned. LUMPS uses a bulk approach, which means that the urban form is represented as a flat horizontal surface with appropriate "bulk" radiative, aerodynamic, and thermal characteristics (Figure 2.8). This means that the LUMPS LSM does not contain a UCL morphology representation, and thus does not attempt to fully simulate UCL temperatures. PILPS-urban showed that more complex LSM do not necessarily improve flux predictions above the UCL. However, a number of studies have shown that LSM that include canopy layer morphology can improve predictions of air temperature observations made in the UCL (Masson, 2000; Kusaka et al., 2001; Hamdi & Masson, 2008).

51
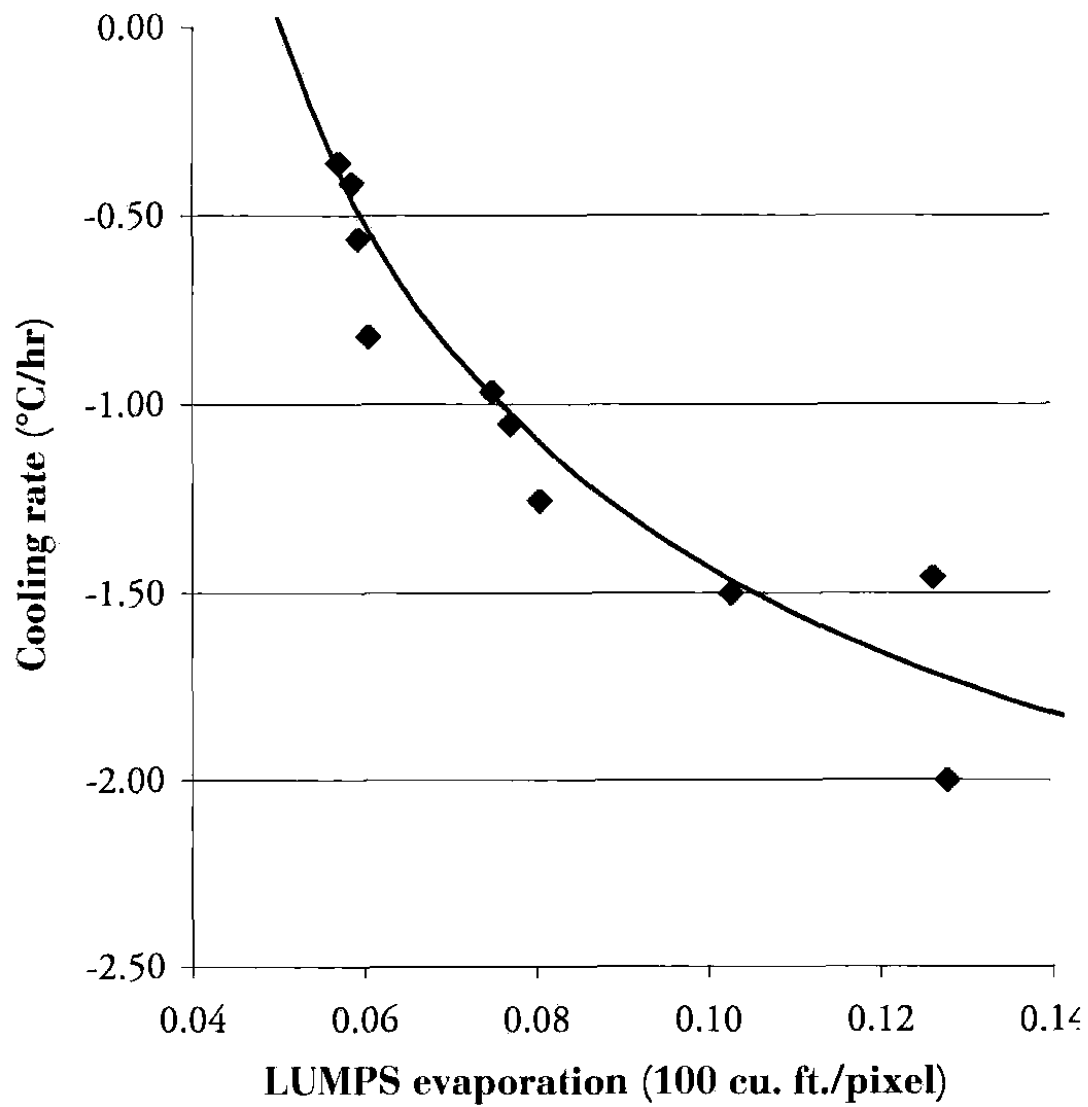
Figure 2.11: The non-linear correspondence between rates of nighttime cooling and ET in Phoenix, AZ. This finding implies that the application of water is inefficient at achieving cooling in areas where water availability is already high. Source: Gober et al. (2010).

Gober et al. (2010) relied on a very simple 1-dimensional boundary layer model to translate changes in LST to air temperature, so these estimates of air temperature therefore do not account for advection or the 3D effects of urban morphology. This lack of UCL representation is a problem for research that is interested in human exposure to heat because the climate of human exposure is not captured. Moreover, the temporal scale of Gober et al. (2010), which looked at 1 month averages, is too low resolution for human exposure research. For human exposure studies, a temporal resolution that captures the dynamics of damaging extreme events is necessary.

Two other studies utilise a very similar approach to the study including a study from Portland, Oregon (House-Peters & Chang, 2011) and a study conducted for Canberra, Australia (Mitchell et al., 2008). These studies used LUMPS and SUEWS, respectively to investigate water-use and urban climate relationships. Both studies use a bulk approach and rely on the simple boundary layer model (mentioned above) to simulate air temperature. House-Peters & Chang (2011) used downscaled general circulation model (GCM) scenarios and LUMPS (0.5 km resolution) to investigate the interplay between future urban planning styles and outdoor water-use consumption in Portland. They found that a 3 °C global warming scenario and an urban sprawl style development increased outdoor water consumption by 4061 L per household (for the month of August); the increased water use also created a small positive trade-off of about 0.1 °C of nighttime cooling. By contrast, a dense development scenario caused less water consumption and caused 0.3 °C of nighttime heating. House-Peters & Chang (2011), much like Gober et al. (2010) did not directly simulate irrigation, and the scale used and UCL representation meant that microscale climate was not captured.

Mitchell et al. (2008) compared six different WSUD and water-use scenarios in a suburb in Canberra (4 km^2) where outdoor irrigation is common (44% of residential water consumption), with a hypothetical desert landscape (a city with no vegetation and no ET) (see Figure 2.12). This is one of only a couple of major urban climate modelling studies that has explicitly con-

Scenario	Summer E (mm day^{-1})	Average heating rate (°C h^{-1})	δT_{amax} (°C)
(1) Conventional urban layout	1·58	1·64	−4·6
(2) Wetland added to conventional urban layout	1·61	1·63	−4·7
(3) Grass swales added to conventional urban layout	1·60	1·64	−4·6
(4) Vegetated roof conversion	1·73	1·59	−5·0
(5) Full vegetated WSUD treatment train	1·76	1·58	−5·1
(6) Full vegetated WSUD treatment train with 50% reduction in garden watering	1·60	1·63	−4·6
(7) Full vegetated WSUD treatment train with 100% reduction in garden watering	1·44	1·69	−4·2
Desert	0·00	2·15	0·00

Figure 2.12: A table showing the summertime E (from Aquacycle simulations) converted to diurnal heating rates and the consequent effect on peak afternoon air temperatures for each of the seven scenarios relative to a "desert". Source: Mitchell et al. (2008).

sidered the effects of WSUD. The authors used SUES (an earlier version of SUEWS), which is an extension of LUMPS, and includes a full water balance including irrigation practices. The results showed that a full WSUD treatment (including WSUD features of vegetated roofs, grass swales and a wetland) was able to maintain similar rates of ET and peak afternoon maximum temperatures (without irrigation) to a conventional urban layout (with irrigation). In comparison with a desert landscape (zero ET), a full WSUD treatment with a 100% reduction in garden watering in the urban landscape, could reduce peak afternoon temperatures by up to 4.2 °C (Figure 2.12). This suggests that the implementation of WSUD can match the cooling potential of irrigated urban landscapes, while using much fewer potable water supplies. In another modelling study that directly considered WSUD practices, Demuzere et al. (2014) implemented biofiltration systems, rainwater tanks, and urban irrigation representation in the Community Land Model-Urban (CLMU) (Oleson et al., 2008b,a). Demuzere et al. (2014), tested the new implementation in Melbourne Australia and found that a large amount of stormwater was available for indoor and outdoor water uses, and ET from the bio-filter was an order of magnitude larger compared to the contributions from the impervious surfaces. While Demuzere et al. (2014) did not directly consider air temperature, the modelling results suggest that WSUD treatments can significantly increases ET and therefore can potentially lead to a cooling of air temperature in urban areas.

The findings from these studies further emphasise the potential for outdoor water-use practices to modify urban climate. Studies such as Mitchell et al. (2008), show how changes in land cover can affect average temperature and water-use. However, much like Gober et al. (2010) the spatial and temporal scale used, and the modelling techniques used, do not actually capture microscale climate nor actual human exposure to heat stress. With regards to exposure to heat stress, there has been little modelling research (although there has been a few observational studies e.g. Shashua-Bar et al. (2011)) that has investigated the potential for outdoor water-use to be used as a mitigation measure during extreme heat events. Cooling via irrigation is appealing because water can be applied during and/or before a heat event, and distributed widely, to promote cooling when and where it is needed most. However, few studies have directly considered the cooling effect of irrigation during extreme heat conditions.

One study that did investigate irrigation during an extreme heat event was Grossman-Clarke et al. (2010). They investigated the impact of land cover/land-use changes on near-surface air temperature during EHE using the Weather Research and Forecasting (WRF) model, the Noah LSM (Chen et al., 1997), and the urban canopy model (UCM) (Kusaka & Kimura, 2004). The Noah LSM does not account for irrigation but assumes a climatological soil moisture content as obtained from WRF initial conditions. Grossman-Clarke et al. (2010) adjusted the soil moisture content for urban vegetation and irrigated agricultural land to the reference soil moisture that corresponds to field capacity. The authors found that land cover/land-use changes associated with urban development caused an intensification and expansion of the area experiencing extreme temperatures during the heatwave and nighttime temperatures in the urban core showed increases of up to 2 °C. Daytime temperatures were not significantly affected when urban development replaced desert land (increase by 1 °C); however, maximum temperatures increased by 2–4 °C when irrigated agricultural land was converted to suburban development. Additionally, urban "landscaping" irrigation caused 0.5–1.0 °C cooling to nighttime air temperature during extreme

events. This is the only study that has directly looked at whether irrigation can cool the urban environment during extreme heat. The Grossman-Clarke et al. (2010) study has a much better temporal resolution for considering human exposure to heat because specific EHE were examined. Furthermore, the use of UCM and WRF means that processes in the UCL and advection are accounted for, but the spatial scale was still quite coarse and probably captured the average mesoscale conditions (not the actual microscale variability) that humans were exposed to during the heatwave.

Overall, none of the urban LSM studies discussed above have attempted to capture microscale temperature variability. As discussed in the section 2.2.3, the variability at the micro to local-scales can be as large as the UHI intensity. This means that in the modelling studies discussed above, the variability within a single grid cell could be very large. As this research is interested in understanding the variability of climate that humans are exposed to, it must attempt to resolve the microscale urban climate variability. For microscale modelling studies there are typically a number of other approaches that are commonly used. CFD based approaches model wind flows around urban landscapes, such as buildings and trees. CFD models solve the Navier-Stokes equation to calculate flow fields within the UCL. While CFD based models are useful for microscale simulations, they are known to be highly computationally demanding. The most commonly used CFD based approach is probably the ENVI-met model (Bruse & Fleer, 1998). ENVI-met has been used for a large number of microscale urban studies, but a number of authors have found deficiencies in ENVI-met simulations including issues relating to radiative fluxes (Ali-Toudert & Mayer, 2006a), wind speed (Krüger et al., 2011), and air temperature (Spangenberg et al., 2008) calculations. Furthermore, this research aims to capture variability in microscale climate across a large spatial area, and generally CFD simulations were deemed to be too computationally expensive. Irradiance models are also commonly used for microscale modelling applications. Irradiance models such as SOLWEIG (Lindberg et al., 2008), are a useful

way to simulate the microscale radiant fluxes (including MRT) and shading patterns in urban areas. However, because radiation models do not fully simulate the urban energy (Equation 2) or water balance (Equation 1) the effects of convective fluxes (Q_H and Q_E) on UCL are not captured. In order to simulate the effects of irrigation and WSUD, this research requires an approach that is computationally efficient, and also simulates the surface energy and water balances, meaning a LSM approach is necessary.

For for finer scale LSM simulations accurate representation of the UCL is essential. Some LSM have more sophisticated representation of the UCL and urban morphology (Figure 2.8 — see urban morphology). PILPS-urban (Grimmond et al., 2010, 2011) showed that more complex representations of urban morphology do not necessarily improve model performance. However, PILPS-urban did not evaluate the models' ability to calculate UCL climate variables. Other research has shown that urban canopy morphology representation can improve simulations at smaller scales and in the UCL (Masson, 2000; Kusaka et al., 2001; Hamdi & Masson, 2008). It is thought that the representation of the UCL (single or multiple layer schemes) is necessary for this research as we wish to simulate street level meteorological variables inside the UCL.

Additionally, for UCL simulations the representation of vegetation in the LSM is important. As seen in Figure 2.8, models can use integrated (vegetation in the canyon) or separate tile (vegetation simulated separately) approaches to simulate vegetation. Tiled approaches build on previous knowledge from ecological land surface modelling, but are probably more suitable at larger scales (i.e. when the urban area is sub-grid scale) (Best & Grimmond, 2014) or when urban areas are highly discretised into urban and natural patches. There are a number of integrated vegetation models that are current available (Lee & Park, 2007; Lemonsu et al., 2012b; Krayenhoff et al., 2015). Lemonsu et al. (2012b) used an integrated vegetation approach (Figure 2.8), an urban canopy layer scheme, and detailed information from two courtyards located in Israel (see (Shashua-Bar et al., 2009) for details) to successfully model microscale air temperature in the

57

courtyards. Lemonsu et al. (2012b) suggest that the integrated approach opens up opportunities to study the urban microclimate down to the micro (or canyon) scale. As such, an integrated approach may be the best option for simulating microscale UCL climates. For this research a LSM that includes vegetation processes within the canyon is needed.

2.5   Urban climate modelling summary

- There are a range of modelling techniques that are available for urban climate studies. The different approaches have strengths and weaknesses and can be used for different modelling applications. However, observed and modelled data need to match the scale of application.

- Despite the potential for irrigation to have a significant effect on urban temperature, most models do not directly account for irrigation or other WUSD features (e.g. bio-filters).

- Only a few studies have considered the effects of irrigation and outdoor water-use in an urban climate modelling context. Modelling suggests that irrigation can be an important source of ET in urban areas, and this can contribute to air temperature. In one study, up to 2–4 °C of cooling was attributed to irrigation during heatwave conditions.

- Although irrigation shows good potential as an urban heat mitigation measure, no modelling studies have attempted to model the effects of irrigation/outdoor water-use on microscale air temperature during heatwave conditions. The potential for irrigation to be used as a heat mitigation measure during extreme conditions, and reduce human exposure to extreme heat, has not been investigated.

- For this research key processes that must be modelled accurately are the urban water cycle (including irrigation), vegetation in the canyon, and the UCL air temperature.

- Microscale models are available for UCL simulations, such as CFD and irradiance models, but such approaches are too computational demanding or do not capture the urban

water/energy balance sufficiently. Actively simulating irrigation and WSUD using these microscale modelling approaches is not currently possible. Additionally, one commonly used microscale model (ENVI-met) has been shown to have some potential problems, and will not be utilised in this research.

2.6 Summary of knowledge gaps and resulting research objectives

Given the theoretical and conceptual background to urban climate observations and heat mitigation modelling research provided in this literature review, the objectives of this research, surrounding the effects of WSUD on urban microclimate (outlined in the introduction), can now be re-examined. These research objectives directly address the knowledge gaps identified in this literature review. In this section the research objectives are outlined in the context of the major knowledge gaps that have been identified.

A major knowledge gap identified in this literature review was that, although there is a lot of observational precedence for the cooling potential of WSUD and irrigation, no published observational studies have directly looked at the effects of WSUD on climate. Despite the interconnected nature of urban water balance and urban climate, the effects of WUSD on microscale and local-scale climate are largely unknown. As such, there is need for observational studies to quantify the effects of WUSD on urban microclimates, particularly in Australia where water shortages are a persistent problem. To approach this knowledge gap we propose the following research objective: **objective 1: identify the observed microscale air temperature and HTC variability in a WSUD suburb.** We conducted a high resolution field campaign in a prototype WSUD suburb called Mawson Lakes, which is located in Adelaide, South Australia. A full description of the Mawson Lakes field campaign is provided in chapter 3.

Another major theme identified throughout the microscale and local-scale urban climate observational literature was that the complex nature of the UCL makes it difficult to infer the

effects of a single feature or mitigation measure on microclimate. In the UCL, many factors contribute to air temperature variability, making it difficult to assess the effectiveness of WSUD at cooling urban microclimate. Nevertheless, designers and architects do require reliable and easily interpretable guidance on the cooling effects of different land surface features. To explicitly address this issue the following research objective has been set: **objective 2: generate robust estimates for the cooling potential of WSUD features on microscale air temperature.** In order to have meaningful understanding of the cooling effects of WSUD, this research must establish a strong link between the drivers of urban microclimate (including WSUD) and observed microclimate variability. To achieve this objective 2 will draw on the Mawson Lakes observational data.

This literature review also revealed that the effect of WSUD (and urban water-cycle management in general) has received a very small amount of attention in the urban climate modelling literature. This dearth of water focused research exists, despite the fact that there is good evidence that irrigation (and outdoor water-use practices) can have cooling benefits. Some water cycle focused urban climate modelling has been done, but the spatial and temporal scales looked at were too coarse to capture microscale variability and HTC effects. In particular, the use of irrigation during heatwave conditions, and the potential for surface watering to reduce human exposure to extreme heat has received minimal attention. In response to these knowledge gaps we propose two additional modelling focused research objectives:

- **objective 3: Calculate the potential for irrigation to reduce exposure to adverse extreme heat conditions (air temperature).**

- **objective 4: Calculate the effect of irrigation on microscale HTC under extreme heat.**

A full description of the modelling techniques used for both of these objectives is provided in

chapter 3.

As shown, this research will employ a combination of observation and modelling approaches to address the research objectives discussed above. The combined results from the field observations and the modelling will provide highly relevant information for urban planners and practitioners in Australian cities. The results from this research can be used to improve understanding of the climate benefits of WSUD and integrated water management approaches. A full description of the methodology and data used in this research is provided in the chapter 3 below.

3 Methodology

3.1 Introduction

The overarching aim of this research is to quantify the potential for WSUD and stormwater reintegration techniques to mitigate urban warmth and improve HTC, during extreme heat events. As outlined in section 2.6, there are four major objectives in this research that address the gaps identified in the urban climate literature. To achieve these objectives a combination of observational and modelling techniques were used. In this chapter the observational and modelling techniques are described in full.

3.2 Summary of research approach

The overall approach of this research, with respect to the different research objectives, is summarised in Figure 3.1. All the research objectives draw on the Mawson Lakes field campaign; and the Mawson Lakes dataset is the basis of all the analysis conducted in this project. Mawson Lakes is a suburb and new residential development in the City of Salisbury, Adelaide. The city of Adelaide was chosen because it has a naturally hot and dry summertime climate, which means it is susceptible to EHE and adverse meteorological conditions. Mawson Lakes was chosen as the focal suburb because it contains a number of WSUD features, and the suburb has a dual water supply system, which provides harvested stormwater for non-potable uses (e.g. irrigation). The nature of the Adelaide regional climate, and the WSUD features already in place, meant that Mawson Lakes represented a good case study site to investigate the potential microscale cooling effects of WSUD and stormwater harvesting.

The field campaign that was conducted in Mawson Lakes was designed to capture the microscale air temperature and HTC variability across the suburb (**objective 1**). The aim was to
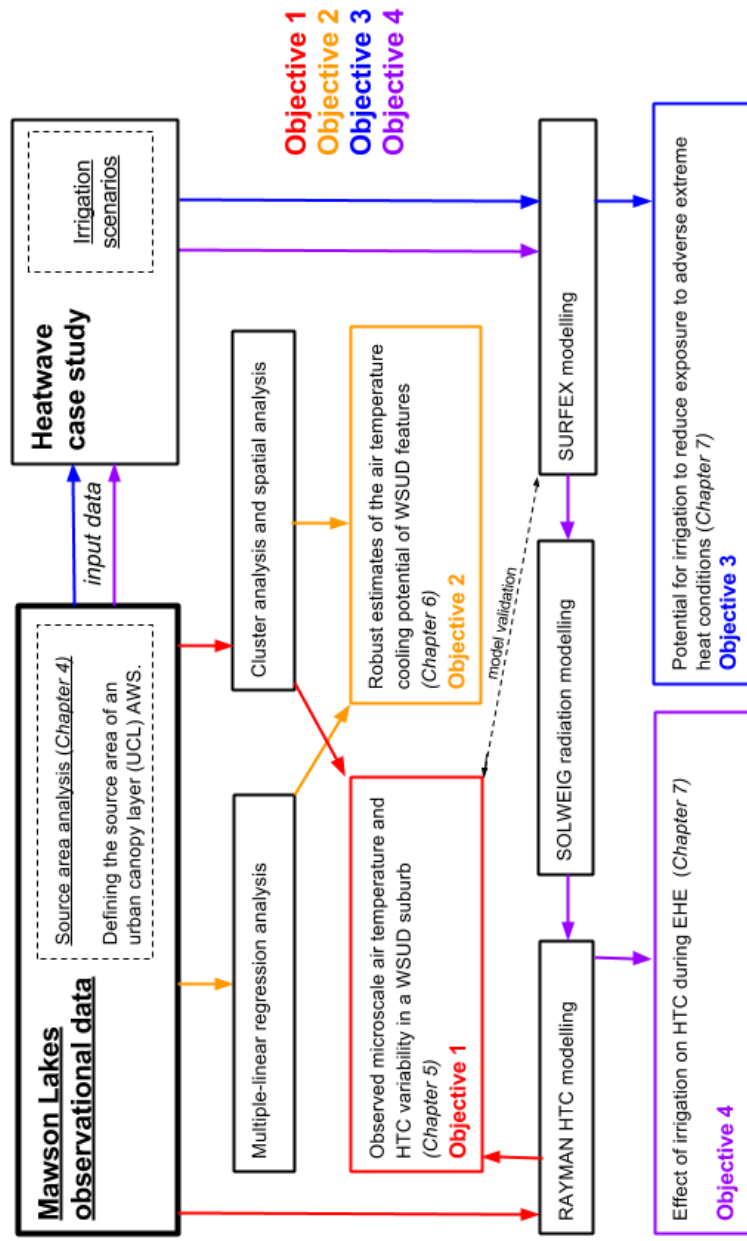
Figure 3.1: An overview of the research approach. The pathway to the research objectives (outlined in the introduction) are indicated by the coloured arrows.

capture both air temperature and HTC variability because these metrics are both important for human health and well-being considerations, and both metrics are influenced by different factors. To capture microscale air temperature and HTC variability a range of observational techniques were used including static weather stations, bicycle transects, and high resolution remote sensing. These observational techniques (described in this chapter) were chosen as they allowed us to capture the microscale climate in the UCL. The range of techniques used were chosen to complement each other and provided a high resolution picture of the microclimate variability in the suburb. All the data collected during the Mawson Lakes campaign are described in this chapter, while the results from **objective 1** are given in chapter 5.

As discussed above, a review of the relevant literature identified that intra-urban observational studies often do not isolate the effects of individual features on microclimate. As such, a major aim of this project is research **objective 2**, which is centered around robustly quantifying the cooling effects of WSUD. To address this objective a source area analysis was also conducted, with a focus on the static weather station data from the Mawson Lakes campaign (Figure 3.1). The source area analysis helped us to isolate the surfaces that a static weather station was affected by. The details surrounding this source area analysis are included in chapter 4. To achieve **objective 2** the meteorological data from the Mawson Lakes field campaign, and the source area estimates (chapter 4) were used to relate land cover variability (collected during the Mawson Lakes campaign) to microscale air temperature variability using multiple-linear regression methods. A description of the data used for this analysis is provided in this chapter, while results and additional methodological information about this analysis are provided in chapter 6.

The literature review showed that the effect of irrigation on urban microclimate has not received much attention in urban climate modelling studies. To look at the effects of irrigation, two numerical modelling focused research objectives were set: **objective 3** and **objective 4**.

The two major reasons that a numerical modelling approach was chosen were (1) the modelling approach allowed us to easily isolate the effects of irrigation on microclimate and (2) to estimate the effects of hypothetical irrigation scenarios during extreme conditions. Capturing heatwave conditions was important because we are interested in the potential for heavy irrigation to alleviate heat stress during heatwaves. However, heatwave conditions were not observed during the Mawson Lakes observational campaign.

The primary modelling tool used in this research was the SURFEX modelling package (Masson et al., 2013). SURFEX was chosen to do the modelling analysis as it contains representation of: irrigation, canyon morphology, and in-canyon vegetation. The literature review identified that these were important requirements for modelling at finer scales. Additionally, SURFEX has been used in a previous study to successfully simulate local to microscale air temperatures (Lemonsu et al., 2012b). Offline simulations using land cover data (collected during the Mawson Lakes campaign) and an atmospheric forcing dataset were used to address **objective 3**.

However, to calculate changes in HTC associated with irrigation (**objective 4**) an estimate of microscale MRT was needed. Therefore, to calculate thermal comfort, MRT estimates from SOLWEIG (irradiance model) were used in conjunction with the meteorological outputs from SURFEX (Figure 3.1) to calculate thermal comfort indices (Figure 3.1). A description of the models and modelling methodology used is provided in this chapter (see section 3.5). Additional information about the modelling analysis and modelling results is given in chapter 7.

This chapter is divided into four major sections: Section 3.3 describes the area of interest, including Adelaide and Mawson Lakes; Section 3.4 summarises the Mawson Lakes observational campaign and data collected; and Section 3.5 describes the models used in this research.
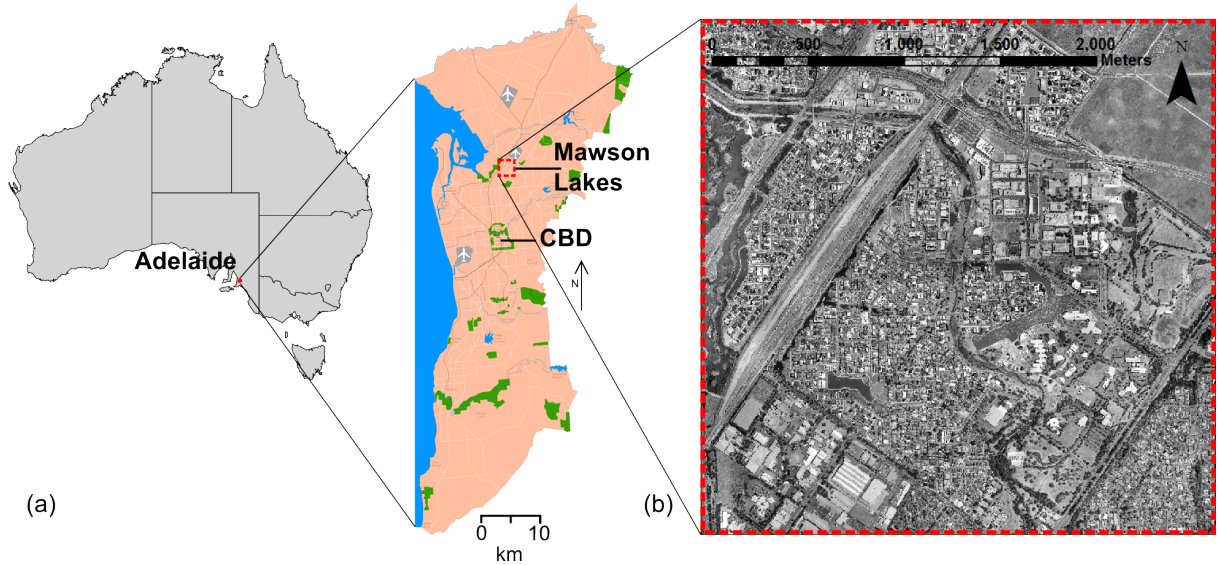
Figure 3.2: A map of the site location: (a) Mawson Lakes, Adelaide, South Australia (source: Wikimedia Commons) and (b) satellite imagery of area of interest (Source: Nearmap). Mawson Lakes is located on the urban fringe of South Australia's capital city, Adelaide.

3.3 Site characterisation

3.3.1 South Australia and Adelaide

South Australia is Australia's 4th largest state, and makes up the southern central portion of the Australian continent (Figure 3.2a). The southern state border is formed by the Great Australian Bight, while the northern and western parts of the state make up a large portion of central Australia and are characterised by very arid and sparsely populated terrain. The majority of South Australia's 1.6 million inhabitants live in Adelaide, which is located in the state's more fertile south eastern regions. Adelaide is the capital city of South Australia, with an estimated population of 1.3 million people (2014) (ABS, 2014); making Adelaide Australia's 5th largest city. It is a coastal city located on the eastern side of the Gulf of St Vincent and north of the Fleurieu Peninsula (Figure 3.2). The city stretches 20 km from the coast to the foothills of the Mount Lofty Ranges. The metropolitan region has a total area of 870 km^2.

Adelaide's climate is classified as Mediterranean (Csa) under the Köppen climate classifica-

tion. This means that winters are generally mild and wet, and summers are hot and dry (Figure 3.3). The average maximum temperature and rainfall in Adelaide during summer is 27.0 °C and 28.0 mm, 29.2 °C and 19.3 mm, and 29.4 °C and 12.4 mm for December, January, and February, respectively. Adelaide's hot and dry summers are frequently punctuated with EHE. The 2009 southeastern Australia heatwave was a recent EHE, which caused record-breaking prolonged high temperatures in the region. The heatwave occurred between the 27th January and 8th February (13 days). On the 28th January, Adelaide reached a maximum temperature of 45.7 °C and an overnight low of 33.9 °C. The average maximum temperature between the 27th of January and 7th of February was 40.5 °C. This caused significant increases in hospital admissions, ambulance call-outs, emergency department presentation, and mortality (especially amongst the elderly) in Adelaide (Nitschke et al., 2011). The hot and dry conditions that frequently cause heat stress in Adelaide necessitate heat mitigation, but this can be difficult when water availability is low.

South Australia is Australia's driest state, with much of the interior of the state receiving less than 200 mm of rainfall per year. As such, Adelaide depends on the Murray-Darling River system for much of its water supply. During drought years up to 90% of Adelaide's water supply comes from the River Murray (SA Water, 2015). A period of prolonged drought from 1997–2009 saw storage levels in many of Adelaide's reservoirs drop to very low levels. Low reservoir levels have stressed water supplies in Adelaide and water restrictions have been enforced. These drought conditions and water-shortages have lead to behaviour and infrastructure changes, which are designed to reduce water-use. Many Adelaide residents have transitioned to drought resistant gardens, with native vegetation types and/or rock features. Other developments have chosen to seek alternative water supplies so that traditional mesic (green) type gardens can be maintained. This includes WSUD approaches, which facilitate the capture, treatment, and re-integration of stormwater runoff. As discussed in detail in chapter 2, these WSUD features, which promote ET, are likely to have positive benefits for urban microclimate. Mawson Lakes is one suburb
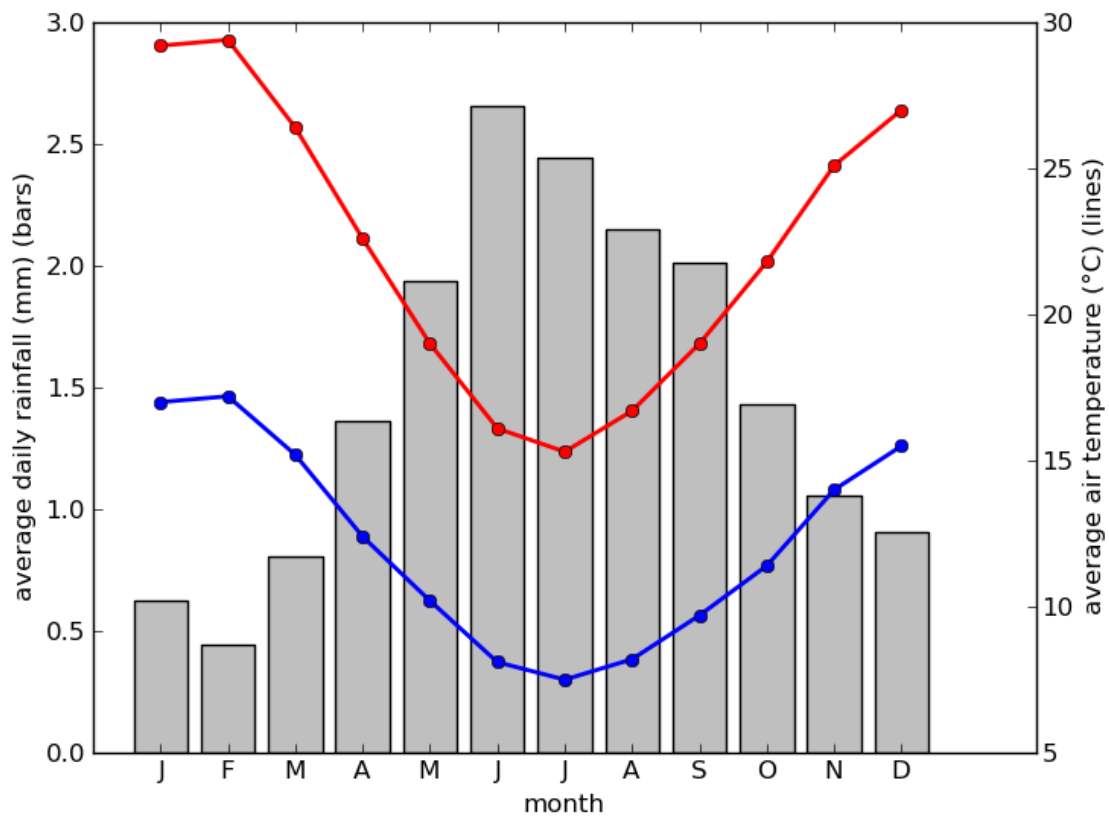
Figure 3.3: A representation of the average monthly rainfall (bars), maximum (red) and minimum (blue) air temperature for Adelaide city (1977-2011) (Bureau of Meteorology—Kent Town—station ID 23090). Adelaide has a hot Mediterranean climate with hot and dry summers and mild and wet winters. Adelaide's climate is characterised by frequent heatwaves during summer. These climate characteristics mean that Adelaide is vulnerable to heat stress conditions.

that has implemented some of these WSUD technologies, including a large stormwater harvesting and storage system. All these factors make Mawson Lakes an excellent site for understanding the potential for WSUD and stormwater reintegration techniques to mitigate urban warmth and improve HTC in urban areas.

3.3.2 Mawson Lakes

Mawson Lakes is a mixed residential suburb located 12 km north of Adelaide, South Australia (Figure 3.2b). Mawson Lakes is a moderate to low density suburb (Figure 3.4). Using the local climate zones (LCZ) from Stewart & Oke (2012), Mawson Lakes consists of open low-rise, open mid-rise, and compact mid-rise LCZ. The mid-rise commercial and residential areas are located north of the Sir Douglas Mawson Lake (SDML) and the majority of low-rise residential areas are located west of the river (named Dry Creek) (Figure 3.4). This prototype development has been built with a number of WSUD features, which could have cooling benefits for urban microclimate. The suburb has a dual water supply system, which delivers potable and recycled water via separate piping systems (Figure 3.5). Stormwater runoff from impervious surfaces is channelled into the Salisbury Wetlands (west of the suburb) (Figure 3.4) where it is treated via bio-filtration methods and pumped into an underground aquifer for storage (Figure 3.5). This treated stormwater is mixed with treated wastewater and pumped back to the surface for use in toilet flushing, domestic irrigation, and watering of public spaces (Figure 3.2c). Mawson Lakes contains a number of large artificial lakes (SDML and Shearwater Lake), which have been built-up using treated stormwater (Figure 3.4). The WSUD features of interest in this study include: large bio-filtration wetlands (e.g. Figure 3.6d), water courses (e.g. Figure 3.6b & 3.6c), irrigated green space (e.g. Figure 3.6e & 3.6f), and artificial lakes (e.g. Figure 3.6g & 3.6h). Although most of these structures were not constructed with urban cooling in mind, all of these features (shown in Figure 3.6) could contribute to increased Q_E and decreased Q_H, which may have
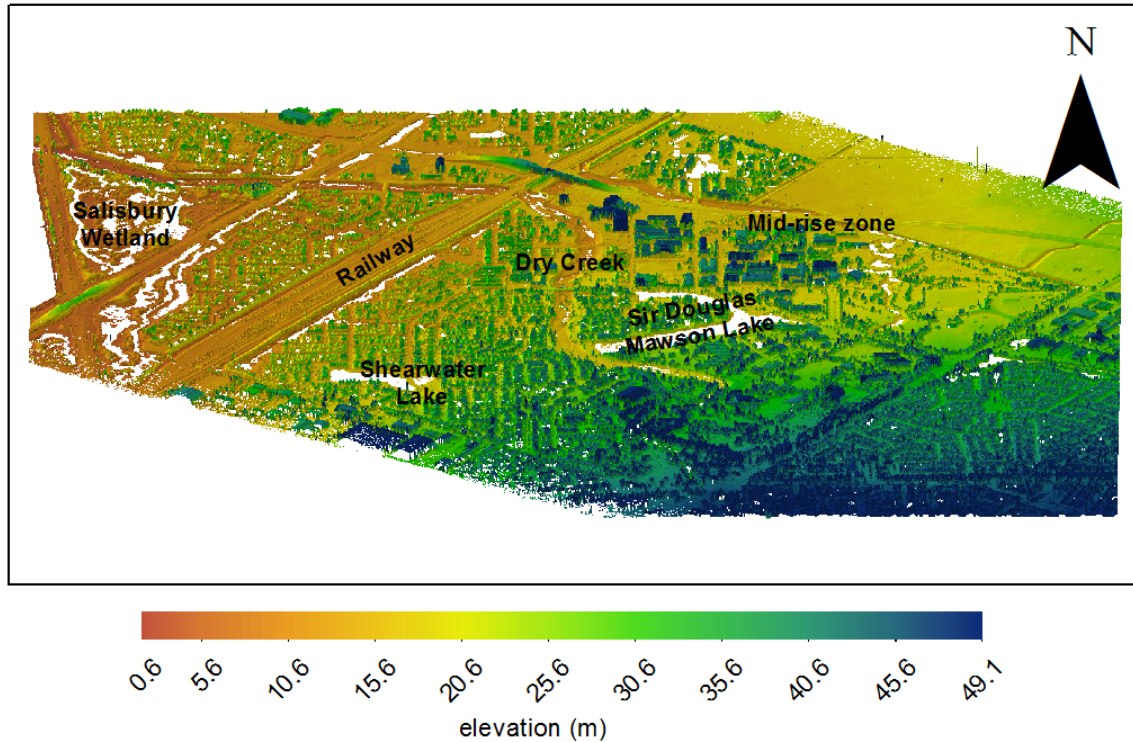
Figure 3.4: A digital elevation model of the Mawson Lakes suburb. The terrain of the area slopes gently downhill towards the west. The suburb contains mostly low-rise residential land-use. However, there is a small mid-rise commercial and residential area located in the north-eastern part of the suburb. As the suburb is relatively new the majority of trees in the area are quite small.

cooling benefits for urban microclimate. This research is interested in the cooling potential of WSUD features for reducing exposure to extreme heat in urban areas. To address the research goal, the Mawson Lakes suburb was chosen as a case study environment to investigate the effects of WSUD on climate.

3.4 Mawson Lakes field campaign

3.4.1 Overview

The Mawson Lakes field campaign was conducted during mid February 2011 (end of austral summer). A range of data acquisition techniques, including static automatic weather stations (AWS), bicycle transects, and aircraft-based remote sensing were used. This ensemble of data
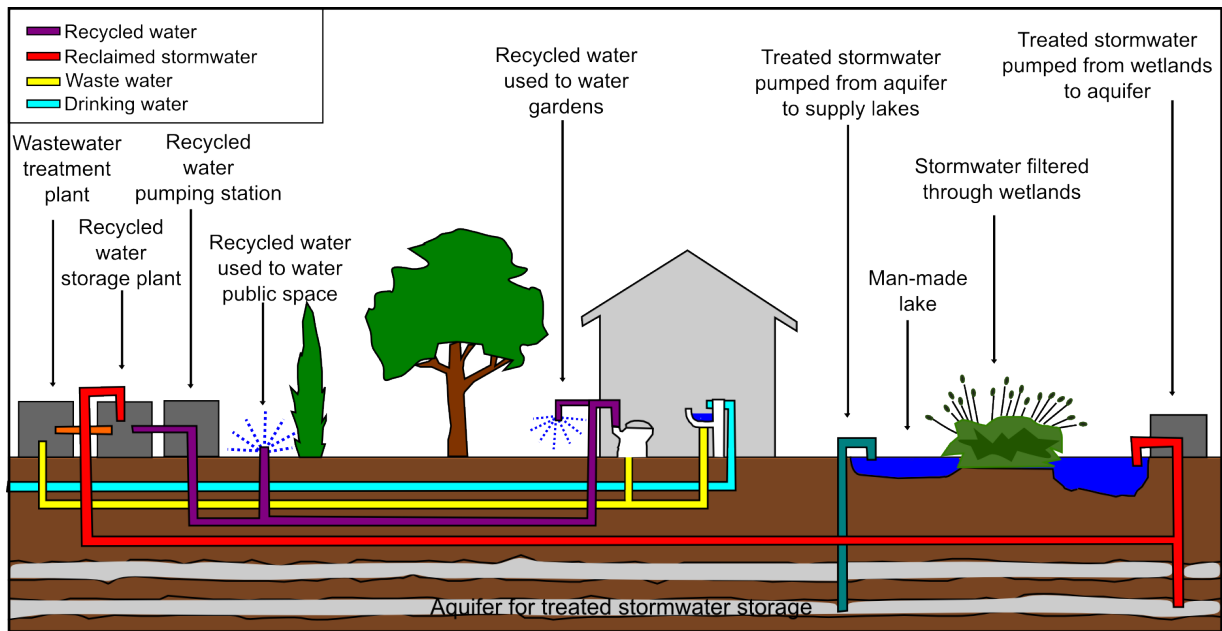
Figure 3.5: A schematic of the Mawson Lakes dual reticulated water supply and stormwater harvesting system. Treated stormwater and wastewater is stored in aquifer underground. Reclaimed stormwater and treated wastewater is pumped from the aquifer to supply artificial lakes and is used for non-potable end uses such as garden irrigation. Recycled water is supplied to households via a separate piping system (purple pipe) to traditional potable grade water (blue pipe). Modified after Lend Lease (2006)

collection techniques was designed to provide spatially detailed datasets that accurately resolved high-resolution microclimate and land surface variability within the suburb. A high resolution (spatial and temporal) approach was essential for capturing the variability in microclimate that urban dwellers are exposed to in the UCL. The combination of high resolution remote sensing data and a dense network of static and mobile weather stations provided the level of detail needed to characterise the complexity of the urban microclimate, and help to reveal the effects of current WSUD practice for urban climate.

More specifically, to answer **research objective 1: identify the observed microscale air temperature and HTC variability in a WSUD suburb**, 27 static weather stations were deployed, measuring air temperature and HTC variables in the UCL at a range of locations around Mawson Lakes. Additionally, to address **objective 1**, 18 bicycle transects measuring air temperature and LST across the suburb were conducted. The meteorological observations

Figure 3.6: The Mawson Lakes study site with example WSUD features labelled: (a) pervious swales, (b & c) water courses, (d) bio-filtration, (e & f) irrigated green space, and (g & h) artificial lakes. The cooling effects of these types of features was the focus of the Mawson Lakes field campaign.

were intended to characterise the UCL, as this is the environment urban dwellers are regularly exposed to. The static and mobile meteorological data were also used to achieve **objective 2: to generate robust estimates for the cooling potential of WSUD features on microscale air temperature**, but for objective 2 high resolution information about the nature of the land surface was required. This research needed empirical data that characterised the land surface in detail so that robust estimates of the cooling potential of WSUD could be quantified. These high resolution land surface data were also used to drive the LSM, which was used to address **objectives 3 and 4** (see Figure 3.1).

The total length of the campaign was approximately 10 days and included an intensive observational period of 5 days (as indicated in Figure 3.7). Data used in this research are taken from the intensive period, where conditions were hot (though not extreme), gradient airflow was south-west/south-easterly and atmospheric conditions were stable with a high pressure system. The long-term (1981–2010) average daily air temperature (T_{max}) in Adelaide during February is 29.5 °C and the average monthly rainfall is 12.8 mm (BOM, 2013). The average T_{max} during the intensive period (29.4 °C) was consistent with the long term average but extreme conditions (e.g. air temperature > 40) were not observed, but do often occur in Adelaide. Wind direction during the intensive period was primarily bi-modal, with predominantly onshore sea breezes (south-westerly) during the day and offshore (south-easterlies) at night. There were two rainfall events (unusual for this time of year): on the 11th February (9.6 mm) and the 18th February (22.6 mm) (Figure 3.7)), which limited the length of the intensive observational period.

3.4.2 Aircraft remote sensing

As mentioned above, a major requirement of the Mawson Lakes campaign was to characterise the land surface in the suburb. To do this a small powered glider aircraft (HK36 Super Diomna) was contracted from Airborne Research Australia (ARA) to perform remote sensing data acquisition
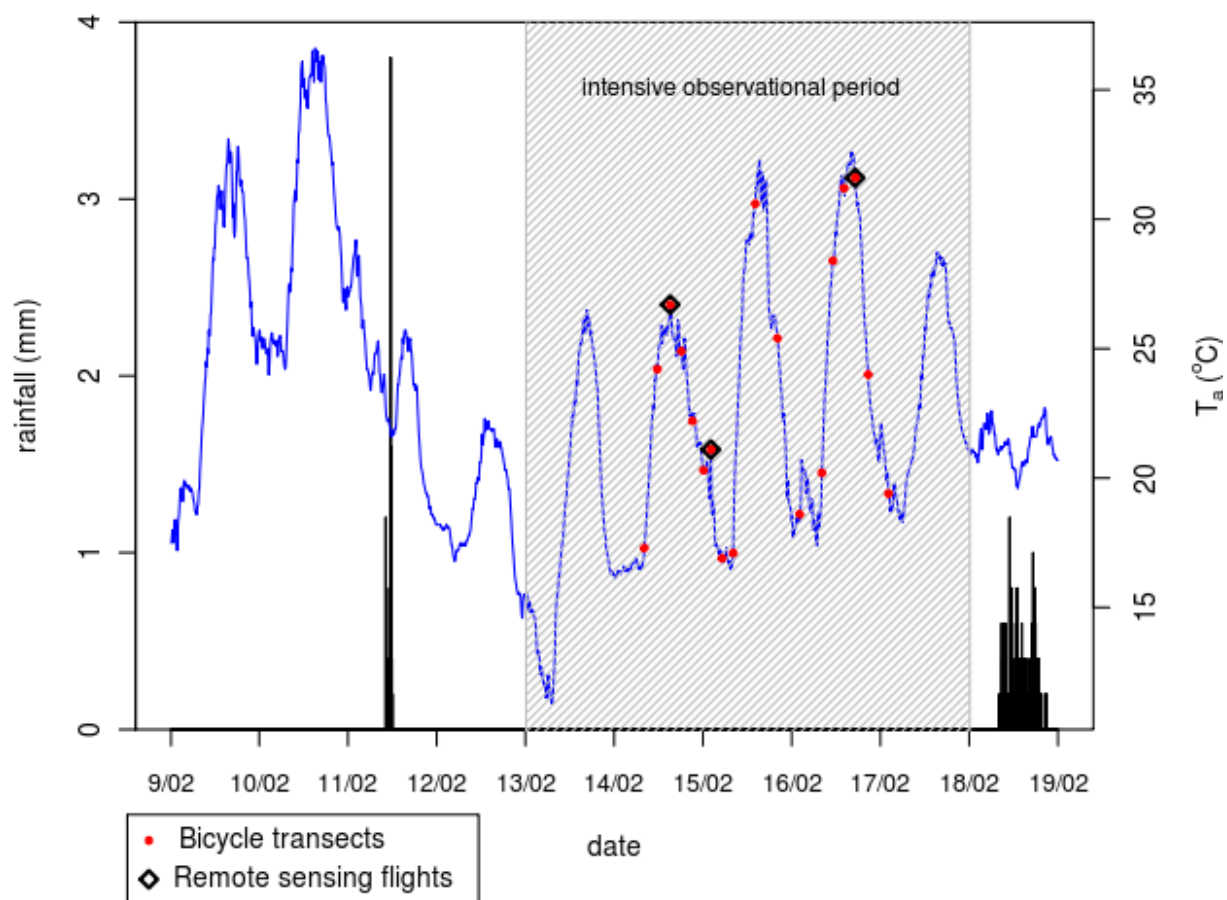
Figure 3.7: A time series overview of the Mawson Lakes field campaign. The timing of bicycle transects and remote sensing flights are indicated. The campaign was hampered by rain, which cut short the intensive observational period. Extreme conditions were not observed during the intensive observational period. However, 5 days of relatively stable and hot conditions were captured. Meteorological data are taken from the Parafield Airport AWS (Bureau of Meteorology—station ID 023013).
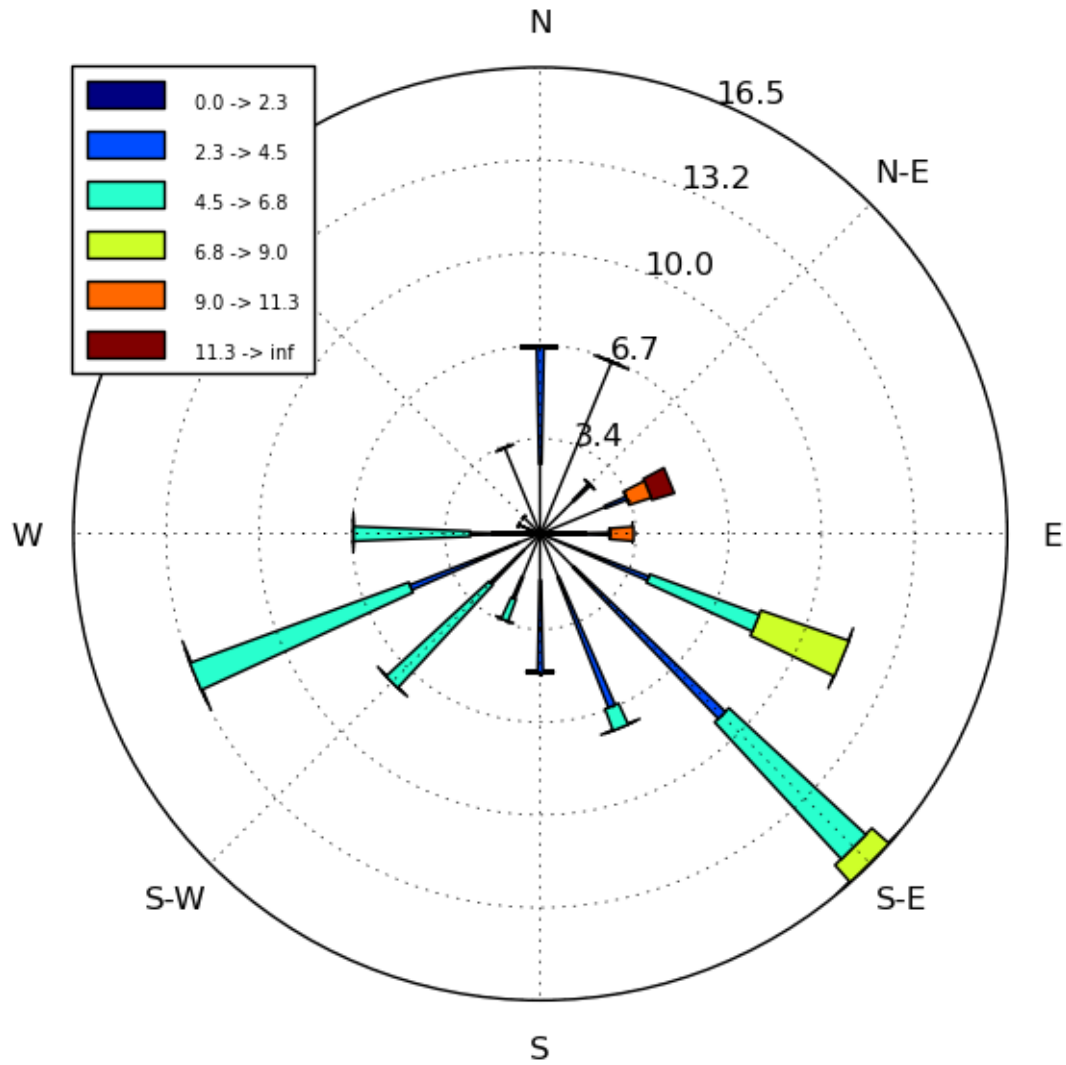
Figure 3.8: The Wind rose for the conditions during intensive observational campaign. The wind regime was characterised by onshore sea breezes (south-westerly) during the day and offshore (south-easterlies) at night. Meteorological data are taken from the Parafield Airport AWS (Bureau of Meteorology—station ID 023013).

over the area of interest. Three flights were conducted during the intensive period: 14th February daytime (3:30 – 5:30 pm), 15th February nocturnal (2:00 – 3:30 am), and 16th February daytime (2:00 – 4:30 pm) (Figure 3.7). These times were chosen to capture day and nighttime conditions. Table 3.1 summarises the instruments used and datasets that were derived from the remote sensing.

The LST provided a very high resolution spatial representation of the temperature of the urban surface. LST is considered to be a key indicator of urban air temperature variability. The LST was used to calculate the average temperature of different surface types (for example irrigated grass) and get complete spatial representation of temperature variability across the suburb. However, there are some limitations associated with high resolution LST measurements. In particular, heterogeneity of emissivity is a major limitation of high resolution LST observations. Inaccuracies associated with emissivity differences are expected to be largest at scales on the order of meters and decrease as averaging occurs over a larger area (Voogt & Oke, 1997). A simple correction for emissivity was conducted using the following emissivities: concrete/asphalt = 0.95, buildings = 0.91, trees = 0.98, irrigated grass = 0.93, dry grass = 0.93, bare ground = 0.96, water = 0.95, other vegetation = 0.98 (Oke, 1987). However, there are a few metal roofing materials (e.g. galvanised sheet steel and aluminum) with very low emissivities that resulted in unreasonably low roof LST. Due to the methodology used to categorise the land cover, metal roofs could not be accurately distinguished from other non-metal roofs. Therefore, to account for the low emissivity of metal roofs, rooftop LST data outside of 2 standard deviations were omitted. Despite these limitations, relatively few studies have explicitly examined high resolution urban emissivity, although temperature-emissivity separation algorithms have been used with hyperspectral data (6 m resolution) to derive per pixel estimates of emissivity (Xu et al., 2008). Approaches for classification of roofing materials using hyperspectral data are being developed (Chisense et al., 2011). Ongoing research is needed to ascertain how important

76

Table 3.1: Mawson Lakes field campaign remote sensing overview: description of instruments used and dataset derived.

Instrument	Data collected	Ground resolution	Data derived*
digital single-lens reflex visible camera	photographs	0.2 – 0.5 m	photographs (not shown)
trispectral linescanner	multi-spectral imagery	1.2 m	land cover (Figure 3.9a) and NDVI (Figure 3.9b)
LiDAR** instrument	LiDAR point cloud data	1.2 m	tree and building heights and SVF† (Figure 3.9d)
infra-red thermal camera	LST	1.2 m	LST (Figure 3.9c)

* information about how these datasets were derived is provided below
** light detecting and ranging
† sky view factor

specific emissivity values are for high resolution thermal imagery. Finally, another limitation of LST remote sensing, that was also neglected, was the directional variation of upwelling thermal radiation (thermal anisotropy) associated with microscale temperature patterns created by the three-dimensional urban surface (Voogt, 2008). It is expected there is some thermal anisotropy in the Mawson Lakes LST dataset, meaning that sidewalls were under-estimated by a downward facing instrument. It should be acknowledged that no attempt was made to lessen this source of error.

Multi-spectral imagery over the Mawson Lakes suburb were also collected. The primary reasons for collecting these data were to calculate normalised difference vegetation index (NDVI) and to derive land cover categories. Land cover categories are essential for characterising the surface and identifying the thermal effects of different surface types (e.g. irrigated vs. unirrigated grass). The multi-spectral data were used to generate land cover categories using a hybrid approach, which utilised land-use planning maps (Department of Planning, South Australian Government), multi-spectral data, tree and building heights, and a supervised classification technique (maximum likelihood classification ArcGIS). The derived land cover categories were designed to capture the key microscale features in the Mawson Lakes suburb, including WSUD elements. The maximum likelihood classification was created using training data from the multi-spectral dataset. These training data sites were identified using the land-use planning maps and visual imagery. The land cover categories derived include: trees, other, water, residential building, mid-rise building, bare ground, grass, concrete/asphalt, low vegetation, and irrigated grass. The tree category included all trees above 1 m in height, low vegetation included bushes and other small plants distinct from grass. Residential buildings (i.e. houses) were those located in residential land-use zones, and also had to be below 10 m in height. The irrigated grass category was identified using NDVI data. The NDVI of grass surfaces showed a clear bimodal distribution (not shown), and the second peak in this distribution was taken to represent green

irrigated grass that was well supplied with water. A threshold value was identified based on this bimodal distribution, and all grass pixels above this threshold were classified as irrigated. There are some limitations associated with this method, as NDVI is not a perfect surrogate for irrigation. However, visual comparison of the land cover classification suggests that areas known to be irrigated (e.g. golf course greens) were very well captured.

NDVI is a simple way to measure the amount of vegetation at the surface (Figure 3.9b). Asides from acting as a key metric of the amount of urban vegetation, it was also used to assist the land cover classification. NDVI was calculated using the following (Goward et al., 1991):

$$NDVI = \frac{(NIR - VIS)}{(NIR + VIS)} \tag{4}$$

where VIS and NIR stand for the spectral reflectance measurements acquired in the visible and near-infrared regions, respectively. SVF is a dimensionless measure between zero and one, representing the fraction of the hemispherical environment not obstructed by objects (Oke, 1988a). SVF was calculated to characterise the three dimensional urban environment. In particular, it is important to account for the effects of urban geometry as that has been shown to influence urban microclimate and HTC. The LiDAR data were converted to a digital elevation model (DEM) and converted to SVF (Figure 3.9d) following (Zhu et al., 2013). The proportion of visible sky at a given point O was calculated at $2°$ azimuth intervals (SVF_a) using:

$$SVFa = sin(\beta)^{2n} \tag{5}$$

where β is the maximum elevation angle along the azimuth interval, and n is the number of the azimuth intervals (180 used here). β was calculated from (Zhu et al., 2013):

$$\beta = \arctan(z_{max}/R) \tag{6}$$
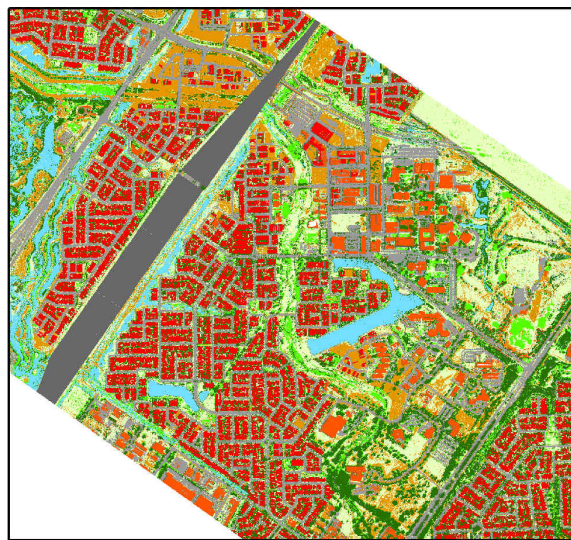
(a) Land cover categories (0.8 m resolution)

■ other		■ bare ground	
■ tree		■ grass	
■ water		■ concrete/ashpalt	
■ residential building		■ irrigated grass	
■ mid-rise building			

(b) NDVI (0.8 m resolution)

0.87 0.79 0.70 0.61 0.52 0.44 0.35 0.26 0.17 0.09 0
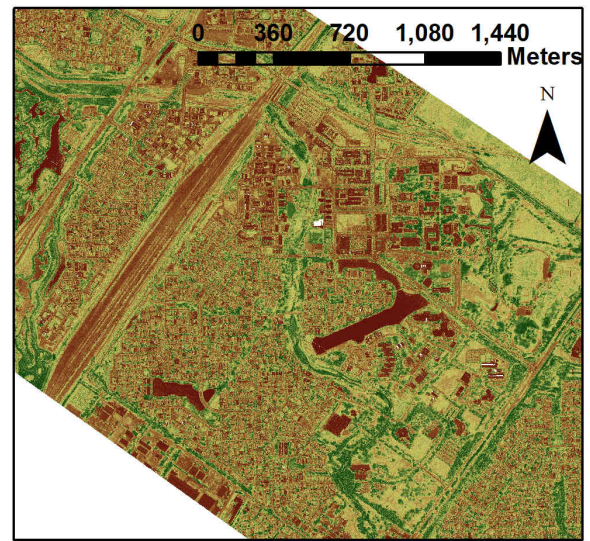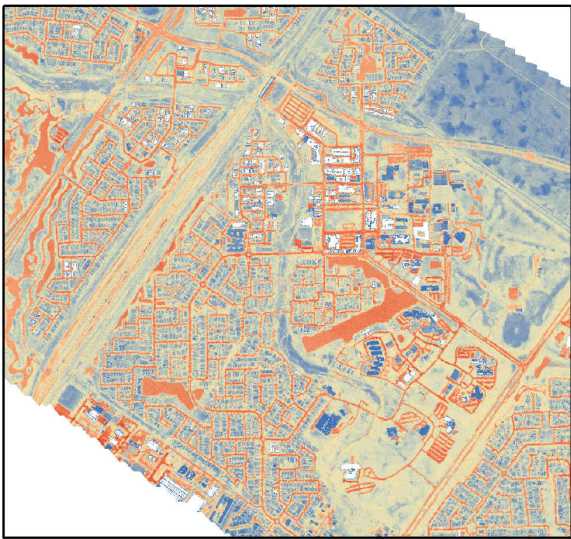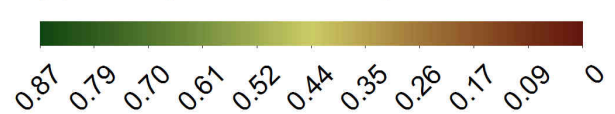
(c) Night surface radiative temperature (°C)
(1.2 m resolution)

29 26 23 20 18 15 12 9 6
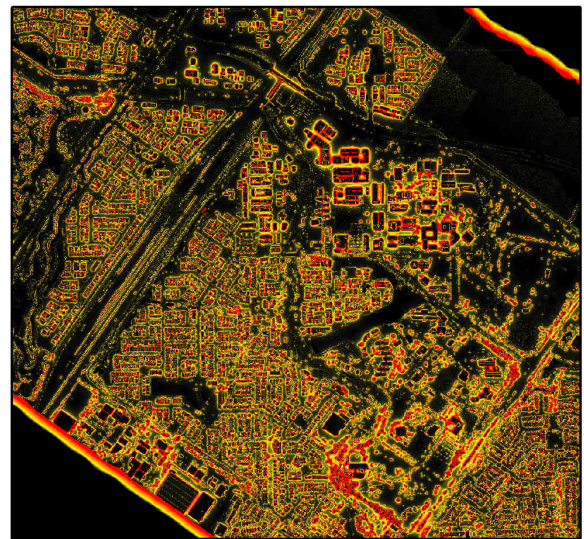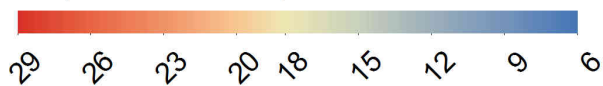
(d) Sky view factor (1.2 m resolution)

1.0 0.9 0.8 0.7 0.6 0.5 0.4 0.3 0.2 0.1 0.0

Figure 3.9: The Mawson Lakes spatial datasets there were derived from remote sensing data: (a) Land cover (supervised classification ArcGIS) (0.8 m resolution) (b) NDVI (1.2 m resolution) (c) LST (2 am) (1.2 m resolution) (d) SVF (1.2 m resolution). These data allowed for the urban surface and form to be characterised in very high resolution. High resolution land surface characteristics are needed as this research is interested in the effects of WSUD on mircoscale climate. Larger versions of all remotely sensed datasets are available in the appendix.

80

where z_{max} is the height difference between the maximum height along the search path z_p and point O, and R is horizontal distance between z_p and O. β was defined along a maximum search path of 50 m. The SVF of O is:

$$SVF = 1 - \sum_{i=1}^{n} SVFa_n \tag{7}$$

n being the number of the azimuth intervals (180 used here). Due to the low average building height in Mawson Lakes (average = 4.6 m), a shorter search path was used to reduce computation time. Longer search paths were tested, but had a negligible effect on SVF calculations.

Using the remote sensing data collected and the datasets derived (Table 3.1) it was possible to generate a high resolution spatial representation of the urban environment. This information characterised the make-up, surface temperature, geometry, and greenness of the urban environment (Table 3.1). These high resolution data are essential for understanding the cooling potential of WSUD at the microscale. They allowed the individual features in the UCL to be resolved; such features can become highly influential at the microscale. The high resolution remote sensing data were used in conjunction with in situ meteorological observation to understand the microclimate variability in the suburb (**objective 1**), and to calculate the effects of different WSUD features on microclimate (**objective 2**). The remote sensing data were also used as a key input to the numerical modelling analysis (**objective 3** and **objective 4**).

3.4.3 Static automatic weather stations (AWS)

A major form of in situ observations made during the Mawson Lakes field campaign were the static weather stations. The primary motivation for deploying these instruments was to capture microscale variability of air temperature and HTC in the Mawson Lakes suburb. To capture microscale variability, 27 static AWS were deployed around the suburb, measuring air tempera-

ture, relative humidity (RH), black-globe temperature, wind speed, and incoming solar radiation ($K\downarrow$). These meteorological variables allowed for HTC indices to be calculated. The AWS were also used to understand the cooling potential of WSUD features on microscale air temperature. As such, the AWS were posted around the suburb at sites that were exposed to different WSUD elements (Figure 3.10). A number of AWS were sited in the Salisbury wetlands (27 and 24), while others we posted adjacent to the Sir Douglas Mawson (6, 8, 9, and 5) and Shearwater Lakes (11). The sites were also chosen to reflect different levels of irrigation and different built form characteristics. Summary satellite images of each AWS are available in the appendix (Figures A.6–A.9). The selection of AWS sites was subjective and targeted towards different WSUD features, but the classification of these sites was done via statistical methods to avoid possible selection biases. See chapter 5 for details of the AWS site classification.

The stations were mounted on lamp-posts (19 AWS) or metal stakes (8 AWS) depending on what was available in the urban environment. The lamp-post stations were mounted at a height of approximately 3 m and the metal stake mounted stations were at a height of 1.5 m. The instrumentation used is described in Table 3.2. The air temperature/RH probes were mounted within radiation shields to shelter the instruments from precipitation and radiation, while allowing air to circulate freely.

Black globe temperature was collected so that MRT could be calculated. As discussed in chapter 2, MRT is considered to be a key metric that influences HTC. Matzarakis et al. (2010, p. 131) state that MRT is defined as *"the uniform temperature of a hypothetical spherical surface surrounding a human (emissivity=1) that would result in the same net radiation energy exchange with the subject as the actual, complex radiative environment"*. The black globe thermometers were constructed using 150 mm diameter copper spheres (painted matt black) with Omega precision thermistors placed in the air cavity. To account for the thermal lag of the sphere, 30 minute averages of black globe temperature were used (Coutts et al., 2015). Black globe

temperature was converted to MRT using (Kántor & Unger, 2011):

$$MRT = \sqrt[4]{(t_g + 273.15)^4 + \frac{h_{c_g}}{\epsilon d_g^{0.4}} \times (t_g - t_a)} - 273.15 \qquad (8)$$

where t_g is the globe temperature, h_{c_g} is the mean convective coefficient ($1.10 \times 10^8 v^{0.6}$ where v is wind velocity in ms^{-1}), d_g is the globe diameter (m), ϵ is the globe emissivity (0.95), and t_a is the air temperature. A limitation of this approach is that the h_{c_g} term is dependent on wind speed, which can potentially fluctuate near the black globe surface. To test the accuracy of the black globes thermometers, three net radiometers (CNR1, Kipp and Zonen) were deployed alongside the black globe thermometers, with separate instruments also measuring wind speed and air temperature. The instruments were deployed in a residential backyard for 5 days, from 29 January to 1 February 2011. The net radiometers were measuring shortwave and longwave radiation from the six cardinal directions. It was found that the MRT of the black globe thermometers was overestimating MRT compared to the directly measured MRT values (Coutts et al., 2015). As such, the h_{c_g} value was adjusted to $0.65 \times 10^8 v^{0.53}$ (Coutts et al., 2015). See Coutts et al. (2015) for a full summary of the black globe thermometer validation methodology. Despite the limitations associated with accounting for fluctuations in wind speed near the black globe surface, the adjusted h_{c_g} black globe estimates of MRT were in good agreement with the net radiometer measurements.

3.4.4 AWS height correction

For a number of the sites that were located away from urbanised areas (stations 23 – 30), we used metal stakes to mount the AWS (Figure 3.10). While near surface mounts were preferred for the AWS, this was not possible at most urbanised sites, where elevated mounts were needed to avoid vandalism. This meant that the AWS were mounted at two different heights during the

Table 3.2: *Mawson Lakes static automatic weather stations instrumentation configuration.*

Variable	Instrument	Sampling frequency	Averaged	Accuracy
Air temperature	Vaisala HPM155A/HMP45C	10 sec	5 min	±0.2 °C
RH	Vaisala HPM155A/HMP45C	10 sec	5 min	1.0–2.0%
Wind speed	RM Young 3-cup anemometer	10 sec	5 min	2.0%
Black-globe temperature*	Black-globe thermome-ter**	10 sec	30 min	0.1 °C
$K\downarrow$	Apogee SP-212/SP-110 pyranometer	10 sec	5 min	5.0%

* converted to MRT using equation 8. ** Omega precision thermistor
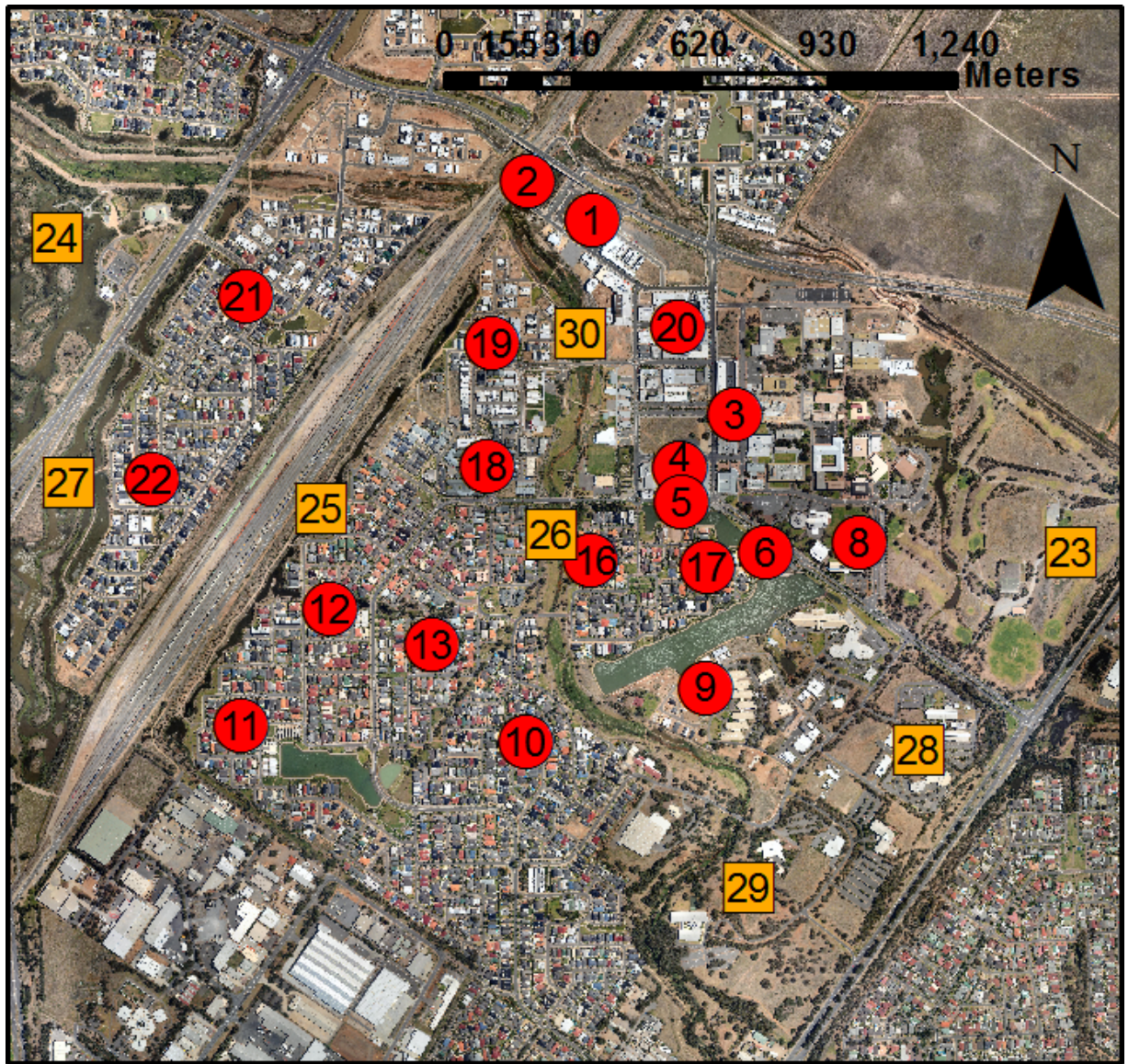
Figure 3.10: A map of AWS locations in Mawson Lakes — lamp-post (red circle) and metal stake sites (orange square) indicated.

campaign. Due to this height difference, there was a tendency for the metal stake mounted AWS to record higher air temperature than lamp-post mounted sites, throughout the diurnal cycle. The metal stake mounted sites, were mounted at a lower height (1.5 m) and were closer to the source of surface heating. The differences in placement height were necessary for security and logistic reasons. To correct for this height difference, data from the bicycle transects (measured at approximately 1.5 m) were compared with static station observations to derive a correction factor for each AWS. Bicycle transect observations (T_b) within 25 m of static stations (T_{AWS})

were used. Four periods were used that reflect the heat/cooling structure of the diurnal cycle: 12 am – 8am (slower cooling), 9am – 11am (rapid heating), 12pm – 4pm (slower heating), 5pm – 11pm (faster cooling). The relationship between T_{AWS} and T_b was linear so we the following linear equations were used:

- 12 am – 8 am: $T_{AWS} = 0.94T_b + 0.47$ $\hspace{2cm}$ $[r^2 = 0.97]$

- 9 am –11 am: $T_{AWS} = 1.05T_b - 2.44$ $\hspace{2cm}$ $[r^2 = 0.96]$

- 12 pm – 4 pm: $T_{AWS} = 0.84T_b + 3.9$ $\hspace{2cm}$ $[r^2 = 0.94]$

- 5 pm – 11 pm: $T_{AWS} = 0.98T_b - 0.02$ $\hspace{2cm}$ $[r^2 = 0.98]$

Given that these relationships are affected by atmospheric stability, they are probably only valid for the campaign period. The 8 AWS at 1.5 m were corrected to 3 m, using these linear relationships; it was considered more suitable to modify the stake mounted sites to the lamp-post mounted sites, as this involved modifying less data. However, wind speeds were not modified for height differences. A simple logarithmic correction was tested using $U = (u*/k)ln(z - d)/z0)$, where $u*$ is the friction velocity, k is the Von Kárman constant (0.41), z is the height above the surface, d is the zero-plane displacement, and $z0$ is the roughness length (Wieringa, 1993). Assuming logarithmic conditions and typical values for $z0$ (e.g. values estimated between 0.25 – 0.5), the difference in wind speed between 1.5 m and 3 m were mostly negligible (approximately 10%). Moreover, there was no bias towards lower wind speeds for the stake mounted sites (see Figure A.21), suggesting a correction was not justified. The effects of differences in mounting heights is an acknowledged limitation of this research.

3.4.5 Physiological equivalent temperature (PET) calculations

The static AWS were purposefully deployed with instruments that allowed for HTC indices to be calculated. This research is interested in the effect of WSUD on both air temperature and

HTC. It is important that both air temperature and HTC are considered simultaneously as HTC indices are affected by meteorological variables other than air temperature. In this research PET is used as the key measure of HTC. To calculate PET the RAYMAN model was used (Matzarakis et al., 2007). Hourly average air temperature, MRT, wind speed, and relative humidity were used to calculate hourly PET for each static AWS site. As MRT was directly measured and used, SVF and urban geometry was not required as an input for RAYMAN. The following variables were used for all PET calculations in this research: height = 1.75 m, weight = 75 kg, age = 35, sex = male, clo = 0.6, and activity = 80.0 W. The clo value of 0.6 is equal to somebody wearing trousers and long-sleeved shirt. The same variables were used for night and daytime calculations to ensure that meaningful comparisons between sites could be made.

3.4.6   Bicycle transects

While the 27 static AWS gave us relatively high spatial resolution; even more detailed coverage can be achieved through mobile transects. In order to fully understand the variability of temperatures in a WSUD suburb (**objective 1**) and how this variability related to WSUD features, a number of bicycle transects were conducted during the Mawson Lakes campaign. This approach provided a very high-resolution "snapshot" dataset of air temperature variability across the suburb. Like the static stations, the transect routes were designed to account for a range of different UCL conditions, WUSD features, and built form types. Bicycles were chosen because they are cheaper to run than vehicles, and can access areas that are inaccessible to vehicles, such as parks and lakeside areas.

During the intensive observational period (13th–18th February) 18 bicycle transects (3 different bicycles riding simultaneously) were conducted (Figure 3.7), measuring air temperature, RH, LST, and global position system (GPS) location (Campbell GPS16) (Table 3.3). Instrumentation was mounted on the back of standard bicycles (Figure 3.11). Air temperature and

RH were measured using the same instrument as used with the static stations (Vaisala HMP45C with radiation shields), but were programmed to take 10 second averages of air temperature and RH. LST was measured using an Apogee S1-121 (10 second average), which has accuracy of ± 0.2 °C. The instruments were connected to a CR1000 Campbell Scientific data-logger, which was housed in a data-logger enclosure.

Figure 3.11: A photograph of the setup of the instrumentation on the back of a bicycle. This setup was used for data collection during the transect data collection.

Three prescribed transect routes (Figure 3.12) were completed at 3 hourly intervals during the intensive observational period (Figure 3.7). The transects took approximately 60 minutes to complete and accordingly air temperature was corrected for change in air temperature with time. Each T_b data point was corrected using the cumulative temperature change of nearby (< 500 m) static weather stations (Section 3.4.4) during transect time period. A number of stop points were made along each transect. These stop points were intended to equilibrate the infrared thermometer measuring LST, so that a reliable LST measurement could be made and compared with the remotely sensed data. However, an unintended consequence of these stop points, was

that air temperature measurements made directly after the stop points were often exaggerated, perhaps because the instrument was not properly aspirated, or because of body heat from the cyclist. As such, data points recorded for 1 minute after a stop point were smoothed using linear interpolation between air temperature at the stop point and the air temperature 1 minute after the stop point. This resulted in some loss of signal in the air temperature data directly after stop points. However, only a small amount of the overall dataset was affected.

Table 3.3: Mawson Lakes bicycle transect instrumentation configuration.

Variable	Instrument	Averaging frequency	Accuracy
T_a	Vaisala HMP45C	1 sec (10 sec average)	$\pm 0.2 - 0.4$ °C
RH	Vaisala HMP45C	1 sec (10 sec average)	$1.0 - 2.0\%$
LST	Apogee SI-121	10 sec	± 0.2 °C
GPS location	Campbell GPS16-HVS	10 sec	< 3 m

3.5 Modelling analysis

3.5.1 Introduction

To complement the Mawson Lakes observational campaign this research also employed a numerical modelling approach. A modelling approach was used to address the effects of irrigation on microclimate in Mawson Lakes during extreme conditions. The effects of irrigation on microclimate were considered as part of the observational analysis (**objective 2**), but this research also looked further at the cooling potential of irrigation using a land surface modelling approach. In particular, this research was interested in the potential for irrigation to reduce exposure to heat and improve human thermal comfort during an EHE. Extreme heat was not observed during the observational campaign (Figure 3.7). Therefore, a modelling approach afforded the opportunity to simulate extreme conditions and directly explore the effects of irrigation on local-scale to microscale climates. The two key research objectives of the modelling analysis were **objective 3: calculate the potential for irrigation to reduce exposure to adverse extreme heat**

Figure 3.12: A map of the transect routes completed during the Mawson Lakes campaign (Source: Nearmaps).

conditions (air temperature) and **objective 4: calculate the effect of irrigation on microscale HTC under extreme heat**. To achieve these objectives two models were used. The primary tool used to simulate urban microclimate was the SURFEX modelling platform (used for both **objective 3 and 4**). SURFEX was used to conduct simulations with different irrigation scenarios (timing and volume varied) during a heatwave case study over Mawson Lakes suburb.

In this section a description of the models is provided. The details regarding model setup are provided in chapter 7 along with modelling results.

3.5.2 SURFEX description

This research used the SURFEX land-surface modelling scheme as the primary numerical modelling tool. SURFEX is a land-surface modelling platform (Masson et al., 2012) that has been developed at Météo-France. The SURFEX package includes a collection of models for simulating energy and radiation balances over a range of different surface types; the model includes the Interaction between Soil Biosphere and Atmosphere (ISBA) model (Noilhan & Mahfouf, 1996) for soil and vegetation, the Town Energy Balance (TEB) model (Masson, 2000), and a range of other modelling schemes that can be used for other surfaces, such as lakes (FLake & WATFLX) and oceans (SEAFLX) (Figure 3.13). TEB is a very commonly used urban-LSM that has been used in many urban climate modelling studies, including the PILPS-urban project (Grimmond et al., 2010, 2011). The TEB scheme uses a canyon approach; representing the city as an ensemble of infinite, isotropic canyons with three surfaces: roofs, walls, and roads. In order to account for solar and wind effects all road orientations are possible, and all exist with the same probability (Figure 2.9) (Masson, 2000). This simple representation allows most of the physical effects associated with the urban energy balance to be reproduced, including radiative trapping (longwave and shortwave) (Masson et al., 2002).

The SURFEX model was chosen because it best suited the requirements of this research. Overall, a model was required that (1) included integrated (in canyon) vegetation simulation, (2) irrigation representation, and (3) UCL morphology effects. For UCL morphology the TEB-Surface Boundary Layer (SBL) scheme has been developed, which improves the predication of meteorological fields inside the UCL (Hamdi & Masson, 2008; Masson & Seity, 2009). As this research is interested in the UCL variables, the TEB-SBL approach was used.

For vegetation representation, SURFEX can be run in two different configurations: the ISBA-TEB setup simulates the natural and built surfaces on separate tiles that do not interact, and the TEB-Veg (integrated vegetation) setup (Lemonsu et al., 2012b) can directly simulate vegetation (natural surfaces) within the urban canyon (Figure 3.14). Lemonsu et al. (2012b) evaluated ISBA-TEB and TEB-Veg at the microscale and found that the TEB-Veg version performs better for UCL simulations than TEB-ISBA for several reasons:

- the actual geometry of urban canyon is better characterized by TEB-Veg than by TEB-ISBA; and

- taking into account the surface and atmosphere exchanges of gardens, in the UCL, seems to improve the results of TEB-Veg.

Lemonsu et al. (2012b) noted that TEB-Veg succeeded in simulating microclimatic conditions inside the UCL, which were warmer than above the canopy. Given that this research is interested in microscale climate, the TEB-Veg approach is considered to be the best option for the microscale urban climate modelling.

For irrigation a recent version of TEB-Veg was used, which allows for garden irrigation and green roof representation (de Munck, 2013). The irrigation regime in TEB-Veg allows for representation of sprinklers, which add extra precipitation to the foliage and soil surfaces inside the canyon, through the following:

$$P_{global} = P + (Irrig \times 24/\Delta t_{Irrig}) = P_{foliage} + P_{soil} \qquad (9)$$

where P is the rate of normal precipitation, $Irrig$ is the amount of water that would be provided by continuous irrigation, P_{global} is the sum of P and $Irrig$. A fraction of this water is intercepted by the ground and foliage. There is also the possibility in TEB-Veg to represent

dripper irrigation systems, which only adds the supply of water to the ground.
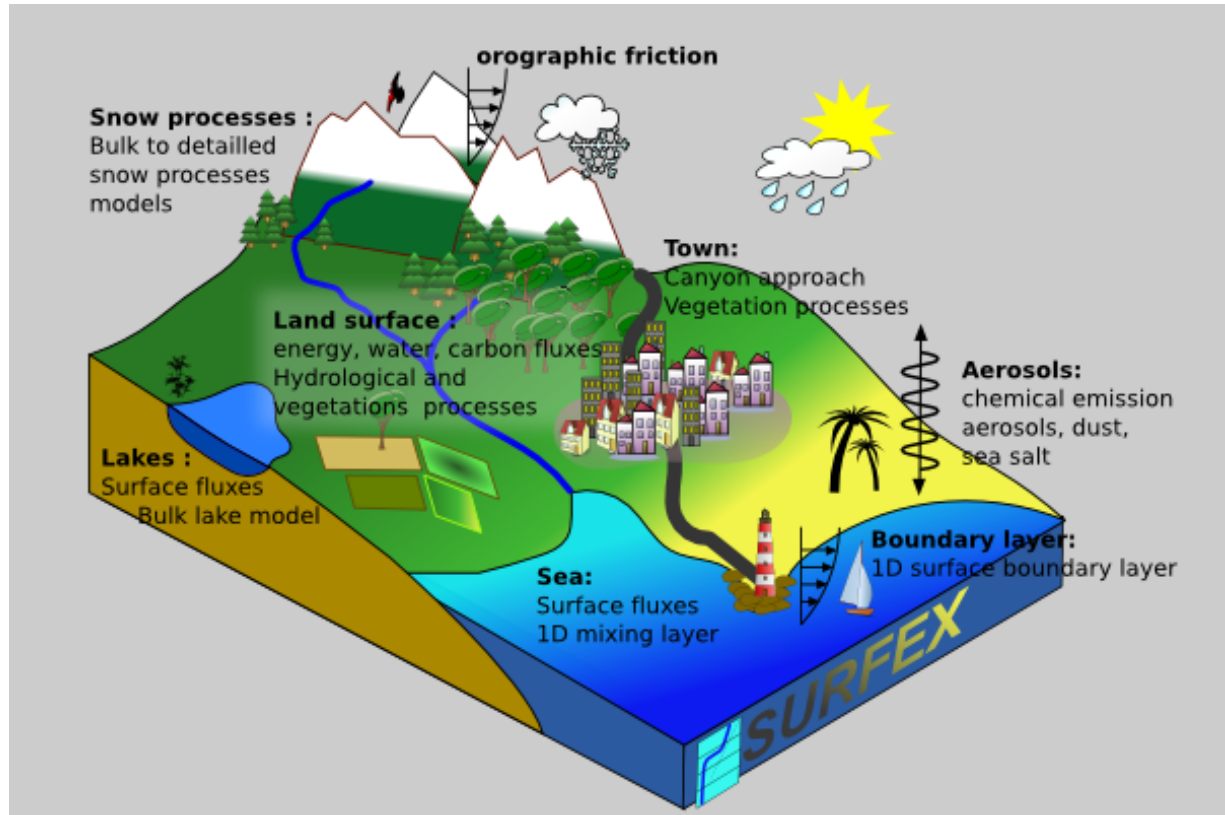
Figure 3.13: An overview of the SURFEX modelling platform. SURFEX is composed of various physical models for natural land surface, urbanised areas, lakes and oceans. It also simulates chemistry and aerosols surface processes and can be used for assimilation of surface and near surface variables (Source: http://www.cnrm.meteo.fr/surfex/).

Full details about the SURFEX set-up and the scenarios that were tested are provided in chapter 7. However, a brief description is provided here for context. Simulations were carried out using the SURFEX model (TEB-Veg and WATFLX) over the Mawson Lakes field campaign for EHE case study period that occurred in February 2009. The heatwave was devastating and affected a large part of south-east Australia and caused 13 days of very hot weather in Adelaide. The upper boundary of the model was forced by a single meteorological dataset that was developed to force the whole domain (offline simulations). There are limitations associated with this offline approach, as no interactions between the atmosphere and the UCL can occur, and these limitations are discussed in detail in chapter 7. While online simulations would have been preferable, it is not possible at the desired modelling resolution (25 m). The model was
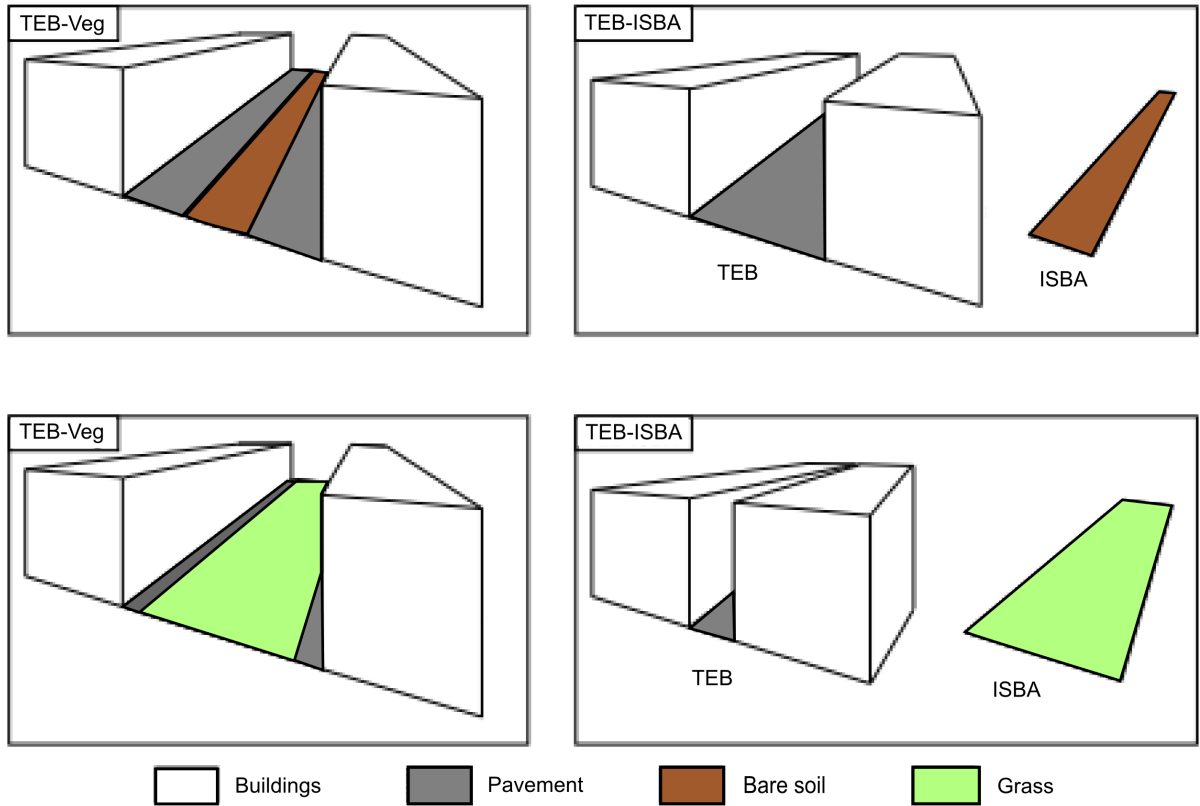
Figure 3.14: A schematic showing the representation of vegetation in SURFEX land surface model. The TEB-ISBA setup creates artificially narrower urban canyons. An integrated approach, such as TEB-Veg, is likely to be better for high resolution studies when the urban area is resolved. In this research the TEB-Veg approach was used. Source: Lemonsu et al. (2012b).

run for the 13 day case study period at 25m resolution, covering the Mawson Lakes suburb. The spatial resolution was chosen to capture microclimate variability and was also informed by the results of the source area analysis (see chapter 4). The land surface parameters were derived from the Mawson Lakes field campaign remote sensing data (Figure 3.9). The TEB-SBL scheme was used to represent UCL processes. A 14 day spin up was used for soil moisture and surface temperatures to stabilize. Different irrigation scenarios were systematically tested with different rates and timing of irrigation. Irrigation scenarios were then compared with a base run, where no irrigation was included, to infer the cooling potential of different irrigation scenarios. A full description and justification of model parameters and modelling scenarios is provided in chapter 7. Additionally, the model's ability to replicate the microscale temperature variability

was validated using meteorological data from the Mawson Lakes field campaign. The results from the SURFEX validation are also found in chapter 7.

SURFEX met all the modelling requirements identified during the review of the literature, and has been used successfully for microscale UCL simulations in a previous study (Lemonsu et al., 2012b). However, SURFEX uses a traditional canyon approach (Figure 2.9), representing the city as an ensemble of infinite, isotropic canyons. Therefore, SURFEX is less suitable for simulating MRT in the UCL, and thus the SOLWEIG model (described below) was used to calculate MRT, so that HTC indices could be calculated (**objective 4**).

3.5.3 SOLWEIG description

While the SURFEX scheme was an efficient way of simulating the effects of irrigation on UCL meteorological variables, a separate model was needed for MRT simulations. To augment the output from the SURFEX simulations the SOLWEIG model was also run for Mawson Lakes. SOLWEIG is a simple irradiance model that can be used to estimate spatial variations in 3D radiation fluxes and MRT (Lindberg et al., 2008). SOLWEIG can accurately represent (in high resolution) the location of objects in space, and the effect of those objects on radiation fluxes (see Figure 3.15). MRT is calculated by modelling shortwave and longwave radiation fluxes in six directions (upward, downward and from the four cardinal points) and taking into account angular factors. SOLWEIG requires simple meteorological inputs, such as direct, diffuse and global shortwave radiation, air temperature, and relative humidity. Therefore, the output from SURFEX (with irrigation changed) can be used to force SOLWEIG. A digital surface model is the other main input, which was derived from the remote sensing data (Figure 3.9). Thom & Coutts (2015) have thoroughly tested the SOLWEIG model using the Mawson Lakes MRT data (Table 3.2). The authors have found that SOLWEIG is able to reproduce the timing and magnitude of daytime MRT, however, the model does not currently work for nighttime MRT

simulations.
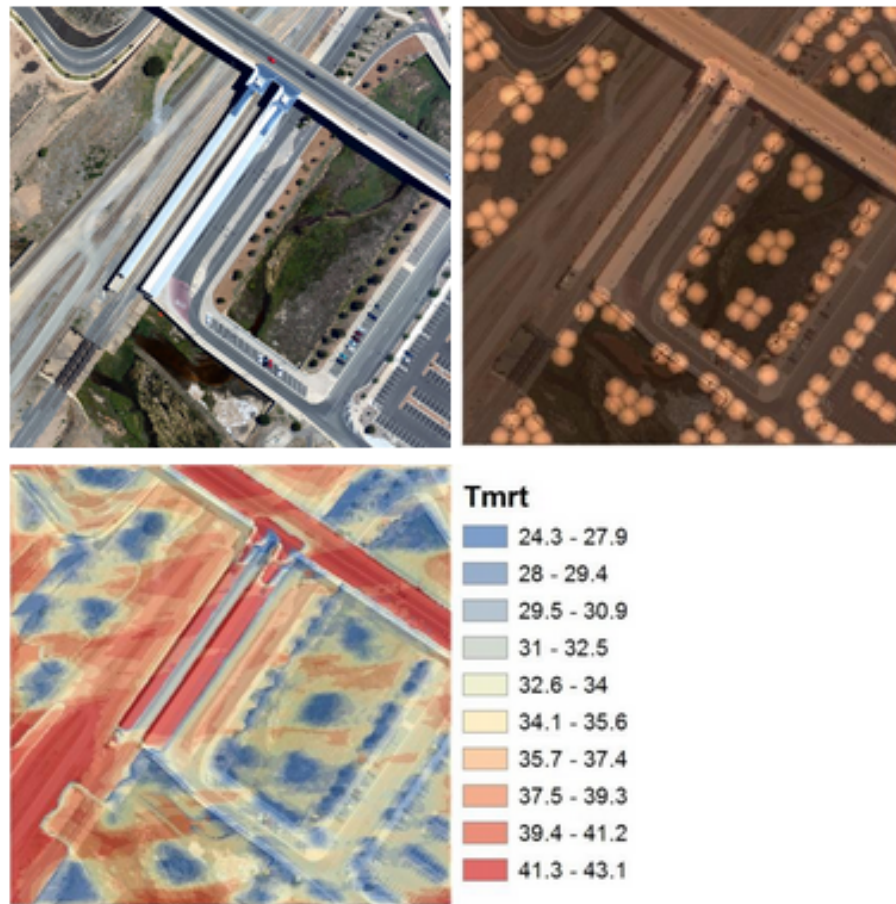
Figure 3.15: An example of a SOLWEIG simulation for Mawson Lakes. Top left: satellite imagery, top right: possible tree planting scenario, and bottom left: MRT output from SOLWEIG. The SOLWEIG model allows for simulation of radiation fluxes, and the calculation for MRT. In this research the output from SURFEX was used to drive SOLWEIG and calculate the effect of irrigation on HTC. Source: (Thom & Coutts, 2015)

3.6   Methodology summary

To meet the 4 research objectives of this research, which are centered around quantifying the potential for WSUD and stormwater reintegration techniques to mitigate urban warmth and improve HTC, a methodological approach that incorporates observational field work and numerical modelling was designed. For this approach the measured and modelled data matches the scale of application (i.e. micro to local-scales). The overall approach of this research is summarised in Figure 3.1. The Mawson Lakes field campaign is the basis of all the analysis in this research

project. In order to assist the observational and modelling analysis a source area analysis of AWS was conducted (chapter 4). The source area analysis provides an estimate of the land surface area that influences the AWS sites. Research **objectives 1 and 2** draw on the Mawson Lakes observational data and the source area analysis. A numerical modelling approach is used to address **objectives 3 and 4**. To investigate the potential for irrigation to reduce exposure to extreme heat (**objective 3**) the SURFEX scheme is used (chapter 7). However, to calculate changes in HTC associated with irrigation (**objective 4**) an estimate of MRT was needed. Therefore, the output from SURFEX was augmented with the MRT estimates from SOLWEIG to calculate PET (also in chapter 7).

4 Defining the source area of an urban canopy layer (UCL) site

4.1 Background

4.1.1 Introduction

A key consideration for urban climate observational studies that are interested in mitigation of urban warmth, is the definition of the source area that influences a given site. Mitigation research must establish a meaningful link between the land surface drivers of urban microclimate and observed microclimate variability. For this research, a meaningful way to connect land surface characteristics and microscale variability is needed so that the cooling effects of WSUD can be quantified. In this chapter a simple source area analysis is presented, which is intended to provide a non-arbitrary value that can be used to characterise the surfaces that directly influence the microscale air temperature at the AWS sites in Mawson Lakes. The analysis in this chapter is not directly related to the overall aim of this research. However, it is a necessary component of the research that allows the research objectives to be directly addressed.

The effect of urbanisation on climate is a widely studied subject (see chapter 2). Traditional UHI studies compare the air temperature of one rural with one urban site. The effect of urbanisation on climate is then inferred from the difference between these two measurements. As interest in urban climate has grown, so too has the sophistication of urban climate research. Researchers have moved beyond the simple UHI rural-urban approach and now often deploy multiple instruments within a city or urban environment. Intra-urban studies have revealed significant intra-urban climate variability at the micro and local-scales. Importantly, it has been shown that this intra-urban air temperature variability can be as large as the UHI intensity (Petralli et al., 2014); some areas within the city are as cool as the rural environment while other areas are much warmer than the rural environment. The high magnitude of intra-urban variability

demonstrates the need for higher resolution intra-urban climate research. Intra-urban variability can be used to identify areas within a city that are potentially exposed to negative heat health conditions (Petralli et al., 2012) and excess energy demand for cooling. However, interpreting intra-urban studies requires a sophisticated understanding of the controls on urban climate at the micro and local-scales. This is particularly true at the microscale where air temperature can be highly variable over short distances, and instrument source areas can be very small (tens of meters) (Oke, 2004). By definition, the source area is the portion of the surface upwind that contributes the main properties of the flux (e.g. Q_H) or meteorological concentration (e.g. air temperature) that is being measured (as shown Figure 4.1) (Schmid, 2002). For a temperature measurement, the source area is the total surface area that is seen by the air temperature sensor. In this research, the term "source area" should be understood as an estimate of the adjacent horizontal surfaces that are most representative of microscale air temperature variability. To draw meaningful links between microclimate variability and the characteristics of the urban surface, observationalists should have some understanding of the source area that influences an UCL site when interpreting data in the urban environment.

However, the characteristics of the UCL (see Figure 4.2 and Section 2.2.4) make it difficult to estimate instrument source areas, and attribute microscale variability to land surface characteristics. This chapter will focus on this problem in the context of the Mawson Lakes dataset by addressing the following question: what is an appropriate source area for an air temperature sensor deployed during the Mawson Lakes field campaign? As this research is interested in the microscale and local-scale cooling effects of WSUD, it is essential that the nature of the surfaces that are influencing UCL sites is understood. The key objective here is to identify an estimate of the source area (planar surfaces only) that captures a best estimate of the surfaces that were influencing UCL air temperature at the AWS sites.
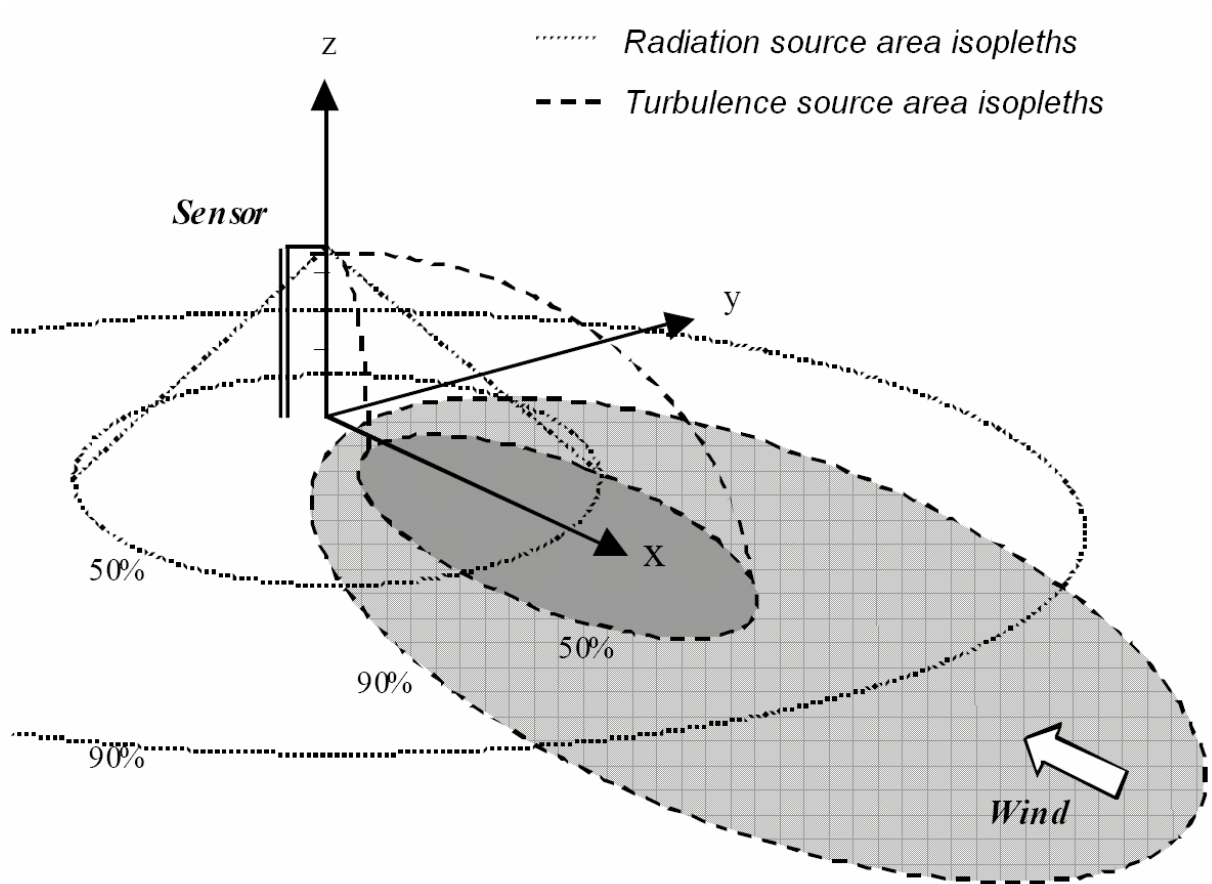
Figure 4.1: A conceptual representation of source areas contributing to sensors for radiation and turbulent fluxes or concentrations. If the sensor is a radiometer, 50 or 90% of the flux originates from the area inside the respective circle. If the sensor is responding to a property of turbulent transport, 50 or 90% of the signal comes from the area inside the respective ellipses. These are dynamic in the sense that they are oriented into the wind and hence move with wind direction and stability. Source: Oke (2004).
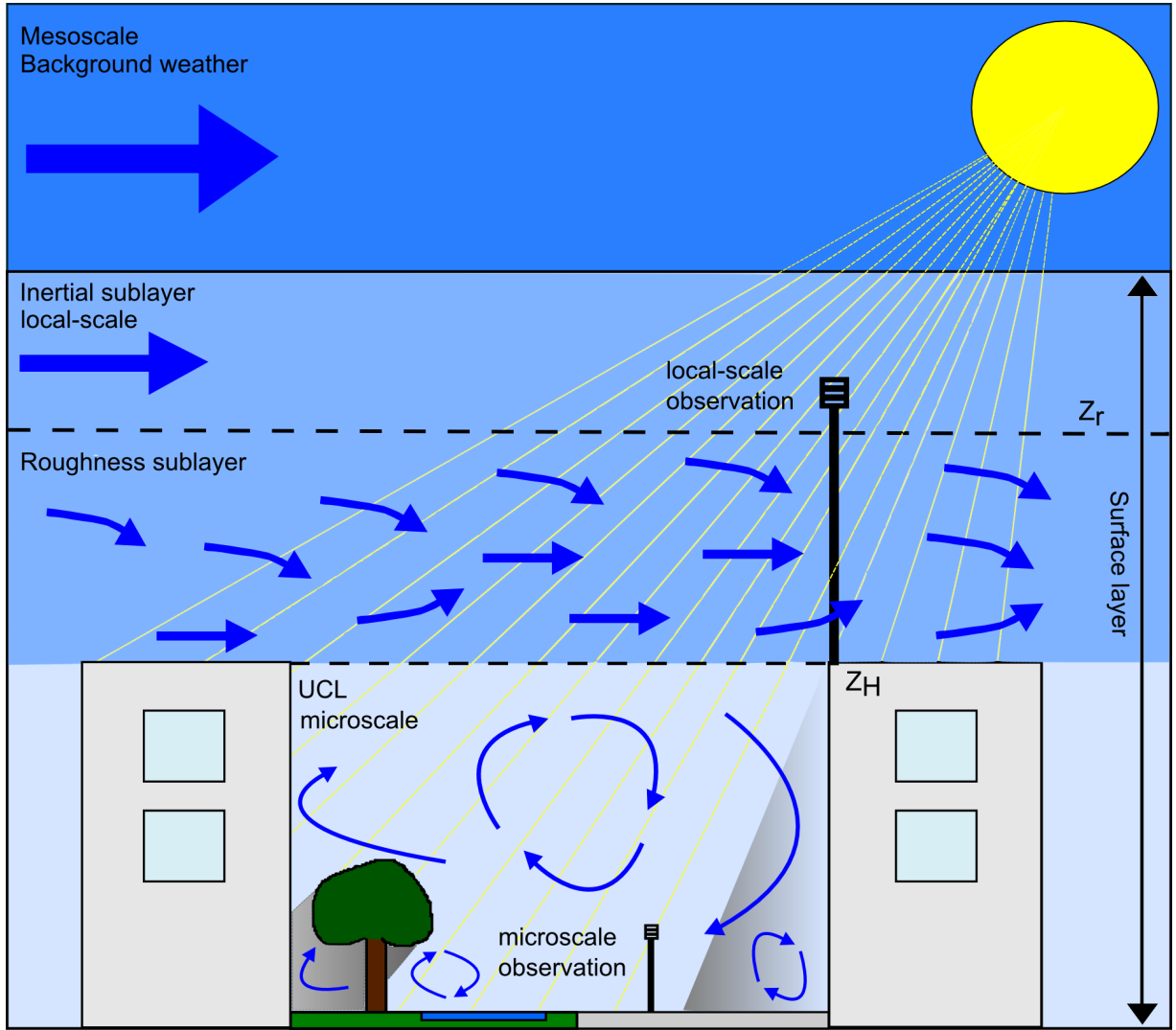
Figure 4.2: A diagram of the urban boundary layer. The urban boundary layer is divided into a series of hypothetical layers, which are characterised by a different scale. UCL = urban canopy layer, Z_H = average building height, and Z_r = the height where the effects of individual roughness elements are no longer detectable. An observational made in the UCL is going to capture microscale climate, while an observation made above the roughness sublayer will be representative of local-scale climate. The microclimate is the scale of urban climate the humans are regularly exposed to. HTC and human health motivated research should try to understand the characteristics of climate in UCL. However, microscale climate is highly variable due to the influence of shading effects, turbulence and wind channelling, interactions between canyon air parcels and air parcels aloft, and highly variable energetic contributions from different surface facets.

4.1.2 Previous estimates of source area

There are a number of different approaches for calculating the source area of a sensor that are based on different mathematical models of turbulence. The methodologies used include: Lagrangian stochastic dispersion models (Flesch et al., 1995; Rannik et al., 2000) and analytical solutions of diffusion advection (Schmid, 1994; Wilson & Swaters, 1991; Horst & Weil, 1992). For such calculations the following (minimum) data is generally needed: the height of measurement, wind velocity, surface roughness, heterogeneous underlying surfaces, and a measure of atmospheric stability (Kljun et al., 2002).

Lagrangian stochastic dispersion models and analytical solutions have been used for estimating the source area of micro-meteorological flux stations (eddy-covariance technique), which are commonly used to measure turbulent fluxes. Such instruments are typically sited well above roughness elements (Figure 4.2), and ideally in flat, horizontally homogeneous environments. These source area modelling approaches are well established in land-atmosphere interaction studies, but are only valid for a sensor that is mounted above the inertial sublayer, where microscale turbulence features have been sufficiently mixed (as shown by the local-scale observation in Figure 4.2). More broadly, the application of analytical solutions (such as Schmid (1994)) in urban areas have been questioned as they assume horizontally homogeneous conditions (Steinfeld et al., 2008). Urban areas are often highly heterogeneous and a horizontally homogeneous surface can be difficult to locate. A number of authors have successfully used micro-meteorological flux measurements (made above the roughness sublayer) in urban areas by carefully siting instruments in horizontally homogeneous urban areas (Grimmond & Oke, 2002; Coutts et al., 2007; Nadeau et al., 2009; Goldbach & Kuttler, 2013). Grimmond & Oke (2002) used the Schmid (1994) analytical solution to calculate the source areas of a number of North America urban flux stations, which were mounted at 18–45m above the surface. In that study, the source areas were

elliptically shaped, lay upwind of the tower sites, and ranged in size from 1.5×10^5 to $5 \times 10^6 \, \text{m}^2$. The use of analytical solutions for calculating source area can work effectively for instruments mounted above the roughness surface layer. However, there are no well-established turbulence approaches for calculating the source area of a sensor that is located below the height of roughness elements and in horizontally heterogeneous terrain. This research is interested in microscale urban climate, and the meteorological observations were made in the UCL, so an alternative approach for calculating AWS source areas is needed.

Stewart & Oke (2012) have pointed out that calculating the source area of an instrument within the UCL is poorly understood. Nevertheless, many urban observational studies use street level observational stations, which rely on instruments that are mounted below surrounding roughness elements in the UCL (e.g. microscale observation shown in Figure 4.2). The ramification of this is that applied urban climate studies, that are interested in intra-urban climate, have no reliable method for estimating the source area of their instruments. However, there have been a number of other studies that have attempted to give a general impression of the area that influences an UCL site. In this research the approach used involved taking the statistical relationship between LST and air temperature to estimate the source area of a sensor in the UCL. This approach was chosen due to the data that were available and the findings from previous research. Before the outcomes of this approach are presented, alternative methods for estimating the source area of UCL sites are discussed below.

There are some "rules of thumb" from the literature that provide very broad guidance around these matters: Oke (2004) suggested that the distance affecting a 3 m high AWS may be from tens of metres up to 300 m depending on atmospheric conditions. While Runnalls & Oke (2006) suggest that a screen-height AWS (in a neutrally stable atmosphere) extends for no more than a few hundred metres. Stewart & Oke (2009) claim that for low instrument heights and among high-rise buildings the source area is often smaller than measurements made high above fields.

Building density and morphology will cause different source areas at sites with variable built form. At a highly built-up site the source area will be defined by the three-dimensional characteristics of the canyon walls and floor, and an open site will have a larger source area defined by the planar characteristics of the adjacent surfaces. Though these observations are useful for urban climate observationalists, they provide at best, a rough approximation of the actual source area. A range of studies have attempted to use alternative methods for estimating the source area of UCL instruments.

In one study, that used an alternative method, Erell et al. (2010) applied simple 22.5° pie-shaped sectors to characterise the source area of a UCL site in Adelaide (Figure 4.3). The sector upwind of the site was identified using hourly average wind direction. The sectors were also divided into concentric rings, at distances of 100–500 m and 500–1000 m from the source. Additionally, a 100 m radius circle surrounding the site was considered as a separative source area, which was not determined by wind direction. Erell et al. (2010) provide no justification for the size and shape of their "pie-shaped sector" source area model. However, the authors were able to show that, during very stable conditions, the source area was determined primarily by the properties of the area immediately adjacent the site (100 m circle), while during unstable conditions the source areas should be calculated using the surface cover of the upwind source area. This study provides some guidance for this research, as it shows that the daytime source area (unstable atmosphere) will likely be determined by the surfaces upwind of the instrument.

In another study, Petralli et al. (2014) indirectly considered the source areas of a network of weather stations mounted at 2 m above the ground in Florence, Italy. The authors conducted regression analysis and compared the average surface characteristics (planning indicators such as Green Cover Ratio) of concentric circles (10 m–500 m) with intra-urban air temperature variability. The statistical significance of different circle radius' varied depending on what air temperature measure was used. For example, the daily mean temperature was negatively

Figure 4.3: The pie shaped source areas used by Erell et al. (2010). Source areas extend 100 to 500 m from the source and the area immediately adjacent to the site (up to 100 m), was treated as a separate source area, independent of wind direction. Source: Erell et al. (2010).

correlated with vegetation indicators, and it was found that these relationships were stronger for circles of higher radius (400 m). By contrast, for daily maximum temperature, only the surfaces directly adjacent the sites (radius < 10 m) were found to be statistically significant ($p < 0.01$). The Petralli et al. (2014) study was not actually trying to determine the source area of a site. The authors were more interested in the effectiveness of different planning indicators at describing intra-urban air temperature variability. However, their statistical approach of comparing land surface variables with air temperature variability, is a useful method for inferring the approximate average source area size.

Statistical approaches were also used by Schwarz et al. (2012) who used a series of concentric circles of different radius' to compare LST and air temperature for static sites in the UCL (1.5 m height). The authors compared the mean LST for circles of size 5 m, 10 m, and 100 m. Schwarz et al. (2012) found that the correlations for air temperature and LST were all statistically significant, and that the correlation decreased with an increasing circle size. The authors explained this finding by stating that increasing the circle size increases the complexity of land cover and consequently, the correlations between the air temperature and LST decrease. This makes sense, as turbulence based methods, typically show that the contribution of surfaces rapidly decreases as you move away from the source (see in Figure 4.1). Overall, Schwarz et al. (2012) suggests that there is a clear relationship between the temperature of the surfaces directly adjacent a site and microscale air temperature. This research will build on the the approach used by Schwarz et al. (2012) and look at the statistical relationship between LST and air temperature to estimate the source area of our AWS in Mawson Lakes.

A number of other studies have looked broadly at the correlation between LST and air temperature (Balling & Brazel, 1989; Dousset, 1989; Mohan et al., 2013), but these studies were for much lower resolution remote sensing platforms. Nevertheless, these studies have shown that the relationship between LST and air temperature is influenced by advection, that arises due

to the spatial configuration of the urban surface, which can have varying patterns of moisture, thermal admittance, and aerodynamic roughness (Voogt, 2008). Advective effects are most pronounced during the day when the atmosphere is well-mixed (Dousset, 1989; Stoll & Brazel, 1992), and consequently the relationship between LST and air temperature is weaker during the day (Dousset, 1989; Voogt & Oke, 2003; Mohan et al., 2013). Roth et al. (1989) suggested that the daytime range in roof temperature causes the apparent daytime range of urban LST (as observed by remote platforms) to be exaggerated. Despite these caveats, the statistical relationship between LST and air temperature is a computationally simple approach that can be used to directly estimate the source area of a sensor in the UCL.

4.2 Methods: estimation of the source area for an AWS in Mawson Lakes

4.2.1 Circular buffer source areas

To ascertain an estimate of the source area of the AWS sites an approach similar to Schwarz et al. (2012) was employed. Circular buffers were used to calculate the coefficient of determination between air temperature and LST at the static AWS sites. Hourly source areas were approximated using circular buffers with increasing diameters: ranging from 12.5 – 150 m (Figure 4.4). Three different configurations of circular buffers were tested with different positioning of the circle relative to the source. The simplest configuration does not take into account wind direction (circular 1) and was always centred on the AWS (Figure 4.4a). However, the other two forms did take into account wind direction. The circular 2 configuration was set up so that the source area is 100% upwind of the point (Figure 4.4b), and the circular 3 buffer is set so that 25% of the circle radius is downwind of the source (Figure 4.4c). Wind direction was defined using the nearby Parafield Airport weather station (Bureau of Meteorology). Hourly average wind direction was grouped into 8 cardinal directions: north (337.5°– 22.5°), north-east (22.5°– 67.5°), east (67.5°–

112.5°), south-east (112.5°– 157.5°), south (157.5°– 202.5°), south-west (202.5°– 247.5°), west (247.5°– 292.5°), and north-west (292.5 – 337.5°). For clarity, a representation of all the possible positions for the circular 2 buffer (50 m diameter shown) is shown in Figure 4.5.

The buffer designs were chosen based on a range of factors. Firstly, circles were chosen for simplicity; other shapes such as sectors (similar to (Erell et al., 2010)) were also tested but these shapes have different areas to the circular buffers, which made inter-comparison difficult. Regardless, it found the sector shaped source areas performed worse than circular buffers (results not shown). Additionally, the positioning of the circular buffers relative to the source had to be chosen. It was important to test source areas that were centred both on the source and upwind of the source. For the upwind source areas (circular 2 and 3), a decision had to be made as to where the circle would be centred in relation to the source. Previous research has suggested that the area upwind of the source and the surfaces directly adjacent (including just downwind of the source) are important. As such, one design was set so that no surfaces downwind of the source were included in the source area (circular 2 — Figure 4.4b), and the other was set so that circle was centred at a point ($distance = 0.25 \times circle\ radius$) downwind of the source (circular 3 — Figure 4.4c). The circular 3 design means that the buffer captures some surfaces that are downwind of the source. The decision to offset the circular 3 buffers by 25% of the circle radius was relatively arbitrary, but it did allow for direct comparison with the circular 2 buffers, which were not offset. These buffers were used to broadly understand the area influencing sites. This was done through a statistical analysis of air temperature and LST, which is described in Section 4.2.3. Additionally, for methodological completeness, an analytical solution is tested alongside the circular source areas.
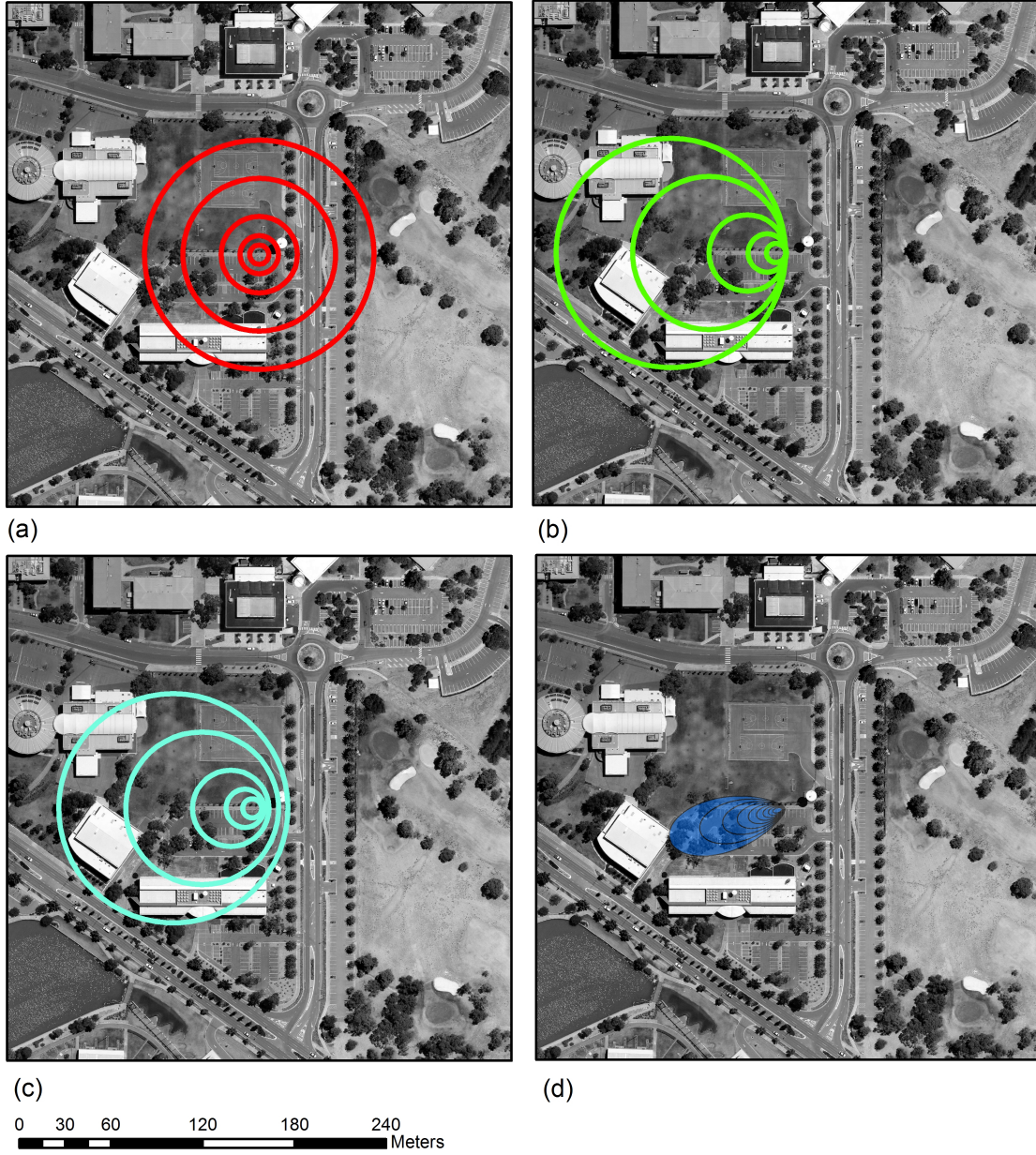
Figure 4.4: A representation of the buffers used in this research: (a) centred on the static AWS (circular 1), (b) 100% of buffer upwind of the static AWS (circular 2), (c) circular buffer centred a distance of 75% of radius distance in the upwind direction (circular 3), and (d) example of a Horst & Weil (1992) source area with 10% - 90% isopleths shown. Horst & Weil (1992) source areas were calculated at hourly timesteps.
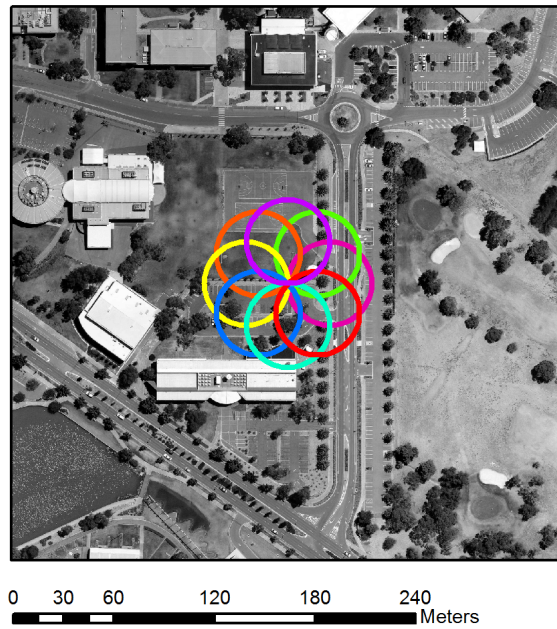
Figure 4.5: A representation of all the possible positions for the circular 2 buffer (50 m diameter example shown). The different colours here correspond to different prevailing wind directions — for example yellow is westerly flow (247.5° – 292.5°) and green is north-easterly flow (22.5° – 67.5°). Overall 8 different categories of prevailing wind flow were used. Both circular 2 and 3 were set up in this way, so that the area upwind of the prevailing flow was captured.

4.2.2 Turbulence source area

In addition to the circular buffers one analytical solution was also tested. The analytical solution from Horst & Weil (1992) was used in this research (e.g. Figure 4.4d). This analytical solution was designed for estimating the scalar sources influencing a micrometeorological flux station, and not a concentration source area, which should be used for meteorological observations such as air temperature. However, Horst (1999) gives a modification of his earlier flux source area model that can be used for vertical concentration profiles (e.g. Bowen ratio systems), and states that that the upwind extent of a source area associated with concentration-profile flux is similar to that of the source area for flux measurements. In this research the original Horst & Weil (1992) flux source area solution was used. This analytic solution (like all analytical solutions) is designed to be used above the roughness sublayer (Figure 4.2)), nevertheless it was tested for comparison with the circular source area estimates. The following inputs for each AWS were used:

- measurement height (m) (measured)

- roughness length (m) (values varied between $0.25 - 0.5$, from Wieringa (1993))

- Monin-Obukhov length (m) (day $=$ -140 and night $=$ 80, from Peña et al. (2010))

- friction velocity (ms^{-1}) (day $=$ 0.30 and night $=$ 0.15, from Peña et al. (2010))

- standard deviation of wind direction (ms^{-1}) (measured)

The Horst & Weil (1992) analytical solution was used to calculate hourly $10 - 90\%$ isopleths for source area contributions (e.g. Figure 4.4d). As such, the Horst & Weil (1992) solution provides a weighted average of surfaces that influence a given point. In order to compare the performance of the analytical solution, the analytical solution results are presented alongside the circular buffers (see Section 4.3).

4.2.3 Statistical analysis

To decide what buffer configuration and size was best used to approximate the source area of the AWS sites, the LST from the thermal images (taken during the Mawson Lakes field campaign — see Section 3.4.2) was compared with the measured in situ air temperature. A separate analysis was conducted for the nocturnal (15th February) and daytime (16th February) thermal images. These two images were captured during a period when atmospheric conditions were consistent with those observed throughout the intensive observational period. The LST of the area inside the buffer for all of the static sites was averaged (not a weighted average for circular buffers), using each of the buffers, and compared with the average air temperature during the period that the thermal images were captured (approximately a 2 hour period). This process was conducted for each buffer type/size — the LST was averaged using the same buffer configuration at all the sites, and for each configuration a linear regression model showing the relationship between LST and air temperature was fitted (Figure 4.6). This means that each r^2 value in Figure 4.6 was calculated using 27 LST-air temperature data points, one from each AWS (for example Figure 4.7). As such, each correlation coefficient in Figure 4.6, describes how well each buffer configuration (Figure 4.4), when applied uniformly to all sites (i.e. the same buffer for all sites), can describe the variability between LST and air temperature across the suburb. A necessary assumption of the circular buffer approach, was that the same buffer size can be used to describe all the AWS sites in the suburb. As a result of this assumption, different combinations of circular buffer configurations were not considered when calculating the correlation coefficients. For the circular buffers the air temperatures that were corrected for height were used (see Section 3.4.4), while for the Horst & Weil (1992) method uncorrected air temperatures were used. This was done because with the Horst & Weil (1992) method (unlike the circular buffers) a unique source area for each AWS was calculated using site specific characteristics, including measurement height.

The limitations of this approach are acknowledged below. To address the issues mentioned by Roth et al. (1989) and test the influence of roof LST on UCL air temperature, the correlation coefficients were also calculated with roof LST excluded from the buffer surfaces (shown in Figure 4.6).

4.3 Results and discussion

4.3.1 Key findings

The analysis of the LST-air temperature relationships has yielded the following best estimates of the source area for an UCL AWS in Mawson Lakes (Figure 4.8):

- day — 50 m (or less) diameter circle upwind of the source (circular 2 or circular 3);

- night — 25 m diameter circle centred on the source (circular 1).

Figure 4.6 shows that for the daytime example, the correlation between air temperature and LST was lower, which is in agreement with previous research (Dousset, 1989; Voogt & Oke, 2003; Mohan et al., 2013). For both the day and night cases, the general trend was for the correlation to increase as buffer size decreased. This pattern was also found by Schwarz et al. (2012) who observed that the correlation decreased as the buffer size increased, as a greater proportion of unrepresentative surfaces were included in the buffer. However, during the day, the different buffer sizes returned more similar results than the nighttime example. This similarity represents the effects of advection and atmospheric mixing, which are more apparent during the day. Overall, for both day and night, the smaller buffers with a diameter of 50 m (or less), effectively covered the canyon floor that surrounded the site. It is thought that the adjacent canyon surfaces were most representative of the surfaces that influenced the microclimate air temperature at these UCL sites, when considering LST from a planar view.
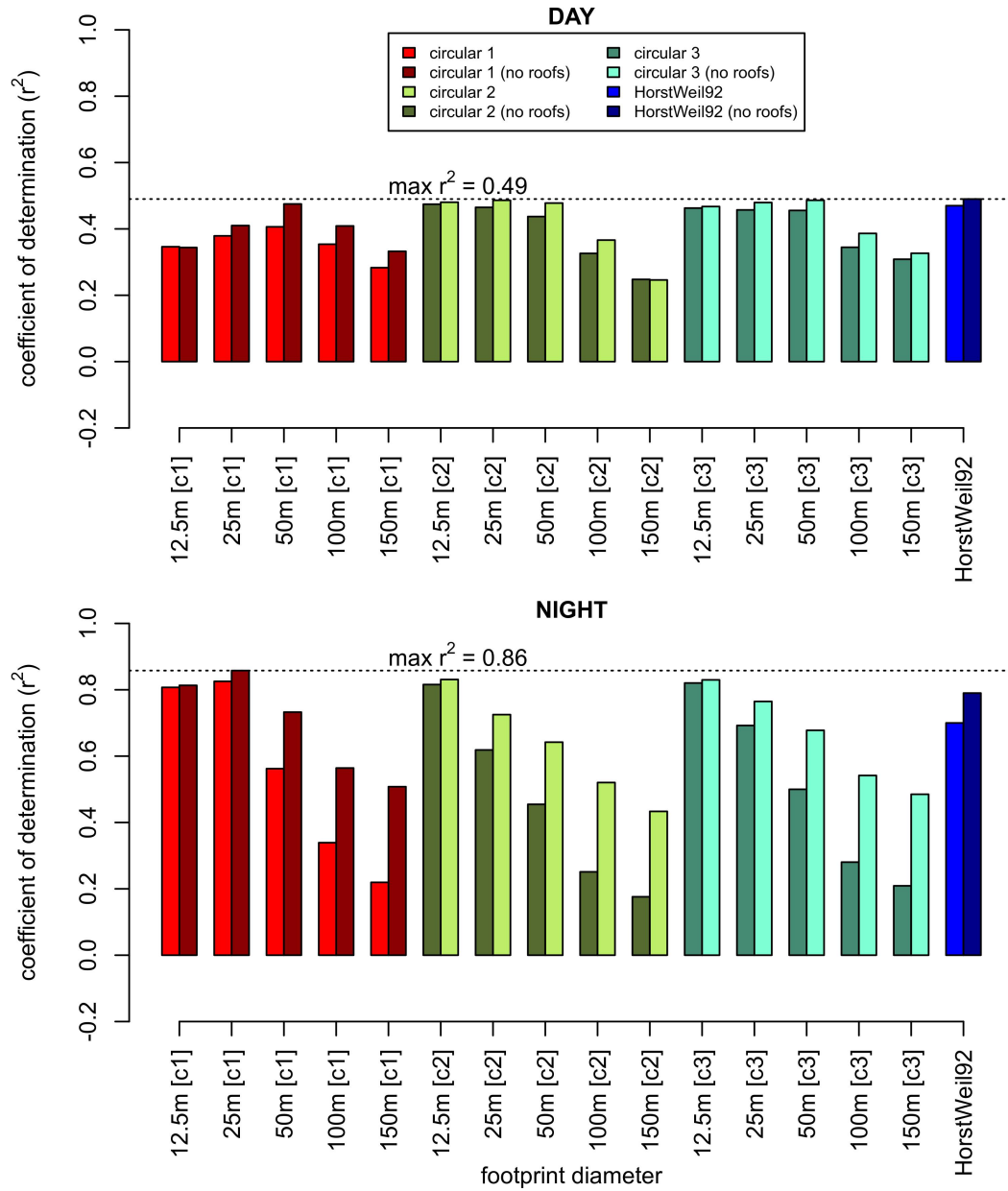
Figure 4.6: The coefficient of determination (r^2) that were calculated for different buffer configurations. The r^2 values were calculated using LST (independent variable) and air temperature (dependent variable) for day (top) and night (bottom) cases. On the basis of these correlations, the the best daytime footprint was judged to be the 50 m diameter circular 2 configuration, and the best nighttime footprint to be the 25 m circular 1 configuration. See Figure 4.7 for the scatter plots and linear regression models that correspond to these configurations.

DAY
50 m diameter circle 2

NIGHT
25 m diameter circle 1

$T_a = 0.06 * LST + 28.2$

$r^2 = 0.5$

$T_a = 0.49 * LST + 9$

$r^2 = 0.9$

(a)

(b)
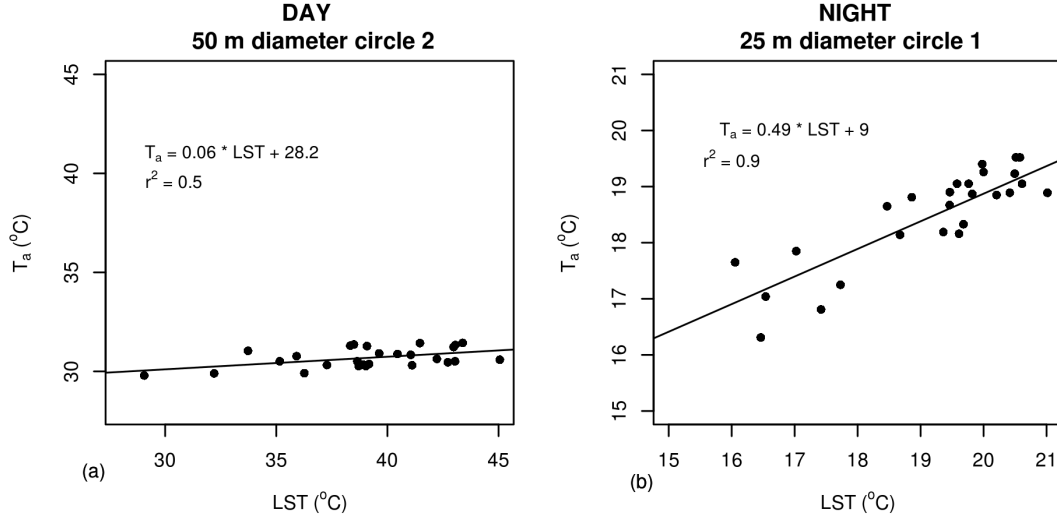
Figure 4.7: The scatter plots and linear regression models for the buffers that produced the best air temperature-LST correlations: (a) daytime case with correlation with LST averaged using a 50 m diameter circular 2 footprint and (b) nighttime case with LST averaged using a 25 m diameter circular 1 footprint.

On the basis of the correlation coefficients, the 25 m diameter circular 1 configuration (centered at the source) was clearly the most appropriate footprint for the nighttime case (Figure 4.6). Given that wind speeds tended to become lighter and more variable at night this centred configuration (as opposed to an upwind setup) also made physical sense. The 50 m diameter circular 2 configuration is used for daytime cases throughout this research, but arguably there was no clear "best" configuration for the day case (Figure 4.6). There was little difference in air temperature-LST correlation observed between the circular 2 and 3 configurations. However, the fact that the 12.5 m, 25 m, and 50 m diameter circular 2 and 3 configuration buffers produced better correlations than the circular 1 buffers, suggests that taking into account wind direction during the day was important. Overall the results suggest the buffer should be up to 50 m in diameter and located upwind of the source. In this research, for the daytime case, the 50 m circular 2 configuration (Figure 4.8) is used.

The Horst & Weil (1992) method when applied to the day case, produced similar sized source areas to the circular buffers (e.g. see Figure 4.4d) and the air temperature-LST correlations

115
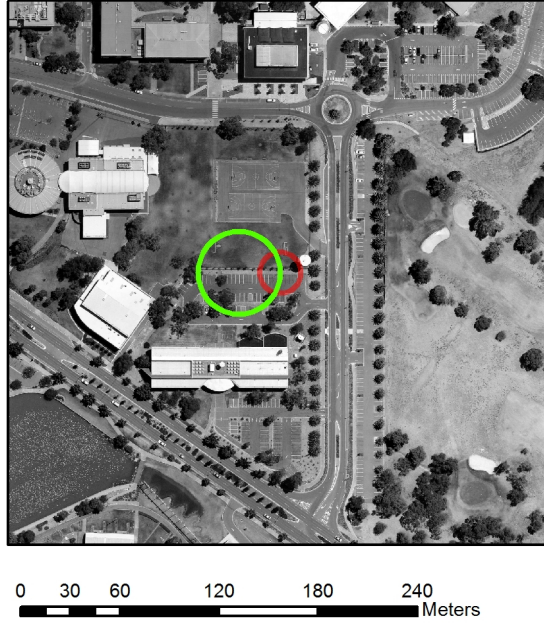
Figure 4.8: A representation of the best estimates of sources area for the microscale AWS sites in Mawson Lakes. Red = night-time 25 m diameter circular 1 and green = 50 m diameter circular 2.

were about the same magnitude as the better performing circular configurations (Figure 4.6). However, at night the Horst & Weil (1992) method generated much larger estimates of source area (see Figure A.10b) than the best performing circular buffers, and the correlation between air temperature and LST was lower than some circular approaches. Given the methodological complexity and assumptions associated with calculating source area using the Horst & Weil (1992) approach, it was deemed unnecessary for this research.

4.3.2 Effects of roofs

Roof surfaces can have a high daytime surface temperature variability. Roth et al. (1989) showed that the daytime range in roof LST causes an exaggeration of the daytime range of the urban LST. In addition to this, it is unclear to what extent roof LST affects air temperature inside in the urban canopy (Figure 4.2). To address this the LST was tabulated both with and without building roofs included (Figure 4.6). This analysis shows that removing roof temperatures im-

proves the LST-air temperature correlation, especially at night (Figure 4.6). This suggests that roof LST are not particularly important for defining the surface street level air temperature. However, roof surfaces have heterogeneity of emissivity, and the improvement of r^2 without roofs may also reflect some error in the emissivity of roofing materials, as uniform emissivity values for roofs were used in this research. Without high resolution roof emissivity data to correct LST, it was difficult to ascertain what factor was causing this trend.

4.3.3 Limitations

An important factor in this source area analysis, is that for circular buffers the LST was taken as an average over a given surface, and not as a distance-from-source weighted average (as in Figure 4.4d). Therefore, the LST from smaller buffers were more representative of air temperature than the larger buffers, which tended to capture less representative surfaces, such as those located in adjoining urban street canyons. The use of unweighted average across the buffer surface meant that these less representative surfaces were treated equally in the calculations. However, this analysis was not attempting to calculate a flux station-type source area estimate. The analysis was attempting to capture the surfaces that are most representative of microscale air temperature variability. Given that the correlation coefficient does not constantly increase as buffer size decreases (3 m and 6 m diameter circular buffers were also tested), we can be confident that we are inferring a reasonable estimate of the buffer size that captures the surfaces most representative of microscale air temperature variability. Nevertheless, source area analysis of UCL sensors is a very important area that requires future research.

Overall, approximately 50% of daytime air temperature variability, and 90% of nighttime air temperature variability can be explained by the average LST of these source area estimates. However, a number of factors were not captured, including 3-dimensional effects (e.g. canyon wall temperatures), local-scale advective effects (such as park and lake breezes), and differences

in characteristics of the upwind fetch. The approach used in this research does not capture these processes, and it's expected that all these factors will have some influence on microscale air temperature variability, especially during the day. However, the good correlation between air temperature and LST suggests that microscale air temperature is highly influenced by the thermal characteristics of the surfaces directly adjacent to the source.

Another limitation of this analysis is the assumption that the same source area can be applied to all the sites. Clearly factors such as surface roughness and the configuration of buildings will affect the actual source area from site to site. It is acknowledged that there will be some variability from site to site in actual source area size and positioning. For example, 7 of the AWS stations were mounted at a lower height, which means that these locations would have had smaller source areas (the Horst & Weil (1992) method confirmed this) than the other sites. However, these locations were mostly quite homogeneous and the effects of this discrepancy were minimal. Overall, given that the Mawson Lakes site is relatively open (see Figure 3.4) it is thought that the method presented here was an acceptable means of getting a broad understanding of the average area influencing air temperature across the 27 static sites. It is thought that the source area estimates presented here are a reasonable estimate of the average area that influences the air temperature of an UCL AWS, in this environment.

4.3.4 Application and broader relevance

The findings of this source area analysis are useful because they provide a non-arbitrary value to characterise the surfaces that directly influence the microscale air temperature in Mawson Lakes. The values obtained in this source area analysis are used throughout this research, including both the observational and modelling analyses (Figure 3.1). These findings also have practical implications for practitioners and urban designers. A key implication is that the effects of the land-surface can be highly localised. The highly localised nature of the UCL source area is

118

one of the reasons why urban microclimates are highly variable. This is both a challenge and an opportunity for practitioners and designers looking to create thermally comfortable environments. Urban designers may be able to create highly targeted cool areas with small patches of so called blue and green infrastructure (e.g. WSUD). These cooling measures could be placed in the areas that have the greatest need for cooling such as schools, hospitals, and retirement homes.

This research also highlights that there is a potential disconnect between urban climate modelling and microscale HTC conditions. There are different modelling approaches that are suited to modelling different scales of urban climate (as shown in Section 2.4.2). However, Oke (2009) has pointed out that urban climatologists and conversationalists commonly use approaches that do not match the scale of interest. Much of the urban climate modelling undertaken in recent times claims to be motivated by urban heat mitigation and improved HTC. This source area analysis reinforces the fact that in order to capture microscale climate variability and accurately understand human heat stress a high resolution approach is needed.

5 The Mawson Lakes observational dataset: spatial variability of air temperature and HTC.

5.1 Introduction

The overarching aim of this research is to understand and quantify the potential for WSUD and stormwater reintegration techniques to mitigate urban warmth and improve HTC. This research aims to understand and quantify the cooling effects of WSUD on urban microclimate, so that future WSUD developments can be purposefully designed for microclimate benefits. As discussed in chapter 2 (literature review), microclimate in urban areas is highly variable. Although cities are generally characterised as being hotter than rural areas, there are in actuality cooler and warmer locations within an urban area. From the perspective of human heat stress, intra-urban variability is more relevant than the UHI, because it reveals more about the conditions people are actually exposed to. Given the importance of intra-urban microclimate variability, a major goal of this research is to **to identify the observed microscale air temperature and HTC variability in a WSUD suburb**. To address this objective a major field campaign was conducted in Mawson Lakes — a WSUD suburb in Adelaide, South Australia. A range of observational techniques were used including static AWS, bicycle transects, and aircraft remote sensing to capture a high resolution picture of microclimate variability in the suburb. A full description of the Mawson Lakes field campaign is provided in section 3.4. This chapter provides an analysis of the data collected during the Mawson Lakes campaign, and will identify the microscale air temperature and HTC variability. This research is also interested in how WSUD contributes to microclimate variability, and to what extent it can provide microclimate cooling benefits. As such, this chapter will also address the following questions:

(1) What are the effects of WSUD on LST, air temperature, and PET during summertime

conditions in Mawson Lakes?

(2) What is the magnitude of these effects?

(3) What is the spatial extent of air temperature cooling from WUSD features?

The chapter will begin with a short data and methods section that will outline some important data analysis methodology information, which was not provided in section 3.4. However, the chapter primarily consists of results and discussion, including the observed microclimate variability in Mawson Lakes, and will follow on from that by exploring how WSUD features contribute to microclimate variability.

5.2 Data and methods

5.2.1 Introduction

In this section the key data analysis relevant to this chapter is described, namely the static AWS statistical clustering methodology (described below in section 5.2.2). The analysis in this chapter focuses on 3 important temperature measures: LST, air temperature, and PET. As shown in chapter 4, LST and air temperature are correlated and therefore LST is a convenient way to capture spatially comprehensive urban temperatures. Air temperature is an important metric because it is an objective measure of the thermal environment in urban areas. Furthermore, air temperature is often used as a key measure for heat health thresholds and to characterise energy use demands in urban areas. It is also important to consider HTC (i.e. PET), which is influenced by a range of meteorological factors, as it is crucial for creating thermally comfortable environments and is a better indicator of heat stress than air temperature.

5.2.2 Static AWS cluster analysis

As part of this analysis, to further understand how the land surface was contributing to microclimate variability, the static sites were classified into thermal categories via a hierarchical cluster analysis approach. The static AWS sites were clustered twice; once using air temperature (see Figure 5.1) and once using PET (see Figure 5.2). The daily average, daily minimum, and daily maximum air temperature/PET were used as clustering criteria. A Ward hierarchical clustering approach (Ward, 1963) was used to identify the clusters. Ward's method was chosen because it tends to divide data in clusters of roughly equal size. Through visual analysis of the cluster dendrogram the subjective decision was made to recognise 6 unique clusters for both air temperature and PET (dendrograms are provided in the appendix). These clusters show the sites that have statistically similar air temperature and PET characteristics. Clustering provided an understanding of the drivers of air temperature and PET variability without inferring selection biases. The average land surface characteristics of these thermal categories were tabulated (see Figure 5.1b & 5.2b) using the source area estimates (described in chapter 4 — see Figure 4.8). It is acknowledged that tabulating the land cover for the PET clusters using the source area estimates is potentially invalid because the source area estimates were derived using LST-air temperature relationships, and not PET. Nevertheless, the clustering allowed us to compare sites with similar PET and air temperature variability, and better understand urban microclimate variability.

The air temperature clusters ('TA' suffix used to indicate air temperature clusters) were given names that reflect the average land surface characteristics of each cluster: urban sites with nearby water (TA-1$_{[Urb+Wtr]}$), mixed land-use with nearby water (TA-2$_{[Mxd+Wtr]}$), urban midrise type sites (TA-3$_{[Urb+Mid]}$), urban residential sites (TA-4$_{[Urb+Res]}$), natural grass dominated sites (TA-5$_{[Nat+Grs]}$), and a single outlier site (TA-6$_{[outlier]}$). Not every site within the clusters fits these characteristics, but these labels represent the average characteristics of each cluster.
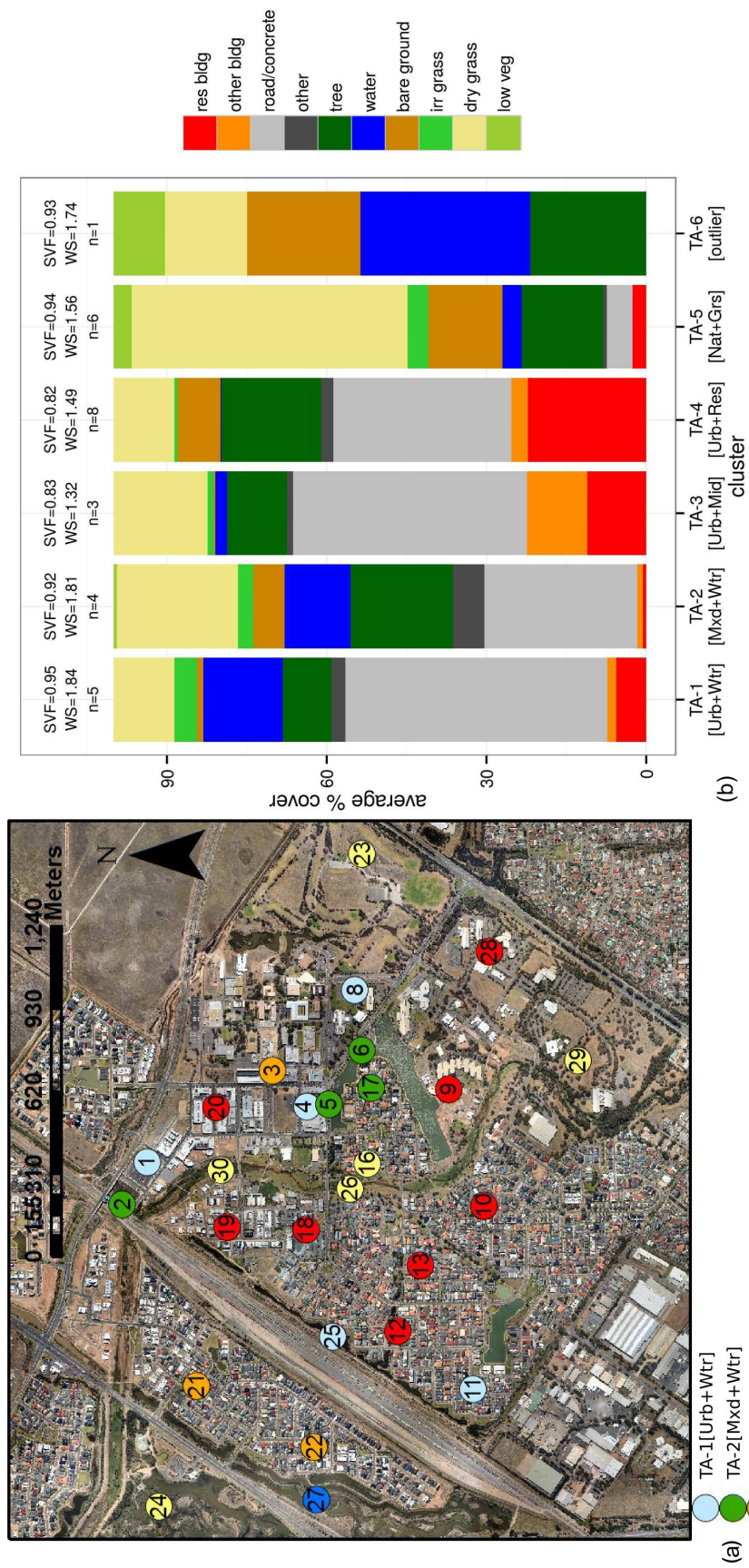
Figure 5.1: *An overview of static AWS air temperature clusters: (a) the location of different cluster types (station numbers also indicated) and (b) the average land coverage characteristics of each cluster (source area estimates from chapter 4 are used). The average wind speed and SVF for each cluster is also show.*

123
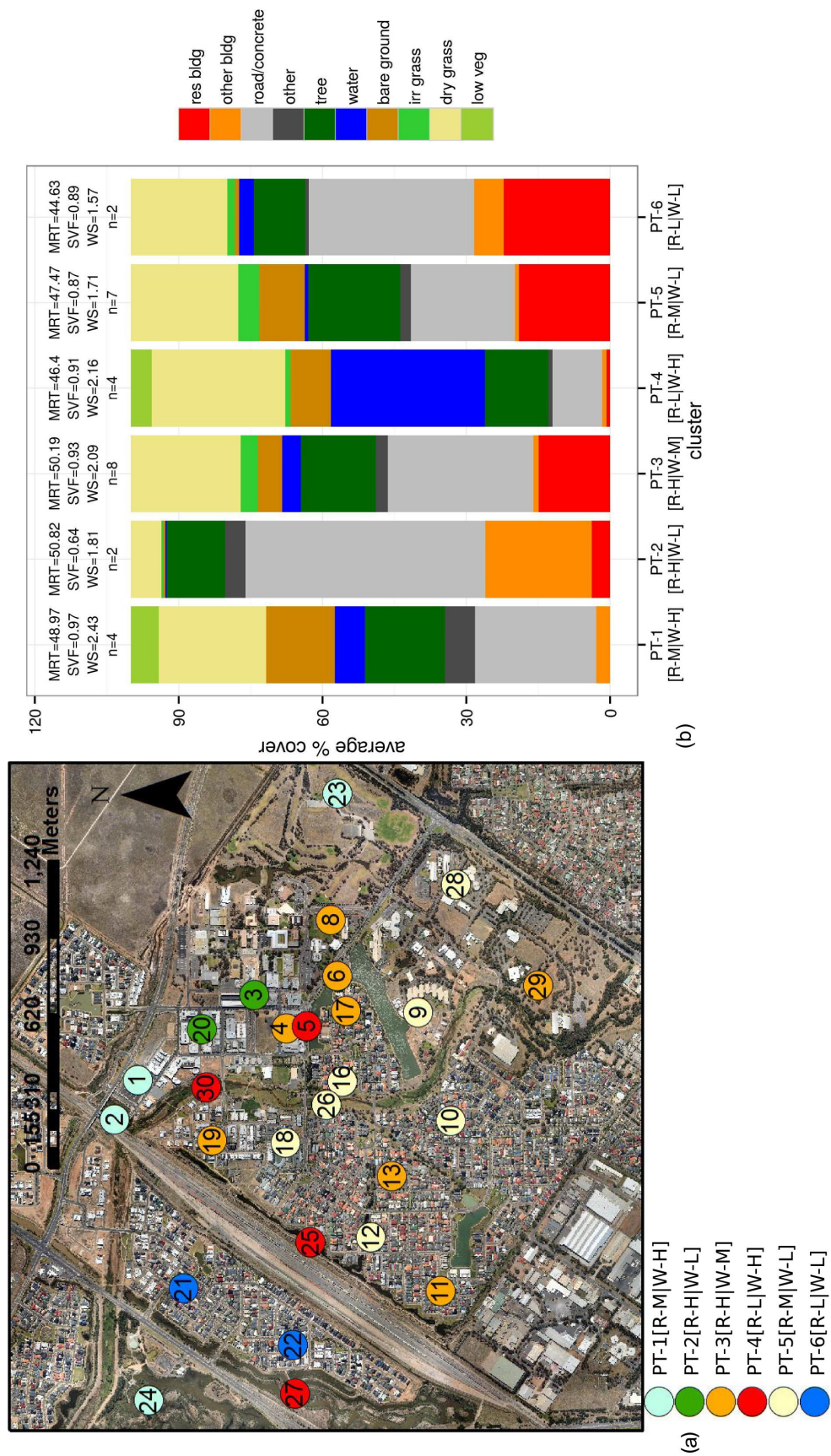
Figure 5.2: An overview of static AWS PET clusters: (a) the location of different cluster types (station numbers also indicated) and (b) the average land coverage characteristics of each cluster (source area estimates from chapter 4 are used*. The average SVF, wind speed (daytime), and MRT (daytime) are shown. Much of the variability in PET was controlled by shading and wind speed differences between the sites. *Note: source area estimates used were derived using air temperature-LST relationships; PET may have a different source area to air temperature. Therefore, these land cover fractions may not be representative of the surfaces that best define PET.

The TA-4$_{[Urb+Res]}$ and TA-3$_{[Urb+Mid]}$ clusters were the most urbanised sites, and had 66.1% and 60.0% impervious surfaces, respectively. The TA-3$_{[Urb+Mid]}$ sites had a greater proportion of taller buildings and lower wind speeds. The TA-1$_{[Urb+Wtr]}$ sites were also categorized by impervious surfaces (57.7% impervious), but had more water (13.4%), and less buildings than categories TA-4$_{[Urb+Res]}$ and TA-3$_{[Urb+Mid]}$, meaning TA-1$_{[Urb+Wtr]}$ sites were more exposed. The TA-2$_{[Mxd+Wtr]}$ sites also had nearby water, but were less urbanized (36.4% impervious) than categories TA-1$_{[Urb+Wtr]}$, TA-3$_{[Urb+Mid]}$, and TA-4$_{[Urb+Res]}$. Lastly, TA-5$_{[Nat+Grs]}$ sites were the more natural sites, with only 9.6% impervious surfaces.

The PET clusters ('PT' suffix used to indicate PET clusters) had less clear representative land surface characteristics (see Figure 5.2b) and were more easily characterised by differences in MRT ('R' used to donate radiant loading) and/or wind exposure ('W' used to donate wind level) (see Figure A.13). The lack of clear land surface characteristics is to be expected as wind speed and the radiant environment (including shading) highly influence PET (discussed further later). The largest differences in PET occurred during the day, and thus the PET clusters were mostly driven by differences in the daytime wind speed and MRT levels. For naming purposes, each cluster was classified in terms of high ('H'), medium ('M'), or low ('L') levels of daytime wind speed and MRT (see Figure 5.2b or Figure A.13 for more details). The PET clusters that were exposed to high levels of wind were PT-1$_{[R-M|W-H]}$ and PT-4$_{[R-L|W-H]}$, which were well ventilated sites that were mostly located on the urban fringe and near water bodies, respectively. There were three clusters of sites that all had low wind speed during the day, but different levels of MRT: PT-2$_{[R-H|W-L]}$, PT-5$_{[R-M|W-L]}$, and PT-6$_{[R-L|R-L]}$. The differences in MRT between these sites were mostly related to differences in shading. The PT-2$_{[R-H|W-L]}$ sites were un-shaded and poorly ventilated urban sites; the PT-5$_{[R-M|W-L]}$ clusters were typically residential-type sites with medium shading and low wind speed; and PT-6$_{[R-L|R-L]}$ were highly shaded but poorly ventilated urban sites, which were sheltered by nearby buildings. Finally, PT-3$_{[R-H|W-M]}$ were

mostly associated with residential areas, but had high MRT and medium wind speeds. The PET and air temperature clusters provided an understanding (in unbiased way) of the factors that contributed to air temperature and HTC variability in Mawson Lakes; these clusters are referred to and discussed further in the analysis below.

5.3 Results and discussion

5.3.1 Intra-urban variability of air temperature and PET

This research is focused on the cooling potential of WSUD from a heat health and human well-being perspective. This focus means that quantifying and understanding intra-urban variability of microclimate is an important part of this research (see **objective 1**). In this section the nature of the observed variability is described in broad terms, and in the proceeding sections the causes/drivers of this observed microclimate variability are addressed and discussed in the context of previous research.

The static AWS reveal that there was a significant amount of variability in microscale air temperature in the suburb. It was found that the intra-urban variability of daytime air temperature was of a similar magnitude to urban-rural contrasts observed in previous UHI observational studies. The average 3 pm air temperature, during the intensive observational period, varied by up to 2.3 °C (Figure 5.3a — 'ALL'). However, the maximum variability of 3 pm air temperature, on a given day, was 3.4 °C (observed on the 14th and 15th February, see Figure 5.3a). The spatial distribution of average air temperature at 3 pm for the static AWS is shown in Figure 5.4a. There were large differences in average air temperature observed over short distances, such as the western part of the suburb (stations 27 and 22), and at the two sites located in the center of the suburb (stations 26 and 16), near the river channel. Despite this variability, there are some trends that are immediately apparent in these data. During the day, there was an observable air

temperature cooling affect associated with the SDML, especially north/north-east of the lake. The cooling potential of water bodies is discussed below in Section 5.3.2. However, the cooling downwind of the lake is consistent with the fact that daytime wind direction was predominately south-westerly during the intensive observational period (Figure 5.4 — inset). Generally speaking, the sites with warmer air temperature were in the more built up areas, which had average 3 pm air temperatures of 28 °C or more (Figure 5.4a). Although the urban sites were warmer, natural sites that were not located near water bodies also had warmer air temperature at 3 pm.
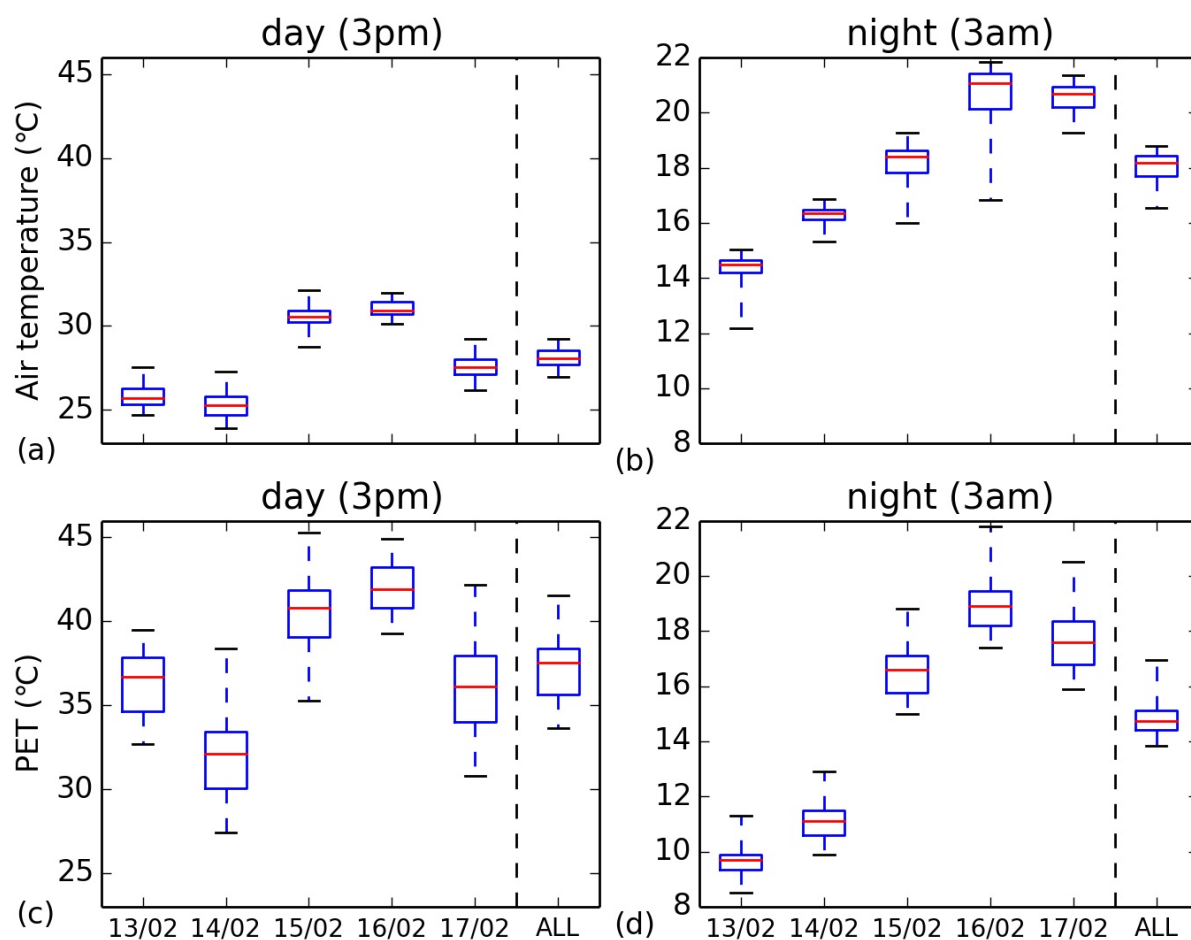
Figure 5.3: Boxplots showing the AWS average intra-urban variability for (a) 3 pm air temperature, (b) 3 am air temperature, (c) 3 pm PET, and (d) 3 am PET, for each day during the intensive observational period. The 'ALL' box shows the variability of the average 3 pm and 3 am temperature throughout the 5 day intensive observational period (n = 27 for all the boxes). In these boxplots the following are indicated: the median (red line), the inter-quartile range (75% percentile – 25% percentile), and the whiskers show the range of the dataset.

The bicycle transects further emphasise how large the spatial variability of daytime air tem-

(a) Static stations average at 3pm

T_a (°C)

26.97 - 27.20
27.21 - 27.43
27.44 - 27.65
27.66 - 27.88
27.89 - 28.11
28.12 - 28.34
28.35 - 28.57
28.58 - 28.80
28.81 - 29.02
29.03 - 29.25

(b) Static stations average at 3am

T_a (°C)

16.53 - 16.75
16.76 - 16.98
16.99 - 17.21
17.22 - 17.43
17.44 - 17.66
17.67 - 17.89
17.90 - 18.11
18.12 - 18.34
18.35 - 18.57
18.58 - 18.79
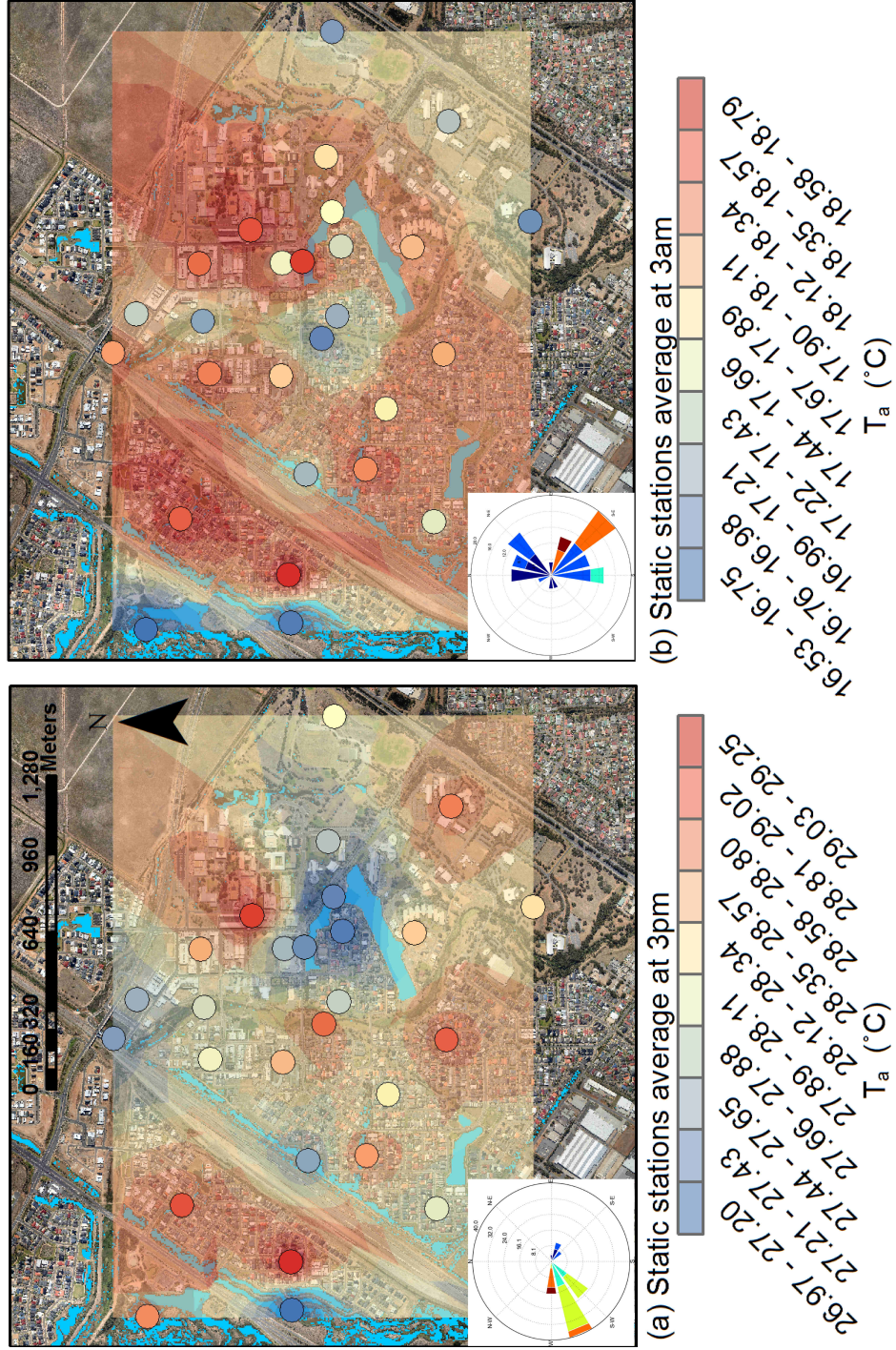
Figure 5.4: The average air temperature for static AWS sites at (a) 3 pm and (b) 3 am. Air temperature data were interpolated using an inverse distance weighted (IDW) approach (ArcGIS algorithm). A variable search radius was used, with up to 3 points used for the calculation. The average wind direction is shown in the inset. The average wind speed = 2.5 ms⁻¹ (3 am) and 5.3 ms⁻¹ (3 pm).

perature can be. Eighteen bicycle transects were conducted during the campaign, which provided high resolution snapshots of microscale air temperature variability across the suburb (spatial plots for all 18 transects can be found in Appendix, Figures A.14–A.16). The variability of the daytime transects (conducted at 2 pm and 3 pm) were 2.2 °C, 2.3 °C, and 1.6 °C (Figure 5.5). Similar trends to those observed at the AWS were observed in the transect data, such as areas of cooling around the Sir Douglas Mawson and Shearwater Lakes, but there does appear to be more fluctuation (e.g. microscale advective effects) in these transect data. The large differences in air temperature over short distances were again observed in the bicycle transect data. This large amount of intra-urban air temperature variability reinforces the need for a high resolution approaches when considering human exposure and heat stress. Furthermore, it shows that it is possible to create (at the microscale) "cool spots" where exposure to higher air temperature is reduced. Overall, the daytime air temperature variability in Mawson Lakes (AWS and transects) was influenced by the presence of WSUD features, which significantly influenced the daytime microclimate variability.

The variability of daytime PET was larger than that of air temperature. The average 3 pm PET had an intra-urban range of 7.9 °C (Figure 5.3c). On a given day the maximum variability of PET reached 11.4 °C (observed on the 17th, see Figure 5.3c). Overall, the AWS data shows that the magnitude of PET was larger than air temperature, and the variability of PET was greater too. The spatial variability of daytime PET is shown in Figure 5.6a. The spatial distribution of PET was different to the spatial distribution of air temperature during the campaign. In particular, the cooling associated with SDML was not as apparent in the PET data. A number of sites that had higher than expected PET, relative to measured air temperature, were those located near to the lake (Figure 5.6a). The reasons that some sites had quite different PET and air temperature characteristics is related to the fact the HTC is also affected by MRT and wind speed — this is discussed further below. Overall, the magnitude of PET variability was
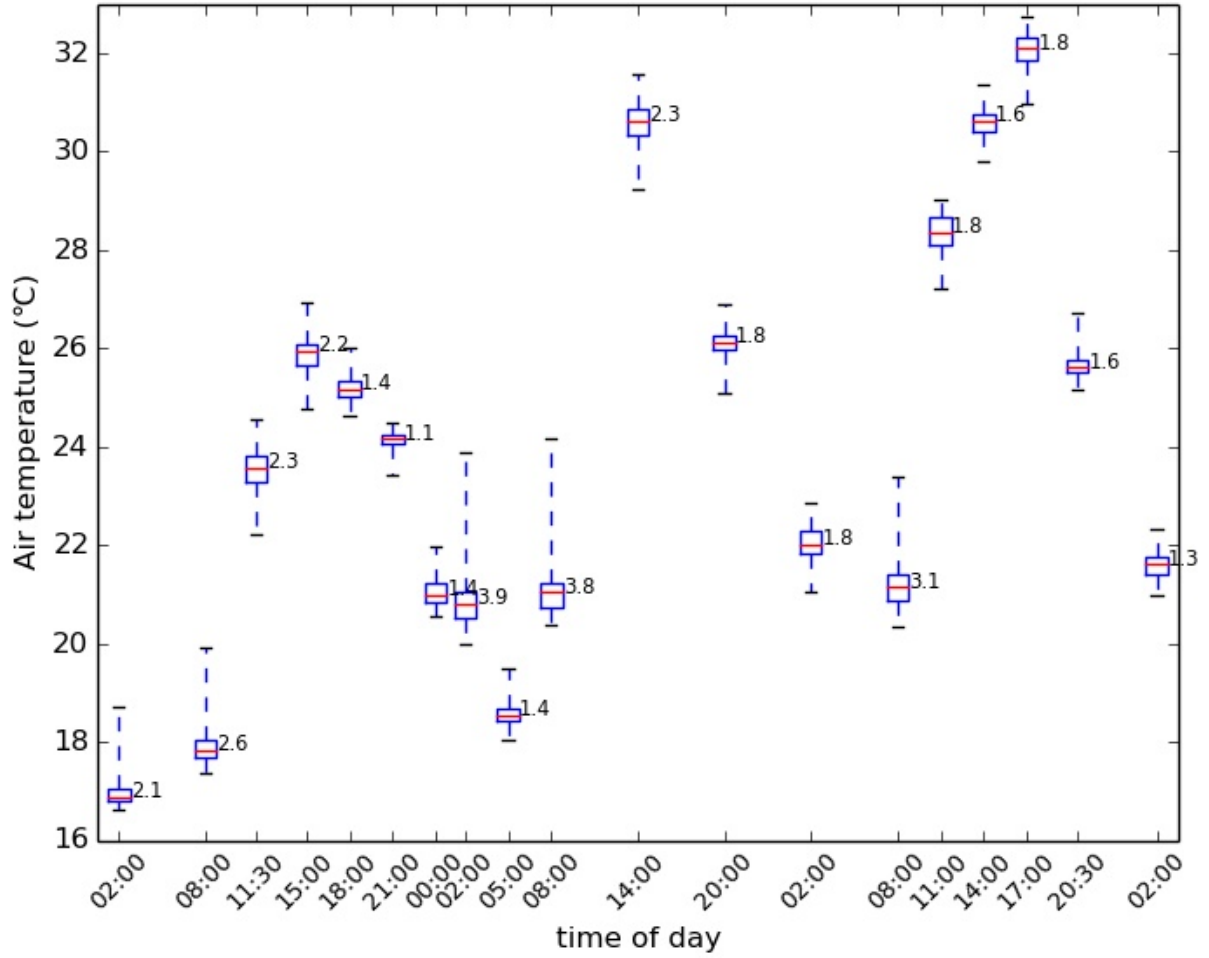
Figure 5.5: Boxplots showing the amount intra-urban variability of air temperature for the bicycle transects conducted during the Mawson Lakes campaign. The number next to each boxplot indicates the range of temperature variability (°C) observed in each transect. In these boxplots the following are indicated: the median (red line), the interquartile range (75% percentile - 25% percentile), and the whiskers show the range of the dataset. The x-axis scale spans from 2 am February 14th – 2 am February 17th.

greater than air temperature, and the general pattern of PET was similar (with some notable differences) to observed air temperature variability.

The nighttime variability of air temperature was similar in average magnitude, but spatially quite dissimilar to the daytime air temperature variability. At night, the average range of air temperature was 2.3 °C — the same as the daytime value. However, this average variability of night air temperature varied more from day-to-day with a maximum value of 5.0 °C observed on the 16th, and a minimum value of 1.5 °C observed on the 14th (Figure 5.3b). The nighttime

(a) Static stations average PET at 3pm

(b) Static stations average PET at 3am
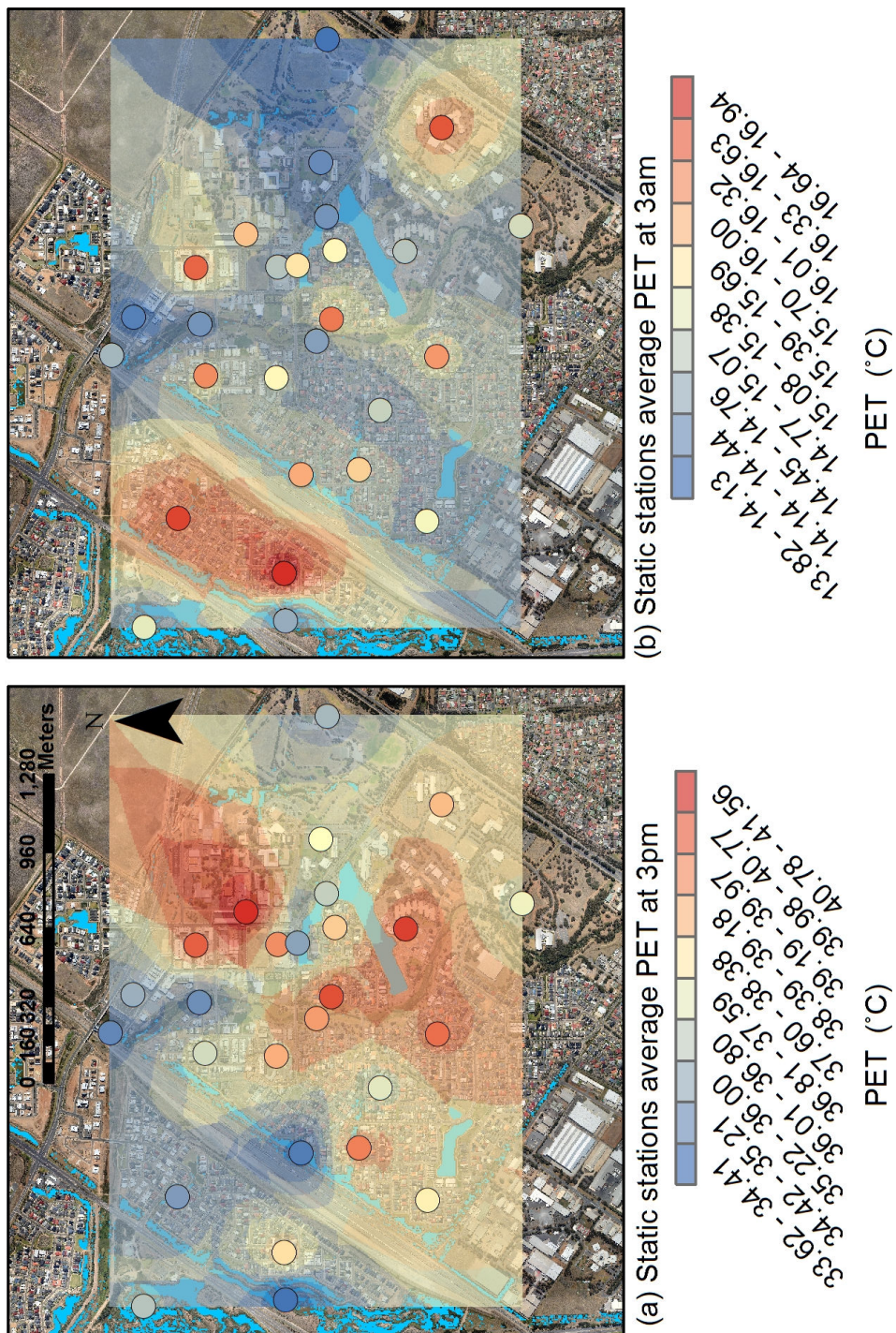
Figure 5.6: The average PET for static AWS sites at (a) 3 pm and (b) 3 am. PET data was interpolated using an inverse distance weighted (IDW) approach (ArcGIS algorithm). A variable search radius was used, with up to 3 points used for the calculation.

bicycle transects reinforce the trends in air temperature variability throughout the suburb, with the following values observed during night (12 am, 2 am, and 5 am transects) transects: 2.1 °C, 1.4 °C, 3.8 °C, 1.8 °C, and 1.3 °C (Figure 5.5). However, the spatial structure of night air temperature variability was different to the spatial variability during the day (Figure 5.7b). In contrast to the daytime case, the SDML did not provide an air temperature cooling effect. At night, the cooler locations were away from built-up areas; including the two sites located in the Sailsubry wetland (stations 24 and 27), the sites located in the grassed areas east of the suburb (stations 29, 28, and 23), and the sites located along the river channel (stations 26 and 30), which runs through the center of the suburb. The more urbanised sites were warmest at night; most had an average 3 am air temperature above 18 °C. Overall, although there was significant nighttime air temperature variability in Mawson Lakes (AWS and transects), it appears that the variability was not highly influenced by the presence of WSUD features (discussed further below).

For nighttime climate, the focus of this research is air temperature, as HTC is a less important metric at night. Nevertheless, the magnitude of nighttime PET variability was found to be smaller than daytime PET, with an average range of 3.1 °C, and a maximum daily variability of 4.4 °C (occurred on the 16th, see Figure 5.3d). The magnitude of nighttime PET variability was comparable to air temperature (Figure 5.3c), though the spatial distribution of PET was quite different (Figure 5.6b). As mentioned, this is because there were factors, other than air temperature, that influence HTC; at night the other highly influential factor was most likely wind speed.

Overall, the static AWS and bicycle transect data did reveal large differences in air temperature and PET over short distances in Mawson Lakes. This finding shows how large the variability of microclimate can be at the scale of human exposure. While the drivers of this variability have not yet been discussed in detail, it is clear that this large variability represents both a challenge

and opportunity for those seeking to reduce exposure to extreme heat. Implementing effective city-wide cooling measures may be difficult, but creating small microscale cool spots in the urban environment is highly feasible. The factors that contribute to night and day variability of both air temperature and PET are discussed further below.

5.3.2 The effects of water bodies on microclimate in Mawson Lakes

5.3.2.1 Water bodies and land surface temperature (LST)

LST is a simple way to capture and assess urban temperatures with extensive spatial coverage. LST for the different land cover categories (see Figure 3.9 for an overview of land cover categories) were averaged for each image acquisition, and are shown in Table 5.1. It was found that water bodies had a significant effect on LST. Water surfaces had the smallest diurnal range of LST, meaning they were the coolest surfaces in the domain during the day, and among the warmer surfaces at night. During the day, the average LST of water bodies was 8.9 °C cooler than concrete and asphalt surfaces and 7.3 °C cooler than dry grass. The cooler LST of water bodies during the day is to be expected, given the thermal properties of water, which has high thermal inertia. The high thermal inertia of water also caused water to remain warmer throughout the night (Table 5.1). At night, the average LST of water surfaces was 3.3 °C warmer than grass and 0.4 °C cooler than concrete and asphalt (Table 5.1). These LST results pose some important questions about the effects of water bodies on air temperature and HTC. How large is the daytime cooling effect associated with water bodies? Is there any observable nighttime warming effects associated with water bodies? The effects of the water bodies on daytime and nighttime microclimate variability are discussed in the sections below.

Table 5.1: The average LST of the entire Mawson Lakes domain by land cover type for nighttime and daytime images.

Land cover type	Domain coverage (%)	Daytime LST (°C ± std dev)	Nighttime LST (°C ± std dev)
Other	5.5	37.5 ± 4.3	17.6 ± 2.1
Trees	16.2	37.5 ± 5.2	17.1 ± 2.0
Water	5.2	30.5 ± 5.3	18.3 ± 1.8
Building residential	14.0	37.2 ± 4.4	14.5 ± 2.2
Building commercial	3.0	33.6 ± 6.1	13.3 ± 4.0
Bare ground	8.5	39.0 ± 4.3	16.8 ± 1.7
Grass	26.8	37.8 ± 3.4	15.0 ± 2.0
Concrete and asphalt	17.4	39.4 ± 3.7	18.7 ± 1.9
Irrigated grass	1.8	31.0 ± 2.3	15.2 ± 1.7
Low vegetation	1.5	33.8 ± 4.5	16.4 ± 1.6
AVERAGE	100	35.7 ± 4.8	16.3 ± 2.6

5.3.2.2   Water bodies and air temperature

The Mawson Lakes suburb contains a number of WSUD water bodies that have cooling benefits for urban air temperature. The cluster analysis shows that during the day, the water dominated sites were cooler than the urbanised sites. Air temperatures at the water affected sites (categories TA-1$_{[Urb+Wtr]}$ and TA-2$_{[Mxd+Wtr]}$) were cooler than the domain average, and up to 1.8 °C cooler than the warmest urban sites (TA-3$_{[Urb+Mid]}$) (Figure 5.7). The warmest daytime sites were the TA-3$_{[Urb+Mid]}$ sites, which had an average daily maximum air temperature of 29.3 °C, while the average daily maximum at the TA-1$_{[Urb+Wtr]}$ and TA-2$_{[Mxd+Wtr]}$ was 27.9 °C and 27.5 °C, respectively. More broadly, the spatial plots clearly show that the average daytime air temperature downwind of the SDML was cooler than most of the domain (Figure 5.4a). The presence of cooling downwind of water bodies, observed in Mawson Lakes was broadly consistent with other observational studies that have shown the cooling effects of open water (Murakawa et al., 1991; Saaroni & Ziv, 2003; Chen et al., 2009). However, the WSUD features in Mawson Lakes were designed for ecological and water preservation purposes, and were not built to target urban climate cooling. While there was clearly a cooling effect associated with the WSUD water

bodies, it was also found that meteorological conditions influenced the effectiveness of daytime cooling from water bodies in Mawson Lakes.
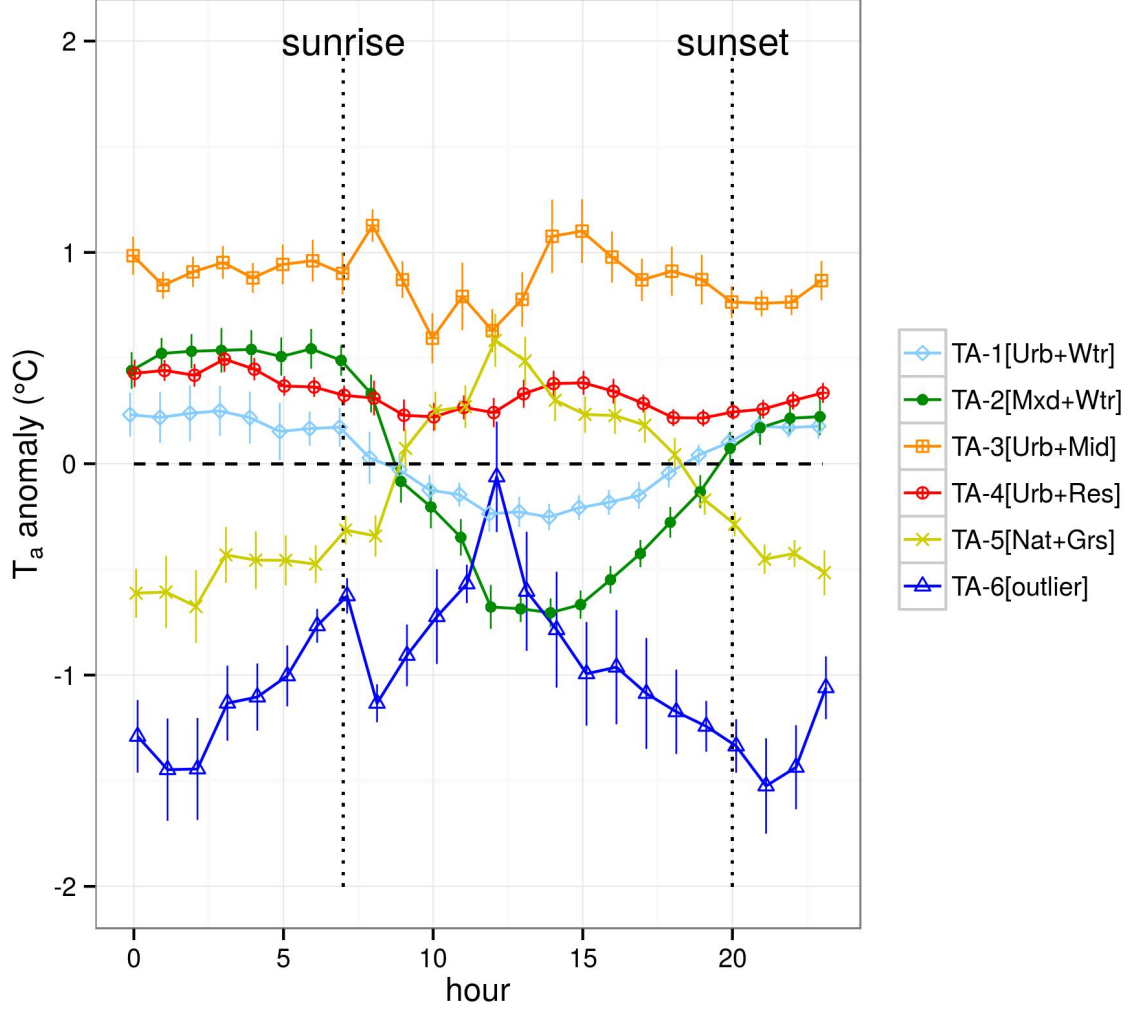
Figure 5.7: The diurnal air temperature variability in Mawson Lakes by air temperature cluster. Daily average temperatures were: TA-1$_{[Urb+Wtr]}$ = 22.0 °C, TA-2$_{[Mxd+Wtr]}$ = 22.0 °C, TA-3$_{[Urb+Mid]}$ = 22.9 °C, TA-4$_{[Urb+Res]}$ = 22.3 °C, and TA-5$_{[Nat+Grs]}$ = 21.8. Daily average minimum temperatures were: TA-1$_{[Urb+Wtr]}$ = 16.9 °C, TA-2$_{[Mxd+Wtr]}$ = 17.3 °C, TA-3$_{[Urb+Mid]}$ = 17.8 °C, TA-4$_{[Urb+Res]}$ = 17.2 °C, and TA-5$_{[Nat+Grs]}$ = 16.2 °C. Daily average maximum temperatures were: TA-1$_{[Urb+Wtr]}$ = 27.9 °C, TA-2$_{[Mxd+Wtr]}$ = 27.5 °C, TA-3$_{[Urb+Mid]}$ = 29.3 °C, TA-4$_{[Urb+Res]}$ = 28.5 °C, and TA-5$_{[Nat+Grs]}$ = 28.4 °C. Note TA-6$_{[outlier]}$ was a single anonymously cool site (site 27).

The meteorological conditions were relatively constant during the intensive period, but there was some variability in wind speed and direction, and this affected microscale air temperature variability in Mawson Lakes. The apparent effect of wind direction on air temperature variability

was most apparent in the AWS data. As shown in Figure 5.4a, the daytime air temperature of AWS sites that were located north/north-east of the Sir Douglas Mawson lake appeared to be receiving a clear cooling benefit. This was likely due to the daytime south-westerly prevailing wind direction (see Figure 5.4a inset), which caused those sites located north of the lake to receive the greatest advective cooling benefits. Though the cooling effects are reasonably clear in the AWS data, the bicycle transects complicated this picture. For example, during the 2 pm bicycle transect on 16th February, the wind was flowing across the Shearwater Lake (from the south-west), resulting in cooling downwind of the lake (Figure A.16c). However, during another event on the 15th, when the wind direction was very similar to the 16th, minimal advective cooling was observed downwind of the Shearwater Lake (Figure A.15e). The shorter averaging period (30 second) of air temperature, for the bicycle transects, meant that the data contains more noise due to microscale effects and variations in wind direction. Therefore the cooling effects of water bodies are not as clear in the bicycle transect data as they are in the static AWS air temperature (hourly average) data (Figure 5.4). Overall, despite the noise in the bicycle transect data, the 3 pm daytime transects (Figures A.14d & A.15e & A.16c) and static AWS (Figure 5.4a) do suggest that the cooling effects of water bodies did extend downwind of WSUD features in Mawson Lakes.

The spatial extent of the cooling associated with lakes and wetlands was variable in Mawson Lakes. The average daytime air temperature for the statics sites, suggests that sites situated a maximum of 150 m downwind of the SDML received some cooling benefit (Figure 5.4a). However, most sites that were in the cooler categories (TA-1$_{[Urb+Wtr]}$ and TA-2$_{[Mxd+Wtr]}$) were within approximately 50 m of a major water body. This result is a similar result to a value of 40 m observed downwind from small lake in Israel (Saaroni & Ziv, 2003) and conforms with the source area analysis from chapter 4.

However, a few stations that were categorised in TA-1$_{[Urb+Wtr]}$ and TA-2$_{[Mxd+Wtr]}$ were lo-

cated between 50 – 150 m away from water bodies (e.g. stations 8 and 11). In part this seems to be related to the effect of wind direction and lake orientation. During our campaign, the dominant daytime wind direction was south-westerly, and this meant that the airflow was often (during the day) flowing directly parallel to the SDML. Station 8 was situated such that it had a long and continuous upwind fetch over the SDML when the wind direction was south-westerly. This may have created a lake induced cooling effect at this site, despite the fact that station 8 was located 150 m away from the SDML. By contrast, station 9 was located directly east of the SDML and appeared to receive minimal cooling benefits. The shape of the SDML (man-made lake) and it's orientation have not been designed to maximize cooling benefits; a long thin lake orientated parallel to the prevailing wind, focuses the cooling benefits on a narrow area, while smaller distributed features orientated perpendicular to flow may provide cooling to a greater area. Practitioners and urban designers should take into account the wind direction when positioning WSUD water bodies. In coastal areas, with relatively predictable sea breeze wind regimes (such as Mawson Lakes), water bodies could be orientated so as to maximise the areas exposed to advective cooling effects. Clearly there is potential to maximise the cooling benefits of water bodies, and this is an area for future research.

Other exceptions were stations 1 and 2, which were classified in TA-1$_{[Urb+Wtr]}$ and TA-2$_{[Mxd+Wtr]}$, but were not located near any major water bodies. Station 1 and 2 were cooler because they were located on the suburban fringe at highly exposed and well ventilated sites. These exceptions emphasise how factors other land surface characteristics influence air temperature, making it difficult to attribute cooling effects to land surface characteristics. During the field campaign, the sensors (AWS and bicycle transects) were detecting a mixed signal (i.e. not just the effects of the lakes/wetlands), and therefore the actual spatial extent of water body cooling is difficult to estimate. Despite the mixed signal, it does seem likely that the cooling from the WSUD water bodies in Mawson Lakes was quite localised. A site that further empha-

sises the case for the localised cooling effects of water bodies is site 24, which was located in the north-west of the domain, on a large island inside the Salisbury Wetland. This site (despite being located inside the wetland) was surrounded by c. 50% dry grass and bare ground, and only a small proportion of the effective footprint was influenced by the nearby water. As a result, it had a thermal regime that was most similar to the other TA-5$_{[Nat+Grs]}$ sites — i.e. cool at night and quite warm during the day. Overall, given the results from the observational campaign and the source area analysis (done in chapter 4), the results suggest that the majority of cooling effects were observed 50 m downwind of the major water bodies in Mawson Lakes.

At night, the overall effect of water bodies on air temperature was probably neutral, providing no beneficial cooling or adverse heating effect. The nighttime air temperature of the water dominated clusters (categories TA-1$_{[Urb+Wtr]}$ and TA-2$_{[Mxd+Wtr]}$) were similar to the residential cluster (TA-4$_{[Urb+Res]}$) and cooler than the mid-rise (TA-5$_{[Nat+Grs]}$) sites (Figure 5.7). The average daily minimum air temperature for the TA-1$_{[Urb+Wtr]}$ and TA-2$_{[Mxd+Wtr]}$ sites was 16.9 °C and 17.3 °C, while the TA-3$_{[Urb+Mid]}$ and TA-4$_{[Urb+Res]}$ sites recorded values of 17.8 and 17.2 °C. No nighttime air temperature cooling effect associated with the lakes in the suburb was observed (Figure 5.4b). However, the sites located in the Salisbury Wetland and the water courses in the western part of the suburb were cooler (Figure 5.4b). As mentioned above, site 24 behaved very much like the other sites that were characterised by natural surfaces (TA-5$_{[Nat+Grs]}$ cluster), while site 27 was an anomalous site that was unusually cold during the day and night. Overall, despite the high LST of water, the average nocturnal air temperature of the sites around SDML were still lower than the air temperature at highly impervious sites. In other words, although water surfaces were warm at night, they were still cooler than hard impervious surfaces like concrete. Therefore, the lakes did not have an adverse effect on nocturnal air temperature during these summertime conditions.

Overall, it was found that the water bodies in Mawson Lakes, including the artificial lakes and

the wetlands, provided a measurable daytime cooling effect and a near neutral nighttime effect on ambient air temperature. This daytime cooling and lack of apparent nighttime warming, meant that the daily average (24 hour) temperature at the TA-1$_{[Urb+Wtr]}$ (22.0 °C) and TA-2$_{[Mxd+Wtr]}$ (22.0 °C) sites were relatively quite low. The TA-5$_{[Nat+Grs]}$ sites had the lowest daily average air temperature, with a value of 21.8 °C, but these sites were 9.6 % impervious. The TA-1$_{[Urb+Wtr]}$ cluster was 57.7% impervious surfaces and had an average daily temperature that was 0.2 °C warmer than the TA-5$_{[Nat+Grs]}$ sites. Given that the TA-1$_{[Urb+Wtr]}$ sites were quite cool, despite the higher amount of impervious surfaces, this suggests that distributed water bodies are an effective way of reducing maximum and daily average air temperature. Overall, the results suggests that urban sites that are less than 50 m downwind of distributed WSUD water bodies will see, on average, up to 1.8 °C cooling of daily maximum air temperature, and a decrease of up to 1 °C of the daily average air temperature (during summertime conditions).

5.3.2.3 Water bodies and physiological equivalent temperature (PET)

The variability in PET across Mawson Lakes was larger than the air temperature variability for both nighttime and daytime cases. The daytime variability was particularly large as MRT and wind speed influence PET. These factors meant that air temperature was not a good predictor of PET variability in Mawson Lakes. In particular, not all the sites near the SDML (which had cooler air temperature) had low PET (for example, stations 4, 6, 9, 16, and 17) (see Figure 5.2a). On the basis of the spatial data (Figure 5.6), it's difficult to attribute any PET cooling to WSUD water bodies. As such, the sites were also clustered using PET (Figure 5.2). The PET clusters were different (in size and make up) to the air temperature clusters. Unlike the air temperature clusters, there was a less clear pattern in average land cover characteristics associated with the PET derived clusters (Figure 5.2b). Three of the PET clusters (PT-1$_{[R-M|W-H]}$, PT-4$_{[R-L|W-H]}$, and PT-6$_{[R-L|R-L]}$) had an average daytime PET that was below the domain average (Figure

5.8). Although one of the coolest PET clusters (PT-4$_{[R-L|W-H]}$) did have a high percentage of nearby water surfaces (see Figure 5.2b), wind speed and MRT variability are shown to be more important predictors of PET in the Mawson Lakes suburb. For example, the PT-1$_{[R-M|W-H]}$ cluster was thermally comfortable due to being located at exposed locations on the suburban fringe. The PT-1$_{[R-M|W-H]}$ cluster shows the importance of promoting airflow to provide better HTC. Additionally, the PT-6$_{[R-L|R-L]}$ sites, which had higher air temperatures, were two urbanised sites where buildings provided shade and reduced MRT (and PET) during the day. The fact that PT-6$_{[R-L|R-L]}$ sites had below average PET despite being urbanised sites, reinforces the fact that shading is an important considerations for practitioners targeting HTC. As such, for WSUD to provide effective HTC cooling, building shading should be taken into consideration, and the use of urban trees and ventilation promotion should also be explicitly encouraged as part of future WSUD developments.

The variability of humidity in Mawson Lakes was also considered, because this is important for HTC. However, the data suggest that there was minimal variability in humidity across the domain (Figure A.17 and A.13d). However for nocturnal humidity, the denser built-up areas were generally drier than the residential areas, which could be associated with nighttime irrigation. Additionally, the sites that were furthest away from the lakes and water bodies (stations 23, 28, and 29) did have lower humidity. These sites mostly had very dry soils and were away from irrigation and water sources. This suggests that there could be a local-scale increase in humidity associated with the Mawson Lakes suburb. However, the overall effect was small, and variability of humidity had minimal affect on HTC during these conditions.
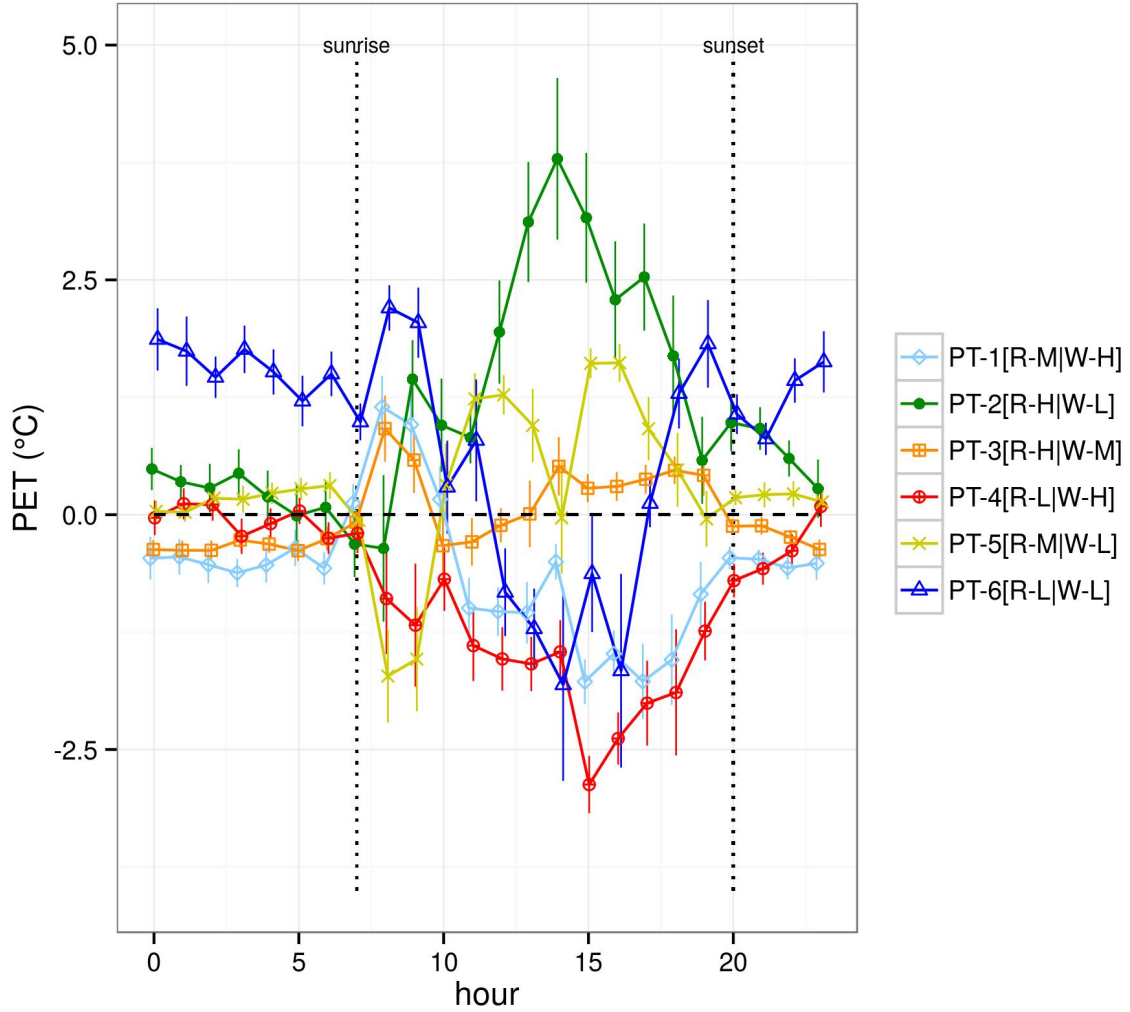
Figure 5.8: The diurnal PET variability in Mawson Lakes by PET cluster. PT-1$_{[R-M|W-H]}$ sites were mostly located on the urban fringe and were well ventilated; PT-2$_{[R-H|W-L]}$ sites were un-shaded and poorly ventilated urban sites; PT-3$_{[R-H|W-M]}$ sites were mostly residential with moderate shading and ventilation; PT-4$_{[R-L|W-H]}$ were well ventilated sites that were often located near water bodies; PT-5$_{[R-M|W-L]}$ sites were similar to PT-3$_{[R-H|W-M]}$ but with lower wind speeds, and PT-6$_{[R-L|R-L]}$ was were highly shaded but poorly ventilated urban sites. Daily average PET were: PT-1$_{[R-M|W-H]}$ = 23.0 °C, PT-2$_{[R-H|W-L]}$ = 24.7 °C, PT-3$_{[R-H|W-M]}$ = 23.6 °C, PT-4$_{[R-L|W-H]}$ = 22.8 °C, and PT-5$_{[R-M|W-L]}$ = 24.0, and PT-6$_{[R-L|R-L]}$ = 24.4. Daily average minimum PET were: PT-1$_{[R-M|W-H]}$ = 13.4 °C, PT-2$_{[R-H|W-L]}$ = 14.2 °C, PT-3$_{[R-H|W-M]}$ = 13.7 °C, PT-4$_{[R-L|W-H]}$ = 13.7 °C, and PT-5$_{[R-M|W-L]}$ = 14.1 °C, and PT-6$_{[R-L|R-L]}$ = 15.1. Daily average maximum PET were: PT-1$_{[R-M|W-H]}$ = 37.2 °C, PT-2$_{[R-H|W-L]}$ = 41.7 °C, PT-3$_{[R-H|W-M]}$ = 38.6 °C, PT-4$_{[R-L|W-H]}$ = 36.1 °C, PT-5$_{[R-M|W-L]}$ = 39.9 °C, and PT-6$_{[R-L|R-L]}$ = 38.2 °C.

5.3.3 Effects of irrigation on microclimate in Mawson Lakes

5.3.3.1 Irrigation and land surface temperature (LST)

The results from this study suggest that irrigation can have a significant cooling effect on daytime LST. It was found that the average daytime LST of irrigated grass was 6.8 °C cooler than dry grass and 8.0 °C cooler than bare ground (Table 5.1). The daytime LST were more or less in agreement with previous research that looked at the LST of irrigated grass surfaces including point measurements (Bonan, 2000) and remote sensing (Spronken-Smith & Oke, 1998). However, at night, the observations suggest there was no difference in LST between irrigated and dry grass (Table 5.1). One might expect a slight increase in nocturnal LST with irrigation, as water on the surface and in the soil retains more heat than a dry grass surface would (Spronken-Smith & Oke, 1998), but that is not apparent in these data. This was observed in Vancouver (climate type Csb) by Spronken-Smith & Oke (1998), who found that the LST of irrigated grass can be warmer than unirrigated grass. However, in the same study, the authors found near negligible nocturnal LST effects associated with irrigation in Sacramento, which also has a Csa (same as Adelaide) type climate. Overall, it seems likely that the effects of irrigation on nocturnal climates will vary depending on the climate characteristics of a given city. Cities with drier and warmer climates (e.g. Mediterranean climate as in Adelaide), are less likely to receive an adverse nocturnal warming effect from irrigation. The data from our observational campaign seems to reinforce this point. Given our focus on human exposure, a key consideration for this research is how (if at all) irrigation influences air temperature and HTC at the microscale.

5.3.3.2 Irrigation and air temperature

Despite the clear effect of irrigation on daytime LST it is difficult to attribute any air temperature cooling effects to irrigation. Although the LST observations confirm the daytime cooling effects

of irrigation, there is no clear observable trend in the air temperature clusters associated with irrigated grass (Figure 5.1). Categories TA-1$_{[Urb+Wtr]}$ and TA-2$_{[Mxd+Wtr]}$ had a higher proportion of irrigated grass, but irrigated grass made up less than 5% of the average effective source area at these sites. However, the absence of irrigation did appear to be associated with warmer daytime air temperatures. It was found that sites with a lot of adjacent dry grass and bare ground (e.g. the TA-5$_{[Nat+Grs]}$ cluster) were quite warm during they day and heated up quickly (Figure 5.7). A similar phenomenon was observed by Jauregui (1991), who found that, after sunrise, a park in Mexico City heated up faster than the surrounding urban areas; the authors attributed this heating to the low thermal inertia of the natural surfaces. Given these observations, and the high LST of dry grass and bare ground (see Table 5.1), unirrigated grass probably will not provide any air temperature cooling benefits, especially in hot dry climates such as Adelaide.

Figure 5.9 shows the average air temperature variability of two sites that had very different amounts of irrigation directly adjacent. Station 17 (residential pocket park - see Figure A.8b) was surrounded by irrigated grass and station 9 (a residential construction site - see Figure A.7b) was surrounded by bare ground. The air temperature at the irrigated site (station 17) was on average up to 1.25 °C cooler than the unirrigated site (station 9) during the day. However, this cooling could be associated with a number of other factors including orientation relative to the SDML, ventilation (airflow), variability in shading (due to tree cover), and other local-scale factors. There are a number of other factors that could contribute to air temperature, and this makes it difficult to robustly quantify the effect of irrigation on air temperature through comparative approaches. In chapter 6 and chapter 7 this issue is addressed directly and the cooling effects of irrigation on air temperature are quantified using multiple linear regression (chapter 6) and numerical modelling (chapter 7). Spronken-Smith & Oke (1998) also noted that confounding variables such as tree coverage and SVF need to be taken into account when considering the effects of irrigation on air temperature. The present research further highlights the difficulties associated

with isolating the effects of irrigation on microscale air temperature variability. Overall, the

results of this chapter suggests that there should be daytime air temperature cooling benefits

associated with irrigation, but more analysis is needed to quantify these effects.
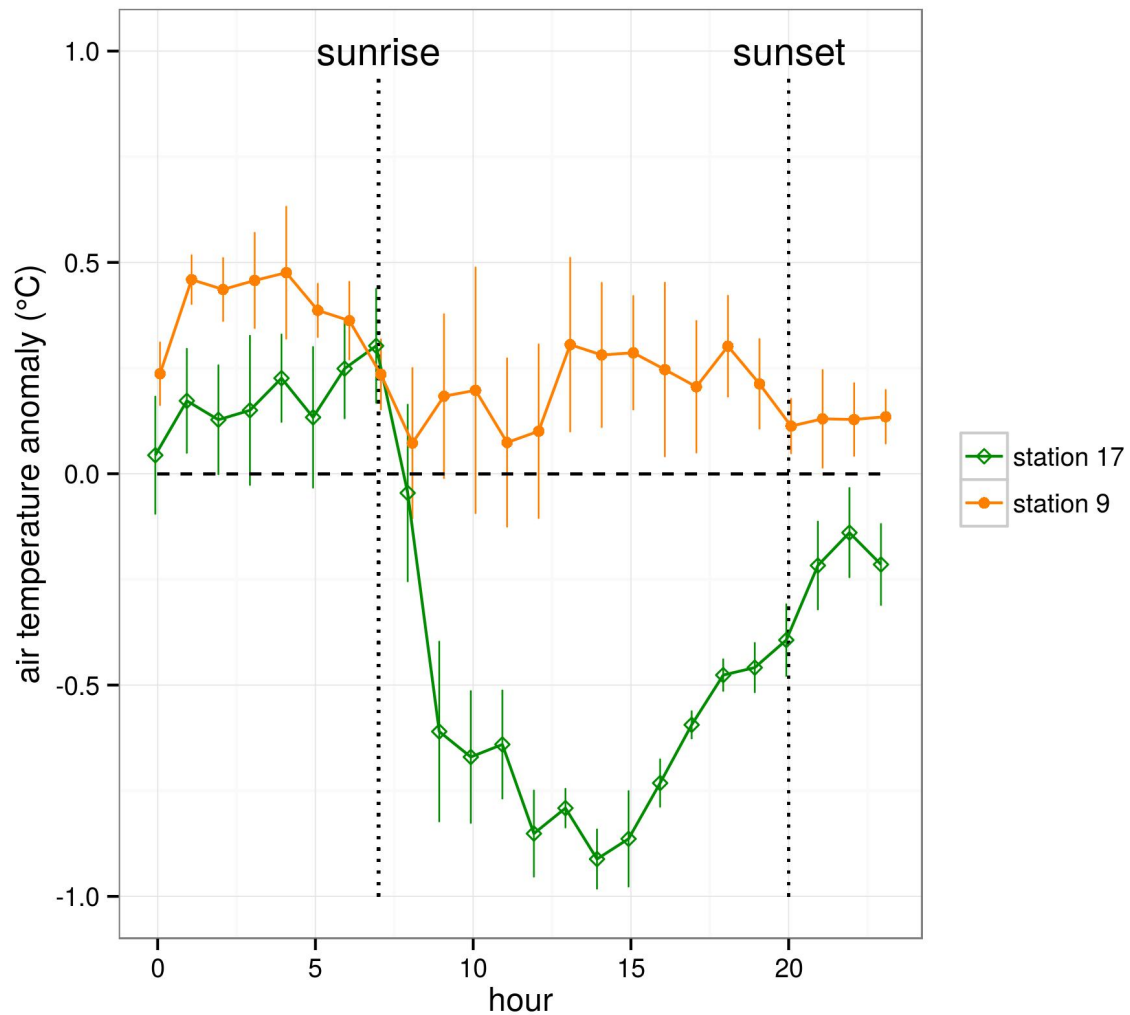
Figure 5.9: The average diurnal air temperature variability (intensive observational period) at stations 17 (more irrigated green space) and 9 (no irrigated green space) with standard errors shown. T_a = air temperature.

5.3.3.3 Irrigation and physiological equivalent temperature (PET)

With regards to the effects of irrigation on PET there were no clear patterns to emerge from

these analyses. Broadly speaking, if irrigation can cool air temperature then one would expect

some HTC benefits associated with irrigation. That said, air temperature is not the key driver of

HTC, and reductions of MRT are more beneficial than air temperature from a HTC perspective. Theoretically, irrigation could increase absolute humidity in the UCL, which could also have an adverse effect on HTC. However, the data suggests that there was minimal microscale variability in humidity across the domain (Figure A.17). Regardless, the rates of irrigation observed during the Mawson Lakes campaign were unlikely to have a significant effect on humidity. Overall, the effects of irrigation on HTC are not apparent in this observational analysis, but microscale modelling in chapter 7 will consider the effects of irrigation on HTC during heatwave conditions.

5.4 Conclusions

- **Intra-urban variability is high and varies spatially and temporally.**

The variability of observed air temperature within the Mawson Lakes suburb was large. This variability was of a similar magnitude to the urban-rural increment observed in typical UHI studies. This analysis shows how variable air temperature can be at the scale of climate that people are exposed to. The variability of PET was also large, meaning intra-urban thermal comfort variability can also be very significant. High spatial variability of air temperature and HTC in urban areas is a major challenge for practitioners and urban designers who are seeking to reduce exposure to heat stress and thermal discomfort. However, this finding also represents an opportunity, as urban designers can create microscale cool spots using small scale interventions. These cool spots can be used to protect vulnerable populations, such as children and the elderly.

- **Water bodies provide downwind cooling, but design and placement are important.**

The results from this observational study suggest that WSUD water bodies can cool suburban air temperature and improve HTC. Air temperature cooling appeared to extend downwind of the water body during the day. The exact distance that this cooling extended was variable, but in Mawson Lakes the most notable cooling occurred up to 50 m downwind of water bodies. Urban

planners and architects should try to design WSUD elements, with climate related objectives in mind, to further increase the cooling benefits of these features. For example, to increase the total area that receives downwind cooling benefits, lakes and wetlands could be smaller and positioned so that they are situated perpendicular to the prevailing wind conditions. This is likely to provide cooling benefits for a greater area than long and thin lakes and water features. Given the potential cooling benefits, planners and landscape architects should take into account the wind regime when incorporating water bodies (WUSD or otherwise) into the urban environment. This is particularly compelling, as WSUD water features have other functional benefits, such as improved stream ecology through reduced runoff (Walsh et al., 2005), flood mitigation, and potable water preservation (Mitchell et al., 2006). If WSUD features are to be integrated into the urban environment for ecological and hydrological benefits, than the thermal benefits should also be maximised where possible. It is recommended that practitioners actively exploit the use of WSUD features, such as lakes and wetlands, to cool urban microclimates.

- **Water bodies can help improve HTC through reductions in air temperature, but greater improvements can be made through promotion of shade and ventilation.**

PET variability was less clearly linked to land surface features in Mawson Lakes. Some of the sites with cooler PET were close to water bodies. However, other sites that were highly urbanised were almost as thermally comfortable due to the effects of shading and increased airflow (ventilation). More research is needed in this area, but it is clear that WSUD features need to be supported by features that provide shade (e.g. irrigated trees), and clever urban design that encourages ventilation. As such, a focus on traditional urban design planning indicators, such as greenspace fraction, is insufficient for effective HTC-focused urban design. In order for WSUD to directly target HTC it must consider surface characteristics, airflow, and shading patterns in urban areas simultaneously.

• **Irrigation shows potential to cool climate, but the effects on air temperature and HTC were inconclusive and more research is needed.**

The data from this study showed that irrigation can clearly cool LST. However, the effects of irrigation on air temperature and PET were inconclusive. Nevertheless, there is some evidence that irrigation can provide positive cooling benefits, particularly for daytime air temperature. Irrigation has two potential thermal benefits. Firstly, irrigation can be used to support vegetation growth providing indirect cooling benefits. In areas where water supplies are limited, WSUD and stormwater harvesting can provide water for irrigation, buffering the potable water supplies. This means that with WSUD implemented, urban trees can be well supplied with water, which will be beneficial for reducing air temperature but also HTC, because trees reduce MRT during the day through solar shading. Secondly, irrigation could potentially provide direct cooling of the urban environment by significantly increasing ET. The direct benefits of irrigation could be particularly useful during EHE, when heat mitigation is highly needed. Chapter 7 of this thesis investigates the potential direct cooling benefits of irrigation during heatwaves. The direct effects of irrigation on air temperature and HTC are unclear in these observational data; however, the indirect longer term effects of irrigation on HTC are likely to be substantial. Harvested stormwater should be used to maintain and support urban vegetation in drought stressed locations.

• **WSUD is just one factor that influences urban climate variability — microclimate at any given point is determined by a mixed signal and a range of factors are likely to influence air temperature and HTC.**

This research has revealed much about the controls on urban climate in Mawson Lakes. However, the mixed signal at each site makes it difficult to completely disentangle the controls of microclimate variability, to understand the cooling potential of WSUD practices. Other authors have noted this problem when conducting microscale observational work (e.g. Spronken-Smith

& Oke (1998)). Untangling the different effects is essential for accurately quantifying the effects of WSUD on microclimate. This is a key consideration for the next chapter in this thesis (chapter 6), which will attempt to generate more robust estimates of the cooling potential of WSUD features on microscale air temperature.

6 Statistical analysis of the land surface controls on microclimate: estimates of the cooling potential of WSUD features on microscale air temperature

6.1 Introduction

Chapter 5 showed that there was a significant amount of microclimate variability across the Mawson Lakes suburb (Figure 5.4). However, a key point made in chapter 5 was that the mixed signal in the UCL makes it difficult to disentangle the controls on microscale air temperature variability, and therefore it is difficult to quantify the cooling effects of WSUD. Consequently, understanding the specific contribution of WSUD land surfaces to microscale climate variability requires additional attention. In the UCL, air temperature is influenced by shading effects, turbulence and wind channelling, interactions between canyon air parcels and air parcels aloft, canyon geometry, and highly variable energetic contributions from different surface facets (Figure 4.2). In addition, the microclimate of a site is affected by the local-scale (inertial sublayer) and mesoscale (background weather) climates (Figure 4.2). The second major objective of this research is **objective 2: generate robust estimates for the cooling potential of WSUD features on microscale air temperature**. However, the complexity of the urban environment means that it is difficult to identify how microclimate is influenced by urban land surface characteristics, which makes it difficult to assess the effectiveness of WSUD strategies (or any cooling methods) at this scale. While quantifying UHI intensity resulting from urbanisation is relatively straight forward, quantifying the influence of land surface characteristics at the microscale, within the urban canyon, for example, is very challenging.

In previous studies, a number of authors have attempted to tease out the role of specific land surface characteristics in defining microscale urban climate. For instance, Saaroni & Ziv (2003)

observed the microscale cooling effects of a small lake in Tel Aviv, Israel. The authors observed a cooling in the order of 1.5 °C, downwind of the lake, with the effects most pronounced during the daytime. Saaroni & Ziv (2003) noted that air temperature around the lake was affected by both turbulence (vertical mixing) and advection (horizontal transport of cooled air) from the lake; they observed a positive linear correlation between wind speed and lake induced cooling, suggesting turbulence does play an important role in enhancing air temperature cooling. Stoll & Brazel (1992) found that increased wind speed decreases the correlation between LST and air temperature, indicating that increased turbulence decreases coupling between the surface and the UCL. This lack of coupling, due to increased turbulence, means that heat can be transported efficiently away from the UCL during the day. Overall, this means that wind speed is an important variable to take into account because, in addition to the effects of advection, it can directly influence vertical turbulent mixing and UCL air temperature.

In another study, Murakawa et al. (1991) investigated the effects of a river on urban microclimate in Hiroshima, Japan. The results showed that sites near the river were up to 5 °C cooler (between 12 pm and 5 pm) than the surrounding area. However, the authors conceded that the cooling effect was more evident where the density of buildings was low and the width of streets and rivers was wide. As such, SVF and urban geometry (not just proximity to the river) were also influencing air temperature variability, and need to be taken into account. Spronken-Smith & Oke (1998) looked at park microclimate variability in Vancouver and Sacramento. They found that parks with more tree coverage were coolest in the afternoon, while more exposed (high SVF) grass parks were coolest prior to sunrise. The picture that emerges from this observational research is complex, with many interacting variables influencing microclimate. The complexity of the UCL means that observations of air temperature are not easily linked to land surface characteristics. Without this link, it is very difficult to robustly quantify the cooling potential of WSUD features on microscale air temperature and provide guidance on design and implementation.

Previous observational studies highlight how difficult it is to disentangle the many variables that influence climate at the microscale and ultimately these complexities make it difficult to quantify the influence of land surface characteristics on microclimate. The actual effect of the land surface features may not be clearly shown, if other variables that influence microclimate (for example, wind speed or SVF) are not controlled for. The primary objective of this analysis is **objective 2: generate robust estimates of the cooling potential of WSUD features on microscale air temperature**. These robust estimates are then applied to provide estimates of the thermal benefits of WSUD.

6.2   Methodology

To calculate the cooling potential of WSUD, multiple linear regressions were conducted to calculate the statistical relationship between land surface characteristics and air temperature variability in Mawson Lakes. Multiple regression has been used previously to link surface temperature with near-surface air temperature (Imamura, 1989; Stoll & Brazel, 1992). Stoll & Brazel (1992) used LST, wind variables, vapour pressure, and solar radiation to predict surface air temperature variability in Phoenix, AZ. A similar approach to Stoll & Brazel (1992) was used in this research, but predictor variables that would be useful for urban planners were used, such as surface land cover fractions. In this research, multiple linear regression (ordinary least squares) was conducted using the dependent variable air temperature and the predictor variables grass fraction, bare ground fraction, SVF, water fraction, building fraction, tree fraction, incoming solar radiation, and wind speed. These variables came from the Mawson Lakes field campaign, which was conducted during typical summertime (not extreme weather) in Adelaide, South Australia (see Section 3.4 for an overview of the campaign and data collected). A mixture of variables that can influence microscale air temperature (including meteorological variables) was included, so as to maximise the chance of filtering out the independent effects of land surface variables. The

land cover variables, for each site, (such as grass fraction, water fraction, and tree fraction) were calculated using the circular buffers from the source area analysis (see Figure 4.8 and chapter 4 for details). The daytime source area estimate captured the surfaces upwind of the source (see Figure 4.8) so as to represent the effects of advection. Therefore, the inclusion of wind speed in the regression model was intended to capture any turbulence effects (discussed above) and help isolate the effects of surface variables. Theoretically, the effects of turbulence will be captured by the wind speed variable, and the effects of cool/warm advection (horizontal transport) will be captured by the surface variables (e.g. % water fraction) that were included in the regression model. The SVF (of the site, not the source area) was included to capture effects associated with the urban geometry, most notably diminished nocturnal longwave radiation loss. Finally, solar radiation was also included in the regression model, to account for the effects of increased solar exposure during the day.

The variables included in the linear regression model were also chosen to avoid covariance between the predictor variables; NDVI and pervious fraction were excluded due to high covariance with other variables. Variance inflation factors were kept below a threshold value of 4. Two models were generated with input data from the 5 day intensive observational period (Figure 3.7) — a nocturnal (12 am–5 am) and a daytime (12 pm–5 pm) model. Each model had input data from 540 data points (27 stations $\times$ 5 days $\times$ 4 hours). Dummy variables were used to account for any possible effects associated with the different days and hours included in the models. The models were also tested for heteroskedasticity (Breusch-Pagan-Godfrey test) and autocorrelation (Breusch-Godfrey serial correlation Lagrange multiplier test).

6.3 Results and discussion

6.3.1 Microscale air temperature variability and land surface characteristics

6.3.1.1 Daytime controls

During the day, the standardised coefficients suggest that wind speed ($b = -0.15$) had the greatest influence on microscale air temperature variability. Wind speed produced an apparent cooling effect of -0.6 °C for a 1 ms^{-1} increase in wind speed (Table 6.1). Saaroni & Ziv (2003) found a linear correlation between wind speed and air temperature, suggesting that turbulence may play a significant role in determining cooling. The linear regression analysis appears to support this because a strong linear correlation between wind speed and air temperature was observed in the Mawson Lakes data. Therefore, higher wind speeds do appear to be independently correlated (i.e. independent of land surface characteristics) with cooler air temperature during the day. Others have noted the importance of ventilation in cities on improved air temperature (Wong et al., 2010) and HTC (Johansson, 2006). This also fits well with the observations from chapter 5, which noted that a number of exposed sites in Mawson Lakes had cooler air temperatures. This microscale cooling from wind speed, is thought to represent a redistribution of heat via vertical transport of heat away from the surface and downward transport of cooler air from aloft. Nevertheless, this observation suggests that promoting ventilation is an effective means of reducing daytime air temperature in the UCL.

An important predictor of air temperature variability was the building cover fraction in the microscale source area (Table 6.1). The building fraction, was associated with a warming effect of 0.20 °C per 25% increase in buildings. This heating is due to the retention of heat in the impervious surfaces associated with buildings, which is a well known phenomenon in urban climate (Oke, 1987). Further, this heat from buildings could be associated with anthropogenic heat

Table 6.1: Daytime air temperature multiple linear regression model results. Only statistically significant variables are included.

Variable	coefficient	standard error	beta coefficient b	t-value	p-value
Intercept	24.16	0.264	-1.54	91.4	0.000
% water	-0.004	0.002	-0.03	-1.879	0.050
% dry grass	0.007	0.002	0.05	3.688	0.000
% bare ground	0.012	0.003	0.05	3.873	0.000
wind speed	-0.601	0.067	-0.15	-9.022	0.000
% buildings (all)*	0.009	0.002	0.07	3.898	0.000
% irrigated grass	-0.018	0.007	-0.04	-2.670	0.008
solar radiation	0.0005	0.000	0.03	2.382	0.017

* residential and non-residential buildings are treated as a single variable here.

sources (Q_F), which is additional heat source in urban areas (Oke, 1987). Dry grass ($b = 0.05$) and bare ground ($b = 0.05$) were important variables during the day (Table 6.1). Dry grass and bare ground were both correlated with a warming effect due to the low heat capacity and diffusivity of dry soils, which causes the surface temperature to increase. A 25% increase in dry grass and bare ground was associated with a warming of 0.18 °C and 0.31 °C, respectively. These unirrigated surfaces were very dry, and warmed up significantly during the day; the average daytime LST of bare ground was almost as high as concrete (see Table 5.1). The regression analysis captures the effect of unirrigated pervious surfaces (e.g. grass and bare ground) contributing to higher air temperature during the day. This is a phenomenon that was also observed in Mexico City by Jauregui (1991), who observed warmer air temperature in an urban park. By contrast, it was found that irrigated grass had a cooling effect of about -0.46 °C per 25% increase in irrigated grass. Given the use of an upwind source area and the inclusion of wind speed, this cooling from irrigated fraction is interpreted as the Q_H and Q_E driven surface cooling. Over irrigated grass increased Q_E partitioning occurs because of enhanced ET, while irrigation causes a decrease in the magnitude of Q_H because moister soils diffuse heat downwards more effectively and take more energy to heat up (higher heat capacity). In chapter 5, it was observed that irrigated surfaces had low LST; this finding supports the claim that irrigation can directly cool air temperature

in suburban environments; the lower surface temperature associated with irrigated surfaces (for reasons discussed above) results in less Q_H exchange from the surface to the atmosphere during the day, resulting in cooler temperatures. While others have noted the cooling effects of irrigation (Bonan, 2000; Spronken-Smith & Oke, 1998), this is the first attempt to isolate that cooling from other factors. The value derived here could be used by urban designers and practitioners, for an estimate of the microscale cooling effects of irrigated grass. Additionally, this estimate of cooling from irrigation is derived from the Mawson Lakes dataset, and therefore is only valid within the bounds of Mawson Lakes dataset, and does not explicitly capture the effects of different irrigation timing and volume of water applied. Given the significant observed cooling benefits of irrigation, chapter 7 will explore the cooling potential of different irrigation timing and volume during heatwave conditions.

Another variable that influenced daytime air temperature variability was water fraction ($b = -0.03$) (Table 6.1). The regression model suggests that a 25% increase in (upwind) water fraction was associated with a cooling of -0.10 °C (assuming constant wind speed and other factors). As mentioned above, given the inclusion of wind speed in the model, this cooling is thought to represent advection of cool air from above the lake surface to the land. The air is cooled by Q_H and Q_E heat exchange between the lake surface and the atmosphere — evaporation can occur over water surfaces, which increases Q_E, while the high heat capacity of water causes it to remain cool during the day, which decreases the Q_H exchange with the atmosphere. Overall, the model suggests that the independent cooling effects of water surfaces in Mawson Lakes were actually comparatively small. However, the observations in chapter 5 suggest that areas located downwind of water bodies were receiving a cooling effect. One potential reason for the lack of apparent cooling from water surfaces in the regression model is that some of the cooling observed around the water bodies (chapter 5) was actually driven by other factors including enhanced airflow (turbulence). A number of sites that were located nearby to lakes and water

bodies tended to record higher wind speeds (particularly locations such as stations 24, 25, 27, 5, and 6). This occurs because water bodies can open up the landscape and increase airflow in the urban environment. Higher wind speeds increase turbulent transport of heat away from the surface providing a cooling effect. However, higher wind speeds also decrease the potential for advective cooling to occur downwind of the water body. The decrease in advection occurs because as wind speed increases an air parcel spends less time above the cool lake surface (Saaroni & Ziv, 2003). Given the relatively small size of the open water features in Mawson Lakes (most were < 50 m width), the lack of advective cooling that was predicted by the regression model makes some physical sense. For example an air parcel travelling at 2.5 ms^{-1} would spend only 20 seconds over the lake surface. This is minimal time for effective transport of heat and moisture to occur (Saaroni & Ziv, 2003). However, the regression model is based on some simple assumptions about the source area that can influence a given point — i.e. the size of upwind source area is constant and does not extend beyond 50 m from the source. It was shown in chapter 5 that some sites (under certain conditions) may have been receiving a cooling benefit from water surfaces at locations beyond 50 m from a water body. If these cooling effects were in fact real they were not captured by this approach. As such, some caution must taken with this finding, as it is possible that the regression model has not fully captured the advective cooling effects of water surfaces. Another possible reason for the apparent lack of cooling from water bodies is that the sites in Mawson Lakes that were located nearby to open water bodies tended to have less surfaces that had a heating effect, including buildings and dry grass. As such, the "cooling effect" observed around the water bodies was as much a lack of a "heating effect" due to the absence of warmer land surface types. Regardless, the finding that the cooling associated with water bodies (observed in chapter 5) was most likely partly driven by other factors that also happen to occur around water bodies, including enhanced airflow and the presence of fewer warm land surfaces, does seem to be a realistic result.

Given that higher wind speeds decrease the potential for advective cooling to occur, wider water bodies with a longer fetch, may provide greater advective cooling benefits in the area directly downwind of the water body. Evidence of this process in Mawson Lakes was found in chapter 5 (see Section 5.3.2.2). However, from a future planning perspective, it is thought that one large water body is unlikely to provide effective cooling for an entire suburb, as a single large water body will only affect the locations that are adjacent to the feature. Rather, smaller distributed water bodies, carefully positioned to maximise upwind fetch, are likely to be more effective at cooling a larger area. The importance of water body placement, for increased advective cooling has already been emphasised (in chapter 5); while those observations are still valid, this analysis suggests that enhancing airflow in urban the environment, with strategic placement of water bodies, may be even more pertinent. With that in mind, practitioners may want to design WSUD features in such a way that they also enhance airflow in urban environments.

This analysis has attempted to provide a robust estimate of the daytime summertime cooling benefits of open water bodies, which could be used in a meaningful way by urban designers and practitioners. Many previous studies have suggested that water bodies can have cooling effects (Ishii et al., 1991; Murakawa et al., 1991; Han et al., 2011; Hathway & Sharples, 2012; Hou et al., 2012), but those analyses did not attempt to isolate the cooling effects of water surfaces from other variables that influence microclimate. This analysis implies that it is probably important to take into account the effects of other variables including wind speed and and the presence of warmer land surfaces. Overall, water bodies can provide cooling benefits through cool advection and increased airflow in urban environments. Moreover, with water bodies in the urban environment the absence of hard impervious surfaces also has a cooling benefit. However, future research is needed to fully understand the contribution of these factors, as well as the advantages and disadvantages of different water body size, distribution, and placement options.

One important variable that was not significant in the daytime linear regression analysis (Table 6.1) was the tree fraction. This was an unexpected result as previous research has shown that tree coverage can have positive benefits for daytime urban climate (Georgi & Dimitriou, 2010; Shashua-Bar et al., 2010; Tsiros, 2010). This could be because cooling from trees was captured by the solar radiation variable; however the effects of this variable were very small (Table 6.1). Additionally, the lack of apparent cooling associated with trees could be related to the source area that was used to characterise the sites. In the daytime linear regression analysis, the upwind 50 m diameter circular buffer was used (Figure 4.4). At the surface, the cooling from trees is primarily caused by the solar shading that the tree canopy provides. With the upwind buffer the trees that are (or are not) shading the site were not as well captured. In other words, the radiation source area of a site is different to the concentration/flux source area (Figure 4.1), and this may explain why trees were not captured. Further, the trees in Mawson Lakes had a relatively low shading potential as they are primarily young eucalyptus trees (yet to have matured as the development is relative new), which generally have low leaf area index (LAI). Overall, the shading effect of trees does improve microscale air temperature, but for a range of reasons the cooling trend was not apparent in these data.

Overall, the linear regression analysis mostly confirms and quantifies the observational trends from chapter 5. Importantly, the regression analysis provides a non-arbitrary means of describing the controls on microclimate in Mawson Lakes, including the effects of different WSUD land cover features. A major finding from this analysis is that the cooler air temperature observed around water bodies (see chapter 5) may have been partly driven by enhanced turbulence due to increased ventilation and a lack of nearby buildings and impervious surfaces. The cooling effect of irrigated grass was also identified by the model, while unirrigated grass and bare ground contributed significantly to warmer air temperatures. The cooling effects of irrigation further makes the case for urban watering as an air temperature cooling measure during summertime

conditions. In suburban environments, the fact that irrigation can be widely distributed with relative ease makes it a compelling heat mitigation strategy. It may not be necessary (from a heat perspective) to have a lot of water body features spread throughout the urban environment, if a high proportion of pervious surfaces are irrigated instead. The use of irrigation is particularly relevant in the context of WSUD, where stormwater harvesting and capture technologies mean that non-potable water sources should be abundantly available for irrigation. A key question that arises from this analysis is how much irrigated pervious area is needed to provide effective cooling? In chapter 7 the cooling potential of widely distributed irrigation during heatwave conditions is explored.

6.3.1.2 Nighttime controls

The nocturnal regression model presents a simpler picture of the controls on air temperature at night (Table 6.2). The key variables were building fraction ($b = 0.10$), wind speed ($b = 0.18$), bare ground ($b = -0.06$) and dry grass fraction ($b = -0.05$) (Table 6.2). The linear regression suggested that a 1 ms^{-1} increase in wind speed was correlated with a warming of 0.49 °C. Wind speeds at night in Mawson Lakes were generally quite low, and 1 ms^{-1} was around the maximum average variability observed during the campaign (Figure A.21). Nevertheless, the effect of higher wind speed caused some mixing of the near-surface atmosphere at night. As noted above, during the day higher wind speed caused heat to be transported away from the surface, whereas at night the effect was the formation of a more uniform near-surface layer, due to nocturnal stability, which diminished the observable air temperature differences. This means that as nocturnal wind speed increased the UCL air was more readily mixed with adjacent air, lessening the air temperature contrasts in the environment. At night, this mixing was correlated with an apparent warming effect at the microscale. This microscale warming was caused by a re-distribution of heat in the urban atmosphere. As such, the data suggests that the effect of

wind speed and mixing mean that the nocturnal cooling benefits of natural land surface features
(e.g. grass) may be less apparent at the microscale during windier conditions.

Table 6.2: Nighttime air temperature multiple linear regression model results. Only statistically significant variables
are included.

Variable	coefficient	standard error	beta coefficient b	t-value	p-value
Intercept	15.34	0.287	-1.22	53.38	0.000
% dry grass	-0.007	0.001	-0.05	-4.77	0.000
% bare ground	-0.013	0.002	-0.06	-5.93	0.000
wind speed	0.486	0.041	0.18	11.74	0.000
% buildings (all)	0.025	0.003	0.10	8.21	0.000
% SVF	-0.078	0.307	-0.03	-2.54	0.012

At night, building fraction was another significant variable. The increased presence of build-
ings caused a nocturnal warming trend of 0.62 °C per 25% increase in building coverage. This
trend is capturing the higher thermal admittance of urban surfaces and the presence of Q_F,
which have been commonly cited to increase nocturnal air temperature in UHI studies (Oke,
1987). Dry grass and bare ground were correlated with cooling rates of -0.16 °C and -0.33 °C per
25% increase in coverage, respectively. This fits with the observations made in chapter 5, and
many UHI studies, which have shown that "natural" (e.g. urban parks) sites with less adjacent
urban surfaces are cooler at night (Barradas, 1991; Oke et al., 1989; Saito et al., 1990; Lindqvist,
1992; Spronken-Smith & Oke, 1998). Furthermore, SVF was correlated with a cooling trend of
-0.08 °C for a 10% increase in SVF, meaning that the regression model is also capturing the well
known effect of lower urban SVF and reduced outgoing longwave radiative heat loss (Oke, 1987).

Water fraction and irrigated grass were not correlated with any trends in nocturnal climate
variability. The observations showed that the nighttime LST of water surfaces were quite high
(Table 5.1). However, this did not translate to a significant trend in air temperature variabil-
ity. Tree coverage was not correlated with any nocturnal air temperature variability. Previous
research has suggested that trees can reduce nighttime temperature cooling in the UCL because

the tree canopy can lessen longwave radiative heat loss, much like buildings can. This trend was not observed in the Mawson Lakes data. It could be that the overall canopy coverage, which was relatively low in Mawson Lakes, was not substantial enough to significantly influence nocturnal air temperature variability. It is also possible that any tree induced warming trend is completely captured by the SVF variable. Overall, the nighttime controls on air temperature variability agree with observations made in chapter 5. Greater cooling occurs at sites with fewer impervious surfaces (buildings) and more pervious surfaces (bare ground and grass). Water bodies and irrigation had no statistically significant effects on nighttime air temperature, while higher wind speeds were correlated with a modest warming effect.

6.3.2 Application of the regression model to idealised sites

To clearly illustrate the impact of the WSUD surfaces on air temperature variability a series of idealised scenarios was explored (Figure 6.1). These scenarios attempt to clearly show the influence of WSUD land surface changes on microscale air temperature. The scenarios represent modelled air temperature using background conditions (based on the model coefficients) from the 16th February. To isolate the influence of surface variables, the effects of wind speed, solar radiation, and SVF were held constant. This is not a physically realistic approach because changing the adjacent surfaces would affect the SVF and wind speed of a given site. However, this exercise is useful for illustrating the effects of WSUD on microscale air temperature, in similar suburban environments, under summertime conditions. The scenarios represent simple hypothetical microscale environments including a grassy parkland site (Rural), a fully urbanised site without any natural surfaces (Urban), and two WSUD sites, which are represented by the inclusion of water (lakes and wetlands) and irrigated grass.

Overall, the output from the regression model shows that daytime air temperature is less sensitive to the characteristics of adjacent surfaces, with a 0.76 °C maximum difference between

the hypothetical sites. As discussed above, wind speed and vertical mixing, were shown to be important daytime variables, and wind speed was held constant in these calculations. Based on the regression model, the independent effect of adjacent surfaces could achieve a daytime cooling of 0.38 °C if 25% of the adjacent surfaces were modified (WSUD1); and 0.76 °C if 50% of adjacent features (WSUD2) were modified. For the nocturnal case there was more variability associated with land surface changes; with 2.07 °C of variability across the sites presented (Figure 6.1). The WSUD scenarios were 0.31 °C (25% land surface change) and 0.68 °C (50 % land surface change) cooler than the conventional fully urbanised site. These idealised sites provide estimates of the amount of cooling that WUSD land surfaces can provide, independent from the effects of other influential factors. In reality, WSUD could provide additional cooling if wind speed and solar shading are also optimized.

6.3.3 Limitations of the linear regression approach

There are a number of limitations associated with this analysis that should be acknowledged. The coefficients that were developed through this analysis were derived from the data in the Mawson Lakes campaign. This means that these relationships may not be applicable in different urban environments and especially in areas with significantly different climate and land surface characteristics. Additionally, these relationships are only valid within the bounds set by the Mawson Lakes dataset. For example, the coefficients probably cannot be used for sites with very low SVF because none of the sites in Mawson Lakes had a SVF < 0.5. Further, the coefficients cannot be used to estimate microclimate variability during heatwave conditions, as these conditions were not observed during the Mawson Lakes field campaign. Additionally, these statistical relationships have yet to be validated against any other datasets.

Another limitation of this analysis is that the methods used probably did not perfectly disentangle the different variables that influence urban microclimate. For example, wind speed
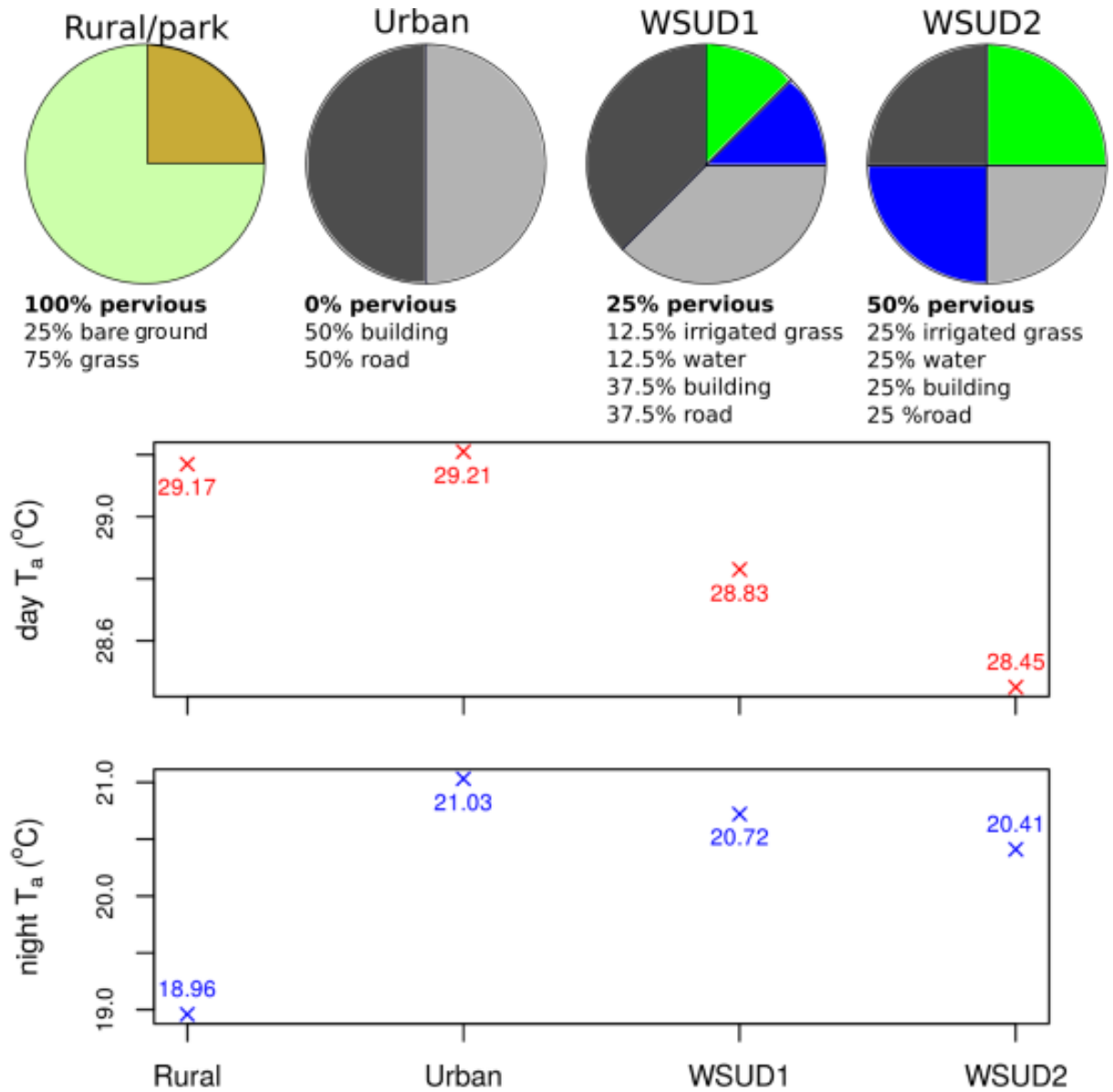
Figure 6.1: The day and night air temperatures from the linear regression models as applied to four idealised sites.

and water fraction were both shown to be predictors of air temperature variability. However, a number of the sites that had a large water fraction, also had higher wind speeds because those sites were exposed. The extent to which the cooling was associated with airflow and mixing (i.e. wind speed) and cool advection from the water body is difficult to disentangle. Nevertheless, it is thought that this approach provides a useful estimate of the cooling potential of WSUD features. Despite the limitations of the statistical approach used here, these results are thought

to be more valid and useful than many observational studies that claim to show cooling benefits associated with different land surface features, but make no attempt to isolate the effects of the feature from other influences (see section 2.3 for more details).

6.4   Conclusions

- **Higher wind speed can provide a significant amount of daytime cooling of microscale air temperature.**

A key finding from this analysis was that wind speed was highly correlated with cooler air temperatures during the day. This microscale cooling was caused by a redistribution of heat in the UCL. In order to get the maximum benefits of WSUD, practitioners should also attempt to promote airflow in the environment during the day. While water bodies can be used to provide some advective benefits, such features also tend to open up the landscape and encourage airflow. As such, promoting cooling through strategic placement of WSUD features could be a method of reducing daytime air temperature and could be considered in future by urban designers and practitioners in future.

- **Irrigation was confirmed to have cooling benefits for daytime microscale air temperature.**

One of the key goals of WSUD is to reduce the runoff of stormwater from urban areas. As such, reintegration of stormwater through irrigation is not only beneficial for the ecology of receiving waterways, but it can also be used to cool urban microclimate. A key outcome from chapter 5 was that irrigation can cool LST, but the effects of air temperature were inconclusive. This analysis suggests that there was a significant cooling effect of irrigation on air temperature during the day. This is an interesting finding because it suggests that cooling can be achieved in suburban areas through a non-permanent measure, i.e. the application of water to pervious

surfaces. As such, irrigation is particularly appealing as a heat mitigation measure, as it allows for some flexibility of spatial and temporal use. Irrigation can potentially be used to cool the urban environment at the time of greatest need, and in the areas where cooling is needed the most.

- **Night microscale air temperature variability in Mawson Lakes can mostly be explained by impervious fraction and wind speed variability.**

The nighttime controls on air temperature variability were relative simple, with impervious surfaces (or the lack of) and wind speed variability explaining most of the variability. It was found that SVF only made a small contribution to nighttime air temperature variability and that pervious fraction encourages nighttime cooling of air temperature, while there was no evidence that irrigation, trees, or water bodies were correlated with a statistically significant warming signal. Overall, the statistical findings in this chapter fit well with observations of nighttime microclimate made in chapter 5.

- **The flexibility of irrigation (stormwater reintegration) means it could be used as an effective emergency heat mitigation measure.**

The most important time to achieve cooling is during heatwave conditions when urban populations are exposed to extreme heat stress. Using WSUD to capture stormwater (and possibly greywater water) and reintegrating this water (through irrigation) during heatwave conditions could be an effective way to achieve cooling during an EHE. WSUD features, such as lakes and wetlands (and rain tanks) can be used for capturing, storing, and treating stormwater; while irrigation is used to distribute the water to areas where cooling is needed. This concept of using alternative water supplies to cool the urban environment during heatwave conditions is in contrast to current outdoor water-use practices in Australia. Potable water has become increas-

ingly scarce and residents have become highly diligent with their water-use practices, especially during heatwaves and droughts. Therefore, encouraging people to irrigate on a hot day may be counter-intuitive and against normal practice for many residents/local-governments. However, if alternative water is available (i.e. harvested stormwater) then that water can be justifiably used to cool the urban environment. The rate and timing of irrigation can be modified and tailored to different seasons/environments to achieve the most efficient cooling benefits when cooling is needed the most. These characteristics of irrigation mean it could be used effectively to cool urban environments during EHE, especially in the context of WSUD where the capture and storage of stormwater is occurring (for ecological reasons) regardless. As heatwave conditions did not occur during the Mawson Lakes field campaign, a modelling approach is used in chapter 7 to look at the cooling potential of irrigation during extreme heat.

7 High resolution modelling of air temperature and HTC in Mawson Lakes: the effect of irrigation on urban microclimate during extreme heat

7.1 Introduction

In chapter 6 it was argued that irrigation could be used to achieve effective distributed cooling in urban developments. In a WSUD suburb the water used for cooling the environment could come from captured runoff, including stormwater and greywater sources. Reducing urban stormwater runoff is a key goal of WSUD, and as discussed has ecological, flood mitigation, and water preservation benefits in urban areas. In addition to these benefits, the reintegration of captured runoff water into pervious surfaces and vegetation could be deliberately used to provide cooling benefits for urban climate. In particular, the reintegration of stormwater (and greywater) could be used as a cooling measure during heatwave events. Heatwaves are well known to cause a short-term increase in mortality and morbidity of exposed populations. Therefore, the need to mitigate heat is greatest during heatwave conditions. Capturing stormwater and greywater water supplies and reintegrating this water during heatwave conditions could be an excellent way to achieve cooling at the time of greatest need. A major benefit of irrigation, as a cooling measure, is that the timing and volume of water application could be varied, thereby maximizing the cooling benefits in areas where cooling is needed. Additionally, given that irrigation is not a permanent modification of the land surface, there would be no adverse thermal effects during winter (i.e. cooling), whereas other permanent cooling measures (such as high albedo surfaces) could be undesirable during the cooler months.

The analysis in chapters 5 and 6 has shown irrigation has clear benefits for cooling daytime LST (Section 5.3.3) and air temperature (Section 6.3.1). However, because the meteorological

conditions during the Mawson Lakes field campaign were not extreme, the potential for irrigation to mitigate extreme conditions has not yet been considered. To explore the cooling potential of irrigation during extreme heat a land surface modelling approach was employed. The objectives of this modelling analysis are:

Objective 3: calculate the potential for irrigation to reduce exposure to adverse extreme heat conditions (air temperature).

Objective 4: calculate the effect of irrigation on microscale HTC during extreme heat.

In the literature review it was shown that there are a range of modelling techniques available for urban climate studies; however LSM approaches were deemed most suitable for the purposes of this analysis. The key processes that had to be modelled accurately were the urban water cycle (including irrigation), vegetation in the canyon, and the UCL air temperature. As such, the SURFEX model was used (see Figure 3.5.2 for a full description) to simulate the effects of different irrigation scenarios on urban microclimate in Mawson Lakes.

Despite the potential for irrigation to contribute significantly to cooling in urban areas, it has received a comparatively small amount of attention in the urban heat mitigation modelling literature. A full description of previous modelling literature is provided in section 2.4. However, a brief description is provided here for convenience. Gober et al. (2010) used LUMPS (Grimmond & Oke, 2002) to investigate variability in air temperature and evaporation in Phoenix, Arizona. The authors found that the rate of nighttime cooling increased as ET increased, but this relationship was non-linear, indicating that the magnitude of nighttime cooling levels off when ET rates (and irrigation) are high (see Figure 2.11). This implies that adding water is a thermally inefficient strategy for reducing temperatures in well watered neighbourhoods. This finding was supported by Demuzere et al. (2014) who found a non-linear relationship between ET and irrigation for a bio-filtration system in Melbourne, Australia. As the relationship between

ET and cooling is non-linear, the possibility that cooling via irrigation can be optimised should be considered, so that cooling can be maximised and water-use minimised.

Two other water-use focused studies utilised a LSM bulk approach, similar to that of Gober et al. (2010), including a study from Portland, Oregon (House-Peters & Chang, 2011) and a study conducted in Canberra, Australia (Mitchell et al., 2008). Mitchell et al. (2008) suggest that, compared to a landscape with no vegetation at all, a full vegetated WSUD treatment increased summer evaporation by 1.44 to 1.76 mm day^{-1} and could reduce peak afternoon temperatures by up to 4.2 °C. Overall, these studies reveal important information about the intertwined issues of irrigation and urban climate. However, the spatial and temporal scale and the modelling techniques used in these studies (Mitchell et al., 2008; Gober et al., 2010; House-Peters & Chang, 2011), did not actually capture microscale climate nor human heat stress.

The possibility that irrigation could be used as an emergency heat mitigation measure during extreme conditions, and reduce extreme heat stress at the microscale, has not been directly looked at. One study that did look at the effects of irrigation during an extreme heat event was Grossman-Clarke et al. (2010), who investigated the impact of land cover and land-use changes on near surface air temperature using the WRF model at 2 km resolution. They found that maximum temperatures increased by 2–4 °C when irrigated agricultural land was converted to suburban development, and urban "landscaping" irrigation caused 0.5–1.0 °C cooling to night-time air temperature during extreme events. Grossman-Clarke et al. (2010) is the only major study to look directly at whether irrigation can cool the urban environment during EHE. However, the spatial scale was quite coarse and probably captured the average mesoscale conditions (not the actual microscale variability) that humans were exposed to during a heatwave. Therefore, the potential for irrigation to be used as an emergency heat mitigation measure and reduce human exposure to extreme heat, has yet to be properly considered. This analysis will look directly at the potential for irrigation to reduce human exposure (microscale climate) to extreme

heat, in the Mawson Lake suburb.

In this chapter results from two simulation periods are discussed: a model validation period (Mawson Lakes field campaign: 11 – 17 February 2011) and a heatwave case study (26 January – 8 February 2009). The model validation period was used to test model performance against observed data, and the heatwave case study was used to test the effects of different irrigation scenarios on urban microclimate during extreme heat.

7.2 Methods

7.2.1 Model description and justification

This modelling analysis was conducted using the SURFEX LSM (see Section 3.5.2 for a full model description). SURFEX includes a number of land surface schemes that can be used for modelling urban, natural, and water surfaces. In this analysis the TEB-Veg scheme was used for urban and vegetative surfaces, and the WATFLX model for lakes and water bodies. The use of the SURFEX model is justified fully in section 3.5.2. However, for convenience a brief summary of this justification is provided here. There are a range of techniques that can be used for modelling urban climate, and these techniques can be used to achieve different ends. The key methodologies commonly used are LSM, radiation modes, and CFD simulations. CFD approaches were deemed to be too computationally expensive for this research and radiation models do not capture the surface energy and water balance, which is essential for modelling the effects of irrigation on microclimate. For these reasons a land surface modelling approach was employed.

This research is interested in the effects of WSUD and stormwater reintegration on UCL microscale variability. Therefore, it was deemed important to use a LSM with a urban canopy parameterisation, so the UCL variables could be simulated. In addition to an urban canopy

parameterisation the use of integrated vegetation (rather than a tile approach) was chosen to improve the accuracy of UCL simulations. Furthermore, a LSM with irrigation representation was needed for these simulations. Grimmond et al. (2010, 2011) revealed that most surface energy balance models do not take into account complicated urban hydrological processes such as runoff, infiltration, interception, or irrigation. Representation of irrigation is clearly of critical importance for this research. As such, for this analysis, we used the Lemonsu et al. (2012b) alteration of TEB, which has integrated vegetation (TEB-Veg) and an irrigation scheme has also been added to the TEB-Veg scheme (de Munck, 2013). See Section 3.5.2 for a description of the SURFEX model and associated land surface schemes.

7.2.2 Model setup

To address the research objectives and explore the effects of irrigation on microclimate during extreme conditions SURFEX was setup for Mawson Lakes. The model was run in offline mode at 25 m resolution (see model domain in Figure 7.1) for two separate periods: a heatwave case study period (26 January – 8 February, 2009) and a model validation period (11 February – 17 February 2011). SURFEX was run at 25 m resolution due to the source area analysis results (chapter 4), which suggested the source area of microclimate observations were highly localised. This highly localised source area was supported by the observations made in chapter 5, which showed large spatial variability of microclimate observed over small distances in the suburb. Further, the TEB-Veg scheme has already been used at a similar resolution in another microscale study where Lemonsu et al. (2012b) modelled the microclimates of two courtyards in the Negev region, southern Israel. An un-nested grid was used because the simulations were run in offline mode. There are limitations associated with this approach (discussed further in Section 7.4), but online simulations at this resolution are currently not possible. A 30 day spin up period was used to determine initial values for surface temperatures and soil moisture. The material

characteristics of the urban surfaces in Mawson Lakes were represented using parameters from phase 2 of the PILPS-urban (see stage 4, table 2 in Grimmond et al. (2011)). The Grimmond et al. (2011) values were estimated for suburban site from Melbourne, Australia (Coutts et al., 2007), which is thought to be comparable to the Mawson Lakes domain. The orientation of the canyon for all grid points was fixed to observed street orientations (Lemonsu et al., 2012b).

(a)   (b)   0   0.2 0.4   0.8   1.2   1.6
                                                                  Kilometers

Figure 7.1: A map of the Mawson Lakes SURFEX domain (25 m grid) used in this research: (a) the whole domain and (b) the residential domain (> 10% residential).

TEB-Veg was used to represent all the vegetation in the domain. TEB-Veg allows for three kinds of vegetation: high, low, and no vegetation. The TEB-Veg categories were represented with the following categories from the ECOCLIMAP database (Champeaux et al., 2005): permanent broadleaf trees (EVER), parks and swamp areas (PARK), and bare soil (NO). The land cover classification from the Mawson Lakes campaign was used to derive the fraction of each vegetation type: EVER = trees; PARK = irrigated grass, dry grass, and low vegetation; and NO = bare ground (see Figure 3.9a for our land cover data). The LAI for each vegetation type was defined using values from the literature. For EVER a value of 2.4 was used for eucalyptus trees (Breuer

et al., 2003), and for NO we used a value of 0. However, for the PARK category, as this represents a range of vegetation types including grass and low vegetation, we defined the average LAI for each grid point using the proportion of each vegetation type. We assumed LAI of 1.6 (Grimmond, 1988) for irrigated grass, 0.75 for dry grass (estimated based visual observations made on site — dry grass was very patchy and much less lush than irrigated grass), and 3.1 for low vegetation (Breuer et al., 2003) (average LAI of modelling domain is available in appendix, Figure A.26). For stomatal resistances the following values were set: EVER = 250 m s^{-1} (Breuer et al., 2003), while the PARK and NO categories were left at the default value of 40 m s^{-1}. For the soil characteristics the Australian Soil Resource Information System (ASRIS) was used, which provided an average value for Mawson Lakes of 15% clay, 70% sand, and 15% silt. A uniform value for soil type was prescribed across the whole domain. Building and tree heights were taken from the LiDAR data (Figure 3.9c). Lake surfaces were simulated using the WATFLX model, and all water bodies were treated as outside the canyon. The SURFEX model with the above setup was run for two separate modelling periods: a model validation period (11 February – 17 February 2011) and heatwave case study period (26 January – 8 February, 2009).

7.2.3   Generation of meteorological forcing data

To run SURFEX for the two modelling periods two meteorological forcing datasets were required. For each simulation conducted with SURFEX a single meteorological dataset was used to force the whole domain. SURFEX requires atmospheric pressure, $L \downarrow$, $K \downarrow_{diffuse}$, $K \downarrow_{direct}$, air temperature, specific humidity, and wind speed from above roof height. A forcing dataset that was independent from the Mawson Lakes observational data was required to run SURFEX, as the Mawson Lakes data were used for model validation. Surface level data were available from the nearby Parafield Airport reference station (Bureau of Meteorology), but data from above roof height were not available. Therefore, to generate the meteorological forcing datasets

SURFEX and a simple iterative correction method (Lemonsu et al., 2012a) (Figure 7.2) were used. It was important to derive a forcing dataset for wind speed, humidity, and air temperature as these variables can vary significantly with height. The Parafield Airport site was used to develop the forcing dataset with a hourly time step. SURFEX was run for a single grid point over the Parafield Airport site, with a forcing height of 40 m, which is well above roof height for the Mawson Lakes domain. In the first iteration the model was forced at 40 m directly using the Parafield Airport near surface meteorological data. The near surface biases were then calculated for the Parafield site, using the difference between the modelled and observed surface values, and the new 40 m forcing data was corrected by subtracting this bias from the previous forcing dataset. Three successive iterations were performed with SURFEX over the Parafield site. Unmodified radiation ($L \downarrow$, $K \downarrow_{diffuse}$, $K \downarrow_{direct}$) data from the Kent Town (Bureau of Meteorology) weather station (approximately 12 km away) were used for the radiation input variables. This entire processes was conducted twice, in order to develop a meteorological forcing dataset for each of the modelling periods considered.
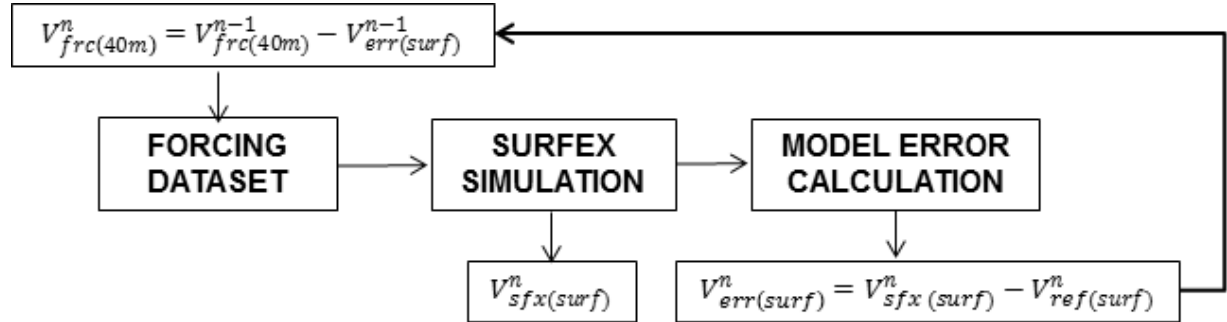
Figure 7.2: A diagram describing the methodology for providing meteorological conditions at a prescribed vertical level, chosen as forcing level for SURFEX simulations. $V_{frc(40m)}$ = meteorological forcing at 40m, $V_{sfx(surf)}$ is the SURFEX simulated near-surface variables, and $V_{err(surf)}$ = the model error for each parameter, calculated as the bias between $V_{sfx(surf)}$ and the reference variables from the Parafield Airport sites. $V_{frc(40m)}^{n-1} = V_{ref(surf)}$ and $V_{err(surf)}^{n-1} = 0$. Source: after Lemonsu et al. (2012a).

7.2.4 Model validation approach

To validate SURFEX a simulation of the Mawson Lakes suburb was conducted for the period that the Mawson field campaign was carried out (11 February – 17 February 2011) (Section 3.4). There were no observed flux data available to validate the modelled fluxes, instead the microscale temperature variability was tested. The model was forced with the Parafield Airport forcing dataset (derived using the processes discussed above) and radiation data from the Kent Town weather station (Bureau of Meteorology). The output from SURFEX (3m canyon air temperature) was compared with the AWS air temperature clusters (as shown in Figure 5.7), which were used as key descriptors of spatial variability of air temperature in chapter 5. These clusters represent sites with statistically similar air temperature characteristics. Statistical analysis was conducted to ascertain if the model could reproduce the variability of air temperature that was observed in the Mawson Lakes suburb.

7.2.5 Heatwave case study

In order to examine the cooling effects of irrigation SURFEX simulations were conducted for a heatwave case study period. The heatwave case study period used was the "early 2009 south-eastern heatwave" (Figure 7.3). This heatwave affected most of south-eastern Australia and resulted in 13 days of very hot weather in Adelaide. There were 8 consecutive days where the maximum air temperature exceeded 40 °C and 3 consecutive days where daily mean air temperature exceed 34 °C (Figure 7.3b), which is an Adelaide specific heat health threshold (Loughnan et al., 2013). The threshold of 34 °C was correlated with an 8% increased in mortality (Loughnan et al., 2013). This heatwave case study was used to model the effect of different irrigation scenarios on air temperature (Section 7.3.3) and HTC (Section 7.3.5). The meteorological forcing dataset came from the Parafield forcing data (iterative correction method, described above) and

radiation data came from Bureau of Meteorology Kent Town weather station.
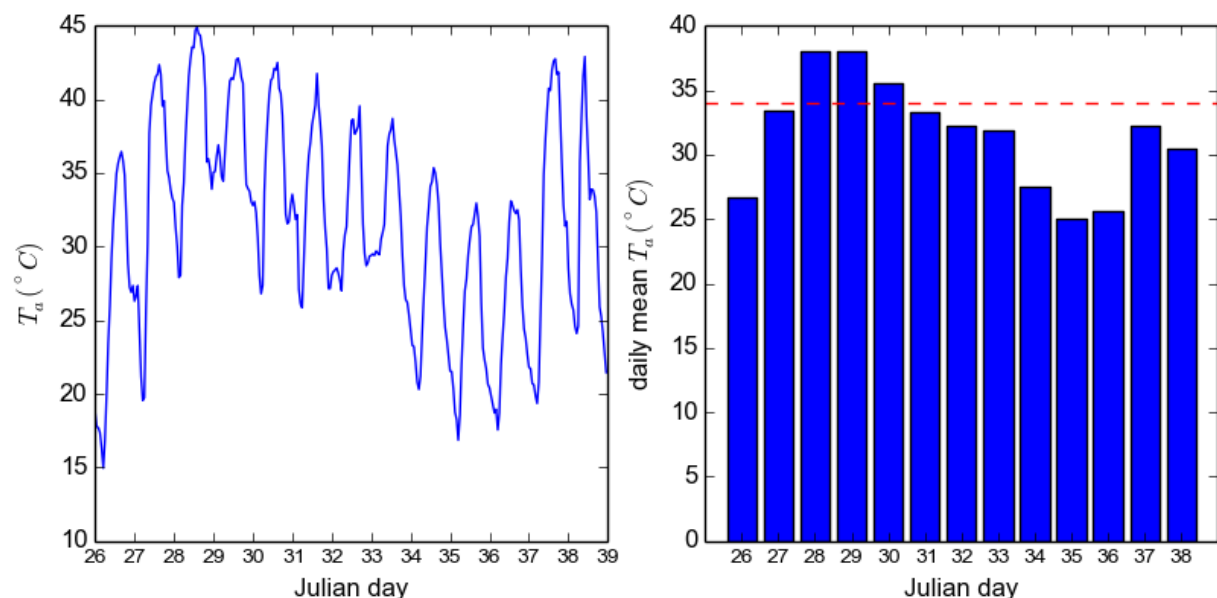
Figure 7.3: An overview of the heatwave case study period 26th January – 8th February 2009: (a) a time series of hourly average air temperature and (b) the daily mean air temperature with a heat health threshold of 34 °C (Loughnan et al., 2013) indicated. There were three days during the heatwave that exceeded the heat health threshold: 28, 29, 30 January.

7.2.6   Irrigation scenarios

For the simulations conducted during the heatwave case study period SURFEX was run with a number of different irrigation scenarios. A range of irrigation rates were tested with incrementally increasing rates of water application to see how changing irrigation affected air temperature and HTC. The only variable that was changed between simulations was the rate and/or timing of irrigation. Irrigation was applied to all pervious surfaces (excluding water) in the domain using the de Munck (2013) irrigation module (see equation 9 for a full description). In total 16 hypothetical irrigation scenarios were tested. Three broad categories of irrigation were simulated, including continuous (24 hour) (Table 7.1), nighttime (6 hours, 11pm–5am) (Table 7.2), and daytime (6 hour, 11am–5pm) (Table 7.2) irrigation. These scenarios were intended to create an array of irrigation regimes, which would allow for a systematic comparison of different

timing and/or rates of water application. The continuous scenarios provided an estimate of the maximum possible cooling that could be achieved for a given rate of irrigation, while the day and night scenarios tested how the timing of irrigation influences microclimate cooling. These scenarios were not intended to be realistic, because water was applied to all pervious surfaces in the domain, and most of the scenarios far exceeded the average outdoor water use for Mawson Lakes. Instead, the irrigation scenarios were intended to provide an estimate of the maximum cooling associated with irrigation across the Mawson Lakes domain. Spatially the irrigation was varied in two ways: whole domain — water was applied to all pervious surfaces (excluding water) across the whole domain (Figure 7.1a), and residential areas only — water was applied to all pervious surfaces (excluding water) in grid cells with residential coverage > 10% (Figure 7.1b). The reason for this spatial variability of application was to explore how targeted application of water could provide localised cooling benefits, and to compare how effectively irrigation provided cooling between residential and non-residential sites. Tables 7.1 and 7.2 summarise the different irrigation scenarios used.

Table 7.1: A description of 24 hour (continuous) irrigation scenarios used.

Scenario	Hourly irrigation	Daily irrigation	Water-use whole domain	Water-use residential
	$(L\ m^{-2}\ hr^{-1})$	$(L\ m^{-2}\ day^{-1})$	(ML) (all cells)	(ML) (10% residential)
24Irr5L	0.21	5	19.2	4.8
24Irr10L	0.42	10	38.5	9.6
24Irr15L	0.63	15	57.7	14.2
24Irr20L	0.83	20	76.9	19.2
24Irr30L	1.25	30	115.4	28.9
24Irr40L	1.67	40	153.8	35.8
24Irr50L	2.08	50	192.3	48.1
24Irr100L	4.17	100	384.5	96.1

ML = megaliters

Table 7.2: *A description of 6 hour irrigation scenarios — day scenarios (11 am–5 pm) and night irrigation scenarios (11 pm–5 am) described below.*

Scenario	Hourly irrigation	Daily irrigation	Total water-use	Water-use residential sites
	$(L\ m^{-2}\ hr^{-1})$	$(L\ day^{-1})$	(ML) (whole domain)	(ML) (10% residential)
Day_6Irr1.25L / Night_6Irr1.25L	0.21	1.25	4.8	1.1
Day_6Irr2.5L / Night_6Irr2.5L	0.42	2.50	9.6	2.6
Day_6Irr3.75L / Night_6Irr3.75L	0.63	3.75	14.2	3.2
Day_6Irr5L / Night_6Irr5L	0.83	5.00	19.2	4.3
Day_6Irr7.5L / Night_6Irr7.5L	1.25	7.50	28.9	6.4
Day_6Irr10L / Night_6Irr10L	1.67	10.0	38.5	8.5
Day_6Irr12.5L / Night_6Irr12.5L	2.08	12.5	48.1	10.6
Day_6Irr25L / Night_6Irr25L	4.17	25.0	96.1	21.3

ML = megaliters

7.2.7   Modelling HTC

To assess the effect of irrigation on HTC an estimate of the MRT was needed so that PET (via RAYMAN) could be calculated. To calculate MRT the SOLWEIG model (description of this model provided in Section 3.5.3) was setup for a number of AWS sites in Mawson Lakes. SOLWEIG can calculate MRT using surface elevation information, SVF, and meteorological forcing input data. The meteorological output from the SURFEX simulations were used as meteorological input to force SOLWEIG, while the three-dimensional land surface characteristics from the Mawson Lakes field campaign were also used to setup SOLWEIG. For the radiation input data, observed data (Kent Town, Bureau of Meteorology) was used. However, for different irrigation scenarios, we did not modify the surface characteristics in SOLWEIG, so the effects of LST cooling on MRT (and PET) were not directly captured. This means that this approach will slightly over-predict PET. However, it is expected that the over-prediction of PET was negligible because solar exposure is the main driver of MRT, not radiant heat from the ground. Thom & Coutts (2015) have validated the SOLWEIG model using the Mawson Lakes field campaign data, they were able to accurately reproduce daytime MRT. The SOLWEIG model is currently

not applicable for nighttime simulations. As such, in this analysis the focus is on the effects of irrigation on PET during the 8 am–7 pm time period.

Three case study sites with different land surface characteristics were used for the HTC modelling. Station 13 was a typical residential site, station 20 was a more urbanised mid-rise site, and station 23 was an open dry grassy site (see Figure 5.1). The effect of three different irrigation scenarios on HTC was calculated: Day_6Irr5L, Night_6Irr5L and 24Irr5L were considered. These scenarios all used an irrigation rate of 5 L m^{-2} day^{-1} of water (see Tables 7.1 & 7.2). Due to the time consuming nature of SOLWEIG simulations, it was not possible to run the model for all irrigation scenarios, so irrigation scenarios that could be categorised as realistic were tested.

7.3   Results and discussion

7.3.1   Model validation

For model validation the output of 3 m air temperature from SURFEX was compared with the AWS air temperature clusters (see Figure A.20). Overall, it was found that SURFEX was able to reproduce the general patterns of microscale air temperature variability observed in the Mawson Lakes suburb. Hourly average air temperature plots for each AWS static station are shown in Figures A.27–A.29 and show good model agreement with predicted values at the hourly timescale. Overall, model performance was good with a high degree of correlation between the observed and modelled datasets (Table 7.3). The RMSE were generally low, but for some clusters (e.g. TA-3$_{[Urb+Mid]}$ and TA-6$_{[outlier]}$) the average RMSE was almost as large as the observed air temperature variability between the clusters, suggesting that those sites were not as well captured. A contributing factor that caused higher RMSE for all clusters, was that the model consistently under-predicted air temperature during the morning period (7–11 am) at all sites (Figure A.20). This is also led to a general over-prediction of daily minimum temperature. The reason for this

consistent under-prediction is unclear, but it could be related to inaccuracies or unrepresentative values in the radiation forcing data, which was taken from a Bureau of Meteorology weather station located 12 km away from Mawson Lakes. Additionally, the model under-predicted daytime and nighttime air temperature at the TA-3$_{[Urb+Mid]}$ sites, causing lower performance scores for those sites. TA-3$_{[Urb+Mid]}$ sites were urbanised and had low wind speeds (Figure 5.1), and the model seemed to over-predict wind speed at theses sites. This over-prediction of wind could be related to microscale canyon airflow effects that were not captured by TEB-Veg. TA-6$_{[outlier]}$ was poorly captured with the worst model performance statistics (see Table 7.3). TA-6$_{[outlier]}$ was actually a single site that had anomalously cool conditions throughout the diurnal cycle. The model was able to predict the cooler daytime temperatures, but the nighttime air temperature was over-predicted (Figure A.20f). This over-prediction could be related to a poor representation of the nocturnal effects of the nearby wetland at this site. The model also over-predicted night-time air temperature at the TA-5$_{[Nat+Grs]}$ sites, which were natural sites with a large amount of adjacent grass. This could be related to poor representation of vegetation parameters in the TEB-Veg scheme. In future work, it could be worthwhile testing the TEB-ISBA scheme to see if this improves nighttime air temperatures at natural sites. Despite these shortfalls, overall the model was able to quite well capture the dynamics and timing of microscale air temperature variability that were observed during the Mawson Lakes field campaign. The 3 pm and 3 am air temperature of different clusters were broadly captured (Figure 7.3), and the relative differences between the sites were correctly modelled.

The decent performance of the model at this resolution further reinforces the source area analysis done earlier (chapter 4). The model was able to reproduce the broad microclimate air temperature characteristics, of the static AWS sites, using only the directly adjacent surface characteristics (i.e. 25 m grid) as surface inputs. It was found that increasing the resolution slightly degraded the performance of the model overall. When the model was tested with a coarser spa-
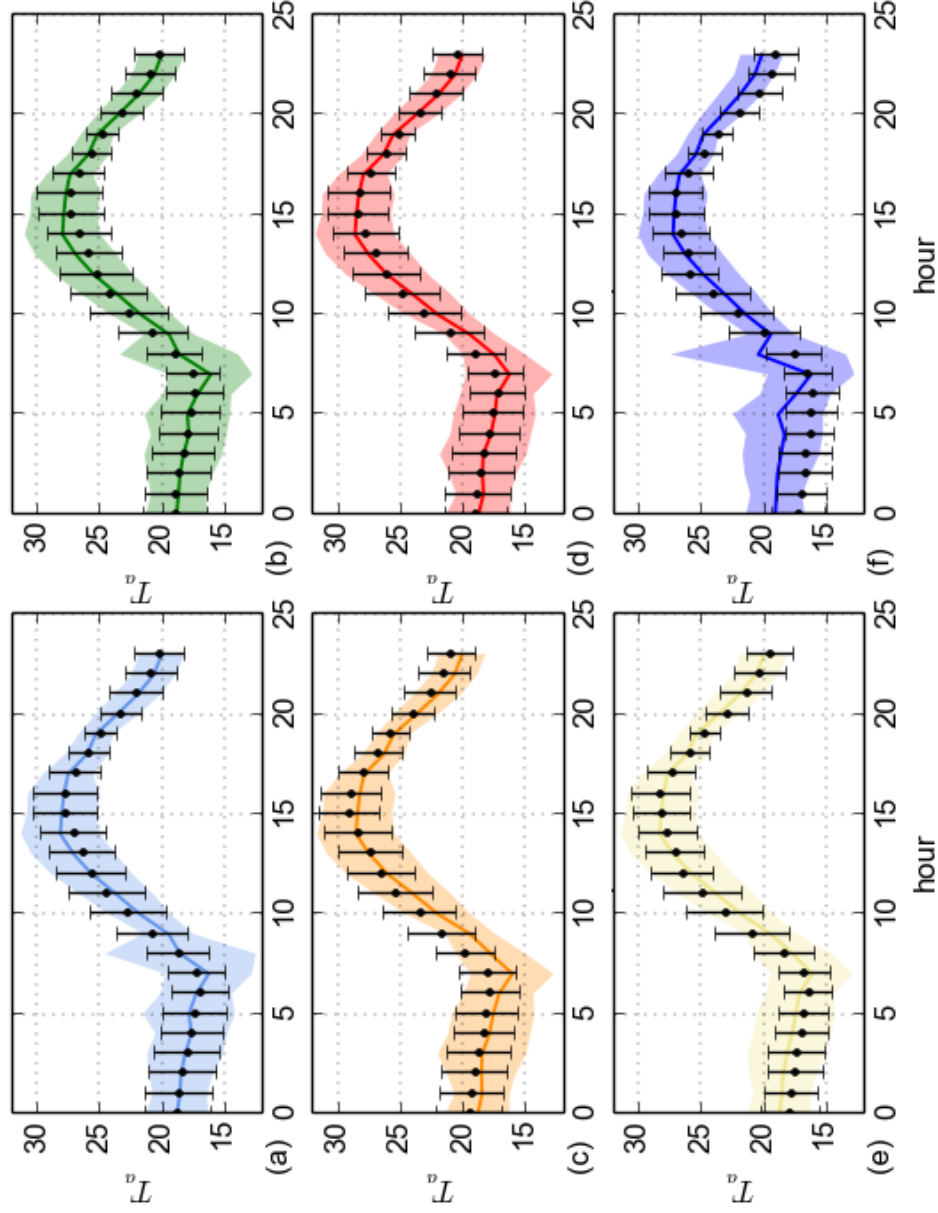
Figure 7.4: The average modelled (line) vs observed (bars) 3 m air temperature during intensive observational period, grouped by air temperature cluster (Figure 5.1): (a) TA-1$_{[Urb+Wtr]}$, (b) TA-2$_{[Mixd+Wtr]}$, (c) TA-3$_{[Urb+Mid]}$, (d) TA-4$_{[Urb+Res]}$, (e) TA-5$_{[Nat+Grs]}$, (f) TA-6$_{[outlier]}$. T_a = air temperature.

181

Table 7.3: *The statistical values from the SURFEX validation: average modelled 3 m air temperature vs observed 3 m air temperature for static AWS clusters.*

Category	σ_o	σ_m	r^2	MAE (°C)	RMSE (°C)	$RMSE_u$ (°C)	$RMSE_s$ (°C)	Δ_{o-m} max (°C)	Δ_{o-m} min (°C)	Δ_{o-m} 3pm (°C)	Δ_{o-m} 3am (°C)
TA-1[Urb+Wtr]	3.7	3.9	0.99	0.0	0.5	0.5	0.2	-0.4	0.8	-0.2	-0.2
TA-2[Mxd+Wtr]	3.5	3.9	0.99	0.0	0.6	0.5	0.3	-0.5	1.2	-0.5	0.0
TA-3[Urb+Mid]	3.9	4.2	0.99	0.8	1.0	0.6	0.8	0.5	1.8	0.7	0.3
TA-4[Urb+Res]	3.9	4.2	0.99	0.2	0.7	0.6	0.4	-0.2	0.9	-0.1	-0.1
TA-5[Nat+Grs]	4.2	4.1	0.99	0.1	0.7	0.7	0.2	-0.1	0.3	0.0	-0.8
TA-6[outlier]	4.0	3.4	0.97	0.9	1.4	0.8	1.2	-0.2	0.1	-0.2	-1.9

o = observations
m = model
MAE = mean absolute error
$RMSE$ = root mean square error
$RMSE_u$ = unsystematic root meant square error
$RMSE_s$ = systematic root meant square error
Δ_{o-m} = difference between observed and modelled

tial resolution the performance was slightly worse at reproducing the observed air temperature variability (output from 50 m and 100 m simulations are shown in appendix). When a 50 m grid was used the output from the model was almost identical, although performed slightly worse for the TA-1$_{[Urb+Wtr]}$ and TA-2$_{[Mxd+Wtr]}$ clusters. At 100 m resolution the model performance was degraded further with the dynamics of TA-1$_{[Urb+Wtr]}$, TA-2$_{[Mxd+Wtr]}$, and TA-6$_{[outlier]}$ poorly captured. As the SURFEX model is not a spatially explicit model, it is thought that the high resolution approach helped to accentuate the highly localised microclimate characteristics observed in Mawson Lakes. However, any larger scale advective processes are completely neglected. Incorporating some form of local-scale mixing into this approach could be an interesting area for future research. Given the caveats of this validation, the SURFEX model was then used to investigate the effect of irrigation on air temperature across the whole domain during a heatwave case study period (Figure 7.3).

7.3.2 Base case

The base case simulation shows the air temperature variability during the heatwave without any irrigation. The average spatial variability of 3 pm and 3 am air temperature throughout the entire heatwave is shown in Figure 7.5. The average 3 pm air temperature varied across the domain by up to 9 °C, with areas near water bodies being below 30 °C and urbanised areas reaching 37 °C. The model is suggesting that the average 3 pm air temperature of locations adjacent to the open water bodies, would be up to 9 °C cooler than the warmest locations during the heatwave. This is much larger than the cooling effects observed during the Mawson Lakes field campaign (moderate conditions), suggesting water bodies may provide greater cooling benefits during heatwave conditions. However, this is an area that requires further research. The large cooling effects of the water bodies during the heatwave meant that large differences in air temperature over short distances can be seen around the lakes and water bodies. The differences

in air temperature over short distances are broadly consistent with the analysis in chapters 4 and 5, which showed that the cooling effects of water bodies are localised. However, the methodology used in this modelling analysis does extenuate these differences in air temperature because each grid point is simulated offline and no horizontal atmospheric mixing (advection) between grid points could occur. The fact that no local-scale atmospheric mixing could occur was a limitation of this modelling approach.

Water bodies aside, the majority of locations in the domain, including urbanised areas (e.g. x = 70, y = 40 in Figure 7.5a) and open grassy areas (e.g. x = 110, y = 60 in Figure 7.5a), were very hot at 3 pm. Although vegetated areas were slightly cooler (0.5 °C) than urbanised sites, most of the domain reached an average 3 pm air temperature > 35 °C during the heatwave. The heating of grassed areas is consistent with observations made in chapter 5, which showed that dry grassy areas can be nearly as hot as concrete during the day. In the base case simulations the initial conditions (i.e. drought) and the lack of irrigation meant that all vegetated areas were dry and provided little daytime cooling benefit. This further illustrates the need to irrigate vegetation, in order to receive cooling benefits from greenspace during hot conditions.

The nighttime (3 am) average variability during the heatwave was much smaller than the day with only about 2 °C variability across the domain (Figure 7.5b). This smaller nighttime variability occurred because the water bodies did not provide as much cooling. However, the model does predict that the average 3 am air temperature of locations near water bodies were the coolest in the domain, suggesting that water bodies do provide some nocturnal air temperature cooling. This is in contrast to the observational analysis, which found no cooling effects associated with water bodies at night during moderate conditions. The model is suggesting that during heatwave conditions, the nocturnal near-surface atmosphere is hot and dry enough for evaporative cooling (Q_E) and/or Q_H heat exchange to occur, which provides a cooling effect.

At night, natural areas were slightly cooler than urbanised areas, which is consistent with
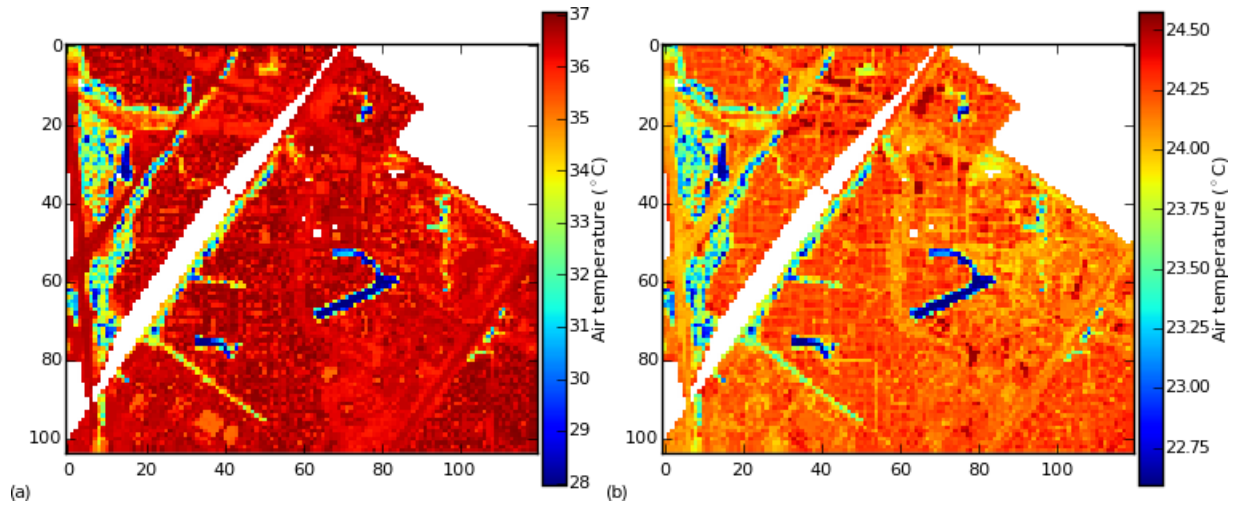
Figure 7.5: The spatial representation of the heatwave average (a) 3 pm and (b) 3 am air temperature (3 m) across the Mawson Lakes domain for the base case (no irrigation) simulation.

the observational analysis. However, the temperature difference was only around 0.5–0.75 °C, which is approximately 1 °C smaller than the differences that were observed between urbanised (e.g. TA-3$_{[Urb+Mid]}$) and natural sites (e.g. TA-5$_{[Nat+Grs]}$) during the Mawson Lakes campaign. It was shown in section 7.3.1 that the SURFEX model tended to over-predict air temperature at the TA-5$_{[Nat+Grs]}$ type sites. This trend also appears to be occurring during the heatwave case study example. Improved predictions of TA-5$_{[Nat+Grs]}$ type sites could be an area for future research. Overall, the base case run mostly conforms to the trends observed during the Mawson Lakes fiend campaign. However, some of the trends discussed, such as the effects of water bodies during heatwave conditions require future research. The focus in this chapter is the cooling effects of irrigation.

7.3.3 24 hour irrigation scenarios

To test the maximum possible cooling benefit of irrigation a series of continuous irrigation scenarios with incrementally increasing irrigation rates were implemented (Table 7.1). In these scenarios water was continuously applied to all pervious surfaces in the domain (Figure 7.1a). The results from the continuous irrigation scenarios show the maximum hypothetical cooling that

could be achieved by integrating water into the urban environment during a heatwave. Across the whole heatwave period, continuous irrigation resulted in a daily average cooling of up to 2.8 °C (Figure 7.6d). However, there was also temporal variability in the domain average cooling that occurred. The heatwave average cooling at 3 pm was as high as 4 °C (Figure 7.6c) and at 3 am the average cooling reached 2 °C (Figure 7.6b). There was more cooling on average at 3 pm because during the day strong positive Q^* meant that there was a higher potential for ET to occur.

Within the domain there was also spatial variability of cooling from irrigation. For example, as shown in Figure 7.6e–g, residential grid points received less cooling than the domain average. The average daily cooling at residential grid points was about 0.5 °C less than the domain average cooling (Figure 7.6g), due to a lower average pervious fraction at residential sites. To further illustrate the spatial variability of cooling the spatial output from three irrigation scenarios (24Irr10L, 24Irr20L, and 24Irr40L) are shown in Figure 7.7. In the spatial data, it is clear that areas that had more pervious surfaces (and therefore more irrigation) were cooler during the heatwave. For the 24Irr40L scenario, the heatwave average 3 pm air temperature of some highly previous areas, cooled down by 4–8 °C, while residential areas only cooled by around 1–4 °C. The tendency for less cooling to occur at residential sites shows that the cooling potential of irrigation could be more limited in residential areas.

A higher pervious fraction meant more irrigation and thus more cooling; however, spatial variability of vegetation also contributed to air temperature variability. Most notable, areas that had a high proportion of bare ground (see Figure A.23 for domain bare ground distribution) received large cooling benefits (e.g. x = 40, y = 20 in Figure 7.7). The reason for this seems to be that for bare ground surfaces minimal infiltration and uptake of water from plants occurred, allowing for very rapid evaporation of surface water to occur. For 24 hour irrigation, the continuous supply of water meant a large cooling effect occurred over bare ground, but when

Figure 7.6: An overview of the output from the continuous irrigation (Table 7.1) scenarios: (a) the domain average diurnal air temperature (3 m) for the entire heatwave case study (26 January – 8 February). Also indicated is the heatwave average domain cooling of (b) 3 am, (c) 3 pm, and (d) daily average air temperature. Lastly, the heatwave average cooling at residential sites for (e) 3 am, (f) 3 pm, and the (g) daily average is shown.

non-continuous (6 hour) irrigation was conducted, bare ground areas rapidly dried out and the cooling effects of irrigation were not prolonged throughout the day (for example see x = 80, y = 100 in Figures A.30c & d). Irrigating hard and dry surfaces, such as bare ground (or perhaps concrete), might provide a large immediate cooling effect during heatwave conditions. However, well vegetated surfaces may provide more sustained cooling effects (e.g. see x = 100, y = 50 in Figures A.31c & d), as some water is stored and evapotranspired later, rather than being immediately evapotranspired. It is likely there will be important differences in the magnitude and timing of cooling provided by different pervious (and soil) surface types, and this area requires future research in order to further optimise the cooling benefits of irrigation during extreme heat.

The results of the 24 hour irrigation scenarios also show, as observed by others (Gober et al., 2010; Demuzere et al., 2014), that there is a non-linear relationship between irrigation and air temperature cooling (Figure 7.8). This occurs when the surface soil becomes saturated and maximum ET is occurring based on atmospheric demand. The 24 hour irrigation scenarios suggest that the average daily air temperature cooling, across the whole domain, begins to plateau at around 2.6 °C at 40 L m^{-2} day^{-1} (Figure 7.8). For residential sites the threshold was also 40 L m^{-2} day^{-1}, but only 2.0 °C of daily average cooling occurred. However, the distance between these non-linear curves diverges as irrigation rate increases, meaning at low irrigation rates (5 L m^{-2} day^{-1}) the cooling in residential areas was almost as large as at sites with higher perviousness (around 0.5 °C, see Figure 7.8). The relationships shown in Figure 7.8 are only applicable for similar environments and climates, and are based on constant and continuous irrigation. However, they provide some useful guidance for practitioners who are interested in providing cooling during heatwave conditions. Overall, regardless of the environment, there are few thermal benefits associated with irrigation at rates of over 40 L m^{-2} day^{-1}, but the higher imperviousness of residential areas did limit the potential for cooling via irrigation in those areas.

The spatial variability of microscale air temperature shown in the base case (Figure 7.5)
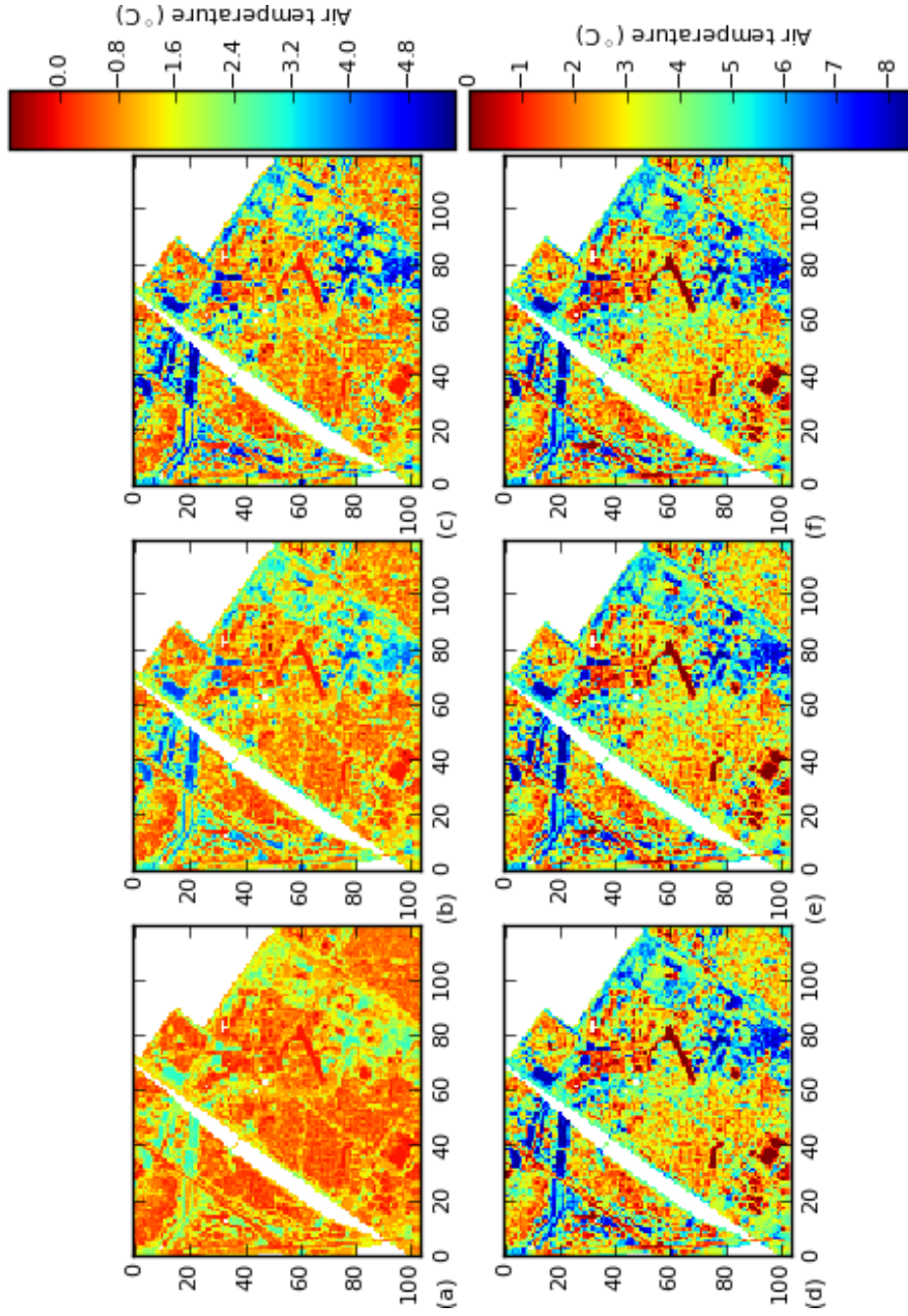
Figure 7.7: A spatial representation of the heatwave average 3 am (top) and 3 pm (bottom) air temperature (3 m) across the Mawson Lakes domain for three different 24 hour irrigation scenarios: (a) average 3 am air temperature for scenario 24Irr10L, (b) average 3 am air temperature for scenario 24Irr20L, (c) average 3 am air temperature for scenario 24Irr40L, (d) average 3 pm air temperature for scenario 24Irr10L, (e) average 3 pm air temperature for scenario 24Irr20L, and (f) average 3 pm air temperature for scenario 24Irr40L.
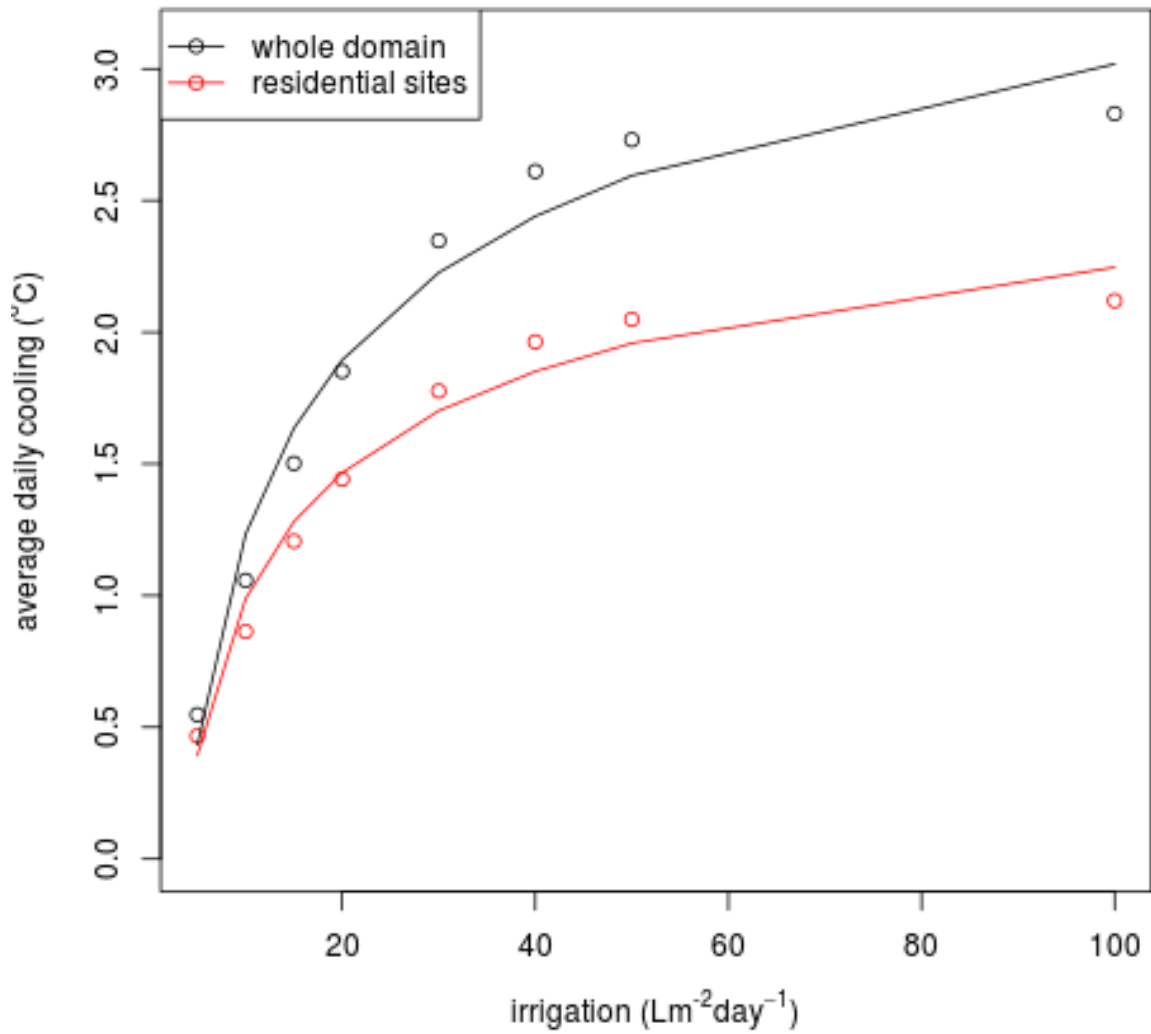
Figure 7.8: The irrigation efficiency (domain average daily cooling (°C)/irrigation (L m^{-2} day^{-1})) for different 24 hour continuous irrigation scenarios. Irrigation cooling begins to plateau around 40 L m^{-2} day^{-1}. Non-linear regression trendlines are shown. The trendline for whole domain is $y = 5.02 - 7.16 \times x^{0.28}$ and for residential sites is $y = 3.43 - 5.04 \times x^{0.32}$.

and in the irrigation scenarios presented (Figure 7.7), indicate that there are areas within the domain (such as more urbanised sites) that receive hotter temperatures during heatwaves. To understand this spatial variability further, the percentage of the domain (whole domain [Figure 7.1a] and residential domain [Figure 7.1b]) that exceeded a daily average temperature of 34 °C (heat health threshold), on the three hottest days of the heatwave (see Figure A.32) was calculated. On January 28 and 29, for continuous irrigation, it found that the percentage of the domain that exceeded the heat health threshold dropped from 90% without any irrigation to below 40% at very high irrigation rates (Figure A.32a). This is a dramatic result, which shows the significant potential cooling benefits of adding very large amounts of water to the landscape. This intra-suburban variability indicates that even when the domain average temperature was below the heat health threshold, there were some areas within the domain, which remained above the threshold. Practitioners need to be aware of variability when evaluating heat stress exposure in urban areas. Taking a larger scale average of air temperature (e.g. as in Figure 7.6) may not provide useful information about the risk of human exposure to heat stress in a given area. The microscale variability of air temperature highlights the challenges and opportunities of reducing human exposure to heat stress in urban environments.

7.3.4   Day and night irrigation scenarios

Another two sets of irrigation scenarios were tested including nighttime (11 pm–5 am) and daytime (11 am–5 pm) irrigation (Table 7.2). The volume of water used in these scenarios was $\frac{1}{4}$ the volume of the original continuous irrigation scenarios. For heatwave average 3 pm air temperature, Night_6Irr25L provided 2.5 °C of cooling and Day_6Irr25L provided 4 °C of cooling. For heatwave average 3 am air temperature, Night_6Irr25L resulted in 2 °C of cooling, and Day_6Irr25L provided 1 °C of cooling. This means that daytime irrigation provided more cooling during the day, and nighttime irrigation provided greater cooling at night. However, the

amount of daily average cooling provided by night and day irrigation was more complicated. The results suggest that nighttime irrigation was most effective at cooling for lower irrigation rates (< 25 L m^{-2} day^{-1}) because the cooling benefit resulting from nighttime irrigation extends for a longer period of the day (Figure 7.9a). However, daytime irrigation was more effective at cooling daily average air temperature at the maximum rate of irrigation tested (25 L m^{-2} day^{-1}). This is because during the day water was more quickly evapotranspired away from the surface, and a large volume needed to be applied during the day (i.e. 25 L m^{-2} day^{-1}) to see a nighttime cooling benefit (Figure 7.9). However, as mentioned above, there was spatial variability of cooling due to differences in vegetation response to day or night irrigation. For the day and night irrigation scenarios, vegetation with higher LAI (such as irrigated grass) tended to provide more prolonged irrigation benefits, by resulting in more cooling after irrigation had stopped (e.g. see well vegetated area at x = 100, y = 50 in Figures A.30c vs. d), whereas less vegetated pervious surfaces only provided cooling at the time of irrigation (e.g. see bare ground at x = 80, y = 100 in Figures A.30c & d). This suggests that greener and more healthy vegetation will provide more prolonged and efficient cooling from irrigation. However the temporal effects of different vegetation types/timing of irrigation is an area that requires further analysis. Overall, the night and day scenarios highlight that there is potential to optimise the timing and volume of irrigation for thermal benefits

For all irrigation scenarios, it is important to consider the total volume of water required to achieve cooling. The volumes of water used in the scenarios discussed above (see Table 7.2) far exceed the January average daily outdoor water-use for Mawson Lakes of 2.56 ML (SA Water, 2013). However, these scenarios were not supposed to be realistic, but rather were intended to provide an estimate of the maximum cooling associated with irrigation across the different environments in the Mawson Lakes domain. To consider what amount of cooling would be possible with more realistic volumes of water the application of water to grid cells with more
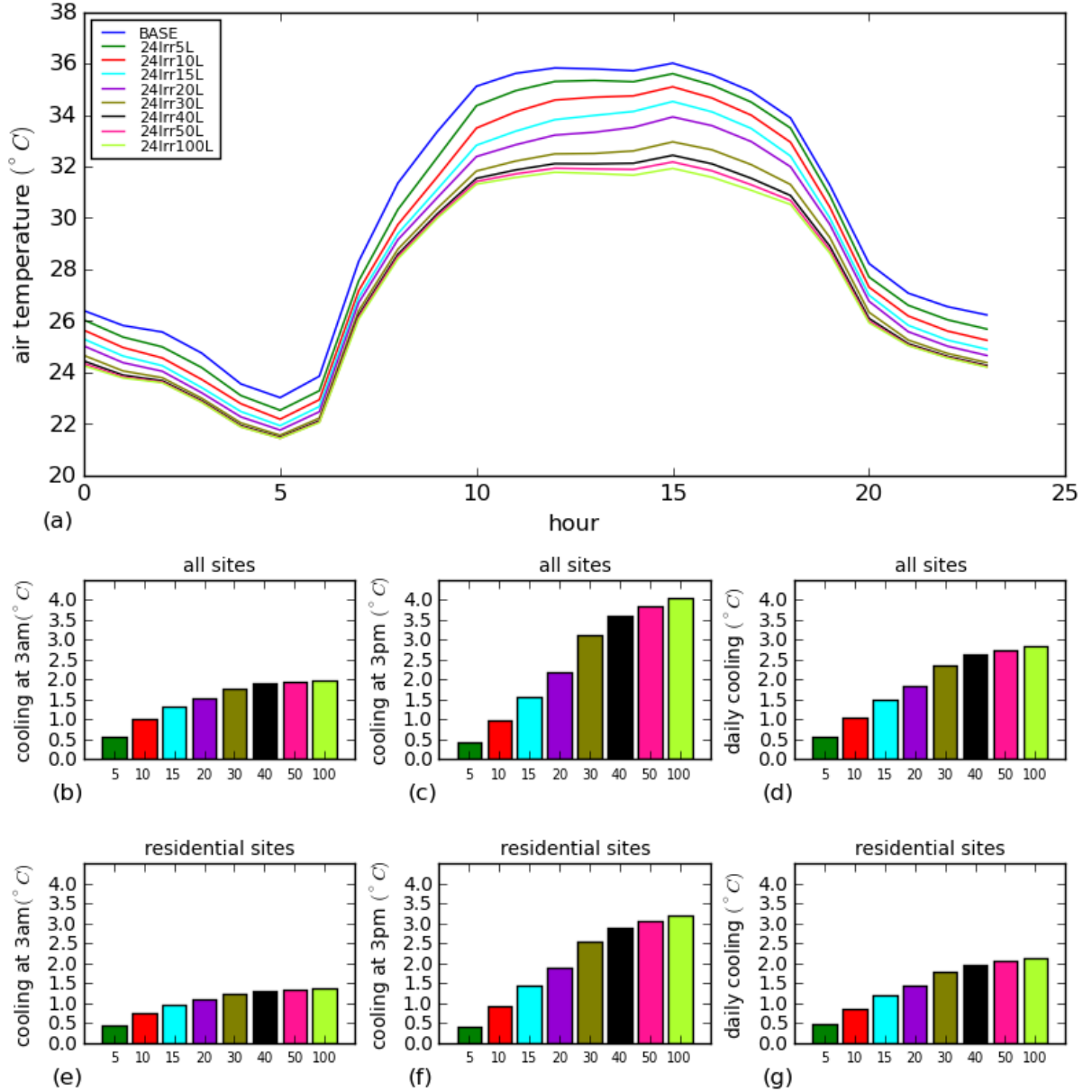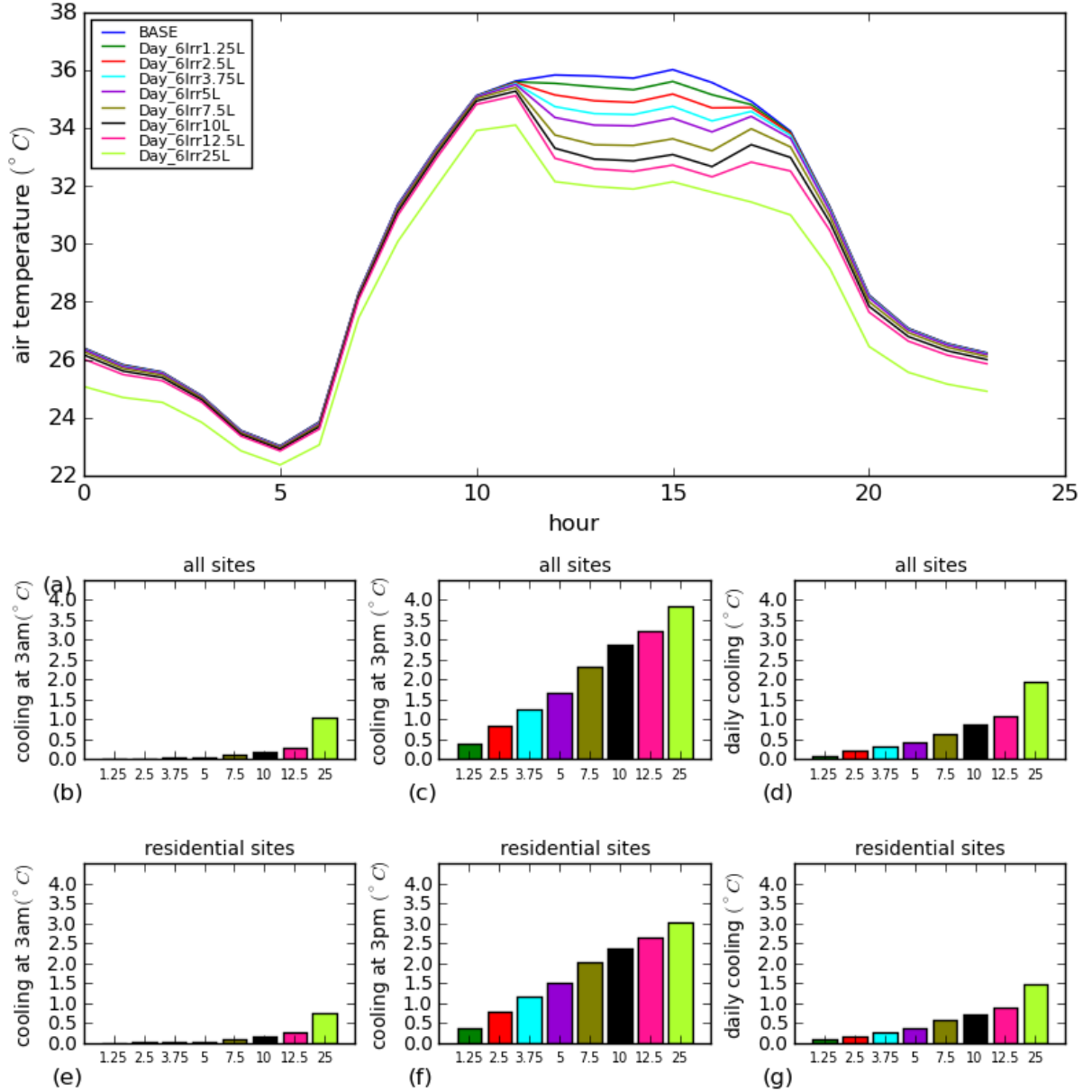
Figure 7.9: An overview of the output from the daytime irrigation (11 am–5 pm) (Table 7.2) scenarios: (a) the domain average diurnal air temperature (3 m) for the entire heatwave case study (26 January – 8 February). Also indicated is the heatwave average domain cooling of (b) 3 am, (c) 3 pm, and (d) daily average air temperature. Lastly, the heatwave average cooling at residential sites for (e) 3 am, (f) 3 pm, and the (g) daily average is shown.
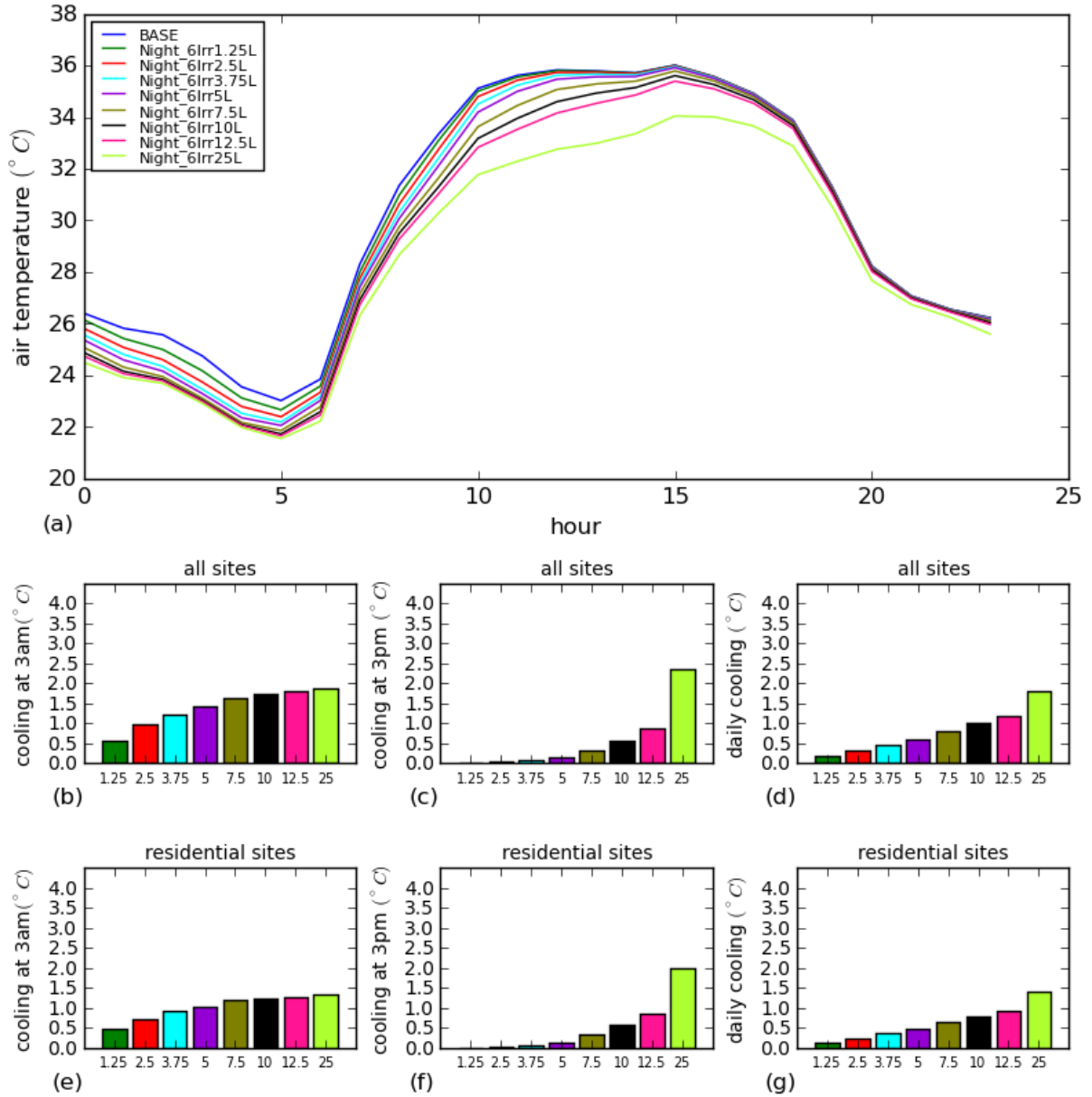
Figure 7.10: An overview of the output from the nighttime irrigation (11 pm–5 am) (Table 7.2) scenarios: (a) the domain average diurnal air temperature (3 m) for the entire heatwave case study (26 January – 8 February). Also indicated is the heatwave average domain cooling of (b) 3 am, (c) 3 pm, and (d) daily average air temperature. Lastly, the heatwave average cooling at residential sites for (e) 3 am, (f) 3 pm, and the (g) daily average is shown.

than 10% residential buildings (Figure 7.1b) was also considered. These scenarios give a sense of how targeted irrigation could be used to provide cooling in areas of need during a heatwave. For example, it was found that if the Night_6Irr12.5L (12.5 L m^{-2} day^{-1}) scenario was carried out in residential areas it could decrease the average daily air temperature at residential sites by about 0.93 °C. This cooling could be achieved in all residential grid cells using 10.6 ML of water per day. This daily reduction of nearly 1 °C at residential sites, is a significant amount of cooling, but note that it was not enough to reduce any of the residential grid cells below the heat health threshold on the 28 and 29 of January (Figure A.32f). This does not mean that irrigation is not effective; however on severe heatwave days (e.g. 28 and 29 January), no amount of irrigation could cool the residential areas enough to fall below the heat health threshold. This suggests that although irrigation is effective, it cannot protect against the most severe heatwave days. Further, this suggests the need for multiple approaches to mitigate excessive urban heat exposure, such as cool roofs, or increasing the amount of pervious surfaces for irrigation through green roofs and walls. Overall, the domain-wide irrigation scenarios provided information about the domain average cooling effects of irrigation across the full distribution of microclimates in Mawson Lakes. However, the residential irrigation scenarios show how more modest irrigation could be used to provide targeted cooling during a heatwave event. This targeted irrigation could be even more focused, for example heavy irrigation could be carried out near age cared facilities and schools during a heatwave, thus providing cooling in those vulnerable areas with a relatively small amount of total water used.

In summary, the irrigation scenarios showed that there is high potential for irrigation to reduce air temperature during heatwaves. It was found that hypothetically, irrigation could reduce the average 3 pm, average 3 am, and daily average air temperature by 4 °C, 2 °C and 2.8 °C, respectively. However, there was significant spatial variability of air temperature with irrigation, and practitioners must be aware of this when attempting to cool the urban environment. The

relationship between average cooling and irrigation was non-linear, with irrigation becoming thermally ineffective at rates greater than 40 L m^{-2} day^{-1}, where the surface is saturated and ET matches atmospheric demand. Finally, the night and day irrigation scenarios showed that there is potential to purposefully optimise the timing and volume of irrigation to maximise cooling benefits.

7.3.5 HTC modelling

The effect of irrigation on PET was considered for three case study sites with different land surface characteristics. The results of the HTC modelling show that all the irrigation scenarios tested reduced average daytime PET (Figure 7.11). For the 24 hour irrigation scenario (24Irr5L), the heatwave average reduction of daytime PET (average of 7am – 8 pm) was 0.8 °C, 0.9 °C, and 0.6 °C, for stations 13, 20, and 23 respectively. The average reductions in daytime PET were similar for the three sites; however, the largest reductions in PET occurred at the more urbanised sites (sites 13 and 20). This is probably because site 23 had a lower baseline PET (see Figure 7.11c), due to higher wind speeds (Figure A.21, see most eastern station) and lower humidity (Figure A.33c), and therefore the PET did not drop as much as at the other sites. Though small differences in PET occured between the sites, it is clear that irrigation can provide some daytime PET cooling; no evidence was found that a small increase in humidity (see Figure A.33) could detract from the PET cooling benefits of irrigation.

However, given the extreme conditions during the heatwave, the irrigation scenarios tested were not sufficient to lower PET to a comfortable level (Figure 7.11). Although higher irrigation rates would have reduced PET by even more, it is unlikely that irrigation could be used to achieve comfortable conditions during extreme heat. MRT has a large effect on HTC during the day, and irrigation can not significantly reduce the MRT of a person standing in direct sunlight. As such, though irrigation can reduce PET, it should be augmented with shading measures to
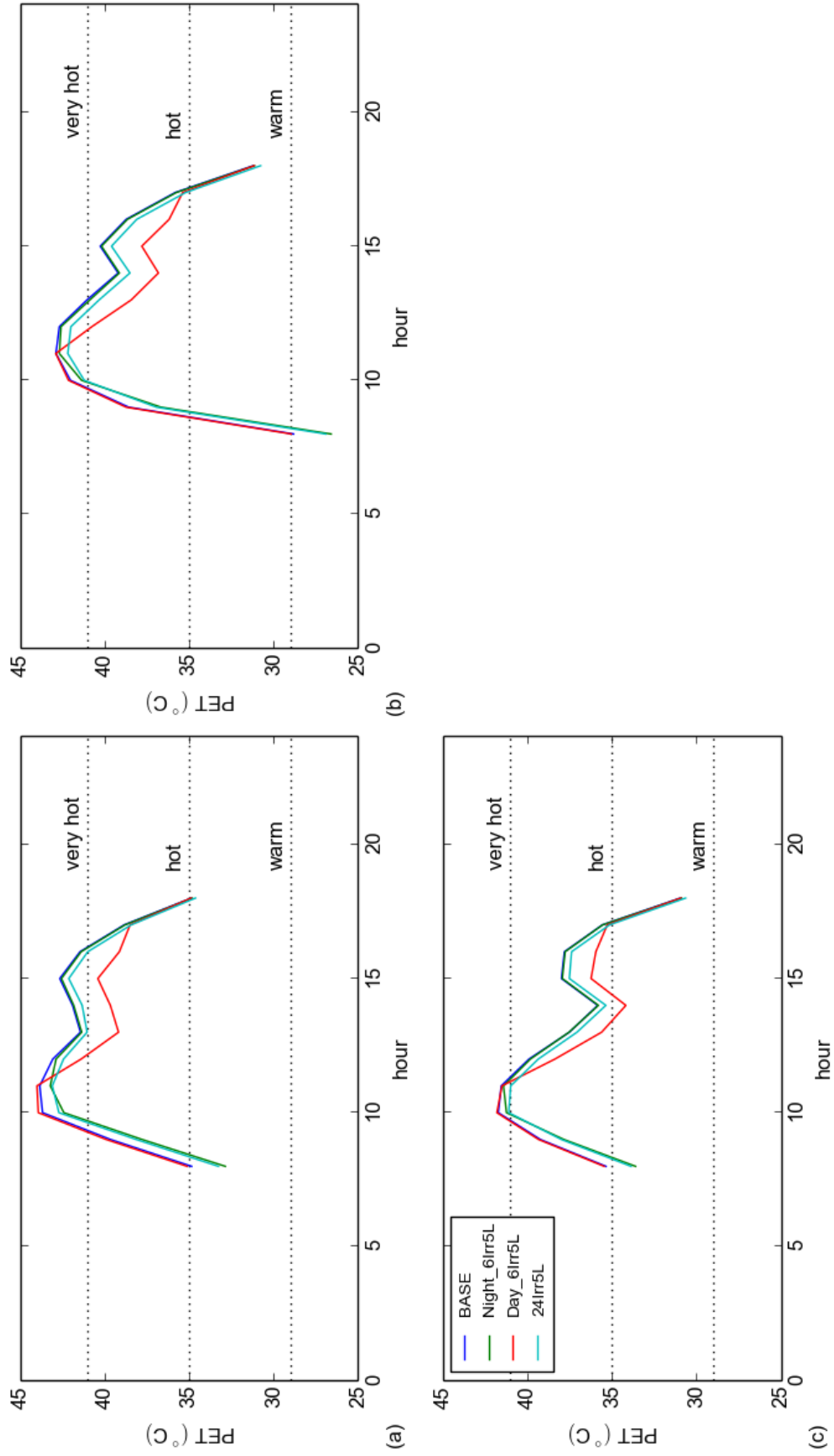
Figure 7.11: The diurnal average PET, during the heatwave period, associated with different irrigation regimes for three case study sites: (a) station 13, (b) station 20, and (c) station 23. Station 13 was a residential site, station 20 was a more urbanised site, and station 23 was an open grassy site.

197

achieve comfortable PET levels during hot conditions.

For the day irrigation scenario (Day_6Irr5L) the heatwave average reduction of daytime PET (7am – 8 pm) was 1.0 °C, 1.2 °C, and 0.8 °C, for stations 13, 20, and 23 respectively. While night (Night_6Irr5L) irrigation resulted on 0.6 °C, 0.6 °C, and 0.4 °C of cooling of daily average PET. For all sites, the most effective scenario for reducing PET was day irrigation. This is unsurprising, as this analysis focused on daytime PET. However, reducing PET is most pertinent during the day, as daytime is when people are most commonly thermally uncomfortable.

The magnitude and timing of maximum PET cooling for different irrigation scenarios was also looked at. For the 24Irr5L scenario the average maximum reduction in PET occured at 8 am for all three sites. The average 8 am cooling ranged from 1.5 – 1.9 °C across the three sites looked at. The Night_6Irr5L scenario also provided average maximum PET cooling at 8 am, with average cooling ranging from 1.8 – 2.2 °C. By contrast, the Day_6Irr5L scenario resulted in maximum PET cooling at 4 pm and an average reduction of PET of 1.9 – 2.5 °C for the three sites. Given the relatively large reduction in PET during the early morning (8 am) for the 24Irr5L and Night_6Irr5L scenarios, this suggests that nighttime irrigation can probably cause approximately 2 °C reductions in nighttime PET. Relatively speaking, this is a large decrease in PET, which makes sense given that nighttime PET is closely linked to air temperature.

The effects of irrigation on daytime PET were, in a relative sense, quite small. The lack of relative PET cooling during the day occurred because daytime PET is highly influenced by MRT. Irrigation can slightly reduce MRT by decreasing the LST of pervious surfaces (although the approach did not capture this), but solar input is the largest contributor to radiant loading during the day. The effects of MRT mean that, although irrigation has a large effect on daytime air temperature (as shown above), irrigation does not have as large an effect (in a relative sense) on daytime PET. Much larger reductions in HTC indices have been observed in the shade of trees in urban areas, including up to 10 °C (UTCI) in Melbourne, Australia (Coutts et al., 2015).

198

This re-reinforces the point that irrigation, without shading measures, is probably not the best strategy for those aiming to improve outdoor HTC in urban areas.

In summary, these results suggests that the air temperature cooling that occurs due to irrigation is large enough to offset any small increase in humidity, and overall lead to a decrease in PET. However, because daytime HTC is highly influenced by MRT, it is recommended that irrigation is augmented with shading measures to provide larger reductions in daytime HTC. Irrigation alone as a heat mitigation measure is probably not the best strategy, for those targeting outdoor HTC, as ultimately trees/shade are needed for comfortable conditions; however, irrigation can certainly reduce air temperature in urban areas and have small positive benefits for HTC, while simultaneously providing other benefits, such as supplying trees with water and improving tree health.

7.3.6   Limitations

The biggest limitation of this modelling analysis is the offline approach. As no atmospheric model was used there were no horizontal interactions between the grid cells and no advection could occur. This means that the modelling approach did not capture the larger scale mixing of heat in the atmosphere or any local-scale effects that contribute to air temperature variability. In chapter 4 we argued that the effects of the land-surface can be highly localised. This analysis appears to support that claim, as the model was able to effectively resolve the air temperature variability using land cover inputs from the surface directly adjacent (25 m) the site. Nevertheless, it must be acknowledged that this approach does not capture all of the processes that influence microscale air temperature in urban areas, and a comparison with an online simulation would be valuable. However, current atmospheric models cannot be used at this resolution.

Given that there is a need to understand microclimate variability for HTC and heat stress reasons, the lack of appropriate modelling tools that can be used at the microscale is of concern.

Urban planners are likely to want to model at this scale to understand exposure to heat stress and HTC variability in urban developments. Therefore, if future urban planners want to assess the benefits of WSUD for different urban layouts, then a microscale model (without the current limitations) would be helpful.

Another limitation of this approach was the simplistic representation of the soil column in TEB-Veg. For example, currently these is no representation of sideways infiltration of moisture in the soil column. Given the importance of soil moisture in these simulations, we acknowledge this limitation could be a non-negligible source of error. However, despite TEB-Veg's limitations, the representation of the water cycle in TEB-Veg is more sophisticated than most other urban land surface models.

A final limitation was the generic parameters for urban and natural surfaces used in this analysis. Grimmond et al. (2011), in Phase 2 of the International Urban Energy Balance Model Comparison (PILPS-urban), found that the performance of most urban land surface models deteriorated when building material information (radiative and thermal parameters) was provided; causing the authors to suggest that, given how difficult it is to gather appropriate values for material characteristics, their provision may not currently be worth the effort. Given the findings of PILPS-urban it is thought that the use of generic urban parameters was justified. However, generic natural parameters were also used and given the complex interactions between vegetation, soil, and irrigation, further refinement of site specific parameters (including LAI and stomatal resistance) is needed for future analyses. Further testing is required to ascertain how sensitive the model is to these natural parameters. Lastly, the effects of different types of vegetation and/or soil on irrigation efficiency is likely to be quite variable, and therefore another important area for future research.

7.4 Conclusions

- **Offline land surface modelling at high resolution was able to capture microscale air temperature variability.**

Overall, the modelling approach used was able to quite accurately capture the microscale air temperature variability that was observed in Mawson Lakes. There are some limitations with the modelling approach used, as discussed above, but despite these limitations we find this approach to be acceptable for modelling urban microclimate in this environment. A key message throughout this research is that microscale climate ("the scale of exposure") is highly variable. It is critical for human exposure studies that microclimate variability is captured. Lower resolution modelling may accurately capture the average air temperature of a suburb (or urban area), but such approaches will not capture the microscale variability within the domain. Ongoing research is needed so that microscale variability can be well captured by urban LSM.

- **Irrigation can significantly reduce air temperature during heatwave conditions. However, over a given threshold (40 L m^{-2} day^{-1}) irrigation is no longer thermally beneficial.**

Previous research has suggested that irrigation can have a cooling effect on both nighttime and daytime urban air temperature (Mitchell et al., 2008; Gober et al., 2010; Grossman-Clarke et al., 2010; House-Peters & Chang, 2011). This research corroborates previous research, suggesting that it's hypothetically possible to cool the daily maximum air temperature and daily average temperature by up to 4 °C and 2.8 °C, respectively. However, given the limitations of the modelling approach and the lack of atmospheric mixing that was captured, these findings should be validated and tested further in future research. It was also found that the relationship between irrigation and cooling was non-linear, and above an irrigation rate of 40 L m^{-2} day^{-1}

there was little thermal benefit from applying water during the heatwave. Furthermore, the results suggest that the 40 L m^{-2} day^{-1} threshold applies for different levels of perviousness. However, the magnitude of daily cooling at residential sites was lower than the domain average cooling, meaning irrigation can provide more cooling in highly pervious areas than in residential areas. These results can be used to inform practitioners about how water should be used to achieve a desired amount of cooling during heatwave conditions.

- **There is the potential to optimise the timing and volume of irrigation for thermal benefits.**

Previous research has not considered the effect of the timing of irrigation on urban microclimate. The results from our analysis show that the timing of irrigation does have an effect on average daily air temperature cooling. Nighttime irrigation was more effective at reducing average daily air temperature at irrigation rates below 25 L m^{-2} day^{-1}, while above 25 L m^{-2} day^{-1} daytime irrigation began to become more effective. These results suggest that the same volume of water can be used to achieve different cooling outcomes. As such, future research will explore the potential for optimising soil water content for cooling benefits.

- **Irrigation does improve HTC but it should be augmented with shading.**

No previous research has directly considered the effect of irrigation on HTC. We tested 3 different irrigation scenarios at 3 sites with different land surface characteristics. In all cases irrigation did improve HTC, and not surprisingly, daytime irrigation created the greatest cooling of average PET during the day. However, irrigation did not provide enough cooling to create thermally comfortable conditions during the heatwave. This is because HTC is highly influenced by MRT, which even with irrigation, can become very high when solar irradiance is high. Overall, irrigation alone is probably not the best strategy for improving HTC in urban areas, as

ultimately trees/shade are needed for thermally comfortable conditions. As such, irrigation must be augmented with other measures that reduce MRT in urban areas, most notably urban trees. Furthermore, longer term irrigation practices (through WSUD) will help to maintain healthy urban trees, even during drought, and a dense canopy of leaves will be maintained, which will have positive effects for HTC.

• **In the context of WSUD there is a good case for using irrigation as an emergency heat mitigation measure during heatwaves.**

WSUD seeks to reduce urban runoff and retain more water in urban areas. This has positive benefits for urban ecology and flood mitigation. Therefore, reducing stormwater and greywater discharge into urban waterways is something that arguably should be done regardless of the thermal benefits. WSUD systems can be used to capture, treat, and store stormwater and greywater supplies. This water can then be re-integrated during heatwave conditions to provide the cooling benefits. Additionally, irrigation provides cooling without permanently modifying the land surface. This means that there are no potential negative cooling effects associated with irrigation during winter.

However, in this research no attempt was made to directly consider the feasibility of irrigation during the meteorological context of the heatwave case study. For example, due to the hot and dry conditions during and prior to the heatwave, there may not have been much much stormwater available for irrigation. However, Mawson Lakes does have a sophisticated water re-use system, including stormwater and recycled water options, meaning availability of water for irrigation during the heatwave may have been high. Future research will directly consider the availability of different sources of water (stormwater, greywater, and potable water) during the heatwave case study, and how much cooling could have been achieved with that volume of water.

8 Research outcomes, implications, and conclusions.

8.1 Introduction

The broad goal of this research was to quantify the cooling potential for WSUD and stormwater reintegration techniques to mitigate urban warmth and improve HTC. Summaries of the key findings are located in the concluding section of chapters 4, 5, 6, and 7. This chapter will draw together the key findings into research outcomes and place these outcomes into the broader context of the research. As discussed in chapter 1, urbanisation, climate change, urban heat, EHE, and drought will leave many urban dwellers regularly exposed to damaging heat stress and thermal discomfort during the 21st century. Indeed, the circumstances of such a culmination have already been experienced in Australia. Excess deaths have occurred during periods of extreme heat, towards the end of a period of severe drought, which included irrigation bans in cities such as Melbourne and Adelaide. It is clear that there is a pressing need to mitigate urban warmth, provide pleasant and safe HTC, and minimise exposure to extreme heat conditions. Creating thermally comfortable, attractive, and more sustainable urban environments is an important task for urban designers and other practitioners. At the same time, interventions for improving urban climates must be efficient and economically viable, meaning that multi-purpose interventions, such as WSUD which has a range of sustainability benefits, are particularly desirable. WSUD is now gaining traction in Australia, as an integrated urban water management approach, but until now very little had been done to quantify its cooling benefits. As such, the overarching aim of this research was to quantify the cooling potential for WSUD and stormwater reintegration techniques to mitigate urban warmth and improve HTC. This chapter will discuss the key findings that have emerged from the observational and modelling analysis and the implications of these findings for urban designers and practitioners who are seeking to create sustainable and liveable

urban environments.

8.2 Key outcomes of the research

(1) The microclimate that people are exposed to in cities (UCL) can vary considerably, which has implications for the thermal experience of the population and for the implementation of urban heat mitigation measures.

- **Intra-suburban microclimate variability (both air temperature and thermal comfort) can be as large as the urban-rural contrast observed in UHI-type studies (chapter 5).** Practitioners that are observing urban climate to address heat mitigation objectives, should be aware of the implications of microclimate variability. The variability means that traditional measures used in urban heat studies, such as UHI intensity, do not provide useful information for designers who wish to reduce heat exposure. For example, when trying to locate hotspots in urban areas, **large scale spatial averages (e.g. 1 km) of LST or air temperature will probably not reveal the true range of heat stress exposure, in the area of interest.**

- Urban microclimate variability also implies that there exist warmer and **less thermally comfortable locations within cities that have the greatest need for cooling measures**. Practitioners should identify these areas, using high resolution heat mapping, so that necessary cooling interventions can be implemented. **Urban designers need to comprehend the variability of urban microclimate to ensure that exposed populations are properly protected from extreme heat**. Hot spots that contain a higher proportion of vulnerable people and/or high activity should be prioritised for cooling measures (see Norton et al. (2015) for further guidance).

- Microclimate variability means that urban designers that are trying to reduce human exposure to heat stress, should **implement targeted cooling interventions that are tailored to site specific microclimatic characteristics.** Some local governments and councils are increasingly committed to protecting and expanding urban green spaces, which is a good thing for urban climate cooling. However, without careful planning, informed by knowledge of UCL microclimate variability, widespread greening measures may not be cost effective. **The effects of microclimate variability mean that to guarantee interventions are effective at providing cooling, they should be highly targeted.**

(2) Air temperature variability is driven by changes in the land surface as well as other (non-surface) factors that that influence urban microclimate. The influence of land surface features is highly localised. Smaller scale interventions (including WSUD) can be used to create targeted cool spots and protect vulnerable people from heat stress.

- The source area analysis conducted in this research suggested that the surfaces that most influence air temperature variability are located directly upwind (within 50 m) during the day, while at night the source area is not affected by wind direction and becomes smaller (within 25 m). **This means that the UCL cooling effects (air temperature) of an individual land surface feature or WSUD invention (such as irrigated green space) will be highly localised.**

- However, this research has highlighted that it is not just land surface features that affect microclimate (chapter 6); a range of factors need to be taken into account when considering urban microclimates. **This research has shown that wind speed (ventilation) is particularly effective at reducing daytime air temperature at the microscale.** It

was found that wind speed had an apparent cooling effect, during the day, of 0.6 °C for a 1 ms^{-1} increase in wind speed. Further, it was shown that MRT and to lesser extent wind speed are critical variables that determine HTC variability.

- **The complexity and variability of urban microclimate represents a significant challenge for urban designers, but it can also be exploited to create targeted cooling interventions.** Good cooling interventions must understand the UCL and leverage the existing environment to maximise the cooling benefits. **Street and neighbourhood scale projects, strategically distributed throughout the landscape, can be used to create microscale to local-scale cooling in urban areas** (see Figure 1.5), which can be used to protect vulnerable populations and areas of high activity from extreme heat. Given the complex factors that contribute to the microscale variability, heat mitigation interventions and **WSUD features should be thoughtfully positioned and designed to maximise cooling benefits**. This will help to ensure that the measures are effective and economical.

(3) The evidence from this research suggests that WSUD can be used as part of a broader urban heat mitigation strategy to effectively and efficiently reduce exposure to extreme heat and improve HTC. Specific recommendations stemming from these findings are given under outcome number (4) (below this section).

- The evidence suggests that the water cycle needs to be a key consideration for urban heat mitigation measures, because **retention of water in the environment can directly and indirectly provide urban cooling benefits and improved HTC.** Broadly, the cooling from water comes in two different forms: (1) direct short-term cooling benefits associated with an increase in in situ water availability and increased ET; and (2) long-

term benefits associated with the retention of urban water in the urban landscape. In this research, the short-term cooling benefits of irrigation were quantified, showing that irrigated grass can have significant effects on both LST and air temperature. The observational analysis showed that under normal summertime conditions, irrigated grass was 6.8 °C cooler than dry grass and 8.0 °C cooler than bare ground (chapter 5). Irrigation was found to have an average cooling effect on daytime air temperature, at the microscale, of 0.46 °C per 25% increase in irrigated fraction in the upwind footprint (chapter 6).

- Additionally, the modelling analysis has shown that **there is high potential for air temperature cooling from irrigation during extreme heat conditions**. The modelling analysis suggests that during heatwave conditions it is hypothetically possible to cool the daily maximum air temperature and daily average temperature by 4.0 °C and 2.8 °C, respectively. However, irrigation cooling efficiency levels off above 40 $Lm^{-2}day^{-1}$. The modelling analysis suggests that irrigation can provide cooling benefits across a range of different urban microclimates, although the evidence suggests that surfaces with greater vegetation coverage will provide a more sustained cooling effect from irrigation.

- The observations suggest that water bodies, such as lakes and wetlands that are primarily built for ecological and amenity reasons, do have incidental microclimate cooling benefits for LST and air temperature. **It was observed that air temperatures at the water affected sites were cooler than the site average, and up to 1.8 °C cooler than the warmest urban sites.** However, the observational analysis also made clear that with additional planning and consideration, water bodies can provide even greater air temperature cooling benefits.

- This research also found evidence that **water bodies can be used to promote airflow in urban areas, which will also generate cooling benefits for urban air temperature.**

This enhancement of airflow around water bodies could be more beneficial than advective cooling. The evidence suggests that practitioners should always consider the local wind regime when designing WSUD interventions.

- It was observed that **reducing MRT is very important for providing thermally comfortable conditions**. This research has shown that **WSUD without shading is less likely to provide thermally comfortable conditions** for urban dwellers. WSUD interventions, such as water bodies and irrigation, can provide cooling benefits for air temperature, but shading measures are needed to significantly reduce MRT during summer, which is of critical importance for improving HTC.

- **No evidence was found that WSUD strategies (including both irrigation and water bodies) can have negative warming effects on nocturnal air temperature.** Further, although the effects of irrigation had a small effect on humidity, this increase was not found to have negative effects for HTC.

(4) Given the evidence and knowledge derived from this research, specific recommendations can be developed to support the implementation of WSUD and maximise the benefits for the urban thermal environment.

- **The use of irrigation is recommended because it has a range of different characteristics that make it a desirable cooling strategy:** water can be rapidly distributed to provide cooling in the areas of greatest need; irrigation can provide cooling without permanently modifying any land surface features; there are no potential negative cooling effects associated with irrigation during winter; capturing stormwater and using it for irrigation is good for the ecology and receiving waterways; and irrigation is arguably the

only way to provide distributed cooling to an urban environment that has already been developed without other cooling interventions in place.

- In order to cool the environment through irrigation substantial water supplies are needed. It's not recommended that potable water is used. **Integrated water management through WUSD, should be used to capture, store and treat stormwater and/or greywater. This water can then be re-integrated during heatwave conditions to provide cooling benefits**. If WSUD features, such as wetlands and man-made lakes, are cleverly designed into the urban landscape they can provide cooling benefits, while also providing valuable alternative water supplies. It is recommended that local governments and water authorities should enable and encourage the capture and treatment of stormwater and greywater.

- **Irrigation has clear cooling benefits for air temperature, which could be particularly useful for providing cooling during heatwaves conditions.** To provide the greatest cooling benefits irrigation should be used in areas that have low in situ water availability. Irrigation should not be used for cooling in areas that are already well watered, and very high irrigation rates (> 40 Lm^{-2}day^{-1}) are not recommended, as cooling efficiency will begin to diminish significantly. Further, **Irrigation alone should not be used to target improvements in HTC, as air temperature cooling for irrigation needs to be supported with shading measures to provide effective HTC.**

- **Designers should directly consider the local wind regime when designing and implementing all types urban heat mitigation interventions, WSUD or otherwise.** To increase advection the wind regime should be considered so that the areas that need cooling are regularly exposed to a large upwind fetch over a cool surface (e.g. a lake or wetland). However, enhancing airflow through an urban canyon will also contribute to day-

time air temperature cooling as turbulence increases heat transport away from the UCL. Understanding the wind regime will help designers to maximise advective and turbulent cooling benefits in urban areas.

- Where possible WSUD measures should be implemented as smaller, distributed features located at regular intervals throughout the urban landscape. Given the localised manner of cooling from water bodies an irrigated greenspace, WSUD features should be distributed throughout the urban environment and placed strategically. Clustering of WSUD features is unlikely to beneficial; **it is also thought that WSUD measures located at regular intervals in urban environment will deliver a larger benefit than large isolated features.** Long thin water bodies, such as the SDML, are less likely to minimize the area exposed to advective cooling, and should be avoided where possible.

- **Maintaining tree cover should be an important part of any WSUD plan**. Aside from adding to overall urban perviousness, which is encouraged in WSUD, trees provide dual cooling benefits by increasing shade and ET. This is particularly important for HTC considerations. As such, **trees should be retained and actively planted (where possible) in urban areas, while harvested stormwater should be used to irrigate trees, thus keeping them healthy.** Healthy trees with thick canopy coverage will provide the greatest benefits for HTC and well-being.

- **Urban vegetation and water management strategies should be developed and considered simultaneously.** Firstly, urban vegetation, particularly in Australia's southern cities needs water to thrive, thus water availability should be part of urban vegetation planning. Secondly, water can be used to maximise the cooling potential of existing green infrastructure, by keeping vegetation well-supplied with water. Vegetation is often already in the urban landscape, but to ensure that it is providing the maximum thermal benefit

to urban climate, vegetation needs to be well watered and protected, especially under a variable and changing climate

- **WSUD interventions are multi-purpose, which enhances their economic imperative.** One of the greatest arguments for actively using WSUD as part of urban heat mitigation measures, is that WSUD has other sustainability benefits independent of heat mitigation. These benefits include: improved stream ecology, water preservation, flood mitigation, and amenity. As such, any additional cooling that can be gained for these features is, in some sense, a bonus for urban sustainability and liveability. Nevertheless, a number of the recommendations above will actively improve the cooling potential of WSUD, and should be considered during the urban planning process.

8.3 Future work

There are a number of areas for future research that have emerged from this research. These include some aspects of the research that could be expanded upon and improved as part of future research projects. Firstly, the statistical relationships derived in chapter 6 could be tested and validated with datasets from other locations. This would show how generally these relationships can be applied, thus indicating whether they can be used in different cities and/or climates, such that practitioners can confidently use the algorithms to inform urban design decision making processes. Secondly, future work on the cooling effects of water bodies, in particular the effects of enhanced airflow vs. advection, would be useful. This research suggests that the cooling effects around small water bodies were more closely related to turbulent mixing than cool advection processes. If this finding is correct, it has implications for WSUD guidelines, regarding the use and positioning of water bodies. Numerical modelling could be a good method to further test these hypotheses because with a numerical model highly controlled experiments can be conducted. Thirdly, the effects of WSUD features under different urban design and urban density config-

urations requires further investigation. This study focused on a low density mixed residential development, however would WUSD be more or less effective in higher or more compact urban spaces? The last major area that could be expanded upon involves a further investigation of the cooling effects of irrigation, including consideration of the actual water availability for irrigation modelling scenarios (chapter 7). This research only considered the effects of hypothetical irrigation scenarios. Future research must be conducted to consider how much cooling can be achieved with realistic estimates of water availability. How much cooling can be achieved during typical heatwave conditions with the actual amount of stormwater and greywater available? Additionally, the effects of irrigation timing could be further considered; an ideal soil moisture level for providing thermal benefits, based on different soil types would be a very useful outcome. These potential areas for further investigation of irrigation cooling measures would provide important information to practitioners and decision makers on the plausibility of reintegrating alternative water supplies (e.g. harvested stormwater) to cool the urban environment during the heatwaves.

There are also some new research questions that have come out of this research. One such questions is how can the effects of advection be accounted for in high resolution LSM? In this research all simulations were done offline, which means that local-scale advection processes were not captured in the simulations. While atmospheric models are available for coupling to LSM (online simulations), due to the underlying physics of such models, simulations at high resolution are not currently plausible. Future research should consider alternative methods for capturing local-scale advective effects in high resolution land surface models. A comparison of this advective approach with offline approaches would be useful for informing future researchers whether coupling is beneficial.

Another major area for new research is the effect of irrigation cooling with regards to different types of vegetation. It is thought that the effects of different vegetation and soil types on the effectiveness of irrigation cooling are likely to be significant, but to limit scope this area was only

briefly touched on in this research. Future modelling research should directly consider to what extent different vegetation types provide cooling benefits from irrigation. This is very important because there are likely to be significant differences between vegetation and soil types owing to plant physiology and soil structure differences. Quantifying and understanding these effects is important so that irrigation cooling approaches can be further improved and optimised based on vegetation and soil characteristics.

Another new question for future work is what are the long-term cooling benefits of WSUD? It is clear that increasing in situ vegetation and water availability has immediate benefits for urban climate, but what are the long-term effects of having healthy, well watered vegetation in cities? Over longer time scales, how much better off is an urban environment with healthy well watered vegetation, compared to an urban environment without WSUD to support vegetation? Analyses such as these could also look at how WSUD cooling effectiveness varies with season and different climatic regions. These long term analyses will help to further quantify the benefits of WSUD, and contribute to the business case for implementation of integrated water management approaches. Further, WSUD cooling approaches should be directly compared with other common heat mitigation measures, including cool roofs, green roofs, trees, general urban greening, and waste heat mitigation. To accurately assess the cooling efficiency of WSUD, such analyses could include a cost benefit analysis of all aspects of the different mitigation scenarios, including the non-market goods/services that each can provide.

Lastly, the Mawson Lakes dataset is a excellent resource that could be utilised by others in future research. The dataset represents a dense network of a range of complementary data types, including in situ meteorological data and high resolution remotely sensed land cover information. There are also other data sources collected that were not utilised in this research, including HTC surveys and on ground-level thermography. This dataset has great potential as a model validation resource, and could be used for land surface, HTC, and irradiance modelling.

214

The Mawson Lakes dataset is currently being used to aid the development of a water sensitive cities modelling toolkit, which will become a modelling tool that can be used to simulate all the benefits (including microclimate benefits) associated with WSUD. It is this author's intention to make this data freely available for interested parties.

8.4 Concluding statement

This research was motivated by the fact that 21st century cities are increasingly facing challenges that threaten their sustainability and liveability. As outlined in the introduction, the interacting processes of changing climate, drought, increased EHE, urbanisation, and the urban warmth mean that many urban dwellers are (and will continue to be) exposed to adverse thermal conditions in cities (Figure 1.3). These interacting processes have generated a pressing need to mitigate urban warmth and reduce exposure to heat. In Australia, the threat of drought and water shortages means that mitigation of urban warmth through the use of vegetation measures is particularly challenging. WSUD has been presented as a possible means for managing urban water and urban climate issues simultaneously. This research sought to understand and quantify the potential for WSUD and stormwater reintegration techniques to mitigate urban warmth and improve HTC, during extreme heat events. It was found that WSUD does in fact help to address the problem of urban warmth and human exposure to heat. This research details the great potential of WSUD, using it to intentionally manipulate water and energy balances, and the combination of green/blue infrastructure can help deliver improved HTC. A broad range of evidence has been presented that specifically shows how WSUD can provide cooling benefits.

This research is significant and highly relevant for both academic and industry parties. The findings from this research can be utilised by Australian municipalities, many of whom are already in the process of planning and implementing integrated water management approaches like WSUD. Guiding principles surrounding irrigation and water body cooling effects can be used

to help create thermally comfortable areas. Further, the cooling benefits cited here can be used by decision making bodies to build a business case for the construction of WSUD infrastructure at their site. The research has contributed significantly to the urban climate academic literature, by highlighting the lack of research that has directly considered the linkages between urban water and climate management. Further, it is the first major piece of work to quantify, using observational techniques, the effects of WSUD on microclimates. The research has quantified these microclimate effects in a robust manner and has pointed out that much of the urban climate observational work lacks this level of robust analysis. As such, this research has clearly demonstrated that WSUD can be used to help maintain liveable and thermally comfortable urban environments.

A Appendix
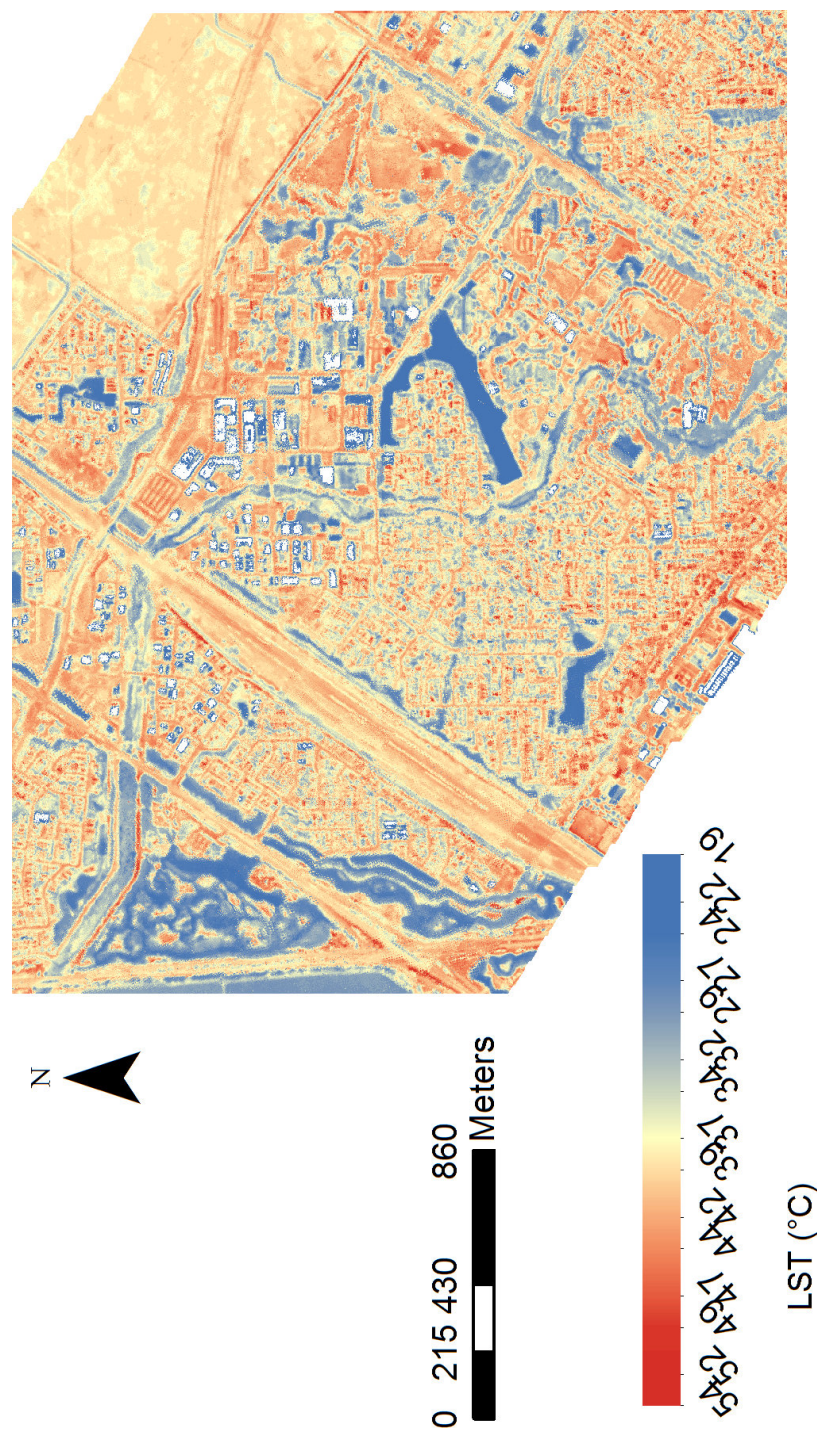
Figure A.1: The airborne thermography for Mawson Lakes captured at 2:00–4:30 pm on the 16th February.
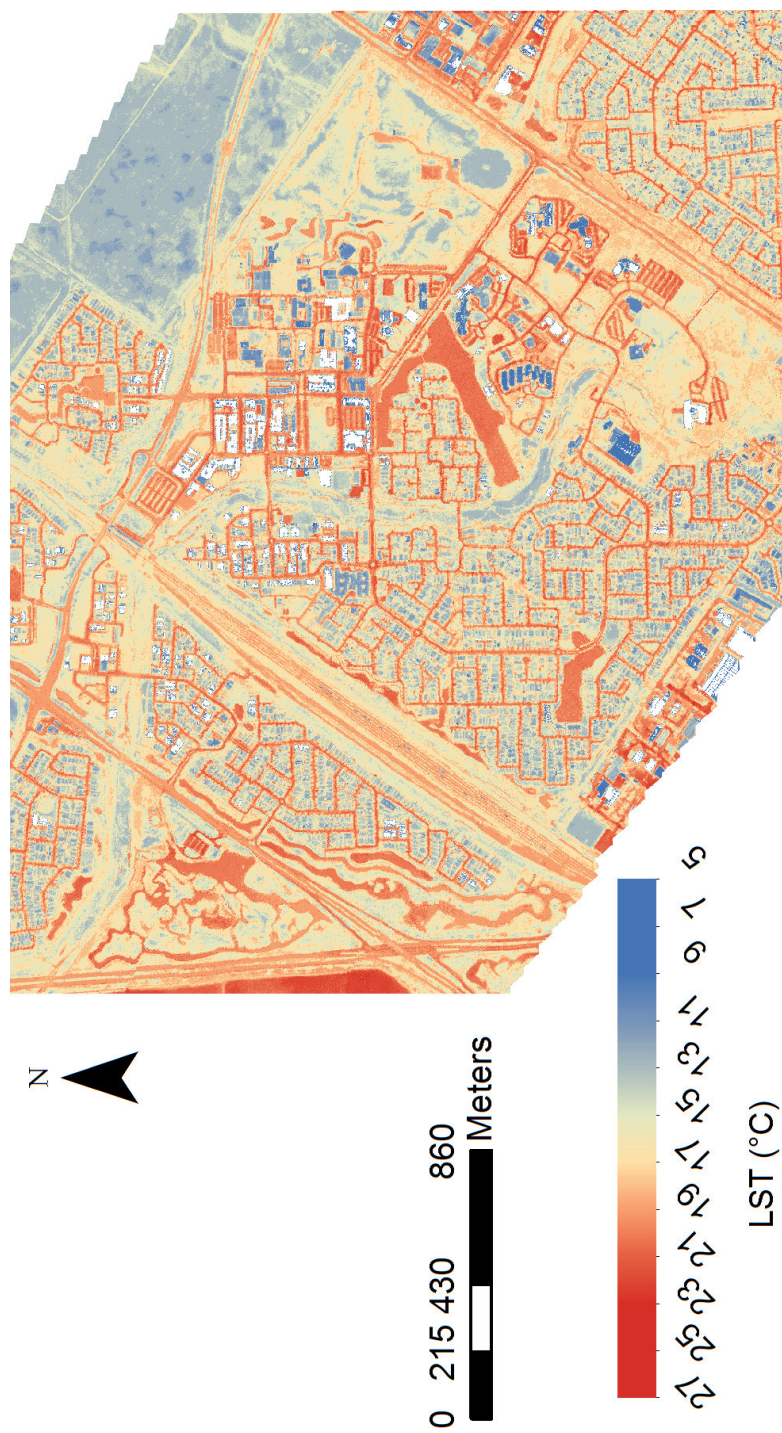
Figure A.2: The airborne thermography for Mawson Lakes captured at 2:00–3:30 am on the 15th February.
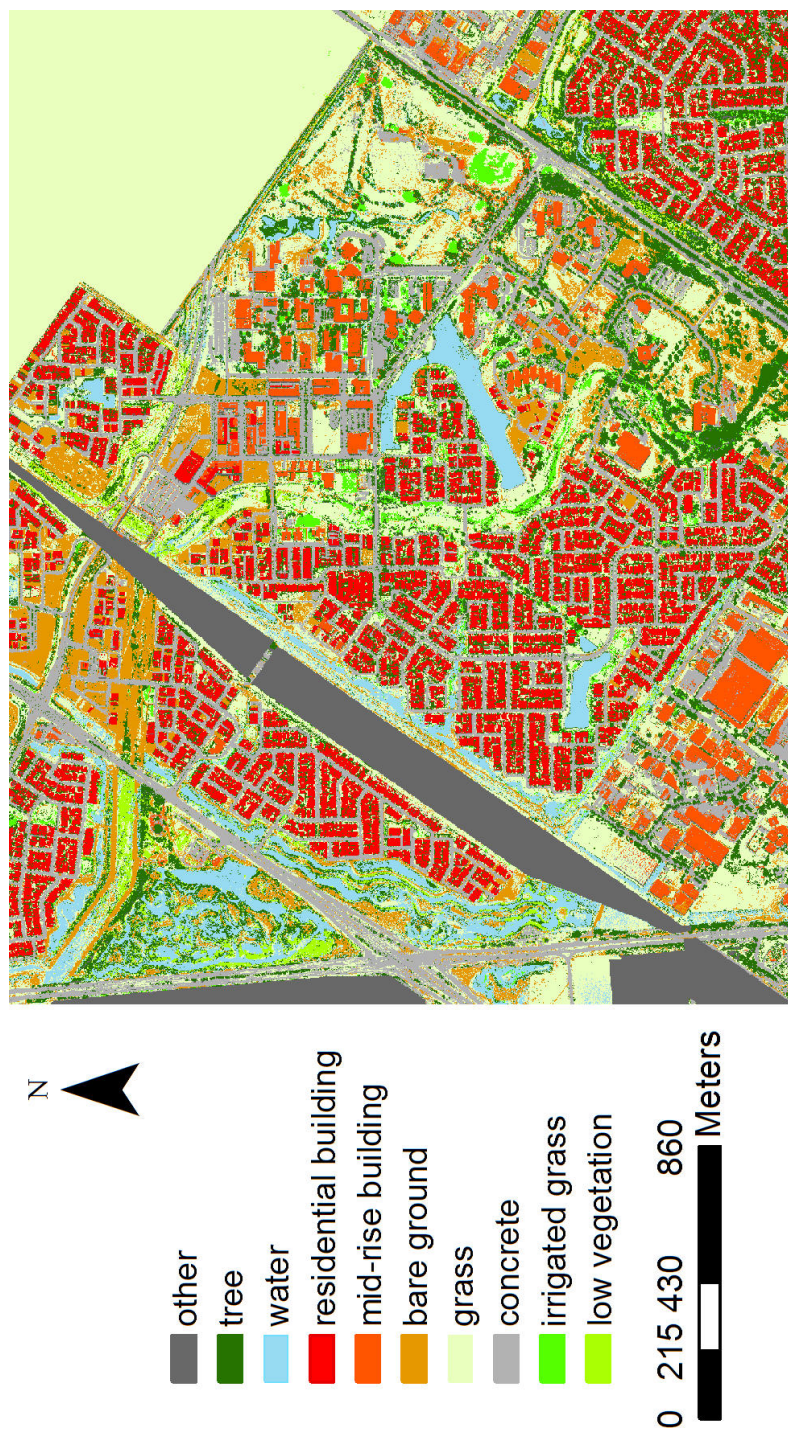
Figure A.3: The land cover categories for Mawson Lakes.
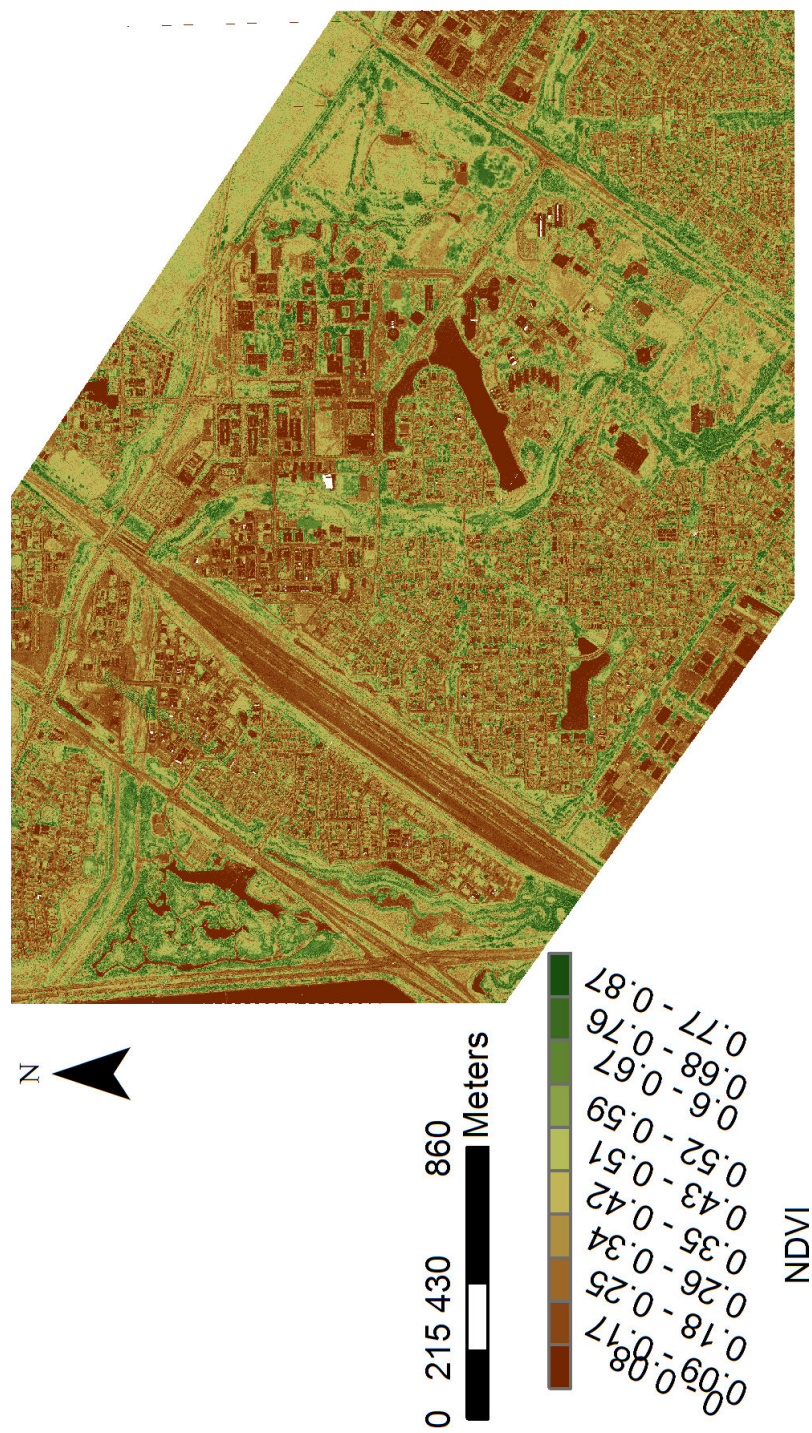
Figure A.4: The NDVI for Mawson Lakes.
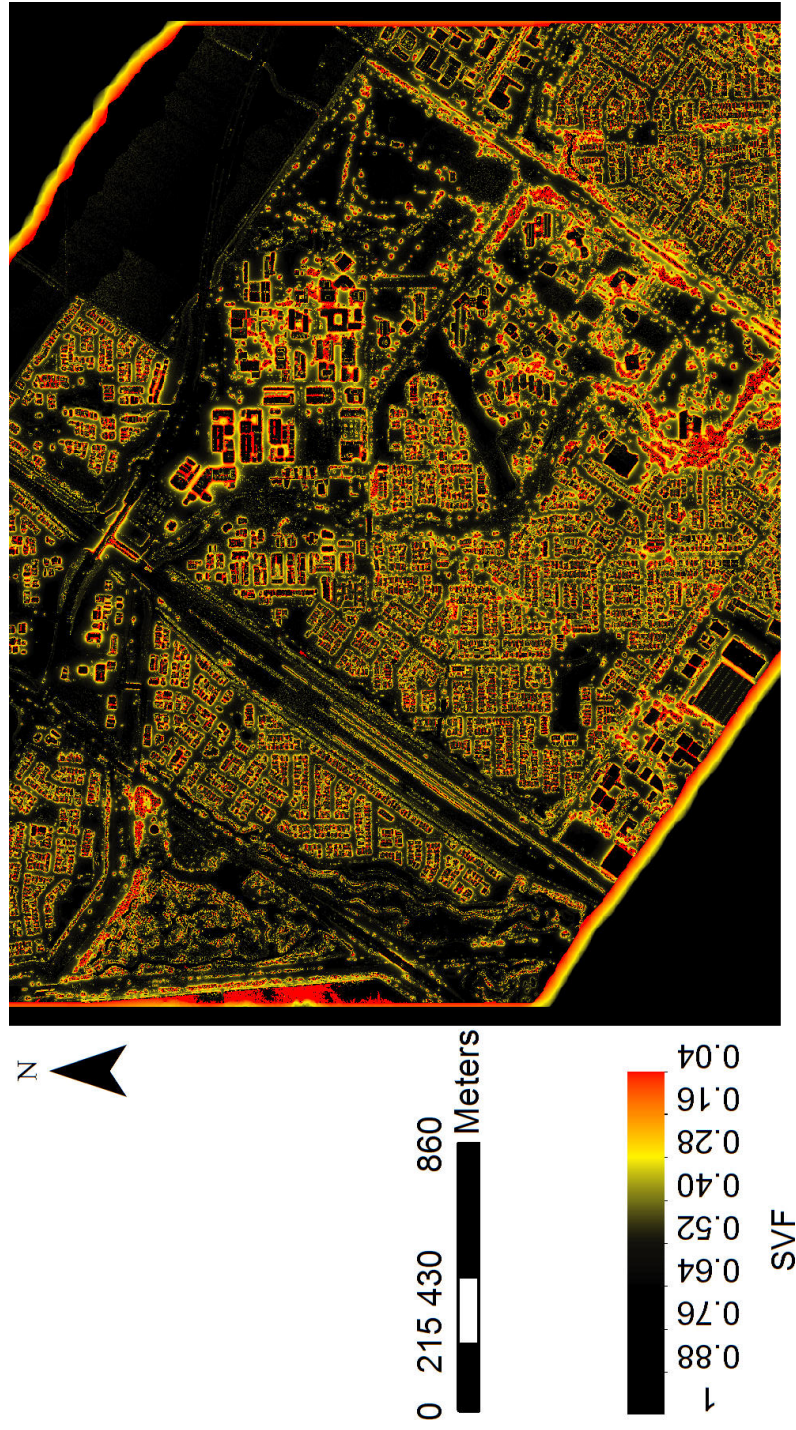
Figure A.5: The SVF for Mawson Lakes.

Figure A.6: Satellite images of AWS stations in Mawson Lakes (a) station 1, (b) station 2, (c) station 3, (d) station 4, (e) station 5, and (f) station 6. The diameter of the circles shown are 100 m.
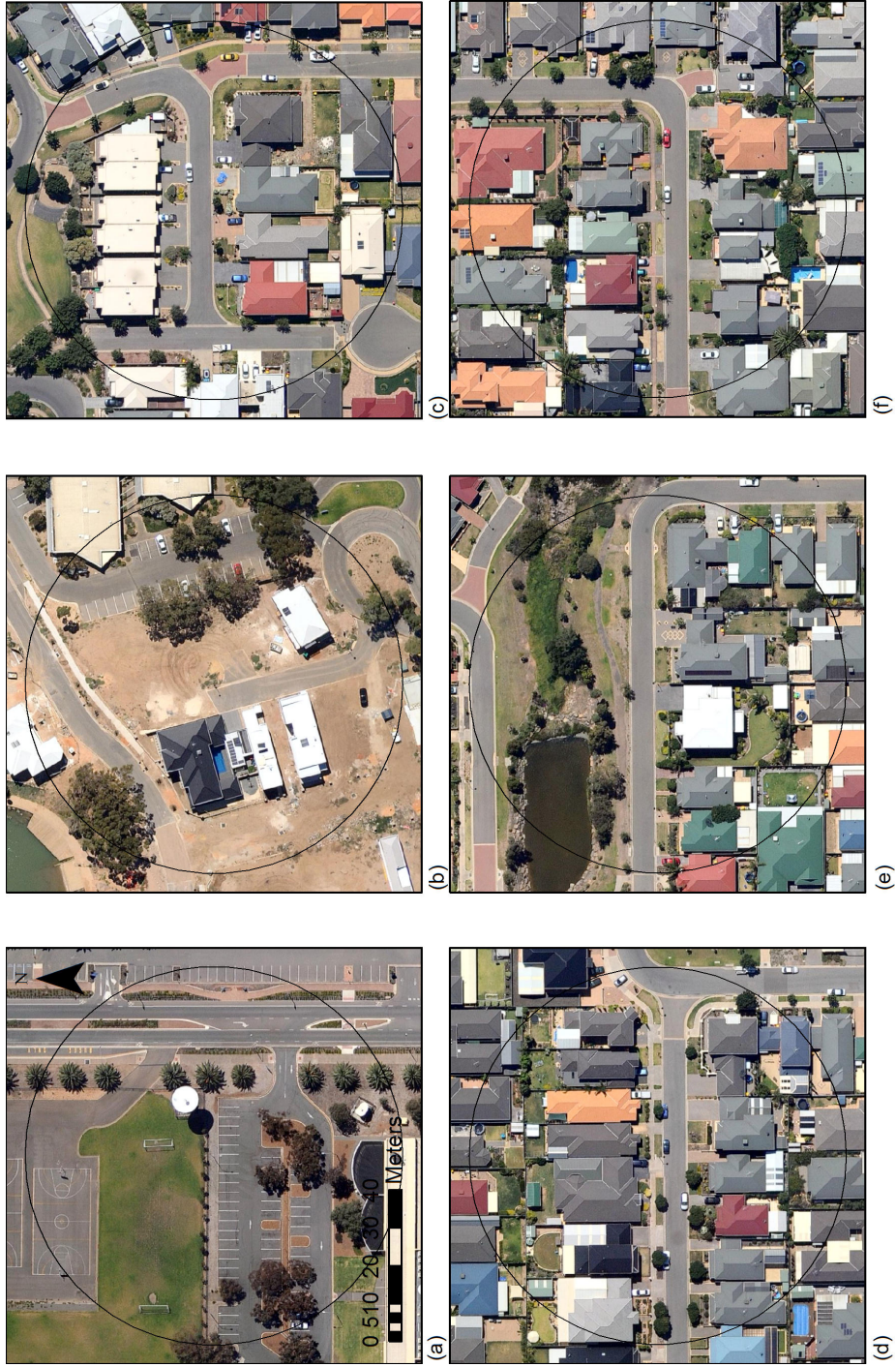
Figure A.7: Satellite images of AWS stations in Mawson Lakes (a) station 8, (b) station 9, (c) station 10, (d) station 11, (e) station 12, and (f) station 13. The diameter of the circles shown are 100 m.

224

Figure A.8: Satellite images of AWS stations in Mawson Lakes (a) station 16, (b) station 17, (c) station 18, (d) station 19, (e) station 20, and (f) station 21. The diameter of the circles shown are 100 m.

225
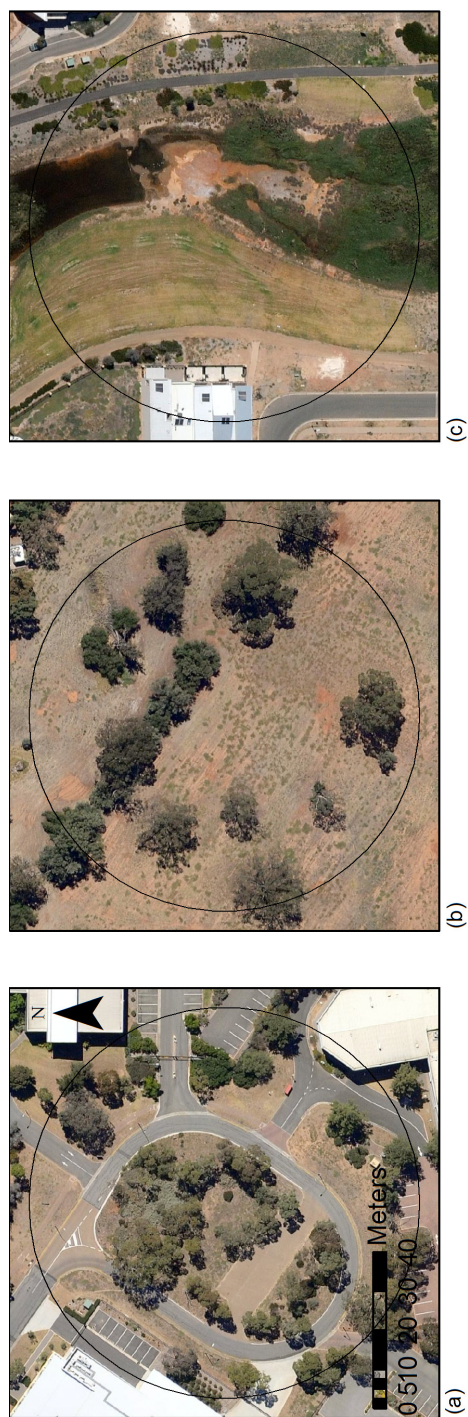
Figure A.9: Satellite images of AWS stations in Mawson Lakes (a) station 28, (b) station 29, and (c) station 30. The diameter of the circles shown are 100 m.

226
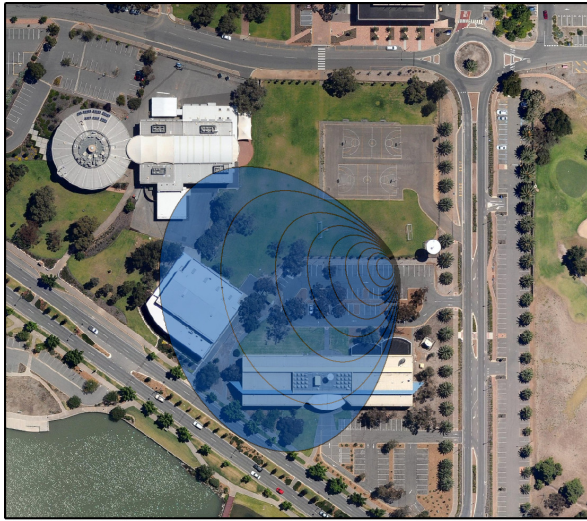
(a.)
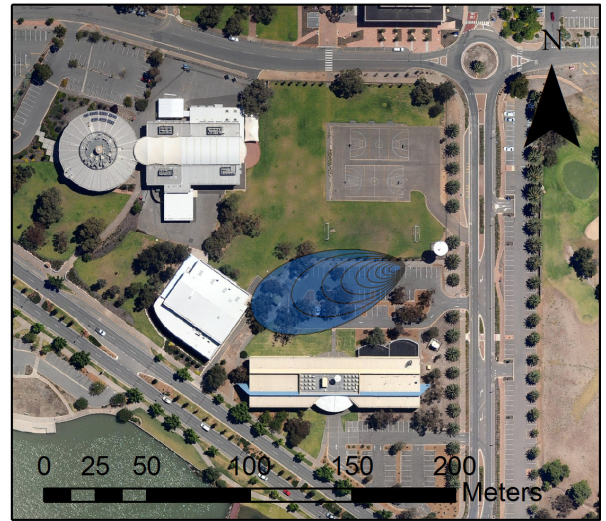
(b.)

Figure A.10: Two examples of hourly source areas estimated using the Horst & Weil (1992) model: (a) nighttime (3 am) and (b) daytime (3 pm).
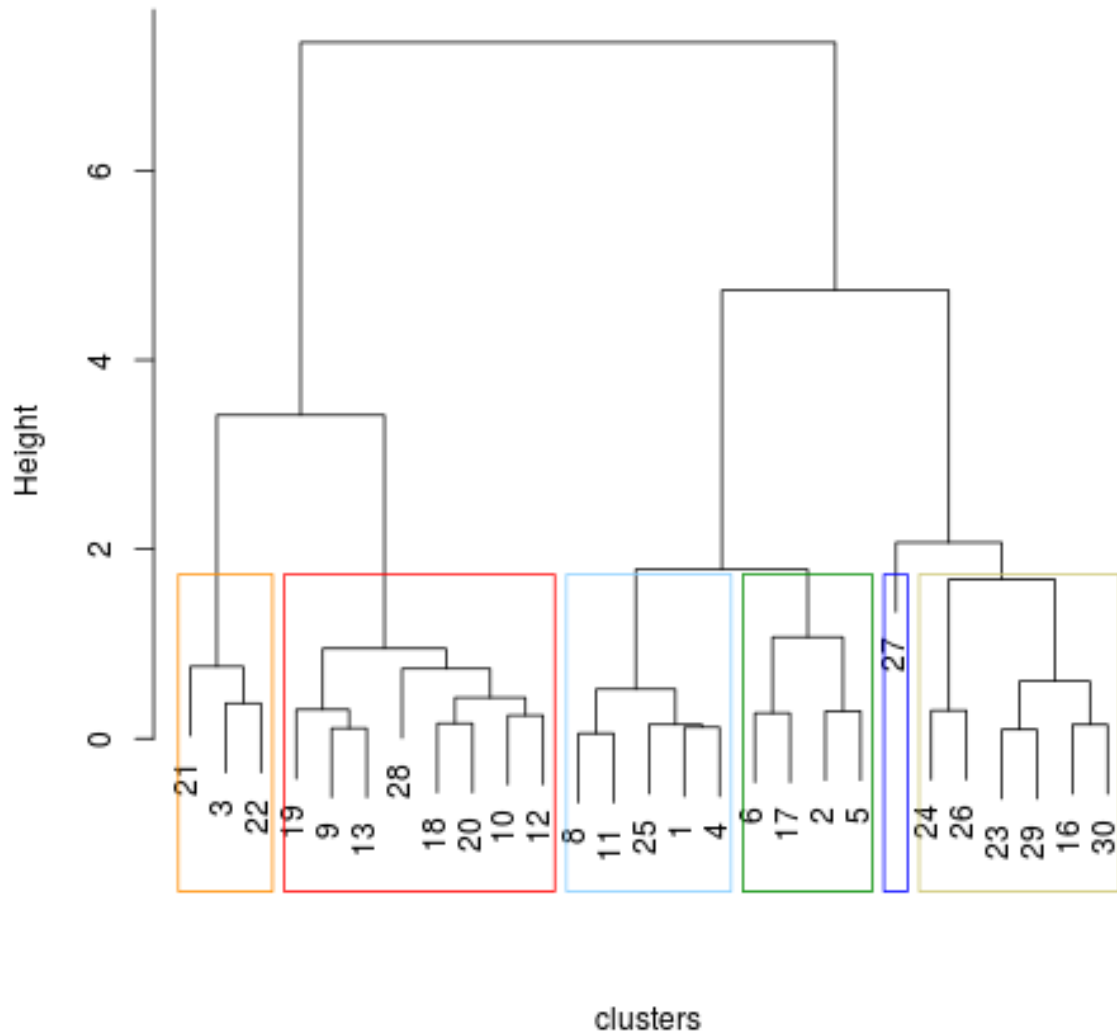
Figure A.11: A dendrogram from the Ward clustering analysis. The inputs to this clustering were: daily average, daily minimum, and daily maximum air temperature. There were 6 clusters identified. Light blue = TA-1$_{[Urb+Wtr]}$, green = TA-2$_{[Mxd+Wtr]}$, orange = TA-3$_{[Urb+Mid]}$, red = TA-4$_{[Urb+Res]}$, yellow = TA-5$_{[Nat+Grs]}$, and blue = TA-6$_{[outlier]}$ (a single outlier site).
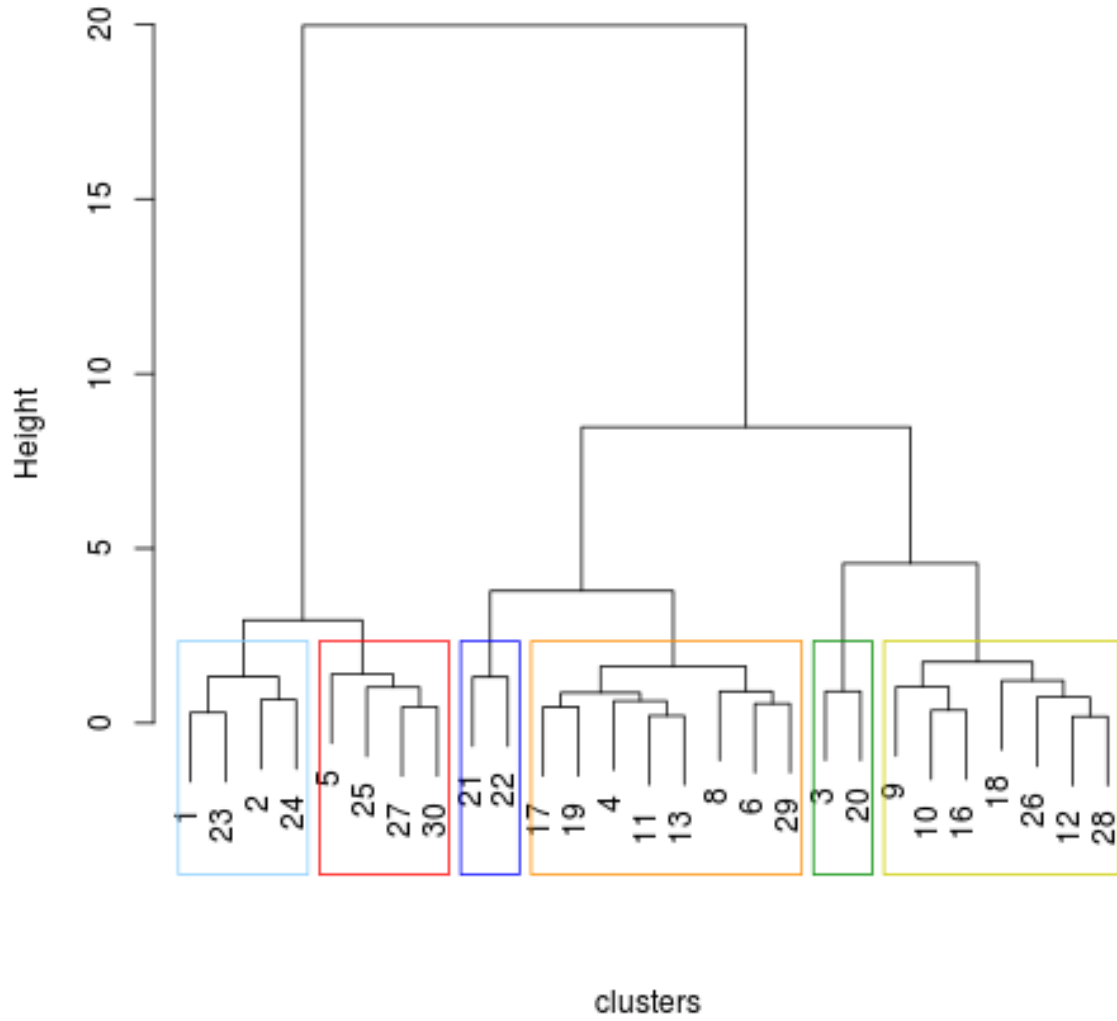
Figure A.12: a dendrogram from the Ward clustering analysis. The inputs to this clustering were: daily average, daily minimum, and daily maximum air temperature. There were 6 clusters identified. Light blue = PT-1$_{[R\text{-}M\,|\,W\text{-}H]}$, green = PT-2$_{[R\text{-}H\,|\,W\text{-}L]}$, orange = PT-3$_{[R\text{-}H\,|\,W\text{-}M]}$, red = PT-4$_{[R\text{-}L\,|\,W\text{-}H]}$, yellow = PT-5$_{[R\text{-}M\,|\,W\text{-}L]}$, and blue = PT-6$_{[R\text{-}L\,|\,R\text{-}L]}$.
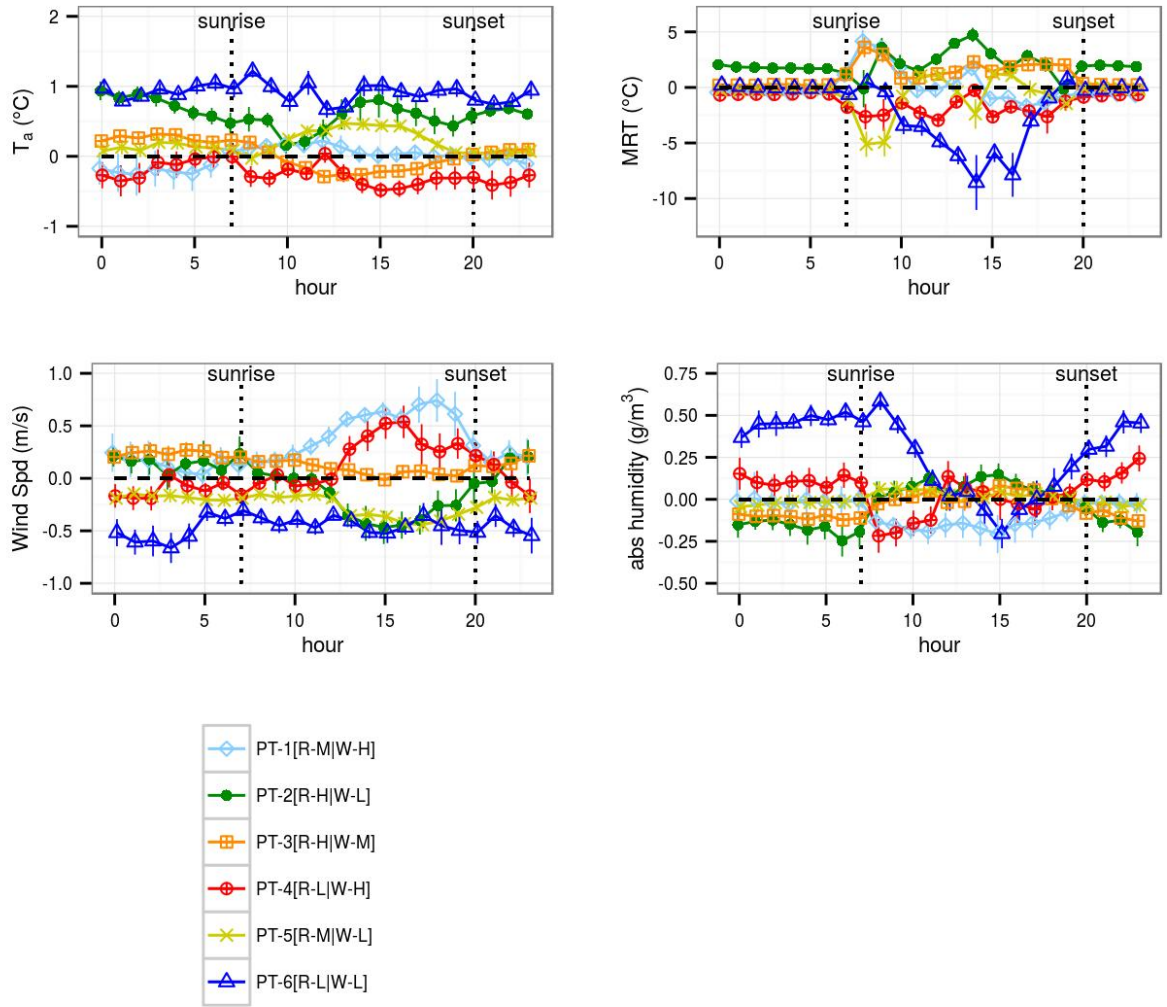
Figure A.13: The variability of meteorological variables by PET cluster.
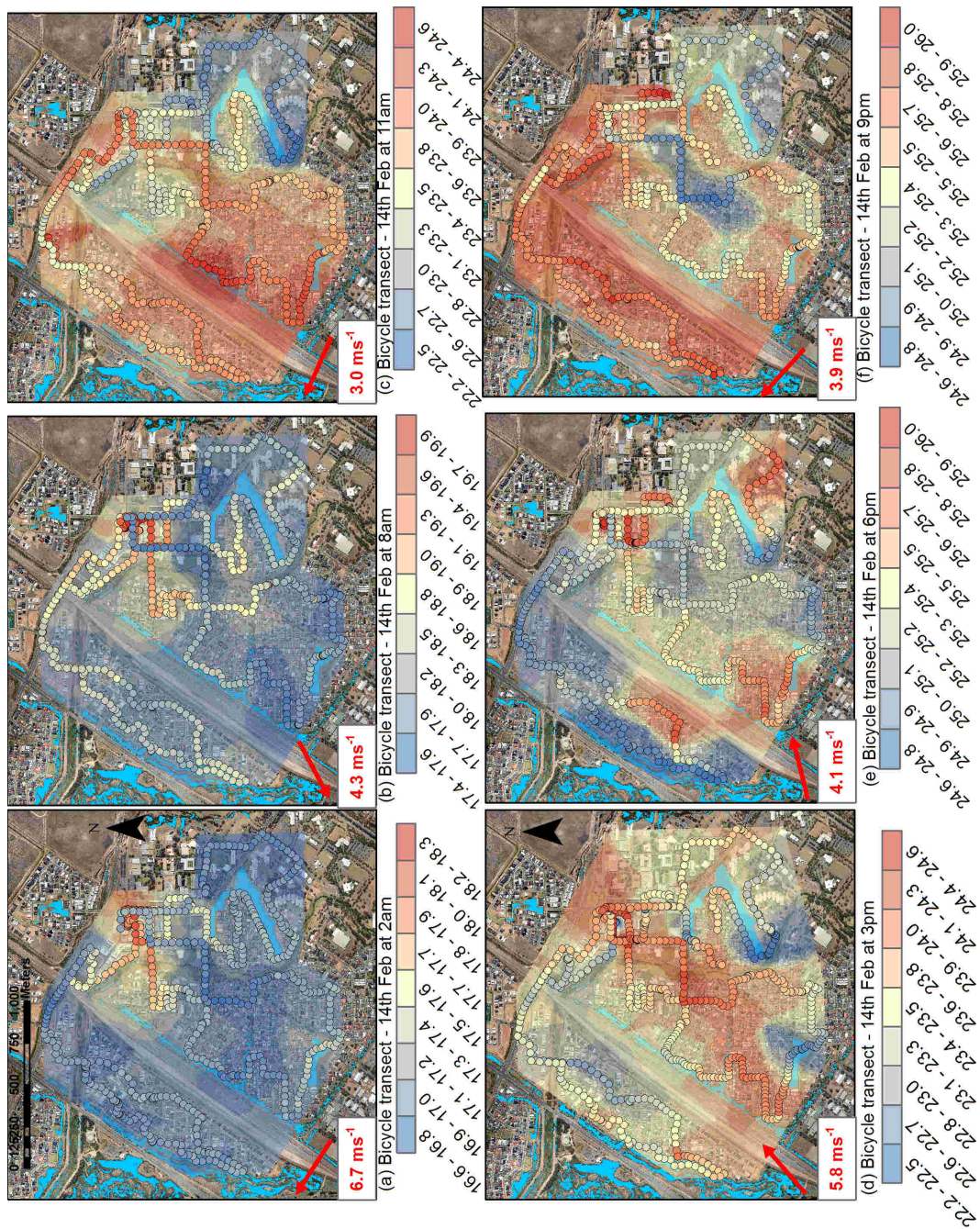
Figure A.14: An overview of all bicycle transects recorded on the 14th February.

231
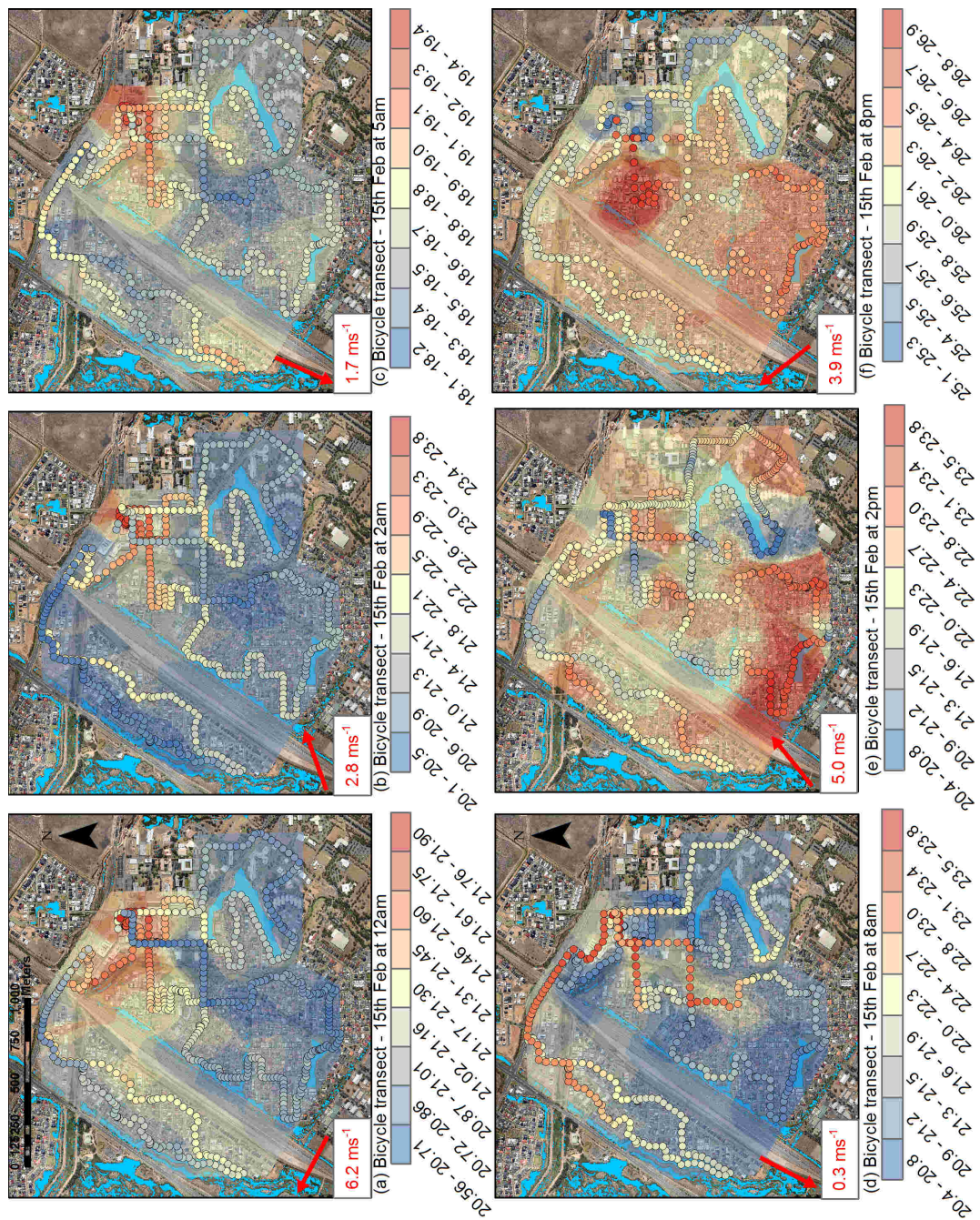
Figure A.15: An overview of all bicycle transects recorded on the 15th February.
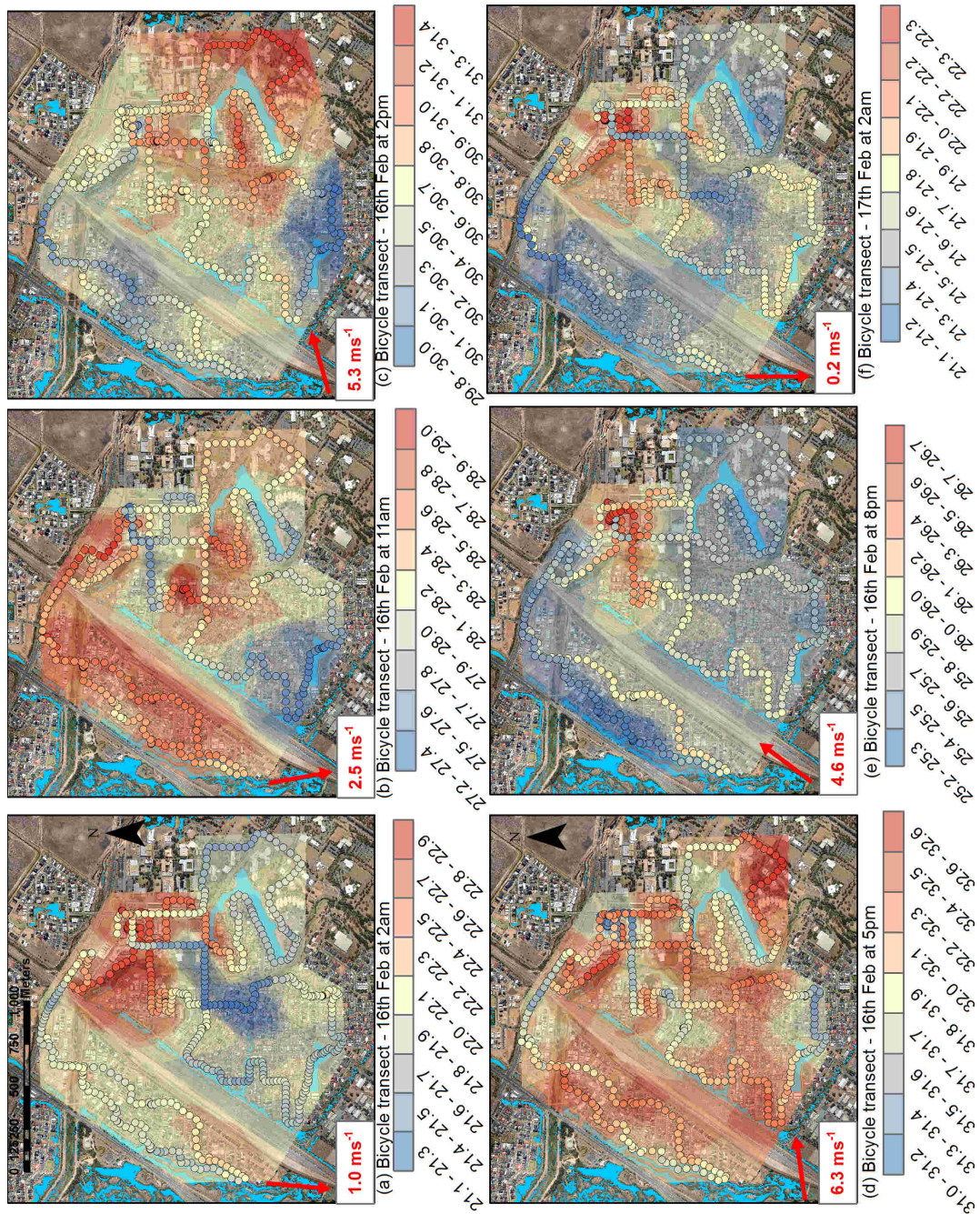
Figure A.16: An overview of all bicycle transects recorded on the 16th February.

(a) Static stations average vapour pressure at 3 pm

absolute humidity (gm^{-3})

(b) Static stations average vapour pressure at 3 am

absolute humidity (gm^{-3})
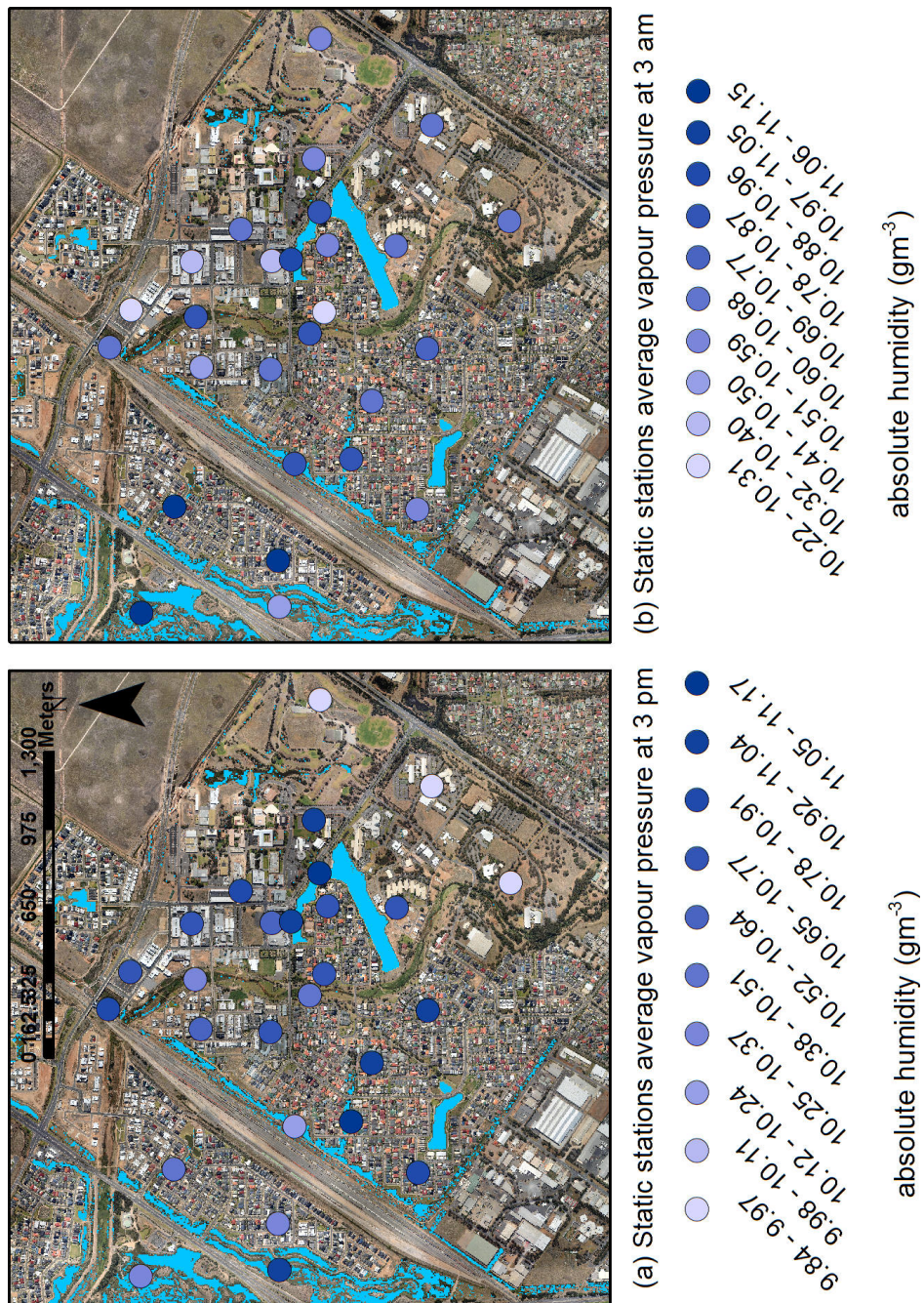
Figure A.17: The average vapour pressure for static AWS sites at (a) 3 pm and (b) 3 am.

234
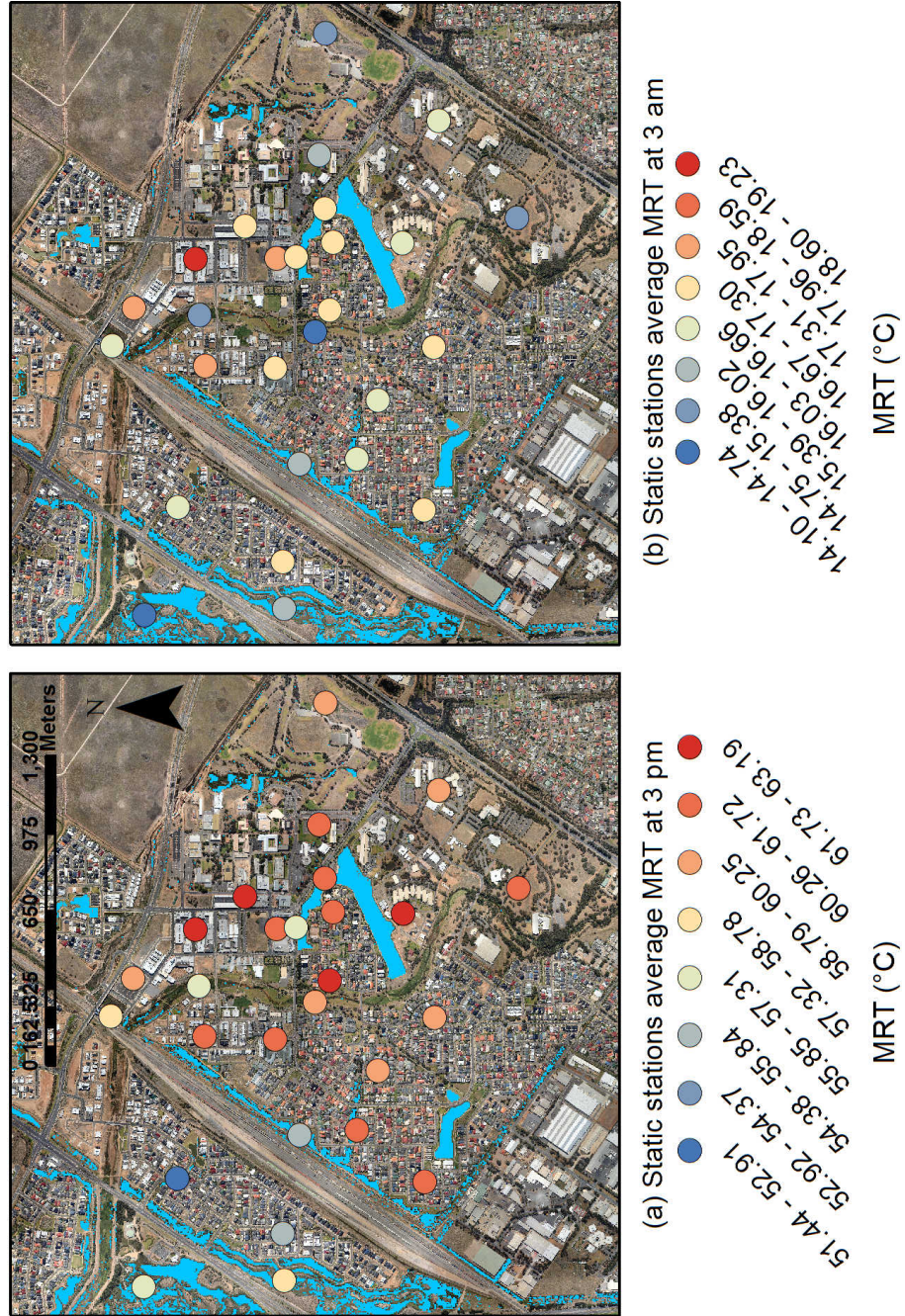
Figure A.18: The average MRT for static AWS sites at (a) 3 pm and (b) 3 am.

Table A.1: The statistical values from the SURFEX validation: average modelled 3 m air temperature vs observed 3 m air temperature for static AWS clusters using 50 m resolution.

Category	σ_o	σ_m	r^2	MAE	$RMSE$	$RMSE_u$	$RMSE_s$	Δ_{o-m} max	Δ_{o-m} min	Δ_{o-m} 3pm	Δ_{o-m} 3am
				(°C)	(°C)	(°C)	(°C)	(°C)	(°C)	(°C)	(°C)
TA-1[Urb+Wtr]	3.7	4.0	0.99	0.0	0.6	0.5	0.2	-0.5	0.8	-0.4	-0.4
TA-2[Mxd+Wtr]	3.5	3.8	0.99	0.0	0.6	0.5	0.3	-0.6	1.2	-0.6	-0.2
TA-3[Urb+Mid]	3.9	4.2	0.99	0.8	1.0	0.6	0.8	0.5	1.7	0.7	0.3
TA-4[Urb+Res]	3.9	4.2	0.99	0.2	0.7	0.5	0.4	-0.3	1.2	-0.2	-0.1
TA-5[Nat+Grs]	4.2	4.0	0.99	0.2	0.8	0.7	0.3	0.0	0.1	0.1	-0.9
TA-6[outlier]	4.0	3.4	0.97	0.9	1.5	0.9	1.2	-0.2	-0.1	-0.1	-2.0

o = observations

m = model

MAE = mean absolute error

$RMSE$ = root mean square error

$RMSE_u$ = unsystematic root meant square error

$RMSE_s$ = systematic root meant square error

Δ_{o-m} = difference between observed and modelled

Figure A.19: The average modelled (line) vs observed (bars) 3 m air temperature during intensive observational period, grouped by air temperature cluster (Figure 5.1): (a) TA-1$_{[Urb+Wtr]}$, (b) TA-2$_{[Mad+Wtr]}$, (c) TA-3$_{[Urb+Mid]}$, (d) TA-4$_{[Urb+Res]}$, (e) TA-5$_{[Nat+Grs]}$, (f) TA-6$_{[outlier]}$. T_a = air temperature. In these simulations a 50 m radius was used — results were very similar to the 25 m resolution simulation, with a minor degradation in performance.

Table A.2: The statistical values from the SURFEX validation: average modelled 3 m air temperature vs observed 3 m air temperature for static AWS clusters using 100 m resolution.

Category	σ_o	σ_m	r^2	MAE	$RMSE$	$RMSE_u$	$RMSE_s$	Δ_{o-m} max	Δ_{o-m} min	Δ_{o-m} 3pm	Δ_{o-m} 3am
				(°C)	(°C)	(°C)	(°C)	(°C)	(°C)	(°C)	(°C)
TA-1[Urb+Wtr]	3.7	4.0	0.99	0.1	0.7	0.5	0.4	-0.8	0.8	-0.7	-0.3
TA-2[Mxd+Wtr]	3.5	3.8	0.99	0.1	0.7	0.5	0.5	-0.8	1.0	-0.8	-0.2
TA-3[Urb+Mid]	3.9	4.2	0.99	0.8	1.0	0.6	0.9	0.6	1.7	0.7	0.4
TA-4[Urb+Res]	3.9	4.2	0.99	0.2	0.6	0.6	0.3	-0.2	0.8	-0.1	-0.1
TA-5[Nat+Grs]	4.2	4.0	0.98	0.2	0.8	0.7	0.5	0.3	0.2	0.4	-1.1
TA-6[outlier]	4.0	4.2	0.98	1.1	1.4	0.8	1.1	-1.6	-0.1	-1.5	-1.7

o = observations
m = model
MAE = mean absolute error
$RMSE$ = root mean square error
$RMSE_u$ = unsystematic root meant square error
$RMSE_s$ = systematic root meant square error
Δ_{o-m} = difference between observed and modelled
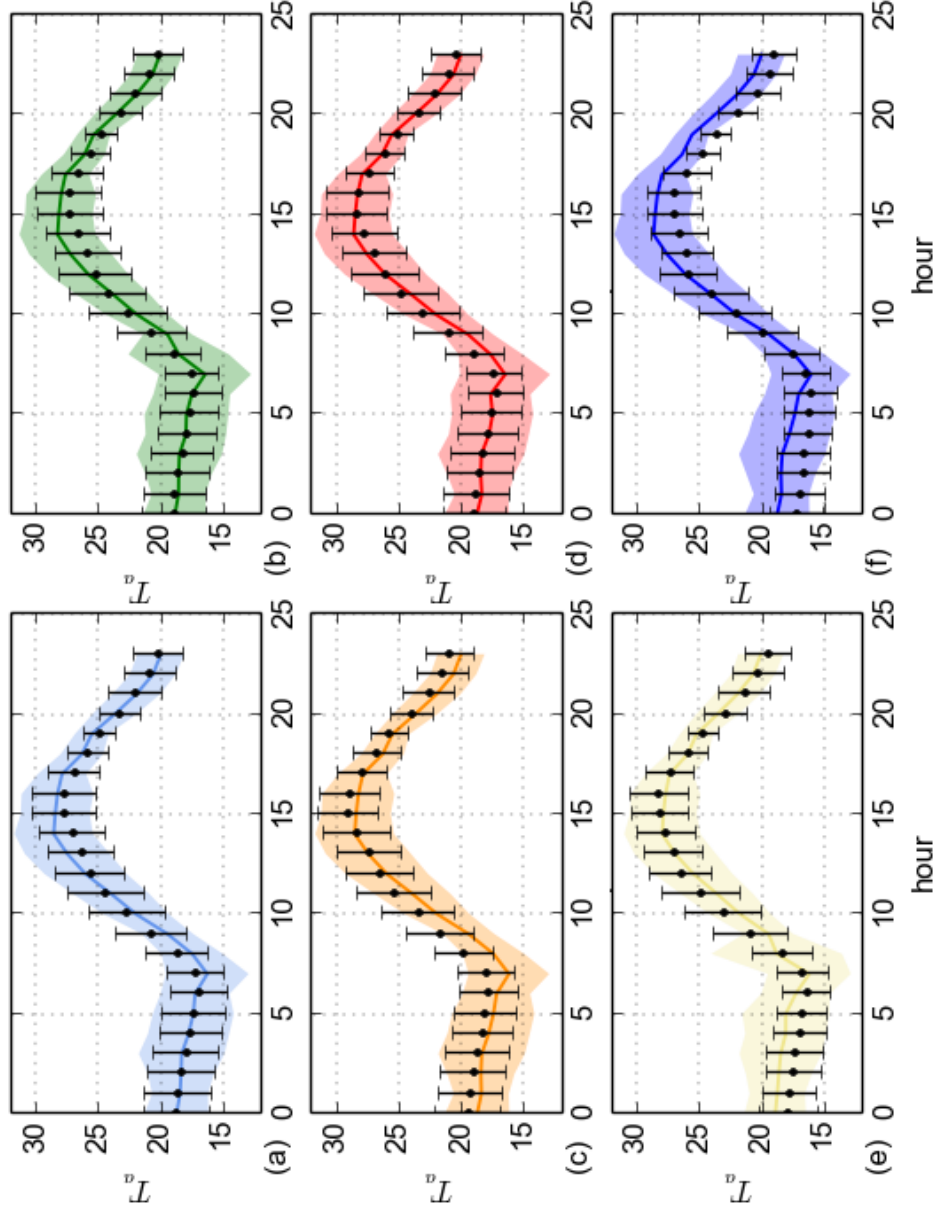
Figure A.20: The average modelled (line) vs observed (bars) 3 m air temperature during intensive observational period, grouped by air temperature cluster (Figure 5.1): (a) TA-1$_{[Urb+Wtr]}$, (b) TA-2$_{[Mad+Wtr]}$, (c) TA-3$_{[Urb+Mad]}$, (d) TA-4$_{[Urb+Res]}$, (e) TA-5$_{[Nat+Grs]}$, (f) TA-6$_{[outlier]}$. T_a= air temperature. In these simulations a 100 m radius was used — results were very similar to the 25 m resolution simulation, with a minor degradation in performance.

Table A.3: *The statistical values from the SURFEX validation: average modelled 3 m air temperature vs observed 3 m air temperature for static AWS clusters using 50 m resolution.*

Category	σ_o	σ_m	r^2	MAE (°C)	RMSE (°C)	$RMSE_u$ (°C)	$RMSE_s$ (°C)	Δ_{o-m} max (°C)	Δ_{o-m} min (°C)	Δ_{o-m} 3pm (°C)	Δ_{o-m} 3am (°C)
TA-1[Urb+Wtr]	3.7	4.0	0.99	0.1	0.7	0.5	0.4	-0.8	0.8	-0.7	-0.3
TA-2[Mxd+Wtr]	3.5	3.9	0.99	0.1	0.7	0.5	0.5	-0.8	1.0	-0.8	-0.2
TA-3[Urb+Mid]	3.9	4.2	0.99	-0.8	1.0	0.6	0.8	0.6	1.7	0.7	0.3
TA-4[Urb+Res]	3.9	4.2	0.99	0.2	0.7	0.5	0.4	-0.3	1.2	-0.2	-0.1
TA-5[Nat+Grs]	4.2	4.0	0.99	0.2	0.8	0.7	0.3	0.0	0.1	0.1	-0.9
TA-6[outlier]	4.0	3.4	0.97	0.9	1.5	0.9	1.2	-0.2	0.1	-0.1	-2.0

o = observations
m = model
MAE = mean absolute error
$RMSE$ = root mean square error
$RMSE_u$ = unsystematic root meant square error
$RMSE_s$ = systematic root meant square error
Δ_{o-m} = difference between observed and modelled

Figure A.21: The average wind speed for static AWS sites at (a) 3 pm and (b) 3 am.
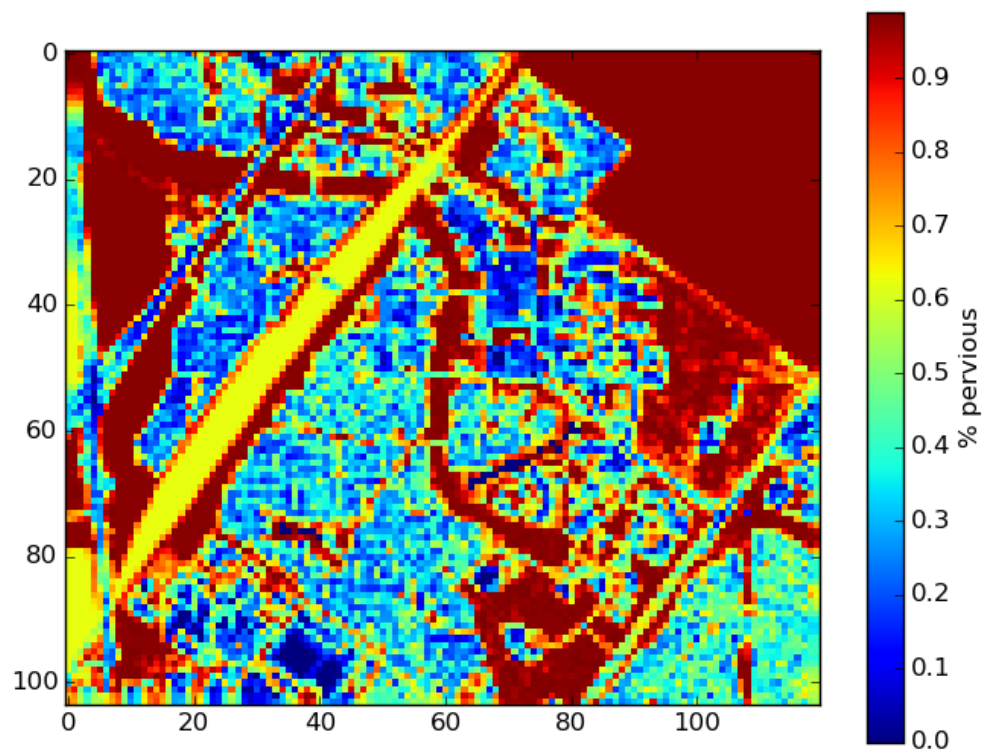
Figure A.22: The percentage of pervious surfaces in the Mawson Lakes SURFEX domain.
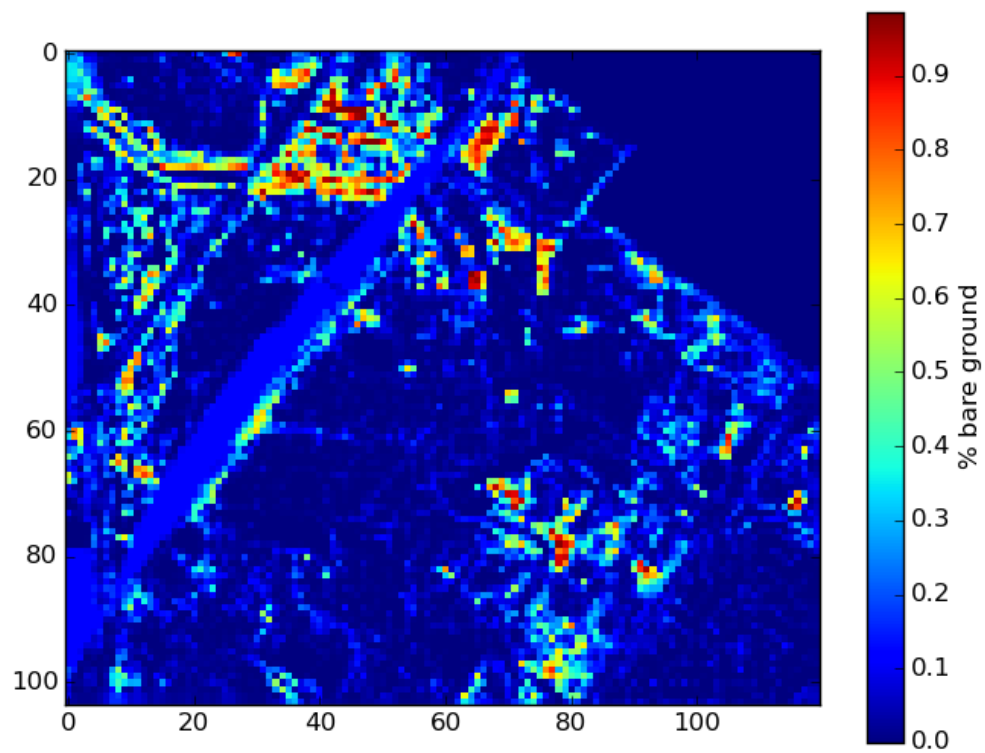
Figure A.23: The percentage of bare ground in the Mawson Lakes SURFEX domain.
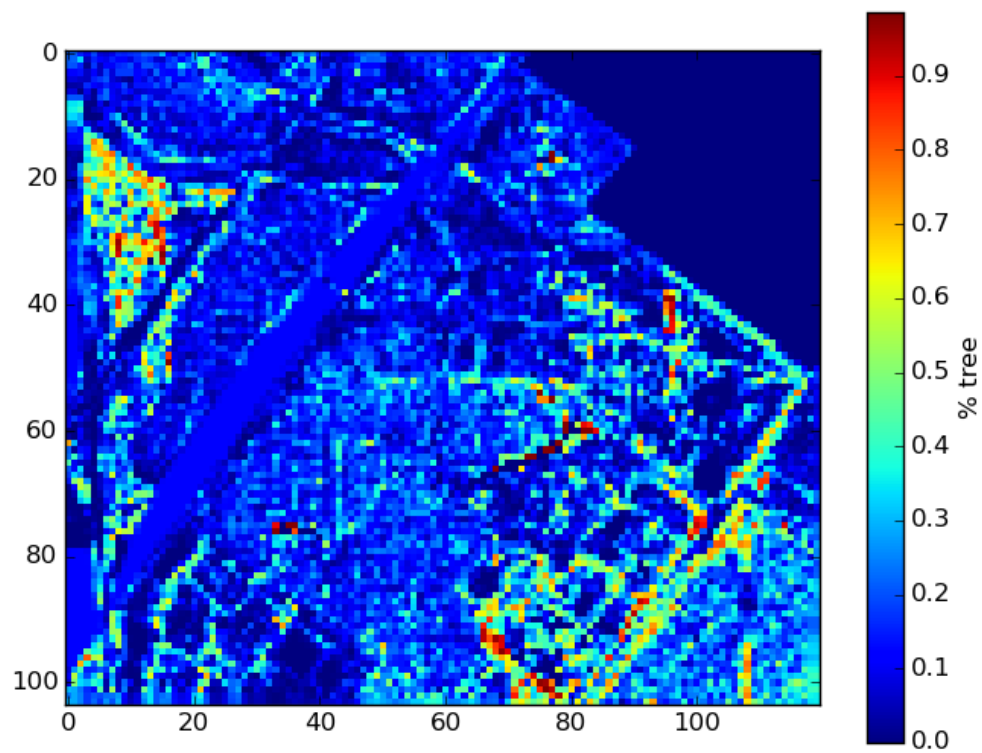
Figure A.24: The percentage of trees in the Mawson Lakes SURFEX domain.
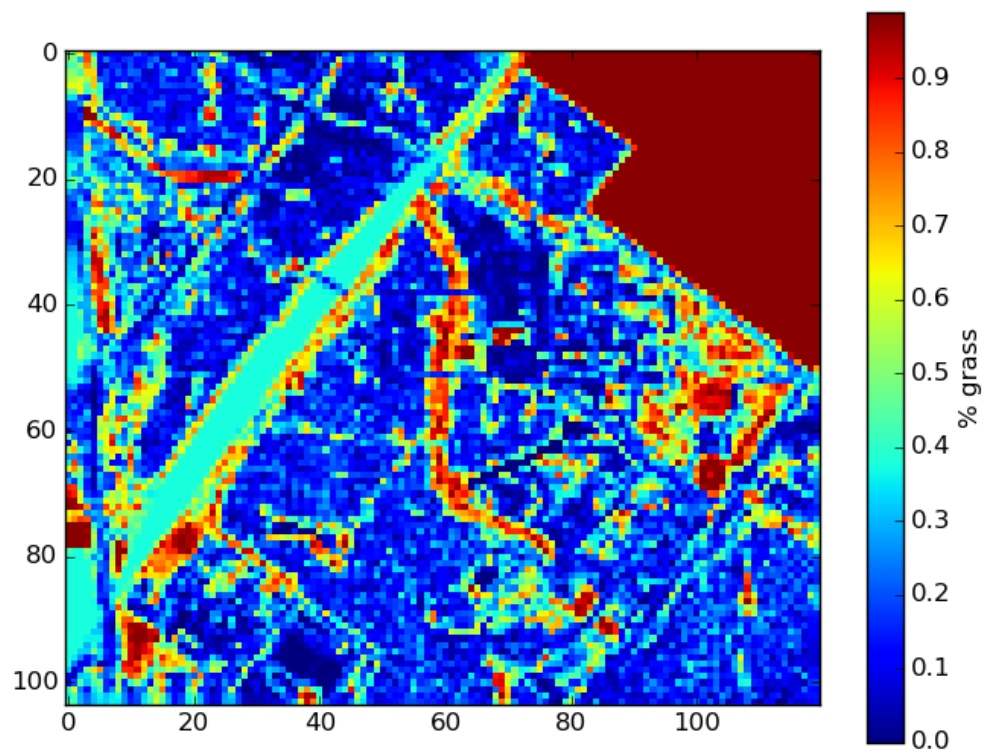
Figure A.25: The percentage of grass in the Mawson Lakes SURFEX domain.
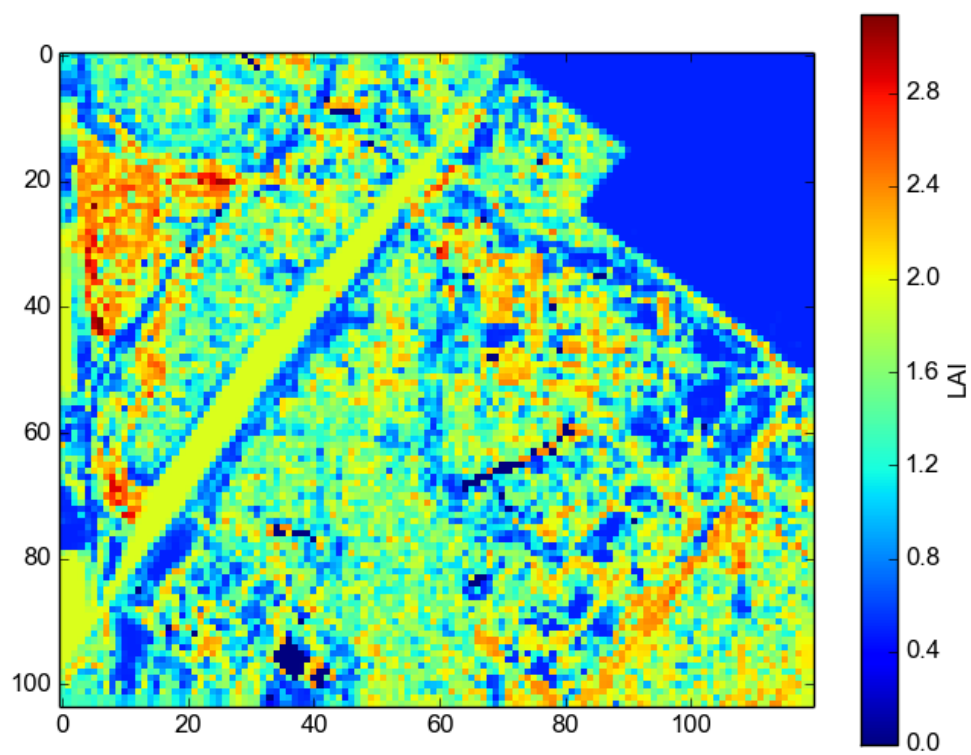
Figure A.26: The LAI in the Mawson Lakes SURFEX domain.
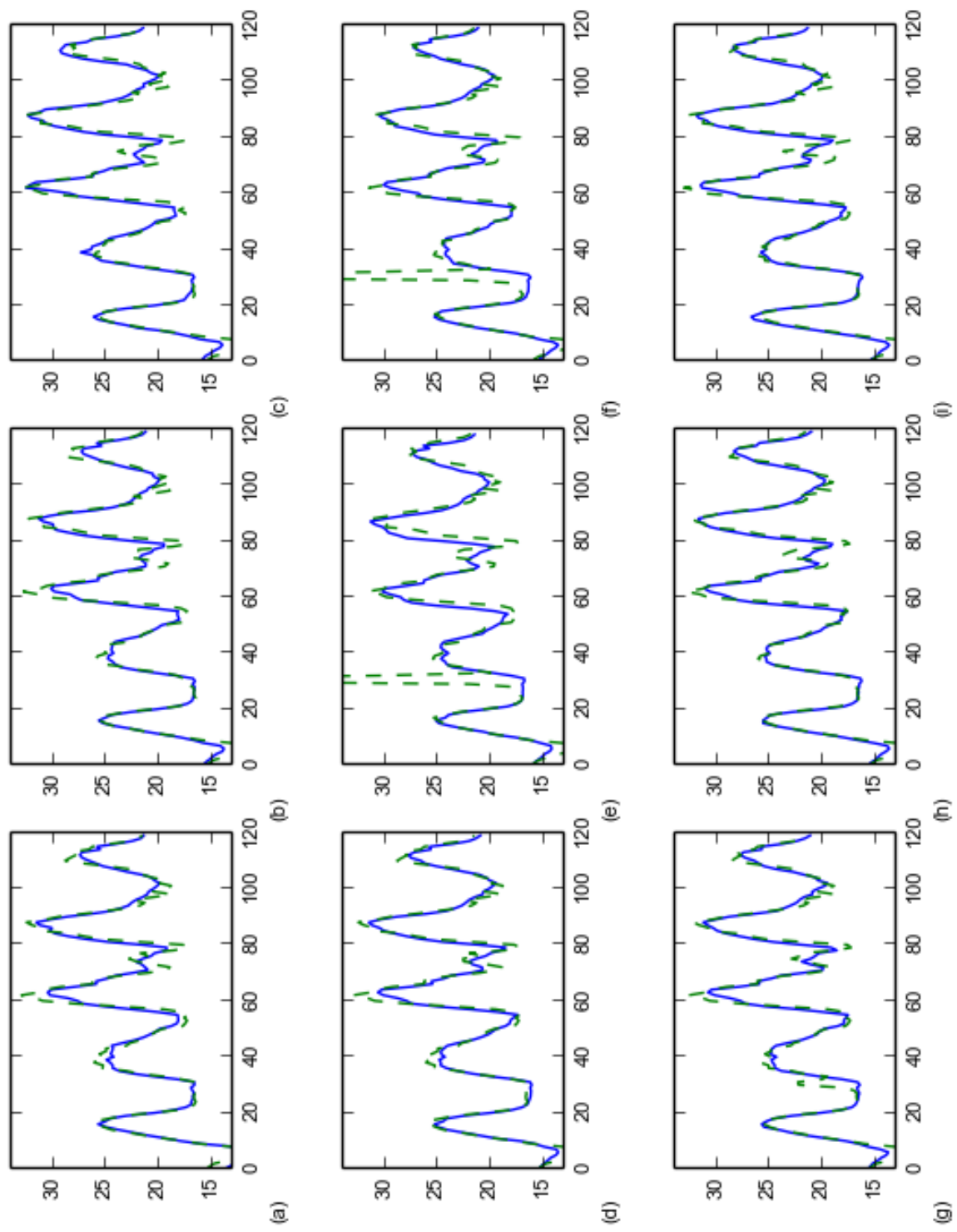
Figure A.27: Hourly average simulated 3 m air temperature (dashed) vs observed 3 m air temperature (line) for the intensive observational period: (a) station 1, (b) station 2, (c) station 3, (d) station 4, (e) station 5, (f) station 6, (g) station 8, (h) station 9, and station 10.
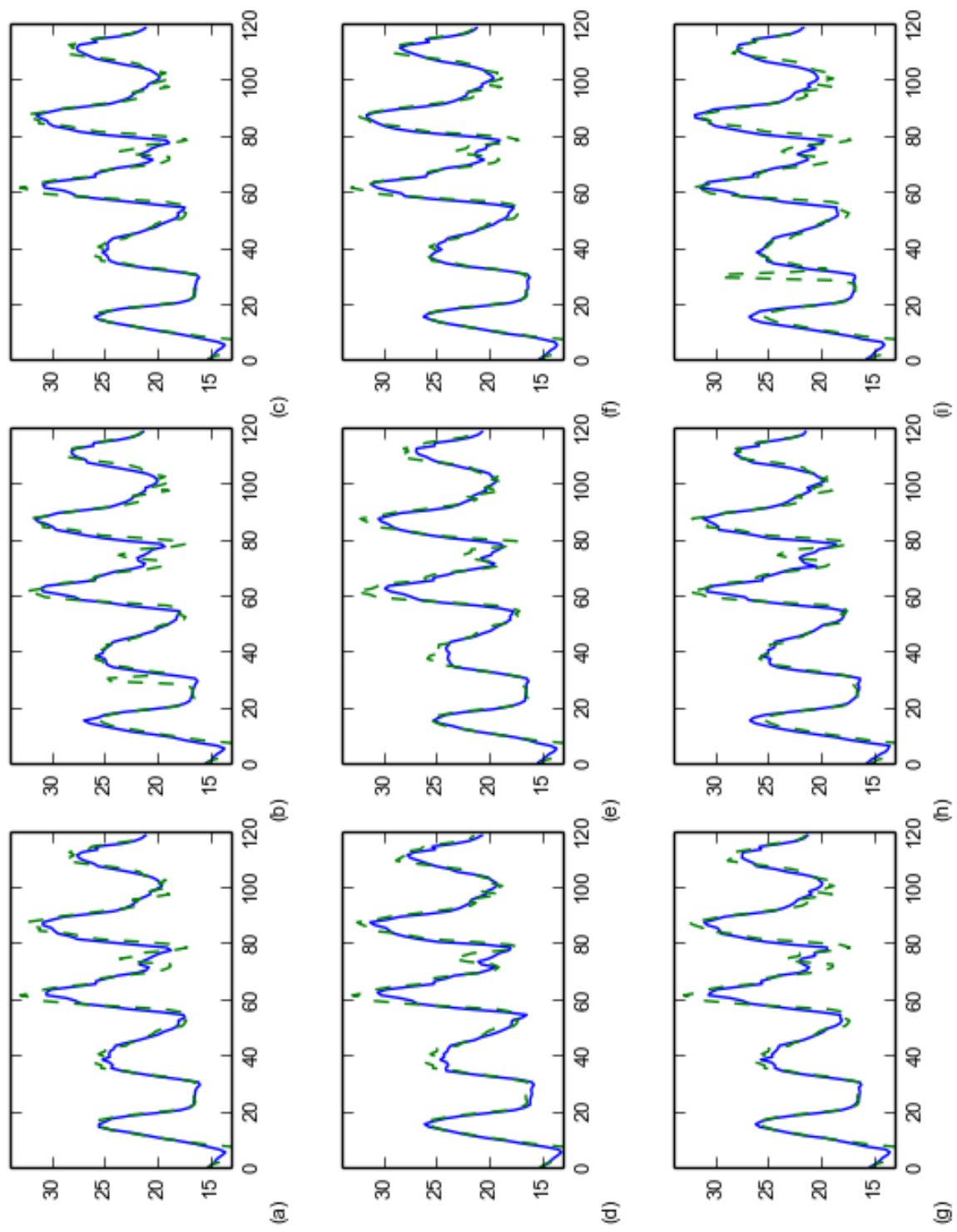
Figure A.28: Hourly average simulated 3 m air temperature (dashed) vs observed 3 m air temperature (line) for the intensive observational period: (a) station 11, (b) station 12, (c) station 13, (d) station 16, (e) station 17, (f) station 18, (g) station 19, (h) station 20, and station 21.
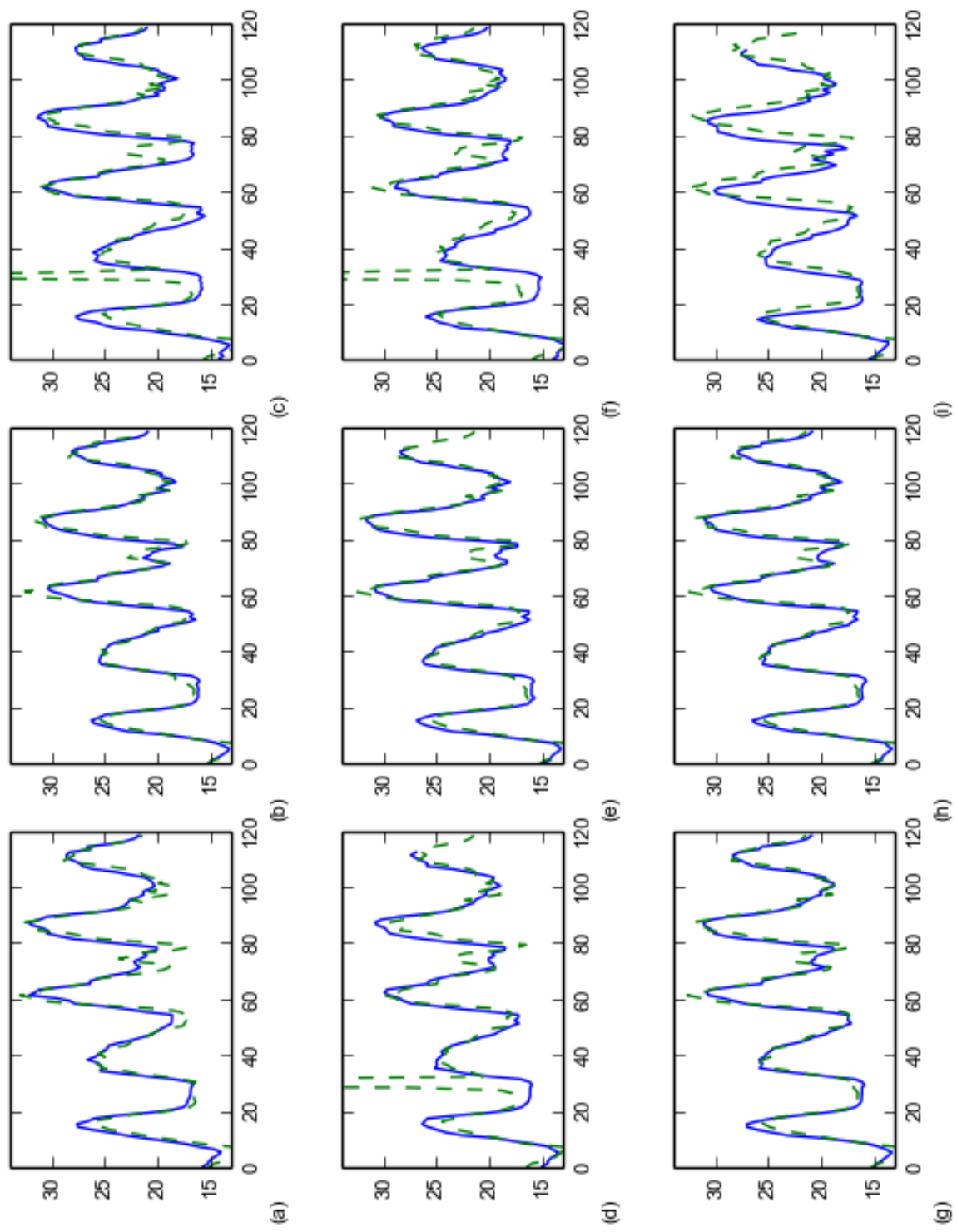
Figure A.29: Hourly average simulated 3 m air temperature (dashed) vs observed 3 m air temperature (line) for the intensive observational period: (a) station 22, (b) station 23, (c) station 24, (d) station 25, (e) station 26, (f) station 27, (g) station 28, (h) station 29, and station 30.

249
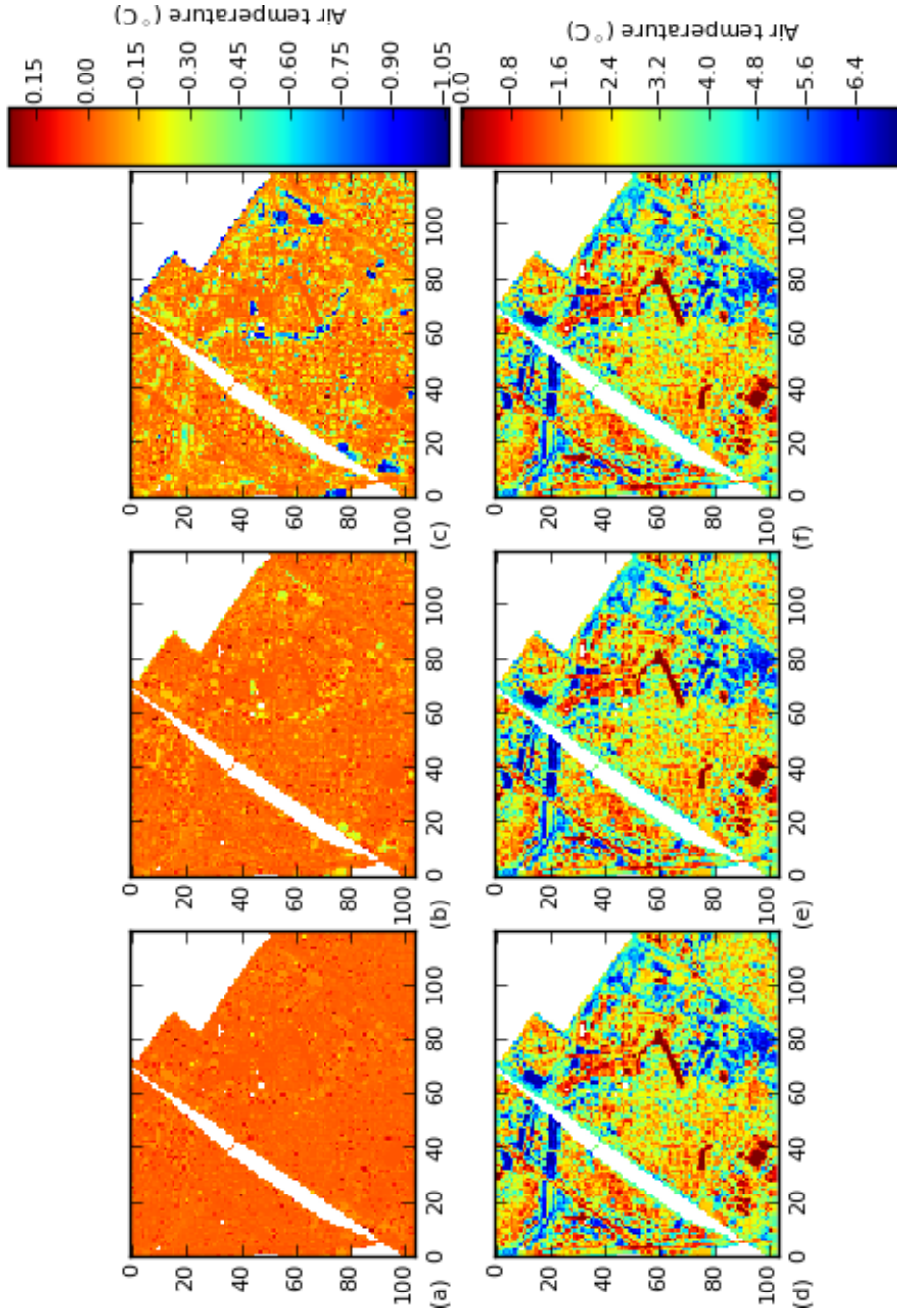
Figure A.30: A spatial representation of the heatwave average 3 am (top) and 3 pm (bottom) air temperature across the Mawson Lakes domain for daytime (6 hour) irrigation scenarios: (a) average 3 am air temperature for Day_6Irr2.5L, (b) average 3 am air temperature for Day_6Irr5L, (c) average 3 am air temperature for Day_6Irr10L, (d) average 3 pm air temperature for Day_6Irr2.5L, (e) average 3 pm air temperature for Day_6Irr5L, and (f) average 3 pm air temperature for Day_6Irr10L.
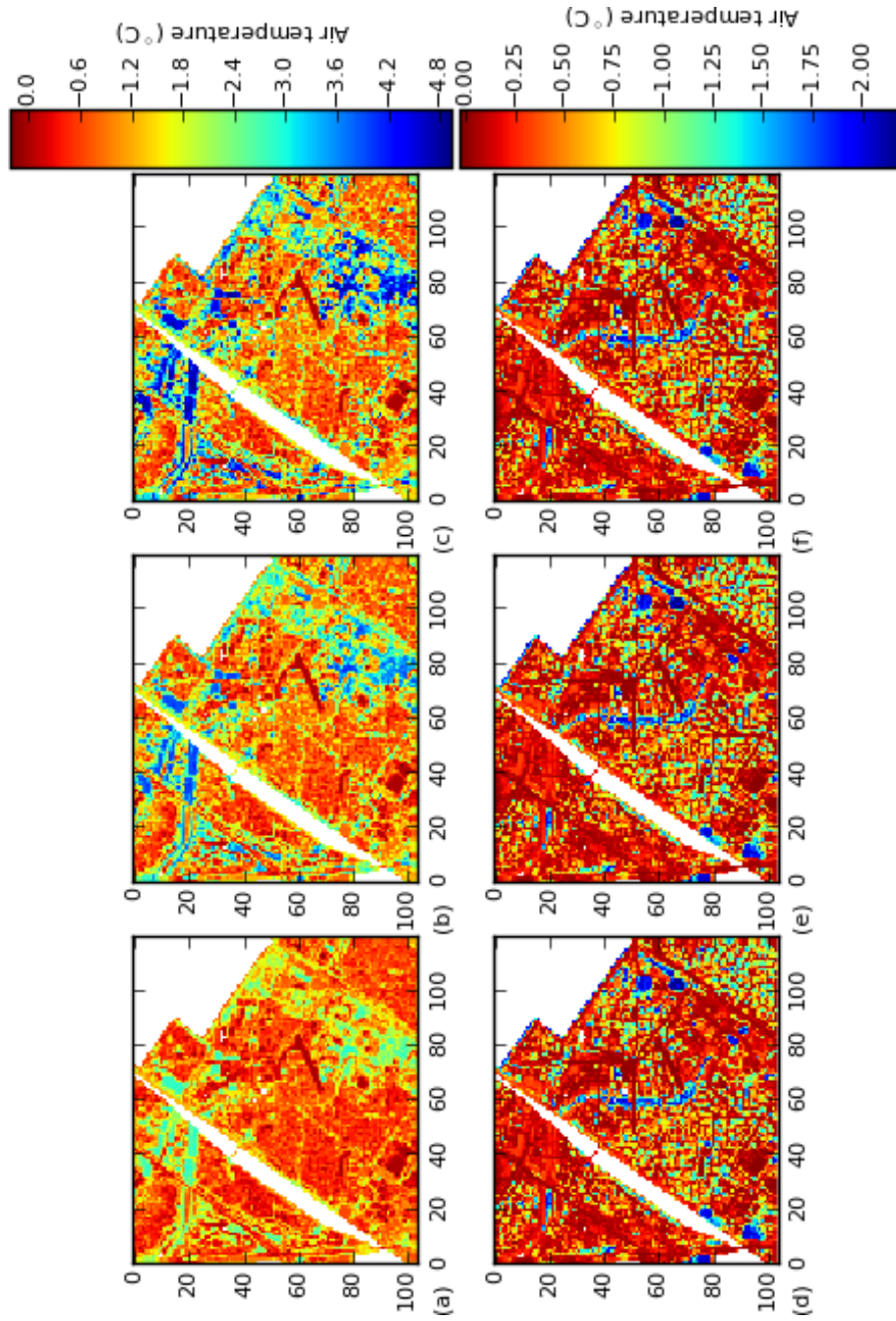
Figure A.31: A spatial representation of the heatwave average 3 am (top) and 3 pm (bottom) air temperature across the Mawson Lakes domain for nighttime (6 hour) irrigation scenarios: (a) average 3 am air temperature for Night_6Irr2.5L, (b) average 3 am air temperature for Night_6Irr5L, (c) average 3 am air temperature for Night_6Irr10L, (d) average 3 pm air temperature for Night_6Irr2.5L, (e) average 3 pm air temperature for Night_6Irr5L, and (f) average 3 pm air temperature for Night_6Irr10L.

Figure A.32: An overview of the proportion of the SURFEX domain that exceeded heat health thresholds during extremely hot conditions (28, 29, and 30 January 2009). Top: the percentage of the whole domain (Figure 7.1a) that exceeded the heat health threshold for: (a) continuous irrigation, (b) day irrigation, and (c) night irrigation. Bottom: the percentage of the residential areas (Figure 7.1b) that exceeded the heat health for (d) continuous irrigation, (e) day irrigation, and (f) night irrigation.

252

Figure A.33: The diurnal average absolute humidity, during the heatwave period, associated with different irrigation regimes for three case study sites: (a) station 13, (b) station 20, (c) station 23, and (d) average PET across the three case study sites. Station 13 was a residential urban site, station 20 was a more urbanised site, and station 23 was an open grassy site.

References

ABS (2014). Australian Bureau of Statistics — Regional Population Growth.

URL http://asb.gov.au

Ahmad, S. A. (1992). Some effects of urban parks on air temperature variations in Kuala Lumpur, Malaysia. In *Tohwa University International Symposium, CUTEST'92*.

Alcoforado, M.-J., Andrade, H., Lopes, A., & Vasconcelos, J. (2009). Application of climatic guidelines to urban planning. *Landscape and Urban Planning*, *90*(1-2), 56–65.

URL http://www.sciencedirect.com/science/article/pii/S0169204608001746

Alexander, L. V., & Arblaster, J. M. (2009). Assessing trends in observed and modelled climate extremes over Australia in relation to future projections. *International Journal of Climatology*, *29*(3), 417–435.

Ali-Toudert, F., Djenane, M., Bensalem, R., & Mayer, H. (2005). Outdoor thermal comfort in the old desert city of Beni-Isguen, Algeria. *Climate Research*, *28*(3), 243–256.

URL http://www.researchgate.net/publication/238451639{_}Outdoor{_}thermal{_}comfort{_}in

Ali-Toudert, F., & Mayer, H. (2006a). Numerical study on the effects of aspect ratio and orientation of an urban street canyon on outdoor thermal comfort in hot and dry climate. *Building and Environment*, *41*(2), 94–108.

URL http://www.sciencedirect.com/science/article/pii/S0360132305000120

Ali-Toudert, F., & Mayer, H. (2006b). Thermal comfort in an eastwest oriented street canyon in Freiburg (Germany) under hot summer conditions. *Theoretical and Applied Climatology*, *87*(1-4), 223–237.

URL http://link.springer.com/10.1007/s00704-005-0194-4

Ali-Toudert, F., & Mayer, H. (2007). Effects of asymmetry, galleries, overhanging façades and vegetation on thermal comfort in urban street canyons. *Solar Energy*, *81*(6), 742–754.

URL `http://www.sciencedirect.com/science/article/pii/S0038092X06002623`

Arnfield, A. (1990). Street design and urban canyon solar access. *Energy and Buildings*, *14*(2), 117–131.

URL `http://www.sciencedirect.com/science/article/pii/037877889090031D`

Ashie, Y., Ca, V. T., & Asaeda, T. (1999). Building canopy model for the analysis of urban climate. *Journal of Wind Engineering and Industrial Aerodynamics*, *81*, 237–248.

ASHRAE (1992). ASHRAE Standard 55 -1992: Thermal environmental conditions for human occupancy. Tech. rep., American Society for heating, Refrigerating and Air conditioning Engineers, Atlanta, USA.

Auliciems, A., & Skinner, J. L. (1989). Cardiovascular deaths and temperature in subtropical Brisbane. *International Journal of Biometeorology*, *33*, 215–221.

Balling, R. C., & Brazel, S. W. (1989). High-Resolution Nighttime Temperature Patterns in Phoenix. *Journal of the Arizona-Nevada Academy of Science*, *23*(1), 49–56.

Barradas, V. L. (1991). Air temperature and humidity and human comfort index of some city parks of Mexico City. *International Journal of Biometeorology*, *35*, 24–28.

Best, M. J., & Grimmond, C. (2014). How does the representation of vegetation within a urban land surface model influence the distribution of energy between the sensible and latent heat fluxes over a number of sites with varying land cover? In *11th Symposium on the Urban Environment*. Atlanta, USA.

BOM (2013). Bureau of Meteorology Climate Statistics.

URL `http://www.bom.gov.au/climate/averages`

BOM (2014). The State of the Climate report. Tech. rep., Bureau of Meterology.

Bonan, G. B. (2000). The microclimates of a suburban Colorado (USA) landscape and implications for planning and design. *Landscape and Urban Planning*, *49*, 97–114.

Bowler, D. E., Buyung-Ali, L., Knight, T. M., & Pullin, A. S. (2010). Urban greening to cool towns and cities: A systematic review of the empirical evidence. *Landscape and Urban Planning*, *97*, 147–155.

Breuer, L., Eckhardt, K., & Frede, H.-G. (2003). Plant parameter values for models in temperate climates. *Ecological Modelling*, *169*(2), 237–293.

Brücker, G. (2005). Vulnerable populations: lessons learnt from the summer 2003 heat waves in Europe. *Euro surveillance: bulletin Europeen sur les maladies transmissibles= European communicable disease bulletin*, *10*(7), 147.

Bruse, M., & Fleer, H. (1998). Simulating surfaceplantair interactions inside urban environments with a three dimensional numerical model. *Environmental Modelling & Software*, *13*(3-4), 373–384.
URL http://www.sciencedirect.com/science/article/pii/S1364815298000425

Buechley, R. W., Bruggen, J. V., & Truppi, L. E. (1972). Heat Island = Death Island? *Environmental Research*, *5*, 85–92.

Burns, M. J., Fletcher, T. D., Walsh, C. J., Ladson, A. R., & Hatt, B. E. (2012). Hydrologic shortcomings of conventional urban stormwater management and opportunities for reform. *Landscape and Urban Planning*, *105*(3), 230–240.
URL http://www.sciencedirect.com/science/article/pii/S016920461100363X

Buzan, J. R., Oleson, K., & Huber, M. (2015). Implementation and comparison of a suite of heat stress metrics within the Community Land Model version 4.5. *Geoscientific Model*

Development, *8*(2), 151–170.

URL `http://www.geosci-model-dev.net/8/151/2015/`

Champeaux, J. L., Masson, V., & Chauvin, F. (2005). ECOCLIMAP: a global database of land surface parameters at 1 km resolution. *Meteorological Applications*, *12*(1), 29–32.

URL `http://journals.cambridge.org/abstract{_}S1350482705001519`

Chen, F., Janić, Z., & Mitchell, K. (1997). Impact of atmospheric surface-layer parameterizations in the new land-surface scheme of the NCEP mesoscale ETA model. *Boundary Layer Meteorology*, *85*, 391–421.

Chen, Z., Zhao, L., Meng, Q., Wang, C., Zhai, Y., & Wang, F. (2009). Field measurements on microclimate in residential community in Guangzhou, China. *Frontiers of Architecture and Civil Engineering in China*, *3*, 462–468.

Chisense, C., Hahn, M., & Engels, J. (2011). Classification of roof materials using hyperspectral data. In *Proceedings Applied Geoinformatics for Society and Environment*.

Civerolo, K. L., Sistla, G., Rao, S. T., & Nowak, D. J. (2000). The effects of land use in meteorological modeling: implications for assessment of future air quality scenarios. *Atmospheric Environment*, *34*, 1615–1621.

Coates, L. (1996). An Overview of Fatalities from Some Natural Hazards in Australia. (p. 49).

URL `http://search.informit.com.au/documentSummary;dn=547566533577889;res=IELENG`

Conti, S., Meli, P., Minelli, G., Solimini, R., Toccaceli, V., Vichi, M., Beltrano, C., & Perini, L. (2005). Epidemiologic study of mortality during the Summer 2003 heat wave in Italy. *Environmental Research*, *98*, 390–399.

Coombes, P. J. (2008). The relative efficiency of water supply catchments and rainwater tanks in cities subject to variable climate and the potential for climate change. *Australian Journal of Water Resources*, *12*(2), 1—-16.

Costello, A., Abbas, M., Allen, A., Ball, S., Bell, S., Bellamy, R., Friel, S., Groce, N., Johnson, A., & Kett, M. (2009). Managing the health effects of climate change: lancet and University College London Institute for Global Health Commission. *The Lancet*, *373*(9676), 1693–1733.

Coutts, A., J, B., & Tapper, N. J. (2010). Changing Urban Climate and CO_2 Emissions: Implications for the Development of Policies for Sustainable Cities. *Urban Policy and Research*, *28*, 27–47.

Coutts, A. M., Beringer, J., & Tapper, N. J. (2007). Impact of Increasing Urban Density on Local Climate: Spatial and Temporal Variations in the Surface Energy Balance in Melbourne, Australia. *Journal of Applied Meteorology and Climatology*, *46*, 477–493.

Coutts, A. M., Tapper, N. J., Beringer, J., Loughnan, M., & Demuzere, M. (2012). Watering our cities: The capacity for Water Sensitive Urban Design to support urban cooling and improve human thermal comfort in the Australian context. *Progress in Physical Geography*, *36*, 1–27.

Coutts, A. M., White, E. C., Tapper, N. J., Beringer, J., & Livesley, S. J. (2015). Temperature and human thermal comfort effects of street trees across three contrasting street canyon environments. *Theoretical and Applied Climatology*.
URL `http://link.springer.com/10.1007/s00704-015-1409-y`

CSIRO (2007). Climate change in Australia: technical report. Tech. rep., CSIRO & Bureau of Meteorology.

CWSC (2010). Project 3: green cities and microclimate — literature review. Tech. rep., {C}entre for {W}ater {S}ensitive {C}ities.

de Munck, C. (2013). Modélisation de la végétation urbaine et stratégies d'adaptation pour l'amélioration du confort climatique et de la demande énergétique en ville.
URL `http://ethesis.inp-toulouse.fr/archive/00002485/`

Demuzere, M., Coutts, A., Göhler, M., Broadbent, A., Wouters, H., van Lipzig, N., & Gebert, L. (2014). The implementation of biofiltration systems, rainwater tanks and urban irrigation in a single-layer urban canopy model. *Urban Climate*, *10*, 148–170.
URL `http://www.researchgate.net/publication/268448888{_}The{_}implementation{_}of{_}biof`

Diem, J. E., & Brown, D. P. (2008). Anthropogenic Impacts on Summer Precipitation in Central Arizona, U.S.A. *The Professional Geographer*.
URL `http://www.tandfonline.com/doi/abs/10.1111/0033-0124.5503011`

Dousset, B. (1989). AVHRR-derived cloudiness and surface temperature patterns over the Los Angeles area and their relationship to land use. In *Proceedings of IGARSS-89*.

DIppoliti, D., Michelozzi, P., Marino, C., Menne, B., Cabre, M. G., Katsouyanni, K., Medina, S., Paldy, A., Anderson, H. R., & Ballester, F. (2008). The Impact of Heat Waves on Mortality in 9 European Cities, 19902004. *Epidemiology*, *19*(6), S286–S287.

Erell, E., Eliasson, I., Grimmond, C. S. B., Offerle, B., & Williamson, T. (2010). The effect pf stability on estimated variations of advected moisture in the canyon air temperature (CAT) model. In *Ninth Symposium on the Urban Environment*.

Flesch, T. K., Wilson, J. E., & Yee, E. (1995). Backward-Time Langrangian Stochastic Dispersion Models and their Application to Estimate Gaseous Emissions. *Journal of Applied Meteorology*, *34*, 1320–1332.

Fouillet, A., Rey, G., Laurent, F., Pavillon, G., Bellec, S., Guihenneuc-Jouyaux, C., Clavel, J.,

Jougla, E., & Hémon, D. (2006). Excess mortality related to the August 2003 heat wave in France. *International archives of occupational and environmental health*, *80*(1), 16–24.

Gaitani, N., Mihalakakou, G., & Santamouris, M. (2007). On the use of bioclimatic architecture principles in order to improve thermal comfort conditions in outdoor spaces. *Building and Environment*, *42*(1), 317–324.

URL `http://www.sciencedirect.com/science/article/pii/S0360132305003409`

Georgi, J. N., & Dimitriou, D. (2010). The contribution of urban green spaces to the improvement of environment in cities: Case study of Chania, Greece. *Building and Environment*, *45*(6), 1401–1414.

URL `http://www.sciencedirect.com/science/article/pii/S0360132309003564`

Gober, P., Brazel, A. J., Quay, R., Myint, S., Grossman-Clarke, S., Miller, A., & Rossi, S. (2010). Using Watered Landscapes to Manipulate Urban Heat Island Effects. *Journal of the American Planning Association*, *76*, 109–121.

Goldbach, A., & Kuttler, W. (2013). Quantification of turbulent heat fluxes for adaptation strategies within urban planning. *International Journal of Climatology*, *33*(1), 143–159.

URL `http://doi.wiley.com/10.1002/joc.3437`

Goward, S. N., Markham, B., Dye, D. G., Dulaney, W., & Yang, J. (1991). Normalized difference vegetation index measurements from the advanced very high resolution radiometer. *Remote Sensing of Environment*, *35*, 257–277.

Grimmond, C. S. B. (1988). *An evaporatranspiration-interception model for urban areas*. Ph.D. thesis, University of British Columbia.

Grimmond, C. S. B., Blackett, M., Best, M. J., Baik, J. J., Belcher, S. E., Beringer, J., Bohnenstengel, S. I., Calmet, I., Chen, F., Coutts, A., Dandou, A., Fortuniak, K., Gouvea, M. L.,

Hamdi, R., Hendry, M., Kanda, M., Kawai, T., Kawamoto, Y., Kondo, H., Krayenhoff, E. S., Lee, S.-H., Loridan, T., Martilli, A., Masson, V., Miao, S., Oleson, K., Ooka, R., Pigeon, G., Porson, A., Ryu, Y. H., Salamanca, F., Steeneveld, G. J., Tombrou, M., Voogt, J. A., Young, D. T., & Zhang, N. (2011). Initial results from Phase 2 of the international urban energy balance model comparison. *International Journal of Climatology*, *31*, 244–272.

Grimmond, C. S. B., M, B., amd J. Barlow, M. J. B., Baik, J. J., Belcher, S. E., Bohnenstengel, S. I., Calmet, I., amd A. Dandou, F. C., Fortuniak, K., Gouvea, M. L., Hamdi, R., Hendry, M., Kawai, T., Kawamoto, Y., Kondo, H., Krayenhoff, E. S., Lee, S. H., Loridan, T., Martilli, A., Masson, V., Miao, S., Oleson, K., Pigeon, G., Porson, A., Ryu, Y. H., Salamanca, F., Shashua-Bar, L., Steeneveld, G. J., Tombrou, M., Voogt, J., Young, D., & Zhang, N. (2010). The International Urban Energy Balance Models Comparison Project: First Results from Phase 1. *Journal of Applied Meteorology and Climatology*, *49*, 1268–1292.

Grimmond, C. S. B., & Oke, T. R. (1991). An Evapotranspiration-Interception Model for Urban Areas. *Water Resources Research*, *27*, 1739–1755.

Grimmond, C. S. B., & Oke, T. R. (1995). Comparison of heat fluxes from summertime observations in the suburbs of four North American cities. *Journal of Applied Meteorolgy*, *34*, 873–889.

Grimmond, C. S. B., & Oke, T. R. (2002). Turbulent heat fluxes in urban areas: Observations and a Local-Scale Urban Meteorological Paramterization Scheme (LUMPS). *Journal of Applied Meteorology*, *41*, 792–810.

Grossman-Clarke, S., Zehnder, J. A., Loridan, T., & Grimmond, C. S. B. (2010). Contribution of Land Use Changes to Near-Surface Air Temperatures during Recent Summer Extreme Heat

Events in the Phoenix Metropolitan Area. *Journal of Applied Meteorology and Climatology*, *49*, 1649–1664.

Hajat, S., Kovats, R. S., Atkinson, R. W., & Haines, A. (2002). Impact of hot temperatures on death in London: a time series approach. *Journal of epidemiology and community health*, *56*(5), 367–372.

Hamdi, R., & Masson, V. (2008). Inclusion of a Drag Approach in the Town Energy Balance (TEB) Scheme: Offline 1D Evaluation in a Street Canyon. *Journal of Applied Meteorology and Climatology*, *47*(10), 2627–2644.
URL `http://journals.ametsoc.org/doi/abs/10.1175/2008JAMC1865.1`

Han, G., Chen, H., Yuan, L., Cai, Y., & Han, M. (2011). Field measurements on micro-climate and cooling effect of river wind on urban blocks in Wuhan city. In *2011 International Conference on Multimedia Technology*, (pp. 4446–4449). IEEE.
URL `http://ieeexplore.ieee.org/articleDetails.jsp?arnumber=6003331`

Harman, I. N., Barlow, J. F., & Belcher, S. E. (2004). Scalar Fluxes from Urban Street Canyons Part II: Model. *Boundary-Layer Meteorology*, *113*(3), 387–410.
URL `http://link.springer.com/10.1007/s10546-004-6205-7`

Hathway, E., & Sharples, S. (2012). The interaction of rivers and urban form in mitigating the Urban Heat Island effect: A UK case study. *Building and Environment*, *58*, 14–22.
URL `http://www.sciencedirect.com/science/article/pii/S0360132312001722`

Henschel, A., Burton, L. L., Margolies, L., & Smith, J. E. (1969). An analysis of the heat deaths in St. Louis during July, 1966. *American Journal of Public Health*, *59*(12), 2232–2242.

Höppe, P. (1999). The physiological equivalent temperature – a universal index for the biometeorological assessment of the thermal environment. *International Journal of Biometeorology*,

43(2), 71–75.

URL `http://dx.doi.org/10.1007/s004840050118`

Höppe, P. R., & Seidl, H. A. J. (1991). Problems in the assessment of the bioclimate for vacationists at the seaside. *International Journal of Biometeorology*, *35*(2), 107–110.

URL `http://link.springer.com/10.1007/BF01087486`

Horst, T. W. (1999). The Footprint for Estimation of Atmosphere-Surface Exchange Fluxes by Profile Techniques. *Boundary-Layer Meteorology*, *90*(2), 171–188.

URL `http://link.springer.com/article/10.1023/A{%}3A1001774726067`

Horst, T. W., & Weil, J. C. (1992). Footprint Estimation for Scalar Flux Measurements in the Atmospheric Surface Layer. *Boundary Layer Meteorology*, *90*, 171–188.

Hou, P., Chen, Y., Qiao, W., Cao, G., Jiang, W., & Li, J. (2012). Near-surface air temperature retrieval from satellite images and influence by wetlands in urban region. *Theoretical and Applied Climatology*, *111*(1-2), 109–118.

URL `http://link.springer.com/10.1007/s00704-012-0629-7`

House-Peters, L. A., & Chang, H. (2011). Modeling the impact of land use and climate change neighborhood-scale evaporation and nighttime cooling: A surface energy balance approach. *Landscape and Urban Planning*, *103*, 139–155.

Hwang, R.-L., Lin, T.-P., & Matzarakis, A. (2011). Seasonal effects of urban street shading on long-term outdoor thermal comfort. *Building and Environment*, *46*(4), 863–870.

URL `http://www.sciencedirect.com/science/article/pii/S0360132310003094`

Ihara, T., Kikegawa, Y., Asahi, K., Genchi, Y., & Kondo, H. (2008). Changes in year-round air temperature and annual energy consumption in office building areas by urban heat-island countermeasures and energy-saving measures. *Applied Energy*, *85*, 12–25.

Imamura, I. R. (1989). Air-surface temperature correlations. In *Controlling summer heat islands. Proceedings of the workshop on saving energy and reducing atmospheric pollution by controlling summer heat islands. Lawrence Berkeley Laboratory, Berkeley, CA*, (pp. 197–203).

IPCC (2014). *Climate Change 2014: Impacts, Adaptation, and Vulnerability. Part A: Global and Sectoral Aspects. Contribution of Working Group II to the Fifth Assessment Report of the Intergovernmental Panel on Climate Change [Field, C.B., V.R. Barros, D.J. Dokken, K.J..* Cambridge, United Kingdom and New York, NY, USA: Cambridge University Press.

Ishii, A., Iwamoto, S., Katayama, T., Hayashi, T., Shiotsuki, Y., Kitayama, H., Tsutsumi, J.-I., & Nishida, M. (1991). A comparison of field surveys on the thermal environment in urban areas surroundings a large pond: when filled and when drained. *Energy and Buildings*, *16*(3-4), 965–971.

URL `http://www.sciencedirect.com/science/article/pii/037877889190091G`

Järvi, L., Grimmond, C. S. B., & Christen, A. (2011). The Surface Urban Energy and Water Balance Scheme (SUEWS): Evaluation in Los Angeles and Vancouver. *Journal of Hydrology*, *411*, 219–237.

Jauregui, E. (1991). Influence of a Large urban park on temperature and convective precipitation in a tropical city. *Energy and Buildings*, *15*, 457–463.

Johansson, E. (2006). Influence of urban geometry on outdoor thermal comfort in a hot dry climate: A study in Fez, Morocco. *Building and Environment*, *41*(10), 1326–1338.

URL `http://www.sciencedirect.com/science/article/pii/S0360132305001952`

Johnson, H., Kovats, R. S., McGregor, G., Stedman, J., Gibbs, M., & Walton, H. (2005). The impact of the 2003 heat wave on daily mortality in England and Wales and the use of rapid weekly mortality estimates. *Euro Surveill*, *10*(7), 168–171.

Jones, T. S., Liang, A. P., Kilbourne, E. M., Griffin, M. R., Patriarca, P. A., Wassilak, S. G. F., Mullan, R. J., Herrick, R. F., Donnell, H. D., Choi, K., & Thacker, S. B. (1982). Morbidity and Mortality Associated With the July 1980 Heat Wave in St Louis and Kansas City, Mo. *Journal of the American Medical Association*, *247*(24), 3327–3331.

Kalanda, B. D., Oke, T. R., & Spittlehouse, D. L. (1980). Suburban energy balance estimates for Vancouver, B.C., using the Bowen ratio-energy balance approach. *Journal of Applied Meteorology*, *19*, 791–802.

Kántor, N., & Unger, J. (2011). The most problematic variable in the course of human-biometeorological comfort assessment the mean radiant temperature. *Open Geosciences*, *3*(1).
URL   `http://www.degruyter.com/view/j/geo.2011.3.issue-1/s13533-011-0010-x/s13533-011-0010-x.xml`

Kikegawa, Y., Genchi, Y., Kondo, H., & Hanaki, K. (2006). Impacts of city-block-scale countermeasures against urban heat-island phenomena upon a building's energy-consumption for air-conditioning. *Applied Energy*, *83*, 649–668.

Kikegawa, Y., Genchi, Y., Yoshikado, H., & Kondo, H. (2003). Development of a numerical simulation system toward comprehensive assessments of urban warming countermeasures including their impacts upon the urban buildings energy-demands. *Applied Energy*, *76*, 449–466.

Kim, Y.-H., Ryoo, S.-B., Baik, J.-J., Park, I.-S., Koo, H.-J., & Nam, J.-C. (2007). Does the restoration of an inner-city stream in Seoul affect local thermal environment? *Theoretical and Applied Climatology*, *92*(3-4), 239–248.
URL `http://link.springer.com/10.1007/s00704-007-0319-z`

Kljun, N., Rotach, M. W., & Schmid, H. P. (2002). A Three-Dimensional Backward Lagrangian

Footprint Model For a Wide of Boundary-Layer Stratifications. *Boundary Layer Meteorology*, *103*, 205–226.

Krayenhoff, E. S., Santiago, J.-L., Martilli, A., Christen, A., & Oke, T. R. (2015). Parametrization of Drag and Turbulence for Urban Neighbourhoods with Trees. *Boundary-Layer Meteorology*, *156*(2), 157–189.

URL http://link.springer.com/10.1007/s10546-015-0028-6

Krüger, E., Minella, F., & Rasia, F. (2011). Impact of urban geometry on outdoor thermal comfort and air quality from field measurements in Curitiba, Brazil. *Building and Environment*, *46*(3), 621–634.

URL http://www.sciencedirect.com/science/article/pii/S0360132310002763

Kusaka, H., & Kimura, F. (2004). Thermal effects of urban canyon stucture on the nocturnal heat island: experiment using a mesoscale model coupled with urban canopy model. *Journal of Applied Meteorology*, *43*, 1899–1910.

Kusaka, H., Kondo, H., Kikegawa, Y., & Kimura, F. (2001). A Simple Single-Layer Urban Canopy Model For Atmospheric Models: Comparison With Multi-Layer And Slab Models. *Boundary-Layer Meteorology*, *101*(3), 329–358.

URL http://link.springer.com/article/10.1023/A{%}3A1019207923078

Lee, H., Holst, J., & Mayer, H. (2013). Modification of human-biometeorologically significant radiant flux densities by shading as local method to mitigate heat stress in summer within urban street canyons. *Advances in Meteorology*, *2013*.

Lee, S.-H., & Park, S.-U. (2007). A Vegetated Urban Canopy Model for Meteorological and Environmental Modelling. *Boundary-Layer Meteorology*, *126*(1), 73–102.

URL http://link.springer.com/10.1007/s10546-007-9221-6

Lemonsu, A., Kounkou-Arnaud, R., Desplat, J., Salagnac, J.-L., & Masson, V. (2012a). Evolution of the Parisian urban climate under a global changing climate. *Climatic Change*, *116*, 679–692.

Lemonsu, A., Masson, V., Shashua-Bar, L., Erell, E., & Pearlmutter, D. (2012b). Inclusion of vegetation in the Town Energy Balance model for modelling urban green areas. *Geoscientific Model Development*, *5*(6), 1377–1393.

URL `http://www.geosci-model-dev.net/5/1377/2012/gmd-5-1377-2012.html`

Lend Lease (2006). Sustainability Initiatives Case Study: Mawson Lakes.

URL `https://www.mawsonlakescommunity.com.au/case/default.aspx`

Lin, B.-S., & Lin, Y.-J. (2010). Cooling Effect of Shade Trees with Different Characteristics in a Subtropical Urban Park. *HortScience*, *45*(1), 83–86.

URL `http://hortsci.ashspublications.org/content/45/1/83.short`

Lindberg, F., Holmer, B., & Thorsson, S. (2008). SOLWEIG 1.0–modelling spatial variations of 3D radiant fluxes and mean radiant temperature in complex urban settings. *International journal of biometeorology*, *52*(7), 697–713.

URL `http://www.ncbi.nlm.nih.gov/pubmed/18523814`

Lindqvist, S. (1992). Local climatological modelling for road streches and urban areas. *Geografiska Annaler*, *74*, 265–274.

Loughnan, M., Nicholls, N., & Tapper, N. J. (2010a). Mortality-temperature thresholds for ten major population centres in rural Victoria, Australia. *Health & Place*, *16*, 1287–1290.

Loughnan, M., Nicholls, N., & Tapper, N. J. (2010b). When the heat is on: Threshold temperatures for AMI admissions to hospital in Melbourne, Australia. *Applied Geography*, *30*, 63–69.

Loughnan, M., Tapper, N., Phan, T., Lynch, K., & McInnes, J. A. (2013). A spatial vulnerability analysis of urban populations during extreme heat events in Australian capital cities. Tech. rep., National Climate Change Adaptation Research Facility, Gold Coast.

URL `http://www.nccarf.edu.au/publications/spatial-vulnerability-urban-extreme-heat-event`

Masson, Moigne, P. L., Martin, E., Faroux, S., Alias, A., Alkama, R., Belamari, S., Barbu, A., Boone, A., Bouyssel, F., Brousseau, P., Brun, E., Calvet, J.-C., Carrer, D., Decharme, B., Delire, C., Donier, S., Essaouini, K., Gibelin, A.-L., Giordani, H., Habets, F., Jidane, M., Kerdraon, G., Kourzeneva, E., Lafaysse, M., Lafont, S., Brossier, C. L., Lemonsu, A., Mahfouf, J.-F., Marguinaud, P., Mokhtari, M., Morin, S., Pigeon, G., Salgado, R., Seity, Y., Taillefer, F., Tanguy, G., Tulet, P., Vincendon, B., Vionnet, V., & Voldoire, A. (2012). The SURFEXv7.2 externalized platform for the simulation of Earth surface variables and fluxes. *ATMOSPHERIC CHEMISTRY AND PHYSICS*.

URL `http://www.researchgate.net/publication/236456205{_}The{_}SURFEXv7.` `2{_}externalized{_}platform{_}for{_}the{_}simulation{_}of{_}Earth{_}surface{_}variables{_`

Masson, V. (2000). A physically-based scheme for the urban energy budget in atmospheric models. *Boundary Layer Meteorology*, *94*, 357–397.

Masson, V., Grimmond, C. S. B., & Oke, T. R. (2002). Evaluation of the Town Energy Balance (TEB) scheme with direct measurements from dry districts in two cities. *Journal of Applied Meteorology*, *41*, 1011–1026.

Masson, V., Le Moigne, P., Martin, E., Faroux, S., Alias, A., Alkama, R., Belamari, S., Barbu, A., Boone, A., Bouyssel, F., Brousseau, P., Brun, E., Calvet, J.-C., Carrer, D., Decharme, B., Delire, C., Donier, S., Essaouini, K., Gibelin, A.-L., Giordani, H., Habets, F., Jidane, M., Kerdraon, G., Kourzeneva, E., Lafaysse, M., Lafont, S., Lebeaupin Brossier, C., Lemonsu, A., Mahfouf, J.-F., Marguinaud, P., Mokhtari, M., Morin, S., Pigeon, G., Salgado, R., Seity, Y.,

Taillefer, F., Tanguy, G., Tulet, P., Vincendon, B., Vionnet, V., & Voldoire, A. (2013). The SURFEXv7.2 land and ocean surface platform for coupled or offline simulation of earth surface variables and fluxes. *Geoscientific Model Development*, *6*(4), 929–960.

URL `http://www.geosci-model-dev.net/6/929/2013/gmd-6-929-2013.html`

Masson, V., & Seity, Y. (2009). Including Atmospheric Layers in Vegetation and Urban Offline Surface Schemes. *Journal of Applied Meteorology and Climatology*, *48*(7), 1377–1397.

URL `http://journals.ametsoc.org/doi/abs/10.1175/2009JAMC1866.1`

Matzarakis, A., & Endler, C. (2010). Climate change and thermal bioclimate in cities: impacts and options for adaptation in Freiburg, Germany. *International journal of biometeorology*, *54*(4), 479–83.

URL `http://www.ncbi.nlm.nih.gov/pubmed/20091322`

Matzarakis, A., Mayer, H., & Iziomon, M. (1999). Applications of a universal thermal index: physiological equivalent temperature. *International Journal of Biometeorology*, *43*(2), 76–84.

URL `http://link.springer.com/10.1007/s004840050119`

Matzarakis, A., Rutz, F., & Mayer, H. (2007). Modelling radiation fluxes in simple and complex environmentsapplication of the RayMan model. *International Journal of Biometeorology*, *51*(4), 323–334.

URL `http://dx.doi.org/10.1007/s00484-006-0061-8`

Matzarakis, A., Rutz, F., & Mayer, H. (2010). Modelling radiation fluxes in simple and complex environments: basics of the RayMan model. *International journal of biometeorology*, *54*(2), 131–9.

URL `http://www.ncbi.nlm.nih.gov/pubmed/19756771`

May, P. B., Livesley, S. J., & Shears, I. (2013). Managing and Monitoring Tree Health and

Soil Water Status During Extreme Drought in Melbourne, Victoria. *Arboriculture & Urban Forestry*, *39*(3), 136–145.

Mayer, H., & Höppe, P. (1987). Thermal comfort of man in different urban environments. *Theoretical and Applied Climatology*, *38*(1), 43–49.

URL `http://link.springer.com/10.1007/BF00866252`

Mayer, H., & Matzarakis, A. (1998). *Human-biometeorological assessment of urban microclimates' thermal component*.

URL `http://www.lib.kobe-u.ac.jp/repository/00044728.pdf`

Michelozzi, P., De Donato, F., Bisanti, L., Russo, A., Cadum, E., DeMaria, M., D'Ovidio, M., Costa, G., & Perucci, C. A. (2005). The impact of the summer 2003 heat waves on mortality in four Italian cities. *Euro surveillance: bulletin Europeen sur les maladies transmissibles= European communicable disease bulletin*, *10*(7), 161–165.

Mitchell, V., Deletic, A., Fletcher, T. D., Hatt, B. E., & McCarthy, D. T. (2006). Achieving Multiple Benefits from Stormwater Harvesting. In *7th International Conference on Urban Drainage Modelling and the 4th International Conference on Water Sensitive Urban Design; Book of Proceedings.*, (pp. 912–919). Monash University.

URL `http://search.informit.com.au/documentSummary;dn=643986473648939;res=IELENG`

Mitchell, V. G., Cleugh, H. A., Grimmond, C. S. B., & Xu, J. (2008). Linking urban water balance and energy balance models to analyse urban design options. *Hydrological Processes*, *22*(16), 2891–2900.

URL `http://doi.wiley.com/10.1002/hyp.6868`

Mohan, M., Kikegawa, Y., Gurjar, B. R., Bhati, S., & Kolli, N. R. (2013). Assessment of urban

heat island effect for different land use–land cover from micrometeorological measurements and remote sensing data for megacity {D}elhi. *Theoretical and Applied Climatology*, *112*, 647–658.

Monaghan, A. J., Hu, L., Brunsell, N. A., Barlage, M., & Wilhelmi, O. V. (2014). Evaluating the impact of urban morphology configurations on the accuracy of urban canopy model temperature simulations with MODIS. *Journal of Geophysical Research: Atmospheres*, *119*(11), 6376–6392.

URL `http://doi.wiley.com/10.1002/2013JD021227`

Murakawa, S., Sekine, T., Narita, K.-i., & Nishina, D. (1991). Study of the effects of a river on the thermal environment in an urban area. *Energy and Buildings*, *15*, 993–1001.

Nadeau, D. F., Brutsaert, W., Parlange, M. B., Bou-Zeid, E., Barrenetxea, G., Couach, O., Boldi, M.-O., Selker, J. S., & Vetterli, M. (2009). Estimation of urban sensible heat flux using a dense wireless network of observations. *Environmental Fluid Mechanics*, *9*(6), 635–653.

URL `http://link.springer.com/10.1007/s10652-009-9150-7`

Nicholls, N., Skinner, C., Loughnan, M., & Tapper, N. (2008). A simple heat alert system for Melbourne, Australia. *International journal of biometeorology*, *52*(5), 375–84.

URL `http://www.ncbi.nlm.nih.gov/pubmed/18058138`

Nitschke, M., Tucker, G. R., Hansen, A. L., Williams, S., Zhang, Y., & Bi, P. (2011). Impact of two recent extreme heat episodes on morbidity and mortality in Adelaide, South Australia: a case-series analysis. *Environmental Health*, *10*, 9.

Noilhan, J., & Mahfouf, J. F. (1996). The ISBA land surface parameterisation scheme. *Global and Planetary Change*, *13*, 145–159.

Norton, B. A., Coutts, A. M., Livesley, S. J., Harris, R. J., Hunter, A. M., & Williams, N. S. (2015). Planning for cooler cities: A framework to prioritise green infrastructure to mitigate

high temperatures in urban landscapes. *Landscape and Urban Planning*, *134*, 127–138.

URL `http://www.sciencedirect.com/science/article/pii/S0169204614002503`

Oke, T. (1987). *Boundary Layer Climates*. London: Methuen.

Oke, T. (2009). The Need to Establish Protocols in Urban Heat Island Work. In *Eighth Symposium on the Urban Environment, Phoenix, AZ*.

Oke, T., Spronken-Smith, R., Jáuregui, E., & Grimmond, C. (1999). The energy balance of central Mexico City during the dry season. *Atmospheric Environment*, *33*(24-25), 3919–3930.

URL `http://www.sciencedirect.com/science/article/pii/S135223109900134X`

Oke, T. R. (1982). The energetic basis of the urban heat island. *Quarterly Journal of the Royal Meteorological Society*, *108*(455), 1–24.

Oke, T. R. (1988a). Street design and urban canopy layer climate. *Energy and Buildings*, *11*, 103–113.

Oke, T. R. (1988b). The urban energy balance. *Progress in Physical Geography*, *12*, 471–508.

Oke, T. R. (2004). Initial Guidance to Obtain Representative Meteorological Observations at Urban Sites. Tech. rep., World Meteorological Organization.

Oke, T. R. (2006). Towards better scientific communication in urban climate. *Theoretical and Applied Climatology*, *84*, 179–190.

Oke, T. R., Crowther, J. M., McNaughton, K. G., Monteith, J. L., & Gardiner, B. (1989). The Micrometeorology of the Urban Forest [and Discussion]. *Philosophical Transactions of the Royal Society B: Biological Sciences*, *324*(1223), 335–349.

URL `http://rstb.royalsocietypublishing.org/content/324/1223/335`

Oke, T. R., & McCaughey, J. H. (1983). Suburban-rural energy balance comparisons for Vancouver, B.C.: an extreme case? *Boundary Layer Meteorology*, *26*, 337–354.

Oleson, K. W., Bonan, G. B., Feddema, J., & Vertenstein, M. (2008a). An urban parameterization for a global climate model. part ii: Sensitivity to input parameters and the simulated urban heat island in offline simulations. *Journal of Applied Climatology and Meterogolgy*, *47*(4), 1061–1076.

Oleson, K. W., Bonan, G. B., Feddema, J., Vertenstein, M., & Grimmond, C. S. B. (2008b). An urban parameterization for a global climate model. Part i: Formulation and evaluation for two cities. *Journal of Applied Climatology and Meterogolgy*, *47*(4), 1038–1060.

Park, M., Hagishima, A., Tanimoto, J., & Narita, K.-i. (2012). Effect of urban vegetation on outdoor thermal environment: Field measurement at a scale model site. *Building and Environment*, *56*, 38–46.
URL http://www.sciencedirect.com/science/article/pii/S0360132312000546

Parsons, K. (2002). *Human Thermal Environments: The Effects of Hot, Moderate, and Cold Environments on Human Health, Comfort and Performance, Second Edition*. CRC Press.
URL http://books.google.com/books?hl=en{&}lr={&}id=4oxA6W{_}Os50C{&}pgis=1

Parsons, K. (2014). *Human Thermal Environments: The Effects of Hot, Moderate, and Cold Environments on Human Health, Comfort, and Performance, Third Edition*. CRC Press.
URL https://books.google.com/books?hl=en{&}lr={&}id=WejMAwAAQBAJ{&}pgis=1

Pataki, D. E., Carreiro, M. M., Cherrier, J., Grulke, N. E., Jennings, V., Pincetl, S., Pouyat, R. V., Whitlow, T. H., & Zipperer, W. C. (2011). Coupling biogeochemical cycles in urban environments: ecosystem services, green solutions, and misconceptions. *Frontiers in Ecology*

and the Environment, *9*(1), 27–36.

URL `http://www.esajournals.org/doi/abs/10.1890/090220`

Pearlmutter, D., Krüger, E. L., & Berliner, P. (2009). The role of evaporation in the energy balance of an open-air scaled urban surface. *International Journal of Climatology*, *29*(6), 911–920.

Peña, A., Gryning, S.-E., & Mann, J. (2010). On the length-scale of the wind profile. *Quarterly Journal of the Royal Meteorological Society*, *136*(653), 2119–2131.

URL `http://doi.wiley.com/10.1002/qj.714`

Peters, E. B., McFadden, J. P., & Montgomery, R. A. (2010). Biological and environmental controls on tree transpiration in a suburban landscape. *Journal of Geophysical Research*, *115*(G4), G04006.

URL `http://doi.wiley.com/10.1029/2009JG001266`

Petralli, M., Massetti, L., Brandani, G., & Orlandini, S. (2014). Urban planning indicators: useful tools to measure the effect of urbanization and vegetation on summer air temperatures. *International Journal of Climatology*, *34*(4), 1236–1244.

URL `http://doi.wiley.com/10.1002/joc.3760`

Petralli, M., Morabito, M., Cecchi, L., Crisci, A., & Orlandini, S. (2012). Urban morbidity in summer: ambulance dispatch data, periodicity and weather. *Central European Journal of Medicine*, *7*(6), 775–782.

URL `http://www.springerlink.com/index/10.2478/s11536-012-0056-2`

Picot, X. (2004). Thermal comfort in urban spaces: impact of vegetation growth Case study: Piazza della Scienza, Milan, Italy. *Energy and Buildings*, *36*, 329–334.

Pirard, P., Vandentorren, S., Pascal, M., Laaidi, K., Le Tertre, A., Cassadou, S., & Ledrans,

M. (2005). Summary of the mortality impact assessment of the 2003 heat wave in France. *Euro surveillance: bulletin Europeen sur les maladies transmissibles= European communicable disease bulletin*, *10*(7), 153–156.

Rannik, U., Aubinet, M., Kurbanmuradov, O., Sabelfield, K. K., Markkanen, T., & Vesala, T. (2000). Footprint Analysis for Measurements over a Heterogeneous Forest. *Boundary Layer Meteorology*, *97*, 137–166.

Roberts, P. (2005). Yarra Valley Water 2004 Residential End Use Measurement Study. Tech. rep., Yarra Valley Water.

Robine, J.-M., Cheung, S. L. K., Le Roy, S., Van Oyen, H., Griffiths, C., Michel, J.-P., & Herrmann, F. R. (2008). Death toll exceeded 70,000 in Europe during the summer of 2003. *Comptes rendus biologies*, *331*(2), 171–178.

Rosenzweig, C., Solecki, W. D., Parshall, L., Lynn, B., Cox, J., Goldberg, R., Hodges, S., Gaffin, S., Slosberg, R. B., Savio, P., Dunstan, F., & Watson, M. (2009). Mitigating New York City's Heat Island. *Bulletin of the American Meteorological Society*, *90*, 1297–1312.

Roth, M., Oke, T. R., & Emery, W. J. (1989). Satellite-derived urban heat islands from three coastal cities and the utilization of such data in urban climatology. *International Journal of Remote Sensing*, *10*(11), 1699–1720.

Runnalls, K. E., & Oke, T. R. (2006). A Technique to Detect Microclimatic Inhomogeneities in Historical Records of Screen-Level Air Temperature. *Journal of Climate*, *19*, 959–978.

Saaroni, H., & Ziv, B. (2003). The impact of a small lake on heat stress in a Mediterranean urban park: the case of Tel Aviv, Israel. *International Journal of Biometeorology*, *47*, 156–165.

Saito, I., Ishihara, O., & Katayama, T. (1990). Study of the Effect of Green Areas on the Thermal Environment in an urban area. *Energy and Buildings*, *15*, 493–498.

Sani, S. (1990). Urban climatology in Malaysia: An overview. *Energy and Buildings*, *15*(1-2), 105–117.

   URL `http://www.sciencedirect.com/science/article/pii/037877889090121X`

Schmid, H. P. (1994). Source areas for scalars and scalar fluxes. *Boundary-Layer Meteorology*, *67*(3), 293–318.

Schmid, H. P. (2002). Footprint modeling for vegetation atmosphere exchange studies: a review and perspective. *Agricultural and Forest Meteorology*, *113*(1-4), 159–183.

   URL `http://www.sciencedirect.com/science/article/pii/S0168192302001077`

Schwarz, N., Schlink, U., Franck, U., & Großmann, K. (2012). Relationship of land surface and air temperatures and its implications for quantifying urban heat island indicatorsAn application for the city of Leipzig (Germany). *Ecological Indicators*, *18*, 693–704.

   URL `http://www.sciencedirect.com/science/article/pii/S1470160X12000167`

Shashua-Bar, L., Oded, P., Arieh, B., Dalia, B., & Yaron, Y. (2010). Microclimate modelling of street tree species effects within the varied urban morphology in the Mediterranean city of Tel Aviv, Israel. *International Journal of Climatology*, *30*, 44–57.

Shashua-Bar, L., Pearlmutter, D., & Erell, E. (2009). The cooling efficiency of urban landscape strategies in a hot dry climate. *Landscape and Urban Planning*, *92*, 179–186.

Shashua-Bar, L., Pearlmutter, D., & Erell, E. (2011). The influence of trees and grass on outdoor thermal comfort in a hot-arid environment. *International Journal of Climatology*, *31*(10), 1498–1506.

Souch, C. A., & Souch, C. (1993). The effect of trees on summertime below canopy urban climates. *Journal of Arboriculture*, *19*, 303.

Spangenberg, J., Shinzato, P., Johansson, E., & Duarte, D. (2008). Simulation of the influence of vegetation on microclimate and thermal comfort in the city of S{ã}o Paulo. *Revista da Sociedade Brasileira de Arboriza{ç}{ã}o Urbana*, *3*, 1–19.

Spronken-Smith, R. A. (1994). *Energetics and cooling in urban parks*. Ph.D. thesis, The University of British Columbia.

Spronken-Smith, R. A., & Oke, T. R. (1998). The thermal regime of urban parks in two cities with different summer climates. *International Journal of Remote Sensing*, *19*, 2085–2104.

Steinfeld, G., Raasch, S., & Markkanen, T. (2008). Footprints in Homogeneously and Heterogeneously Driven Boundary Layers Derived from a Lagrangian Stochastic Particle Model Embedded into Large-Eddy Simulation. *Boundary-Layer Meteorology*, *129*(2), 225–248.
URL http://link.springer.com/10.1007/s10546-008-9317-7

Stewart, I. D. (2011). A systematic review and scientific critique of methodology in modern urban heat island literature. *International Journal of Climatology*, *31*, 200–217.

Stewart, I. D., & Oke, T. R. (2009). Classifying urban climate field sites by "local climate zones": the case of Nagano, Japan. In *The seventh {I}nternational {C}onference on {U}rban {C}limate, {Y}okohama, {J}apan*.

Stewart, I. D., & Oke, T. R. (2012). Local Climate Zones for Urban Temperature Studies. *Bulletin of the American Meteorological Society*, *93*(12), 1879–1900.
URL http://journals.ametsoc.org/doi/abs/10.1175/BAMS-D-11-00019.1

Stoll, M. J., & Brazel, A. J. (1992). Surface-air temperature relationship in the urban environment of Phoenix, Arizona. *Physical Geography*, *13*(2), 160–179.

Taha, H., Konopacki, S., & Gabersek, S. (1999). Impacts of Large-Scale Surface Modifcations

on Meteorological Conditions and Energy Use: A 10-Region Modeling Study. *Theoretical and Applied Climatology*, *62*, 175–185.

Takebayashi, H., & Moriyama, M. (2009). Study on the urban heat island mitigation effect achieved by converting to grass-covered parking. *Solar Energy*, *83*, 1211–1223.

Tan, J., Zheng, Y., Tang, X., Guo, C., Li, L., Song, G., Zhen, X., Yuan, D., Kalkstein, A. J., & Li, F. (2010). The urban heat island and its impact on heat waves and human health in {S}hanghai. *International Journal of Biometeorology*, *54*, 75–84.

Thom, J., & Coutts, A. (2015). Unpublished report: Modelling MRT variability with SOLWEIG. Tech. rep., Monash University.

Thompson, R. D., & Perry, A. H. (1997). *Applied Climatology: Principles and Practice*. Psychology Press.
URL https://books.google.com/books?id=FAYty1uyfboC{&}pgis=1

Tong, H., Walton, A., Sang, J., & Chan, J. C. L. (2005). Numerical simulation of the urban boundary layer over the complex terrain of Hong Kong. *Atmospheric Environment*, *39*, 3549–3563.

Tsiros, I. X. (2010). Assessment and energy implications of street air temperature cooling by shade tress in Athens (Greece) under extremely hot weather conditions. *Renewable Energy*, *35*(8), 1866–1869.
URL http://econpapers.repec.org/RePEc:eee:renene:v:35:y:2010:i:8:p:1866-1869

Upmanis, H., Eliasson, I., & Lindqvist, S. (1998). The influence of green areas on nocturnal temperatures in a high latitude city (Goteborg, Sweden). *International Journal of Climatology*, *18*(6), 681–700.

Velazquez-Lozada, A., Gonzalez, J. E., & Winter, A. (2006). Urban heat island effect analysis for San Juan, Puerto Rico. *Atmospheric Environment*, *40*, 1731–1741.

VicGov (2009). January 2009 Heatwave in Victoria: an Assessment of Health Impacts. Tech. rep., Victorian Government Department of Human Services.

Voogt, J. A. (2008). Assessment of an Urban Sensor View Model for thermal anisotropy. *Remote Sensing of Environment*, *112*, 482–495.

Voogt, J. A., & Oke, T. R. (1997). Complete Urban Surface Temperatures. *Journal of Applied Meteorology*, *36*, 1117–1132.

Voogt, J. A., & Oke, T. R. (2003). Thermal remote sensing of urban climates. *Remote Sensing of Environment*, *86*, 370–384.

Walsh, C. J., Fletcher, T. D., & Ladson, A. R. (2005). Stream restoration in urban catchments through redesigning stormwater systems: looking to the catchment to save the stream. *Journal of the North American Benthological Society*, *24*(3), 690–705.
URL http://dx.doi.org/10.1899/04-020.1

Ward, J. H. J. (1963). Hierarchical Grouping to Optimize an Objective Function. *Journal of the American Statistical Association*, *58*(301), 236–244.
URL http://www.jstor.org/discover/2282967?sid=21105652729063{&}uid=4{&}uid=2{&}uid=2134{&}uid=3737536{&}uid=70

Wieringa, J. (1993). Representative Roughness Paraneters for Homogeneous Terrain. *Boundary Layer Meteorology*, *63*, 323–363.

Wilson, J. D., & Swaters, G. E. (1991). The Source Area Influencing a Measurement in the Planetary Boundary Layer: The {\grqq}Footprint and the {\grqq}Distribution of Contact Distance. *Boundary Layer Meteorology*, *55*, 25–46.

Wong, M. S., Nichol, J. E., To, P. H., & Wang, J. (2010). A simple method for designation of urban ventilation corridors and its application to urban heat island analysis. *Building and Environment*, *45*(8), 1880–1889.

URL `http://www.sciencedirect.com/science/article/pii/S0360132310000776`

Wong, N. H., Chen, Y., Ong, C. L., & Sia, A. (2003). Investigation of thermal benefits of rooftop garden in the tropical environment. *Building and Environment*, *38*, 261–270.

Wong, T., & Hoban, A. (2006). WSUD resilience to Climate Change. In *1st International Hydropolis Conference,*. Perth, WA.

Wong, T. H. F., Allen, R., Brown, R., Deletic, A., Gangadharan, L., Gernjak, W., Jakob, C., Johnstone, P., Reeder, M., Tapper, N., Vietz, G., & Walsh, C. (2013). blueprint2013 - Stormwater management in a Water Sensitive City. Tech. rep., Cooperative Research Centre for Water Sensitive Cities, Melbourne.

Xu, W., Wooster, M. J., & Grimmond, C. S. B. (2008). Modelling of urban sensible heat flux at multiple spatial scales: A demonstration using airborne hyperspectral imagery of Shanghai and a temperature{â}{\grqq}emissivity separation approach. *Remote Sensing of Environment*, *112*(9), 3493–3510.

URL `http://www.sciencedirect.com/science/article/pii/S0034425708001296`

Zhang, D. L., X., Y., & Dickerson, R. R. (2009). Upstream urbanization exacerbates urban heat island effects. *Geophysical Research Letters*, *36*, 5.

Zhang, Z., Lv, Y., & Pan, H. (2013). Cooling and humidifying effect of plant communities in subtropical urban parks. *Urban Forestry & Urban Greening*, *12*(3), 323–329.

URL `http://www.sciencedirect.com/science/article/pii/S1618866713000368`

Zhou, Y., & Shepherd, J. M. (2010). Atlanta's urban heat island under extreme heat conditions and potential mitigation strategies. *Natural Hazards*, *52*, 639–668.

Zhu, S., Guan, H., Bennett, J., Clay, R., Ewenz, C., Benger, S., Maghrabi, A., & Millington, A. C. (2013). Influence of sky temperature distribution on sky view factor and its applications in urban heat island. *International Journal of Climatology*, (pp. 1837–1843).

URL `http://dx.doi.org/10.1002/joc.3660`